Universidad Autónoma de Madrid

Departamento de Bioquímica

Contribución de las prostaglandinas producidas por la ciclooxigenasa-2 al desarrollo del carcinoma hepatocelular

Ana Cristina Llorente Izquierdo

Madrid, 2013

Departamento de Bioquímica

Facultad de Medicina

Universidad Autónoma de Madrid

Contribución de las prostaglandinas producidas por la ciclooxigenasa-2 al desarrollo del carcinoma hepatocelular

Memoria de Tesis Doctoral presentada por:

Ana Cristina Llorente Izquierdo

Madrid, 2013

Licenciada en Bioquímica, para optar al grado de Doctor

por la Universidad Autónoma de Madrid

Dirigida por:

Dra. Paloma Martín Sanz

Dr. Rafael Mayoral Moñibas

Realizada en:

Instituto de Investigaciones Biomédicas Alberto Sols CSIC-UAM

CSIC
CONSEJO SUPERIOR DE INVESTIGACIONES CIENTÍFICAS

INSTITUTO DE INVETIGACIONES BIOMÉCICAS "ALBERTO SOLS"
CSIC-UAM

UAM
UNIVERSIDAD AUTONOMA DE MADRID

La directora **Dra. Paloma Martín Sanz** y el codirector **Dr. Rafael Mayoral Moñibas** certifican que **Ana Cristina Llorente Izquierdo**, licenciada en Bioquímica por la Universidad Complutense de Madrid, ha realizado el trabajo de investigación titulado: **"Contribución de las prostaglandinas producidas por la ciclooxigenasa-2 al desarrollo del carcinoma hepatocelular"** bajo su dirección en el Instituto de Investigaciones Biomédicas Alberto Sols, para optar al grado de Doctor por la Universidad Autónoma de Madrid.

Revisado el presente trabajo, expresan su conformidad para la presentación del mismo considerando que reúne los requisitos necesarios para ser sometido a discusión ante el Tribunal correspondiente.

Firmado, para que conste a todos los efectos, en Madrid, a 19 de Noviembre de 2012.

Fdo. **Paloma Martín Sanz**
Directora de Tesis
Investigadora Científica, CSIC

Fdo. **Rafael Mayoral Moñibas**
Codirector de Tesis
Investigador Contratado, UCSD

V^{o}B^{o} Tutora
Ángela María Martínez Valverde
Investigadora Científica, CSIC

MINISTERIO
DE ECONOMÍA
Y COMPETITIVIDAD

Esta memoria de tesis ha sido realizada con ayuda de la Beca Formación de Personal Investigador (FPI) con referencia BES-2008-009275 en el Departamento de Bioquímica del Instituto de Investigaciones Biomédicas Alberto Sols CSIC-UAM.

A mis padres Ana y Alfredo

A mis hermanos Alfredo, José Miguel y María Elena

A Paloma y Rafa

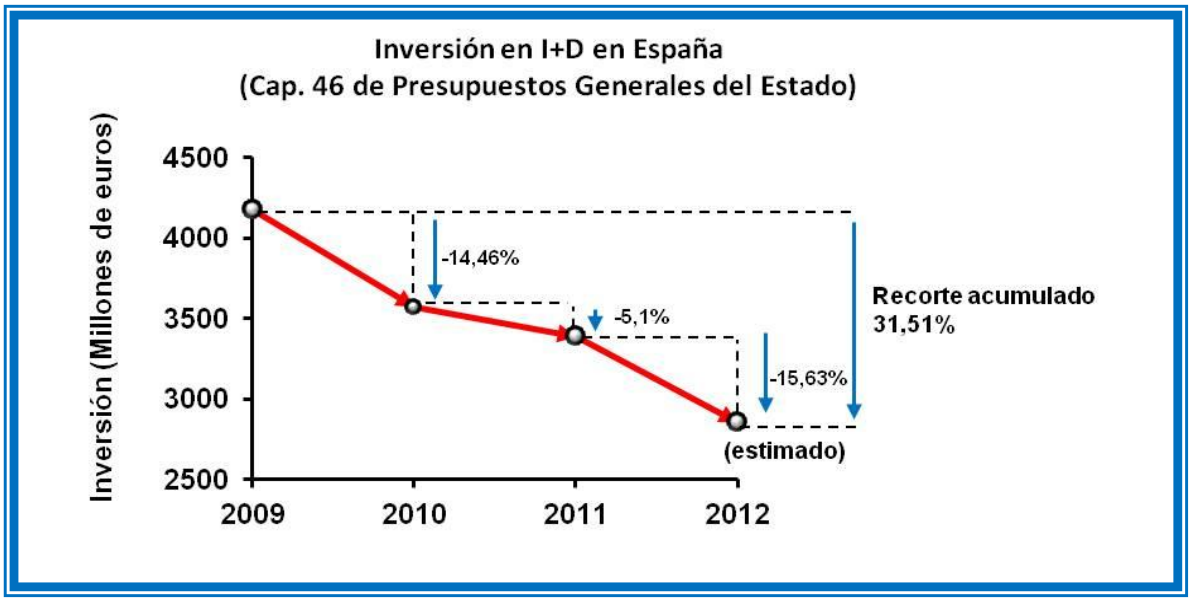

"Al carro de la cultura española le falta la rueda de la ciencia"

Santiago Ramón y Cajal

"Si el conocimiento te parece caro prueba con la ignorancia"

Derek Bok

Me fui a Chichester, Inglaterra, para mejorar mi inglés y pensar en mi futuro mientras estudiaba mis dos últimos exámenes de la carrera. Después de acabarlos, el **Dr. Manuel Guzmán** me pregunto a qué me iba a dedicar. Yo le dije que me gustaría investigar. Al día siguiente se abrió el plazo para solicitar las becas FPI. El me aconsejo a la **Dra. Paloma Martín** y me redactó una carta de recomendación. Era muy difícil conseguir la beca. Se lo agradezco porque desde ese momento comienza mi tesis.

Recuerdo perfectamente el día que me concedieron la beca. Era el último sábado de Agosto. Yo estaba en Berlanga de Duero, Soria. El lunes siguiente iba a comenzar una beca Leonardo de 9 meses en Dow Chemical Company, en Oxford. Solamente me quedaba hacer las maletas e irme. Estaba todo preparado. Ese mismo día, mi amigo Jaime me llamó felicitándome por haber conseguido la beca. La beca cambió mi futuro.

Agradezco infinitamente y con cariño a **la Dra. Paloma Martín** la oportunidad de realizar la Tesis. Me siento afortunada por haber trabajado y compartido este tiempo contigo. Gracias por tus sublimes directrices, por tu constancia, tu calidad humana y por enseñarme personalmente a mejorar cada día. Sin tu esfuerzo y ayuda desde el primer día hasta el último día hubiese sido imposible.

Por supuesto, dedico reconocido agradecimiento al **Dr. Rafael Mayoral**, por tu lucha diaria por enseñarme desde la base, por querer perfeccionarme cada día. No siempre ha sido sencillo. Aprecio enormemente tus aportaciones y el que gracias a ti pudiese hacer la estancia en el laboratorio del Dr. Jerrold Olefsky. Gracias no solo laboralmente si no personalmente. Son considerables las veces que me has brindado tu ayuda. Muchas gracias con cariño.

Sin duda, también quiero agradecer a la **Dra. Marta Casado** por haberme acogido cálidamente durante estancias breves en su laboratorio en el Instituto de Biomedicina de Valencia (IBV). Te agradezco tu enseñanza, calidad técnica y dedicación por el trabajo bien hecho. Fue un placer aprender en tu laboratorio.

Quiero hacer un afectuoso agradecimiento al **Dr. Lisardo Boscá** por tus excelentes aportaciones al proyecto, tu inteligente actitud positiva, amabilidad y por tus historias y anécdotas durante el día a día.

A **Jerrold M. Olefsky** no le puedo estar más agradecida por la gran oportunidad de hacer una estancia breve en su laboratorio en la Universidad de California, San Diego (UCSD). *Frankly, I am really grateful for the opportunity to perform a short internship in your lab. Working there was great, agreeable and has given me a good insight into the exiting field of obesity and diabetes research. It was particularly exciting to discover the good quality of your projects and your passion at work.*

Gracias a la **Dra. Ángela María Martínez**, al **Dr. Antonio Castrillo** y la **Dra. Susana Alemany** por enseñarme de primera mano técnicas, darme consejos y dejarnos amablemente pequeñas alícuotas de anticuerpos.

Gracias al **Dr. Carmelo García** por dejarnos reactivos, ser cordial y amable con nosotros.

Gracias a la **Dra. Sonsoles Hortelano** por compartir conmigo buenos momentos en los congresos de la SEBBM, por tus consejos, por tu ayuda y por tus donaciones.

A la **Dra. Francisca González,** me has apoyado y ayudado siempre que lo he necesitado en el laboratorio y fuera de él tantas veces que no tengo espacio para enumerarlas aquí. He disfrutado muchas y muy buenas experiencias contigo. Te agradezco de corazón tu generosidad y amabilidad conmigo.

A la **Dra. Ana Julia Fernández,** no solo te agradezco por enseñarme técnicas durante mi estancia en el IBV, sino que además, debo agradecerte que me acogieras amablemente en tu casa y me dedicases esos días con un trato excelente. Estoy encantada de haber compartido el tiempo de mi estancia en Valencia contigo y el trabajo de epigenética. Tampoco puedo olvidar reconocer el agradable trato, aportaciones y enseñanzas durante mi estancia en Valencia a la **Dra. M. Soledad Álvarez**, a la **Dra. Carme Cucarella** y a **Carlos Graw**.

A la **Dra. Patricia Sancho** y a la **Dra. Águeda González** gracias por ser amables conmigo y por enseñarme las técnicas que necesitaba.

Y por tan buenos momentos pasados en el laboratorio y fuera del laboratorio, por haber hecho los días más sencillos y agradables, por apoyarme en los buenos y malos periodos, por ayudarme en mi trabajo, explicarme dudas y mantener el orden en el laboratorio B11, gracias a **María Pimentel, Patricia Prieto, María Fernández, Gemma Benito, Verónica Terrón, María José Guillén, Noelia Agra, Daniel Francés, Luis Alberto Castro, Omar Motiño y Luciane A. Faine**. Todos y cada uno de vosotros me habéis ayudado personalmente y laboralmente en mil ocasiones. Gracias.

También quiero agradecer a la gente de otros laboratorios del IIB por su generosidad, buen trato y convivencias, en especial a **Leticia Martínez, Elsa, Carlos Sanz y Carolina Muñoz.**

Qué decir de todos los compañeros que conocí durante mi estancia en California en la UCSD. No puedo estar más encantada de la excelente experiencia vivida con vosotros. *I couldn't be more grateful for the excellent and very pleasant manner that I daily received. I am totally glad for sharing that awesome experience with all of you. I immensely appreciate the friendly atmosphere lived there. Thank you so much especially to* ***Evelyn Walenta, Da Young Oh, Jan Heinrichsdorff, Andrew Dillin, Denise, Joanne McNelis, William Ricketts, Livy, PingPing Li, Min Lu, Marina, Lin Lin,***

Leo, Nai-Wen Chi, Betsy, Dorothy Sears and Hyun-Shik Son. *It is a nice memory that I will treasure forever. I would also like to keep on record my sincere thanks to other extraordinary people that I met in California*

Sin la colaboración del personal de los servicios de **Informática**, **Citometría de Flujo, Imagen, Genómica, Microscopía Confocal, Animalario, Almacén, Recursos Humanos y Gerencia** la realización del proyecto no habría sido posible.

Quiero hacer especial mención a todos mis **amigos**. Me siento afortunada por compartir mi vida con cada uno de vosotros, por esos momentos insuperables, por darme la alegría del día a día, por hacerme reír y por escucharme cuando lo necesito. Gracias a mis **amigos de la Universidad** (Nacho, Jaime, Tere, Julio, Bea, Hector e Irene)**, de la Residencia** (Bea e Ire)**,** a mis **compañeros de piso** (Helen, Aurelio y Yoana), a mis **amigos de Soria** (Diego, Chechu, Kike, Edu, Dafne, Dani, Eli, Bea y Miri) **de Anguiano**, **de Garcillán y a toda "la familia segoviana".** Gracias a todas mis grandes e inseparables amigas del **grupo HDH** que incluso algunas acabasteis viviendo conmigo (Nata, Cris Kunkun, Bego, Bea, Ele, Cris B, Sara, Sandra y Lucía). Y por supuesto gracias a ti, **Laura**, gracias por compartir mi vida desde el día en que nací. Tú estás en casi todos los grupos de amigos. También a ti, **Irene,** tú también estás en muchos grupos, gracias por las innumerables e inmejorables experiencias vividas.

Y para terminar quiero dar las gracias a toda **MI FAMILIA** tanto a **LOS LLORENTES** como a **LOS IZQUIERDOS** a todos los tíos por darme vuestro ilimitado cariño, por enseñarme y cuidarme. A todos los primos, los nuevos primos, los novios de mis hermanos y a mi cuñada Marta, por ser amigos fieles.

Gracias a mi primo **Jorge**, a mi tía **Begoña** y a mis **Abuelos.** Nadie muere hasta que no mueren sus recuerdos. Mis recuerdos están vivos. Jamás os olvidaré.

Y finalmente, por ser lo más importarte de mi vida, por apoyarme incondicionalmente, por aguantarme, por enseñarme, por cuidarme y por quererme, mi más profundo agradecimiento a **MIS PADRES Y A MIS HERMANOS.**

Gracias a todos por compartir mi vida.

Resumen/Abstract

La ciclooxigenasa (COX) es la enzima que cataliza el paso limitante en la biosíntesis de prostanoides. Existen dos isoformas de COX, COX-1 que se expresa de manera constitutiva en muchos tejidos y COX-2 que es inducible por diversos estímulos como factores de crecimiento, estímulos pro-inflamatorios y otros tipos de estrés celular. Además de los procesos pro-inflamatorios, COX-2 es un gen crítico en proliferación celular, remodelación tisular y cáncer.

En hígado, COX-2 no se expresa ni se induce en el hepatocito adulto con diversos estímulos pro-inflamatorios, pero si en el hepatocito fetal. COX-2 solamente se expresa en el hepatocito adulto en aquellas situaciones que implican procesos de des-diferenciación, regeneración y proliferación como en el carcinoma hepatocelular (CHC). En el CHC, COX-2 no se expresa en estadios avanzados pero sí en las fases iniciales y hay mayor expresión en la zona no tumoral adyacente al área tumoral que en la tumoral. Por lo tanto, la contribución de COX-2 al CHC no está bien establecida. Para esclarecer el efecto de las PGs derivadas de COX-2 en el CHC se generó un modelo de ratón TG para COX-2 en el hepatocito y una línea celular hepática TG para COX-2. Además, se analizó la implicación de las alteraciones epigenéticas del gen de COX-2 en el CHC, en células de hepatoma y en biopsias humanas.

Los resultados obtenidos sugieren que a pesar de que el aumento de las PGs en el hepatocito promueve una ligera hepatitis, no contribuyen al desarrollo de fibrosis hepática después de un daño hepático crónico con dieta deficiente en colina y metionina. La inducción de una hepatocarcinogénesis química con dietilnitrosamina (DEN) reveló que COX-2 acelera la proliferación inicial de los hepatocitos y favorece moderadamente el desarrollo de nódulos pre-neoplásicos sin que esté directamente vinculada con la transformación tumoral. Para corroborar estos resultados, se empleó un modelo de hepatocarcinogénesis genética donde ratones dobles TG para c-Myc/TGF-α desarrollan espontáneamente CHC. Se generaron animales triples TG c-Myc/TGF-α/COX-2 para evaluar la implicación de las PGs al CHC. En concordancia con nuestros resultados previos, se confirmó que las PGs derivadas de COX-2 juegan un papel poco relevante en el desarrollo del CHC murino**.** Sin embargo, hemos definido que los cambios epigenéticos en el promotor de COX-2 modifican su expresión y que tienen importancia en el pronóstico de CHC humano. La hipermetilación del promotor de COX-2 y la hipoacetilación de la histona H3 están correlacionadas con la disminución en la expresión de COX-2 en las biopsias humanas y en algunas líneas de hepatoma así como con la reducción de la supervivencia de los pacientes.

Cyclooxygenases 1 and 2 (COX-1 and COX-2) catalyze the first step in prostanoid biosynthesis. COX-1 is constitutively expressed in many tissues; COX-2 is induced by a variety of stimuli such as growth factors, pro-inflammatory stimuli, hormones and other cellular stresses. Moreover, COX-2 has been associated with cell growth regulation, tissue remodeling and carcinogenesis.

Adult hepatocytes fail to induce COX-2 expression, regardless of the pro-inflammatory factors used, however, Kupffer, stellate, fetal hepatocytes and hepatoma mouse liver cells retain the ability to express COX-2 on stimulation with pro-inflammatory cytokines. COX-2 is solely expressed in adult hepatocytes in those situations that involve de-differentiation, regeneration and proliferation such as human hepatocellular carcinoma (HCC). In HCC, COX-2 expression has been found in early stages but is downregulated in advances stages, and with changes in the areas of expression in tumor versus non-tumor adjacent tissue. Therefore, many questions remain unsolved regarding the contribution of COX-2 dependent PGs to induce HCC. The regulation of COX-2 expression by epigenetic modulation could be crucial in HCC. To clarify the role of COX-2 in liver tumorigenesis models of COX-2 transgenic (TG) mice and human hepatocyte-like TG cell line were generated. Besides, the involvement of epigenetic alterations of the COX-2 gen in HCC in human biopsies and in human hepatoma cell lines were analyzed.

The obtained data suggests that the increased of PGs in hepatocytes promoted mild hepatitis, but failed to contribute to the development of liver fibrogenesis after chronic liver damage with methionine and choline deficient diet. The induction of chemical hepatocarcinogenesis with diethylnitrosamine (DEN) revealed that COX-2 expression in hepatocytes favors moderately the development of pre-neoplastic foci without affecting malignant transformation**.** To confirm these results, further experiments were performed in a well-defined genetic hepatocarcinogenesis model where double TG mice that express c-Myc/TGF-α spontaneously develop HCC. Triple c-Myc/TGF-α/COX-2 TG mice were generated to evaluate the involvement of COX-2 in HCC. According to our previous results, the triple TG model confirms that COX-2 dependent PGs play a minor role in the hepatocarcinogenesis course mediated by c-Myc/TGF-α. However, changes in the epigenetics marks at the COX-2 promoter are closely associated with its expression and with the prognosis of human HCC. Hipermethylation in the COX-2 promoter and histone 3 hypoacetylation are correlated with low levels of COX-2 in human biopsies and in some HCC cell lines as well as with a reduction of overall survival of the patients.

Índice

Abreviaturas

15d-PGJ_2	15-deoxi-Δ12,14-PGJ_2
15-PGDH	15-hidroxiprostaglandina deshidrogenasa dependiente de NAD^+
2-AAF	2-acetilaminoflurano
3'-UTR	Región 3' no traducida
4-DAB	3'-metil-4-dimetilamino-azobenceno
5mC	5-metilcitosina
8-OHdG	8-hidroxi-2'-deoxiguanosina
AA	Ácido araquidónico
aa	Aminoácido
AAT	Alfa antitripsina
Ac-H	Acetil-Histona
ADN	Ácido desoxirribonucleico
ADNc	ADN complementario
AINE	Anti-inflamatorios no esteroideo
ALT	Alanina transaminasa
AMPc	Adenosín monofosfato cíclico
AOX	Acetil-CoA oxidasa
AP	Proteína activadora
APAP	Acetaminofeno
APC	Poliposis adenomatosa coli
ApoE	Apolipoproteína E
ARE	Elementos ricos en AU (adenina y uracilo)
ARF	Factor de ribosilación del ADP
ARN	Ácido ribonucleico
ARNm	ARN mensajero
Ask	Quinasa activadora de la fase S
AST	Aspartato transaminasa
AzadC	5'-aza-2'-deoxicitidina
C	Citosina
C/EBP	Proteína potenciadora de unión a CCAAT
Ca^{2+}	Calcio
CCdn-1	Ciclina D1
CCl_4	Tetracloruro de carbono
Ccne1	Ciclina E1
CdK	Quinasa dependiente de Ciclina
CFH	Factor H del complemento
CHC	Carcinoma hepatocelular
CHL	Chang Liver
c-Jun	Quinasa N-terminal
Ck	Promotor de citoqueratina
cMOAT	Transportador de aniones multiespecíficos orgánicos de la membrana canalicular
COX	Ciclooxigenasa
COXIB	Inhibidor selectivo para COX-2
cPGES	PGES citosólica
CRE	Elementos de respuesta a AMPc
CSDM	Células supresoras derivadas de progenitores mieloides
c-Src	Oncogén del virus del sarcoma de Rous
CXCR	Receptor de quimioquinas
CYP450	Sistema citocromo P450
DCM	Deficiente en colina y metionina
DEN	Dietilnitrosamina
DMBA	7,12-dimetilbenzo(α)antraceno
DMN	Dimetilnitrosamina
DNMT	DNA metiltransferasa
DTG	Doble TG
EGF	Factor de crecimiento epidérmico
EGFR	Receptor de EGF
EHGNA	Enfermedad de hígado graso no alcohólica

EPI	Epinefrina
ERK	Quinasas reguladoras de señales extracelulares
FBS	Suero bovino fetal
FGF	Factor de crecimiento de fibroblastos
FSH	Hormona folículo estimulante
Gadd45b	Proteína de parada del crecimiento inducible por daño al ADN
GFP	Proteína verde fluorescente
GnRH	Hormona liberadora de gonadotropina
GSH	Glutatión
GSTP1	Glutatión S transferasa clase P1
Gtse1	Proteína 1 expresada en la fase S y G2
H	Histona
HAT	Histona acetiltransferasa
HBsAg	Antígeno de superficie del VHB
HBx	Proteína X del VHB
hCOX-2	COX-2 humana
HDAC	Histona deacetilasa
HGF	Factor de crecimiento hepatocitario
HMT	Histona metiltransferasa
HO-1	Hemo oxigenasa-1
HOX	Hidroperoxidasa
IFN	Interferón
IGF	Factor de crecimiento insulínico
IGF-R	Receptor del factor de crecimiento insulínico
iHDAC	Inhibidores de la actividad de HDAC
IKK	Proteína de la quinasa IκB
IL	Interleuquina
IL-R	Receptor de IL
Inhbc	Inhibina beta C
iNOS	Óxido nítrico sintasa
JNK/SAPK	Quinasa c-Jun N-terminal
LH	Hormona luteinizante
LPS	Lipopolisacárido
Ltab	Linfotoxina a o b
Lys	Lisina
MAPK	Proteína quinasa activada por mitógenos
MARP3	Proteína 3 anquirina de músculo repetida
MAT	Metionina adenosiltransferasa
MBD	Proteína de unión a la 5mC
MDR	Proteína de resistencia a múltiples fármacos
MMP	Metaloproteasa
MN	Membrana nuclear
mPGES	PGES microsomal
MRP	Proteína relacionada con la resistencia a fármacos
MSRA	Metilación sensible a enzimas de restricción por PCR
MTG	Mono TG
mTOR	Proteína diana de la rampamicina en mamíferos
MYO1E	Miosina 1E
MYRIP	Proteína de interacción miosina VIIA y Rab
NaB	Butirato sódico
NEMO	Proteína moduladora esencial de NF-κB
Nfr-2	Factor nuclear de transcripción eritroide-2
NF-κB	Factor nuclear potenciador de las cadenas ligeras kappa de las células B
NOREPI	Norepinefrina
NOS	Óxido nítrico sintasa
NOX	NADPH oxidasa
NS5A	Proteína no estructural 5A
ORF	Marco de lectura abierto

PAF	Factor de activación plaquetario
PARP	Poli-ADP-ribosa polimerasa
pb	Pares de bases
PB	Fenobarbital
PCNA	Antígeno nuclear de células en proliferación
PCR	Reacción en cadena de la polimerasa
PDGF	Factor de crecimiento derivado de plaquetas
PG	Prostaglandina
PGES	Prostaglandina E sintasa
PGHS	Prostaglandina G/H sintasa
PGT	Transportador de PG
PI3K	Fosfoinositol 3-quinasa
PKA	Proteína quinasa A
PKB	Proteínas quinasa B/Akt
PKC	Proteína quinasa C
PLA_2	Fosfolipasa A_2
PLC	Fosfolipasa C
PMA	Acetato de forbol miristato
PPAR	Receptores activados por proliferadores de peroxisomas
PPRE	Elemento de respuesta a PPAR
PSRC1	Proteína helice superenrrollada 1 ricos en prolina/serina
PTEN	Homólogo de la fosfatasa y la tensina
PTH	Hormona paratiroidea
RASSF	Proteína de la familia con dominio de asociación a Ras
Rb	Retinoblastoma
RE	Retículo endoplasmático
ROS	Especies reactivas de oxígeno
SAHA	Ácido hidroxámico suberoilanilida
SAM	S-adenosin-metionina
SIRT1	Sirtuina 1
Slc16a2	Miembro 2 transportador de monocarboxilatos de la familia de transportadores de solutos 16 a
SP-1	Proteína específica 1
SRE	Elemento de respuesta a suero
Stat3	Activador de la transcripción 3
TAM	Tioacetamida
TBARS	Especies reactivas al ácido tiobarbitúrico
TERT	Telomerasa transcriptasa inversa
TG	Transgénico
TGF	Factor de crecimiento transformante
TIMP	Inhibidor de la metalopeptidasa
TKR	Receptores tirosina quinasa
TLR	Receptor tipo Toll
TNF	Factor de necrosis tumoral
TNF-R	Receptor de TNF
Tnfrsf	Receptor de TNF
TSA	Tricostatina A
TTG	Triple TG
TXA_2	Tromboxanos
uPA	Activador del plasminógeno de tipo uroquinasa
UV-B	Ultravioleta B
VEGF	Factor de crecimiento endotelial vascular
VHB	Virus de la hepatitis B
VHC	Virus de la hepatitis C
WT	Fenotipo salvaje
α-SMA	α-actina de músculo liso

Introducción

1. Ciclooxigenasa-2

1.1 Biosíntesis de prostanoides

Los prostanoides (prostaglandinas, prostaciclinas y tromboxanos) son mensajeros lipídicos de vida media corta que derivan del ácido araquidónico (AA) procedente de los glicerofosfolípidos de la membrana [5]. La liberación del AA requiere de la acción de la fosfolipasa A_2 (PLA_2) o de la fosfolipasa C (PLC) [32]. El AA puede ser metabolizado por tres vías principales: 1) ciclooxigenasa (COX), 2) lipooxigenasa y 3) citocromo P-450 monooxigenasa. La vía de COX es la que ha sido más estudiada debido a que las prostaglandinas (PGs) juegan un papel importante en diferentes procesos biológicos.

COX, (EC 1.14.99.1), también conocida como prostaglandina G/H sintasa (PGHS) o prostaglandina-endoperóxido sintasa, es la enzima que cataliza el paso limitante en la biosíntesis de prostanoides. Se caracteriza por presentar doble actividad enzimática, ciclooxigenasa (COX) e hidroperoxidasa (HOX). Mediante su actividad COX cicla y oxigena al AA para la formación de prostaglandina G_2 (PGG_2) que es un metabolito de gran inestabilidad. A continuación, por su actividad HOX, reduce PGG_2 a una forma hidroxilada denominada prostaglandina H_2 (PGH_2) [51]. Finalmente, actúan una serie de isomerasas y oxidoreductasas específicas de tejido que emplean como sustrato PGH_2 generando los diferentes productos; prostaglandinas (PGE_2, PGD_2, PGF_2), prostaciclinas (PGI_2) y tromboxanos (TXA_2) (Fig.1). Las acciones biológicas de los prostanoides son múltiples. PGE_2 participa en procesos de regulación del tono vascular, agregación plaquetaria, ovulación, remodelación ósea, así como en procesos febriles, dolor y otros mecanismos fisiológicos de defensa, incluyendo respuesta inflamatoria e inmune. PGF_2 produce contracción uterina. PGI_2 inhibe la agregación plaquetaria, es vasodilatadora e imprescindible para la implantación del embrión. TXA_2 estimula la agregación plaquetaria y la vasoconstrición.

Una vez sintetizadas, las PGs pueden ejercer su acción de forma autocrina o paracrina. La señalización paracrina requiere de proteínas relacionadas con la resistencia a múltiples fármacos (MRP4) que secretan las PGs al medio extracelular [149]. Las PGs pueden ser reconocidas por receptores específicos de membrana plasmática y receptores nucleares que median su acción por la activación de diferentes vías de transducción de señales. Después de ejercer su acción, las PGs se internalizan en la célula por difusión pasiva o por el transportador de PGs (PGT) para ser catabolizadas e inactivadas por la acción enzimática de la 15-hidroxiprostaglandina deshidrogenasa dependiente de NAD^+ (15-PGDH)[100].

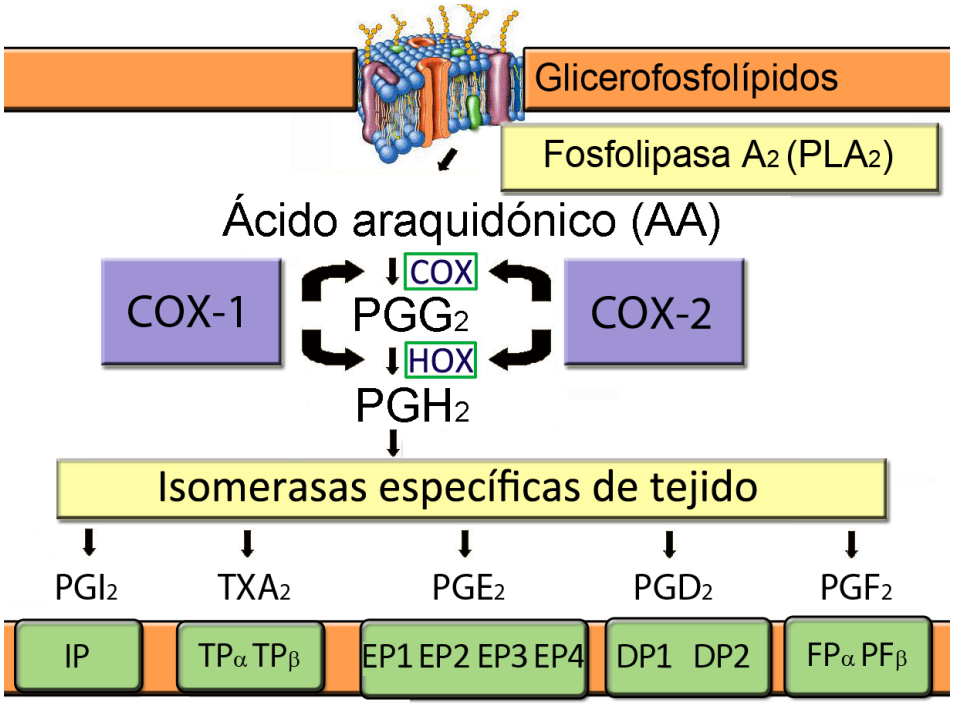

Figura 1. Vía metabólica para la conversión del ácido araquidónico en prostaglandinas, prostaciclinas y tromboxanos. *PLA_2 libera el AA de los glicerofosfolípidos de la membrana. El AA es transformado por la enzima COX mediante sus dos actividades enzimáticas secuenciales COX y HOX. A continuación, prostaciclinas, prostaglandinas y tromboxano sintasas específicas de tejido actúan para formar los distintos productos activos finales que serán reconocidos por diversos receptores. Adaptado de Samuelsson et al. [121].*

1.2 Evidencia de diferentes ciclooxigenasas

Existen dos isoformas de COX: una de expresión constitutiva denominada COX-1 y otra de expresión inducible en respuesta a diversos estímulos conocida como COX-2. COX-1 se purificó en 1976 de glándulas vesiculares bovinas [102]. En 1989 Simmons identificó el ADNc de COX-2, cuyo ARNm se inducía al transformar fibroblastos de pollo con v-Src [134].

Se ha comprobado que ambas proteínas están localizadas en la porción de la bicapa lipídica más próxima al lado luminal del retículo endoplasmático (RE) y en las porciones externa e interna de la membrana nuclear (MN), estando COX-2 preferentemente localizada en la MN. Su localización en diferentes membranas está directamente relacionada con sus funciones fisiológicas [154]. Se ha descrito que COX-2 se localiza también en la membrana mitocondrial y en los cuerpos lipídicos en células tumorales [1]. Las secuencias aminoacídicas de COX-1 y de COX-2 presentan aproximadamente un 60% de homología. Desde la región N-terminal hasta la C-terminal, los dominios que conforman la estructura proteica de COX-1 y COX-2 son: el péptido señal, el domino de dimerización, el dominio de unión a membrana y el dominio catalítico. Ambas isoformas tienen N-glicosilaciones que regulan el plegamiento de las proteínas. Una de las diferencias más importantes en su estructura proteica es que el sitio catalítico de COX-2 es un 17% más grande que el de COX-1, permitiendo la entrada de sustratos de mayor tamaño. Esto es debido a la sustitución en la posición 434 de una

isoleucina en COX-1 por una valina en COX-2. El desarrollo de inhibidores selectivos para una u otra isoforma de COX se basa en esta diferencia. Además COX-2 puede procesar sustratos alternativos como ésteres y derivados de amidas (endocanabinoides endógenos) [116].

En 1971, el grupo de Vane demostró que la aspirina e indometacina inhibían la producción de PGs bloqueando la actividad enzimática de COX [145], siendo ambos compuestos anti-inflamatorios no esteroideos (AINEs). Los AINEs inhiben la actividad catalítica de COX modificando covalentemente la enzima de manera irreversible (exclusivamente la aspirina) o compitiendo con el sustrato por el centro activo (resto de los AINEs). Los AINEs tienen propiedades antipiréticas, analgésicas y anti-inflamatorias. Debido a que las PGs derivadas de COX-1 regulan múltiples procesos fisiológicos, la inhibición crónica de COX-1 producida por un consumo prolongado de inhibidores conduce a efectos secundarios gastrointestinales. El descubrimiento de la diferencia de tamaño del centro activo entre ambas isoformas dio lugar al desarrollo de AINEs selectivos para COX-2 (COXIBs). Posteriormente se comprobó que la inhibición de COX-2 puede tener efectos secundarios cardiovasculares y renales [25]. El hecho de que prácticamente todos los AINEs, a excepción de la aspirina, sean inhibidores reversibles competitivos de COX es importante ya que se ha descrito que producen una acumulación de la proteína, de forma que al retirar el inhibidor reversible puede provocar una sobre-producción de PGs [14]. Estudios recientes han demostrado que los AINEs pueden mediar sus efectos anti-inflamatorios y anti-neoplásicos por vías alternativas a la vía de COX-2. De hecho, los efectos anti-neoplásicos de los AINEs se observan a concentraciones que son superiores a las necesarias para inhibir la síntesis de PGs y son capaces de inhibir la proliferación e incrementar la apoptosis en células que no expresan COX-2 [18].

1.3 Estructura génica de COX-1 y COX-2

El gen que codifica para COX-1 humana se localiza en el cromosoma 9, su tamaño es de 22.5 kb, posee 11 exones y sus tránscritos tienen una longitud de 2.8, 4.5 y 5.2 kb. El más abundante es el de 2.8 kb (Tabla 1).

	COX-1	COX-2
Cromosoma	**Cromosoma 9**	**Cromosoma 1**
Tamaño del gen	**22.5 Kb, 11 exones**	**8.3 Kb, 10 exones**
Masa molecular	**72 kDa**	**72-74KDa**
Nº de aminoácidos (aa)	**600-602 aa**	**603-604 aa**
Cinética	**Similar V_{max} y K_m para el AA**	
3' UTR	**0.7 Kb**	**2 Kb, enriquecida en AUUUA**
Expresión	**Constitutiva**	**Inducible**
Localización	**RE y MN**	**Principalmente en la MN**

Tabla 1. Propiedades de COX-1 y COX-2 humanas.

El gen de COX-2 humana se localiza en el cromosoma 1, su tamaño es de 8.3 kb, está formado por 10 exones y las variantes del tránscrito de ARNm son de 2.6, 4.0 y 4.5 kb. Los tránscritos más abundantes son el de 2.6 y el de 4.5 Kb. El tránscrito de 2.6 kb, está poliadenilado y carece de la región 3' no traducida (3'-UTR). Las mayores diferencias en la estructura génica de ambas isoformas consisten en la longitud de los intrones y en que COX-2 carece del primer intrón. Además, cada una tiene diferentes elementos reguladores de los promotores que les confieren determinadas características funcionales (Fig.2) [26].

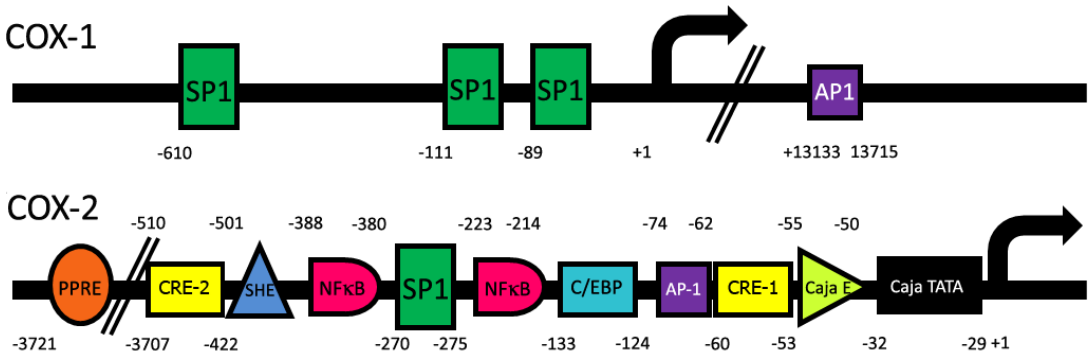

Figura 2. Elementos reguladores de los promotores de COX-1 y COX-2 humanas. *Adaptado de Kang et al. [68].*

El promotor del gen humano y murino de COX-1 carece de caja TATA, contiene tres motivos de unión a la proteína específica 1 (SP-1) implicados en la iniciación de la transcripción del gen y un sitio de unión a la proteína activadora 1 (AP-1) que interactúa con los motivos SP-1. A pesar de que estas características hacen de COX-1 un gen constitutivo por excelencia, es particularmente inducido por algunos estímulos mediante la regulación de los motivos SP-1 en determinadas células que se diferencian durante el desarrollo.

La región 5' flanqueante del gen humano de COX-2 contiene varios elementos reguladores de la transcripción. Incluye un sitio PPRE, dos elementos de respuesta a AMPc (CRE), un elemento de respuesta a suero (SRE), diversos sitios SP-1, dos sitios de unión a NF-κB, un sitio de reconocimiento de la proteína potenciadora de unión a CCAAT (C/EBP), dos sitios AP-2, una caja E y la caja TATA. Los dominios CRE, C/EBP, NF-κB y la caja E son claves en la regulación del gen [140]. Hay algunas pequeñas diferencias entre el gen de COX-2 humano y el de ratón. El gen murino de COX-2 solo tiene un sitio NF-κB en lugar de dos y dos sitios C/EBP [68]. Por otra parte, la región 3'-UTR del gen de COX-2 contiene 23 copias del elemento desestabilizador ATTTA que confieren control post-transcripcional actuando como determinante de la inestabilidad del ARNm. Una vez transcrito, la presencia de elementos enriquecidos en secuencias AU en la región 3'-UTR del ARNm (AREs) es reconocida por proteínas que pueden estabilizar o desestabilizar el tránscrito [34]. Hasta ahora se han descrito 16 proteínas que regulan la estabilidad del ARNm de COX-2 [161]. Además, las secuencias AREs pueden

interactuar con microARNs regulando el silenciamiento transcripcional de COX-2. Estás características génicas hacen que la expresión de COX-2 sea regulada por un amplio espectro de mediadores implicados en inflamación, cáncer y otras patologías [54].

1.4 Regulación de la expresión de COX-2

COX-1 y COX-2 comparten gran homología estructural y actividad catalítica, sin embargo, su patrón de expresión y sus funciones biológicas son muy diferentes. COX-1 está presente prácticamente en todas las células del organismo, aunque sus niveles varían según el tipo celular. Esta isoforma promueve la producción de PGs cito-protectoras jugando un papel fundamental en la homeostasis de diversos procesos fisiológicos como la agregación plaquetaria, el mantenimiento de la mucosa gástrica y la regulación de la función renal. En cambio, COX-2 sólo se expresa de manera constitutiva en cerebro, riñón y placenta, mientras que su expresión es inducida en otros tejidos en diversos procesos fisiológicos (secreción de renina, función reproductiva, metabolismo óseo, protección vascular, secreción pancreática, neurotransmisión e inmunidad), así como en determinados situaciones fisiopatológicas (inflamación, dolor, fiebre, isquemia, Alzheimer y cáncer). La expresión del gen de COX-2 se restringe a ciertos tipos celulares o tejidos en respuesta a determinados inductores (Tabla 2) [68].

Factores de crecimiento	**EGF, PDGF, FGF, IGF, TGF-α, TGF-β, VEGF.**
Mediadores pro-inflamatorios	**IL-1α, IL-1β, IL-6, IL-8, IL-11, TNF-α, IFN-α, LPS.**
Hormonas	**FSH, LH, GnRH, EPI, NOREPI, PTH, insulin.**
Oncogenes	**v-Src, v-Ras.**
Promotores tumorales	**PMA, dioxinas, benzo-α-pirenos.**
Otros inductores	**Hipoxia, estrés mecánico, bradiquinina, 25-hidroxicolesterol, ácidos biliares, radiación UV-B, forscolina, altas concentraciones de sal y de glucosa, triglicéridos, suero.**

Tabla 2. Agentes inductores de la expresión de COX-2 [68].

Además, los productos de la vía metabólica de COX-2 ejercen una regulación positiva en la expresión del propio gen. PGE_2 incrementa la expresión de COX-2 a través de un aumento de los niveles de AMPc en varios tipos celulares [88].

Por el contrario, los glucocorticoides, las interleuquinas anti-inflamatorias (IL-4, IL-13, IL-10) y los ligandos de los receptores activados por proliferadores de peroxisomas (PPAR) inhiben la expresión de COX-2 [140]. A pesar de que el promotor de COX-2 presenta un sitio de reconocimiento al elemento de respuesta a PPAR (PPRE) que puede trans-activar el promotor, se ha relacionado a los ligandos de PPARα, ácido piriníxico, y de PPARγ, 15d-PGJ_2, con la supresión de la de expresión del gen COX-2 por interferir con la vía de señalización de NF-κB [127].

1.5 Modulación epigenética

Desde un punto de vista clásico, la epigenética es el patrón de marcas heredables que influencian la expresión de genes sin alterar la secuencia del ADN. En la actualidad se debe puntualizar que algunos fenómenos de tipo epigenético no son heredables [6]. La regulación epigenética tiene lugar en la cromatina aportando niveles adicionales de regulación entre el genotipo y el fenotipo. La cromatina es el conjunto de ADN, histonas y proteínas no histónicas que se encuentra en el núcleo de las células eucariotas y que constituye el cromosoma. La unidad básica de la cromatina es el nucleosoma. El nucleosoma contiene aproximadamente 165 pb de ADN enrollado que da 1,8 vueltas alrededor de un núcleo proteico compuesto por un octámero de histonas. Las histonas que forman el octámero son; H2A, H2B, H3 y H4, estando cada una por duplicado. De manera simplificada, la cromatina es una estructura dinámica con dos estados conformacionales inter-convertibles; inactivo y activo. En la conformación inactiva la cromatina presenta una estructura condensada, conocida como heterocromatina, que se mantiene en un estado transcripcional inactivo. En la conformación activa la cromatina posee una estructura laxa, denominada eucromatina, que está preparada para comenzar la transcripción. El estado conformacional de la cromatina puede ser alterado por la modulación epigenética de sus componentes. Los mecanismos epigenéticos mejor cararacterizados son: la metilación del ADN, modificaciones covalentes y no covalentes de histonas así como la expresión de ARNs no codificantes.

1.5.1 Metilación del ADN. De las 4 bases nitrogenadas que componen el ADN, solo la citosina (C) es modificada a un análogo llamado 5-metilcitosina (5mC) por la adición de un grupo metilo procedente de la S-adenosin-metionina (SAM). Las enzimas responsables de la metilación del ADN son las ADN metiltransferasas (DNMTs) que se dividen en dos grupos: 1) metiltransferasas *de novo* (DNMT3a y DNMT3b), que son responsables de metilar residuos de C que no han sido metilados con anterioridad, 2) la metiltransferasa de mantenimiento (DNMT1), que copia patrones de metilación preexistentes [101].

En los mamíferos, la metilación del ADN ocurre predominantemente en el nucleótido de C que precede al de guanosina (G), formando dinucleótidos CpG localizados en zonas determinadas denominadas islas CpG [48]. Las islas CpG se localizan frecuentemente en la región 5’ de los genes, en elementos de repetición dentro del promotor. La metilación del ADN promueve la conformación compacta de la cromatina impidiendo el ensamblaje de la maquinaria de transcripción y por tanto favoreciendo el silenciamiento génico. Pero la metilación no bloquea la expresión génica *per se,* sino que también requiere de la intervención de otros elementos como las proteínas de unión a la 5mC denominadas MBDs, junto con otras proteínas como las histonas deacetilasas (HDACs). Las MBDs ejercen su capacidad represiva sobre la expresión

génica imposibilitando la unión de factores de transcripción a los sitios de iniciación de la transcripción [66]. Por otro lado, las enzimas DNMTs también juegan un papel no enzimático en el silenciamiento transcripcional, por interaccionar con HDACs y con histonas metiltransferasas (HMTs) que favorecen el estado condensado de la cromatina [4]. Todo este mecanismo molecular en conjunto media el silenciamiento génico (Fig. 3A).

Debido al papel de la metilación en la expresión génica, la alteración en la metilación del ADN está relacionada con numerosas patologías. La pérdida en la metilación global del ADN (hipometilación) es característica de células cancerígenas y está relacionada con inestabilidad genómica, reactivación de transposones, pérdida de la impronta génica y activación de genes que normalmente se encuentran reprimidos. Las células cancerígenas, también pueden presentar ganancia en la metilación del ADN (hipermetilación) en islas CpG que resultan en el silenciamiento de genes, muchos de los cuales son genes supresores de tumores. Cada tipo de tumor posee un patrón distintivo de metilación conocido como "hipermetiloma"[123].

1.5.2 Modificación de histonas. La modificación de histonas es un mecanismo epigenético que modula el estado conformacional de la cromatina. Las histonas, particularmente las histonas H3 y H4, pueden ser modificadas por acetilación, metilación, fosforilación, ADP-ribosilación, ubiquitinación y sumoilación. La acetilación y la metilación de histonas son las modificaciones más importantes siendo la acetilación la mejor caracterizada.

La acetilación en las lisinas (Lys) de la región N-terminal de las histonas supone la neutralización de la carga positiva de la Lys que favorece el estado relajado y estable de la cromatina, permitiendo la interacción del ADN con complejos proteicos reguladores de la transcripción. Por lo tanto, la acetilación de histonas favorece la activación de la transcripción (Fig.3B). La acetilación y deacetilación de histonas es llevada a cabo por histonas acetiltransferasas (HATs) y HDACs respectivamente. Las HATs generalmente se asocian con la activación transcripcional y se agrupan en tres familias principales: Gcn5/PCAF, p300/CBP y MYST. Las HDACs se consideran elementos de represión transcripcional porque además de deacetilar impiden la unión de factores de transcripción al ADN [106]. Las HDACs se subdividen en tres clases: clase I (HDAC1-3, HDAC8, HDAC11), clase II (HDAC4-7, HDAC9-10) y clase III (SIRT1-7). La pérdida de expresión de HATs y el aumento de la expresión de HDACs se ha relacionado con transformación y progresión tumoral [65]. Para impedir la deacetilación de histonas y promover la expresión génica de supresores tumorales se han desarrollado una amplia gama de inhibidores de la actividad de HDACs (iHDAC) que han demostrado tener efectos antitumorales [115].

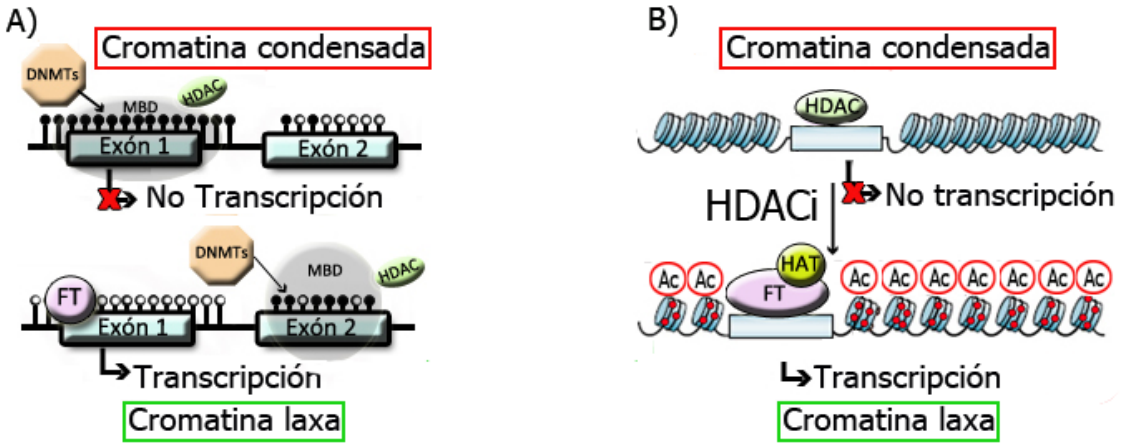

Figura 3. Regulación de la transcripción por modulación epigenética. *A) Regulación de la transcripción en función del estado de metilación en la isla CpG. Isla CpG metilada (círculos negros), isla CpG no metilada (círculos blancos), factores de transcripción (FT). B) Regulación de la transcripción por acetilación/deacetilación de histonas. Los puntos rojos corresponden a acetilaciones en las Lys de las colas de las histonas. Adaptado de Jones et al. y de Marks et al. [66, 91].*

1.6 Modulación epigenética de COX-2

Cambios en la metilación del ADN de COX-2 y modificaciones de histonas se han relacionado con la alteración de la expresión génica de COX-2 principalmente en procesos relacionados con la progresión tumoral. De hecho, la sobre-expresión de COX-2 por alteración de la actividad de las HDACs y por hipometilación del promotor de COX-2 está relacionada con leucemia mieloide aguda, cáncer colorrectal y cáncer gástrico. Sin embargo, en contraposición a estos estudios también se ha descrito que la expresión de COX-2 y de genes de su vía de señalización está disminuida por la hipermetilación del promotor o por la deacetilación de histonas en diferentes tipos de cáncer, como cáncer de mama, cervical, colorrectal, esofágico, hepático, nasofaríngeo, ovárico, pancreático, de próstata y en leucemia mieloide crónica [17].

1.7 Vías de señalización implicadas en la activación del gen de COX-2

El mecanismo de transducción de señales que media la activación de la expresión de COX-2 varía dependiendo del estímulo y del tipo celular. Las vías de señalización más importantes son la de NF-κB y la de las proteínas quinasas activadas por mitógenos (MAPK) (Fig. 4).

La vía de señalización de NF-κB se activa por los estímulos TNF-α/β, IL-1α/β y lipopolisacárido (LPS), al unirse a sus respectivos receptores TNF-R, IL-R y TLR4, así como por endotelina e hipoxia en determinados tipos celulares. Estos estímulos inducen la fosforilación de las proteínas IκB por el complejo IKK y su subsecuente ubiquitinización y degradación por el proteasoma. Esto permite la translocación de p65/p50 al núcleo donde participa en la activación de genes pro-inflamatorios, incluyendo el de COX-2 [143].

La familia de las MAPK está formada por tres grupos de quinasas (ERK, JNK/SAPK y p38 MAPK). Las vías de JNK/SAPK y p38 comparten activadores: citoquinas pro-inflamatorias, LPS y estrés

[89]. La vía de ERK se activa preferentemente por factores de crecimiento al unirse a los receptores tirosina quinasa (TKR), por oncogenes como el v-Src y el v-Ras así como por promotores tumorales como el acetato de forbol miristato (PMA). Una vez activadas, las MAPK pueden fosforilar y activar factores de transcripción que regulan la expresión de ciertos genes como el de COX-2 [27].

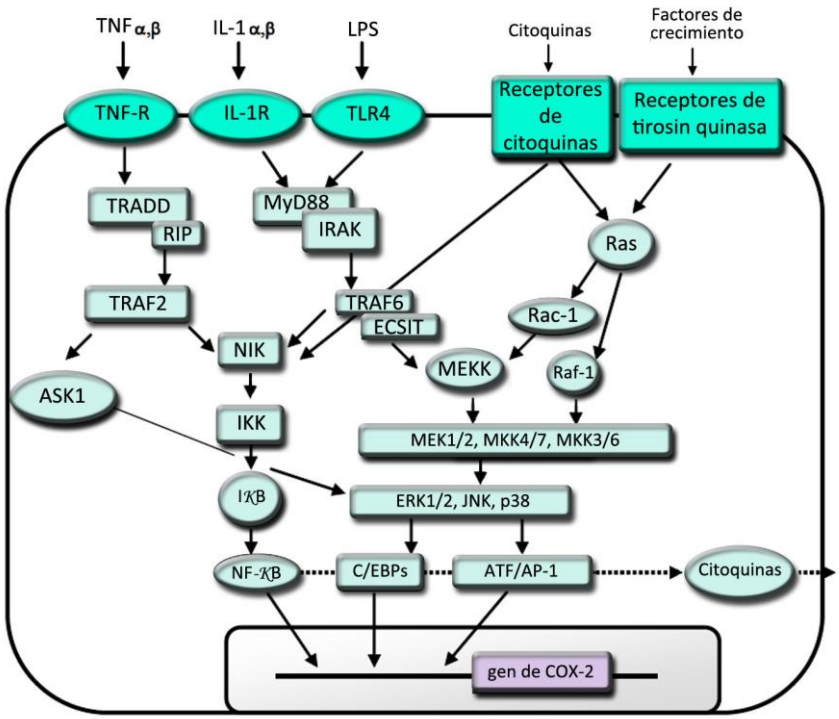

Figura 4. Vías de señalización implicadas en la inducción del gen de COX-2. *Adaptado de Tanabe et al. [140].*

1.8 Acción biológica de las prostaglandinas

La acción biológica de las PGs es mediada por receptores específicos de membrana y por receptores nucleares.

1.8.1 Receptores de PGs específicos de membrana. Los receptores de PGs específicos de membrana pertenecen a la familia de receptores con siete dominios transmembrana acoplados a proteínas G heterotriméricas. Los prostanoides PGE_2, PGD_2, PGF_2, PGI_2, TXA_2 interactúan con sus respectivos receptores EP (EP1, EP2, EP3, EP4), DP (DP1, DP2), FP (FPα, FPβ), IP y TP (TPα, TPβ). De todos los metabolitos finales producidos por acción de COX-2, la PGE_2 es el mayoritario. La PGE_2 es producida por la acción de la prostaglandina E sintasa (PGES). Hay diferentes subclases de PGES, la citosólica (cPGES) y las microsomales (mPGES-1 y mPGES-2). Los diversos efectos biológicos que se observan dependen de su interacción con los subtipos de receptores EP1-4 (Fig. 5). Los receptores se localizan principalmente en la membrana plasmática, pero también se ha descrito una localización nuclear de EP1, EP3 y EP4.

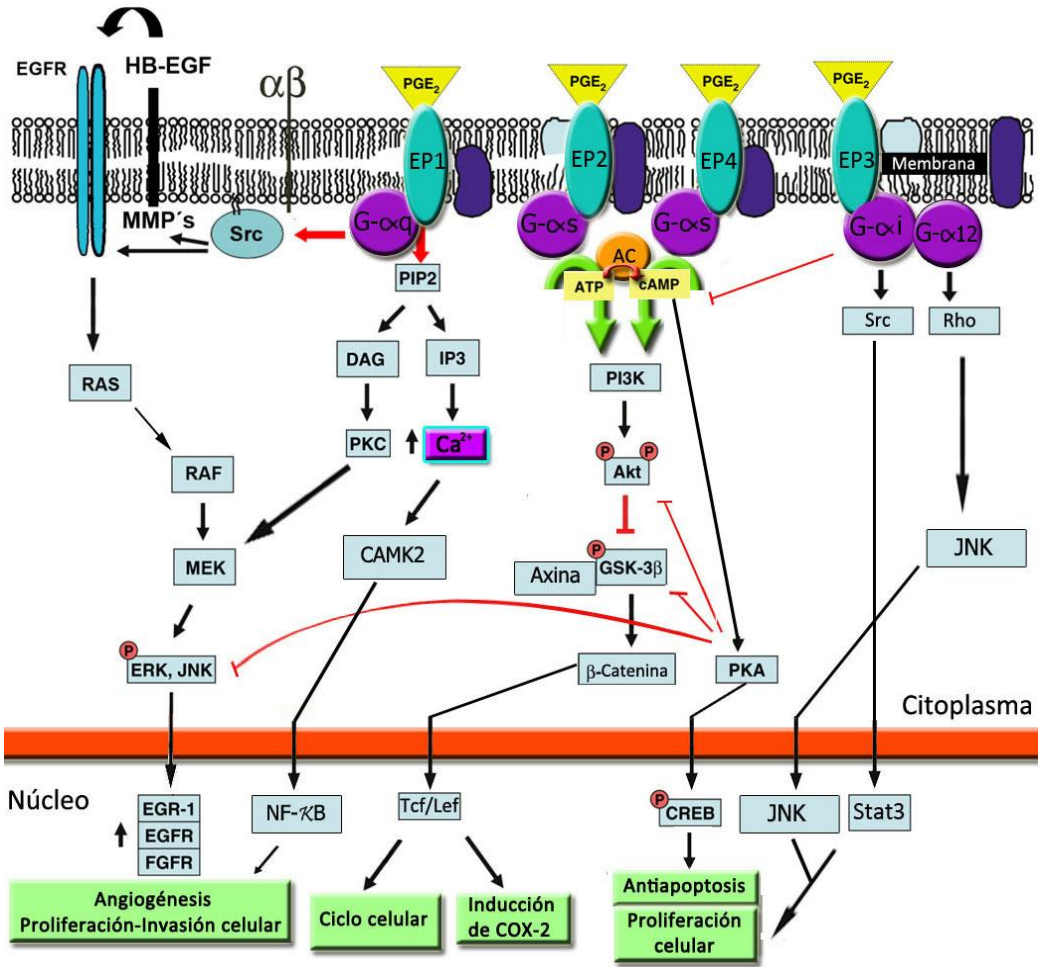

Figura 5. Vías de señalización mediadas por los receptores de PGE_2. *Adaptado de Dey et al. [33].*

El receptor EP1 se une a proteínas G-αq y su activación resulta en un incremento del Ca^{2+} intracelular que promueve la activación de la proteína quinasa C (PKC). Por mediación del receptor EP1 también se activa al proto-oncogén c-Src que induce la trans-activación del receptor del factor de crecimiento epidérmico (EGFR). Los receptores EP2 y EP4 están acoplados a proteínas G-αs y su activación promueve la producción de AMPc estimulando la señalización mediada por fosfoinositol 3-quinasa (PI3K) y la activación de la proteína quinasa A (PKA). Por último la estimulación del receptor EP3 puede conducir a la activación de la proteína Rho, al incremento de los niveles de Ca^{2+} y a la disminución de los de AMPc cuando se asocia a las proteínas G-α12, G-αq, o G-αi respectivamente [155]. La presencia de distintos subtipos de receptores EPs co-expresados en la misma célula y con niveles diferentes dependiendo del tipo celular contribuye a la complejidad de la señalización de PGE_2.

1.8.2 Receptores nucleares de prostanoides. Los derivados de PGD_2 (PGJ_2 y 15d-PGJ_2), de la PGE_2 (PGA_2) y PGI_2 tienen afinidad por los PPAR. Cuando PPAR se une a eicosanoides interfiriere con determinados factores de transcripción inhibiendo la transcripción de genes implicados en inflamación [127].

1.9 Modelos animales de disrupción y sobre-expresión génica de COX-2

Ensayos epidemiológicos, farmacológicos y clínicos llevados a cabo en modelos de disrupción y sobre-expresión génica de COX-2 demuestran la importancia de la señalización de las PGs en los procesos fisiológicos y patológicos, incluyendo el desarrollo de diferentes tipos de cáncer.

1.9.1 Modelos animales deficientes para COX-2. Los modelos animales deficientes para COX-2 presentan anomalías en la reproducción, malformación renal postnatal, fallo del cierre del *ductus arteriosus* y fibrosis miocárdica. En cuanto al sistema nervioso, los ratones deficientes en COX-2 muestran una reducción significativa del daño cerebral inducido por isquemia y por tóxicos. Concerniente al cáncer, se ha observado que reducen la formación de tumores de piel en un 75% y de pólipos intestinales en un 70-80% [94].

1.9.2 Modelos de animales transgénicos para COX-2. La expresión de COX-2 de manera ubicua en modelos murinos causa muerte postnatal debido a que presentan malformaciones esqueléticas [133]. Por esta razón se utilizan modelos de transgénesis de COX-2 en tejidos concretos usando promotores específicos de tejido. Estos modelos han permitido demostrar que la expresión de COX-2 en neuronas está relacionada con un incremento del daño neuronal en modelos de isquemia cerebral y con el desarrollo de deficiencias cognitivas, sugiriendo que COX-2 puede jugar un papel importante en la enfermedad del Alzheimer [35, 99]. Relativo al cáncer, no hay muchos estudios que indiquen una clara relación entre la expresión de COX-2 y la iniciación tumoral pero si con la progresión tumoral. COX-2 se ha relacionado con inducción de tumorigénesis en glándula mamaria, empleando el promotor del virus del tumor de mama de ratón, y en la célula gástrica, usando ratones transgénicos (TG) que expresan simultáneamente COX-2 y mPGES-1 bajo el promotor de citoqueratina 19 (Ck19) [28, 111]. Sin embargo, la mayoría de estudios en modelos TG para COX-2 indican que el TG *per se* no desarrolla tumores y se requiere el uso de agentes iniciadores y/o promotores tumorales. La expresión constitutiva de COX-2 en la lámina basal del epitelio, en ratones, mediante el promotor Ck5, causa un fenotipo pre-neoplásico con hiperplasia, displasia y quistes en varios órganos como piel, glándula mamaria, vejiga urinaria y páncreas, y además sensibiliza frente a carcinogénesis [21, 90, 151]. Otros grupos empleando el promotor Ck5 y Ck4 dirigieron la expresión de COX-2 directamente a las células de la epidermis basal y al folículo piloso de la piel de ratón. Los animales experimentaron alopecia por alteración en la morfogénesis del folículo piloso, no obstante, se necesitó el uso de agentes carcinógenos como DMBA o PMA para la formación de tumores de piel [107, 117]. Se ha descrito que los ratones TG que expresan COX-2 en el epitelio intestinal regulada por el promotor de la proteína de unión a ácidos grasos (FABPL) no desarrollan tumores espontáneos. Solamente cuando se trataron con azoximetano, un carcinógeno de colon, los ratones TG para COX-2 desarrollaron más tumores

que los controles [2]. Los modelos de transgénesis de COX-2 en el hepatocito no muestran ninguna alteración hepática de manera espontánea [16, 53, 162].

2. Hígado y carcinoma hepatocelular

2.1 Hígado

El hígado es el órgano principal en la homeostasis metabólica ya que es responsable del metabolismo, síntesis, almacenamiento y redistribución de nutrientes, carbohidratos, grasas y vitaminas. Además el hígado elimina los productos biológicos tóxicos y agentes xenobióticos por conversión metabólica y excreción biliar. El hepatocito que desempeña la mayoría de las funciones descritas en el hígado, constituye el 80% del total de células hepáticas.

La unidad funcional del hígado es el lóbulo hepático. Los lóbulos hepáticos son estructuras hexagonales formadas por hileras de hepatocitos de una o dos células de grosor en cuyo centro se encuentra la vena central, que desemboca en las venas hepáticas y estas a su vez en la vena cava inferior. Los vértices del hexágono lo componen seis triadas portales formadas por una rama de la arteria hepática, una rama de la vena porta y un conducto biliar que conduce la bilis hacia los conductos biliares mayores. El hígado tiene un doble aporte circulatorio, mediante la vena porta y la arteria hepática. Los hepatocitos tienen distintas funciones dependiendo de su localización peri-portal o peri-central en el lóbulo hepático (Fig. 6).

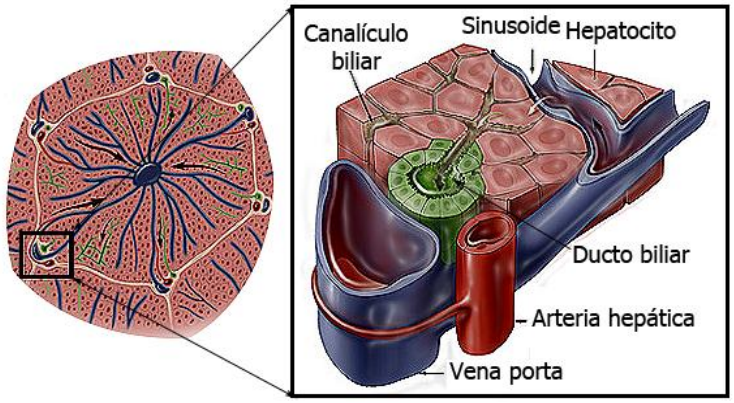

Figura 6. Estructura del lóbulo hepático. *Adaptado de Kanel et al. [67].*

El otro 20% de células hepáticas está integrado por células no parenquimáticas que incluyen a células de Kupffer, células endoteliales, células epiteliales biliares (colangiocitos), linfocitos y células hepáticas estrelladas o de Ito. Las células de Kupffer son macrófagos que junto con los linfocitos se encargan de fagocitar y destruir cualquier partícula extraña que llegue al hígado. Las células endoteliales constituyen la mayor parte de las células de la pared de los sinusoides. Los colangiocitos conforman el canal de Hering en el cual confluye la bilis. En cuanto a las

células hepáticas estrelladas tienen una función mecánica, además de metabolizar lípidos, almacenar vitamina A y sintetizar varios componentes del sistema conjuntivo (colágeno I, III y IV)[67].

2.2 Etiología y desarrollo del carcinoma hepatocelular

El carcinoma hepatocelular (CHC) es el sexto cáncer más frecuente y es la tercera causa de mortalidad relacionada con cáncer. El 90% de los cánceres de hígado son CHCs, el otro 10% son angiosarcomas, colangiocarcinomas y hepatoblastomas. La frecuencia del CHC es mayor en el este de Asia y en África subsahariana y la más baja es en Norte América, en el Norte de Europa y en Australia. Además es la principal causa de mortalidad en los pacientes con cirrosis hepática [41]. La etiología del CHC está asociada con afecciones crónicas como el virus de la hepatitis B (VHB) y C (VHC), alcoholismo, exposición a aflatoxina-B1, cirrosis, hemocromatosis, porfiria cutánea tarda, deficiencia en α-1 antitripsina, tirosinemia y enfermedad de hígado graso no alcohólica (EHGNA). El CHC afecta en mayor proporción a hombres que a mujeres aunque, después de la menopausia en las mujeres, no se encuentran diferencias entre sexos [130]. El CHC se clasifica según el criterio de la OMS equivalente al criterio de Edmonson y Steiner en bien diferenciado, moderadamente diferenciado, poco diferenciado o indiferenciado, donde el grado de malignidad está inversamente correlacionado con el grado de diferenciación [36] (Fig. 7).

Una lesión celular aguda en el hígado se manifiesta con la muerte de los hepatocitos. Posteriormente, se produce una respuesta regenerativa de los hepatocitos aumentando su capacidad proliferativa hasta que se restablece la arquitectura hepática normal. Ante lesiones hepáticas crónicas se generan repetidos ciclos de inflamación, muerte y regeneración de los hepatocitos que pueden derivar en la formación de nódulos hiperplásicos rodeados de una cápsula fibrosa. Este fenómeno neoplásico benigno se conoce como adenoma hepatocelular. Los procesos de daño hepático crónico también pueden culminar en una cirrosis hepática. La cirrosis está caracterizada por fibrosis y por la formación de nódulos de hepatocitos regenerantes estructuralmente anormales. La fibrosis es consecuencia de la cicatrización continua para la reparación de las lesiones del tejido hepático que provoca la alteración de la estructura de los nódulos y de la estructura global hepática. En el entorno hepático durante las lesiones crónicas se activan y aumenta el número de fibroblastos, células hepáticas estrelladas, células de Kupffer, macrófagos infiltrados asociados a tumores, células dendríticas, células inflamatorias y células endoteliales. Estos tipos celulares activados liberan citoquinas, factores de crecimiento, enzimas lisosomales, leucotrienos, el factor de activación plaquetario (PAF), etc. Estos factores crean una red de señalización paracrina entre todos los

componentes celulares del entorno hepático alterado y un estrés oxidativo que promueve la aparición de mutaciones. Además, durante procesos proliferativos como en la regeneración hepática, se acortan los telómeros de los hepatocitos induciendo inestabilidad genómica. Esta inestabilidad puede derivar en la adquisición de mutaciones, pérdidas de heterocigosidad, oscilaciones alélicas en oncogenes, en genes supresores de tumores, en genes responsables del mantenimiento de la integridad del genoma, de la proliferación y del ciclo celular. Las mutaciones en los hepatocitos de los nódulos hiperplásicos cirróticos pueden dar lugar a la formación de nódulos displásicos pre-malignos con hepatocitos fenotípicamente anormales que con el tiempo y el acúmulo de mutaciones derivan en un CHC. El CHC es una neoplasia maligna, los hepatocitos anormales se multiplican sin control, pueden migrar e invadir los tejidos cercanos y diseminarse a otros órganos del cuerpo a través del torrente sanguíneo y del sistema linfático (Fig.7) [41].

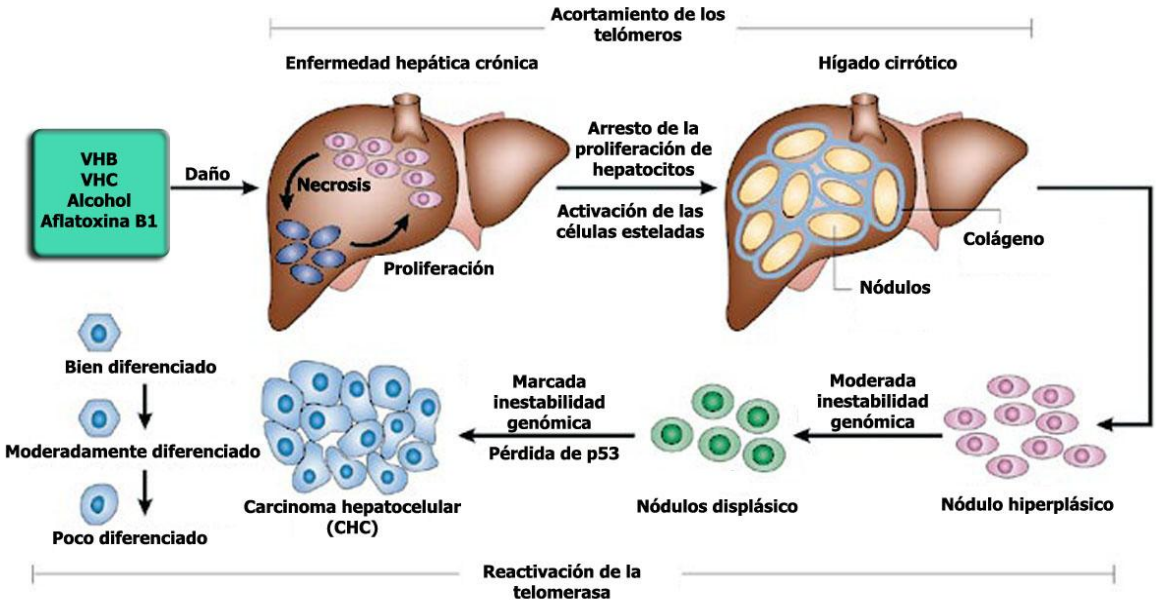

Figura 7. Progresión histopatológica y cambios moleculares en el CHC. *Adaptado de Farazi et al. [41].*

2. 3 Modelos animales de carcinoma hepatocelular

Existen modelos quirúrgicos, químicos, nutricionales y genéticos que derivan en CHC y que se utilizan para estudiar los mecanismos moleculares implicados en esta patología hepática (Tabla 3) [80].

Modelos quirúrgicos	**Ligación portal**
Modelos químicos	**CCl_4, TAM, APAP, GalN, DEN, DMN, 2-AAF, 4-DAB, ciprofibrato y etanol.**
Modelos nutricionales	**Dieta DCM**
Modelos genéticos	**Modelos TG para: proteínas del VHB (HBsAg y HBx), proteínas del VHC (proteínas de la envuelta E1-E2, proteína core, poliproteína viral FL-N, proteína estructural S-N), antígeno T del SV40, E2F1, TGF-α, c-Myc, E2F1/c-Myc, TGF-α/ c-Myc, FGF19, IGF-2, EGF/c-Myc, HGF, HGF/c-Myc, HGF/TGF-α, uPA, PDGF-C, AAT, LTab.**
	Modelos deficientes en: p53, p53/INK4a/ARF, TERT, TERT/p53, PTEN, AOX, Mdr2P, MAT1A, IKK, NEMO/IKKγ.

Tabla 3. Modelos animales de CHC.

3. Expresión de COX-2 en cáncer

En el cáncer de colon, el papel de las PGs derivadas de COX-2 en el desarrollo neoplásico está bien establecido. Estudios epidemiológicos muestran que los pacientes a los que se les administran AINEs de forma regular presentan menor incidencia de cáncer colorrectal y disminuyen el número de pólipos en poliposis adenomatosa familiar. Estos resultados fueron confirmados en estudios usando modelos murinos de poliposis adenomatosa delecionando el gen de COX-2 y usando AINEs selectivos para COX-2. Se ha demostrado que COX-2 se sobre-expresa en una amplia gama de tumores epiteliales pre-malignos y malignos, incluyendo los de piel, mama, esófago, estómago, colon, recto, páncreas, vejiga y cáncer de piel de tipo no melanoma. También hay evidencias de que la expresión de COX-2 está inducida en tumores de origen no epitelial como en los melanomas y se ha comprobado su expresión en macrófagos y células no tumorales cercanas al área del tumor. Además, existen determinados polimorfismos de COX-2 asociados al desarrollo de cáncer. De hecho, la administración de AINEs selectivos y no selectivos de COX-2 reducen la incidencia de cáncer de mama, próstata, pulmón, cuello uterino, gástrico, esofágico y colorrectal [94, 100].

COX-2 está implicada en cáncer porque regula el metabolismo de carcinógenos, contribuye a la inhibición de la apoptosis a través Bcl-2, interviene en la vía de señalización de la proteína quinasa B (PKB)/Akt, favorece el proceso angiogénico mediante la producción del factor de crecimiento endotelial vascular (VEGF), actúa directamente en invasión y metástasis y participa en la supresión de la respuesta inmune [49, 94].

4. COX-2 e hígado

4.1 COX-2 en hígado

COX-2 no se expresa en el hepatocito adulto y tampoco se induce por estimulación con factores pro-inflamatorios. Sin embargo, COX-2 si se expresa en las células no parenquimáticas, en el hepatocito fetal que tiene un fenotipo menos diferenciado que el hepatocito adulto y en algunas líneas celulares hepáticas [92]. Se ha demostrado que la

expresión diferencial del factor de transcripción C/EBPα en el hepatocito adulto y fetal juega un papel fundamental en la inducción de COX-2. C/EBPα se encuentra altamente expresado en el hepatocito adulto interfiriendo en la expresión de COX-2 [13]. COX-2 sólo se expresa en el hepatocito adulto en aquellas situaciones que implican procesos de des-diferenciación y proliferación como en respuesta a una hepatectomía parcial, a daño hepático agudo y en enfermedades hepáticas crónicas [93, 94].

4.1.1 COX-2 en regeneración hepática. COX-2 se induce en modelos experimentales de regeneración hepática después de una hepatectomía parcial, favoreciendo el proceso de proliferación y recuperación de la masa hepática [15, 97]. En regeneración después del daño hepático agudo con tioacetamida (TAM), se ha demostrado una importante disminución en los niveles de C/EBPα y C/EBPβ coincidiendo con la inducción de COX-2 [42]. Los animales tratados con COXIBs muestran un retraso en la iniciación de la regeneración hepática [15]. De hecho, la disrupción simultánea de COX-2 junto con otros genes relevantes para la regeneración hepática como la óxido nítrico sintasa-2 (iNOS) resultan en la inhibición del proceso de regeneración [42, 58, 165].

4.1.2 COX-2 en enfermedad hepática aguda. En modelos de daño hepático agudo usando el estímulo Jo2 (ligando Fas), LPS/D-galactosamina y Concanavalina-A, los animales TG que sobre-expresan COX-2 específicamente en el hepatocito muestran protección frente al daño hepático. Por otro lado, los COXIBs revierten la protección [16, 79, 97]. Las PGs ejercen un efecto protector frente al daño hepático agudo por tener efecto anti-apoptótico/anti-necrótico sobre los hepatocitos y además estimulan su proliferación temprana [43, 97].

4.1.3 COX-2 en enfermedad hepática crónica. COX-2 se expresa en el hígado como consecuencia de procesos de inflamación crónicos como el causado por la infección del VHB o el VHC. La proteína X del VHB (HBx) y otras proteínas del VHB, así como la proteína no estructural 5A (NS5A) y la proteína del núcleo del VHC activan el promotor de COX-2 [62, 110]. Determinados estudios han mostrado discrepancias en cuanto a la correlación entre el grado de expresión de COX-2 y el grado de infección, pero estudios recientes corroboran la correlación tanto en la infección por el VHB como por el VHC [83, 103].

La hepatopatía alcohólica y la EHGNA son enfermedades crónicas que presentan esteatosis hepática. En la esteatosis, las células de Kupffer cumplen un papel predominante en la inducción de COX-2 [118]. La expresión de COX-2 se asocia con la intensidad de la lesión necro-inflamatoria, con el aumento de endotoxinas, del TXA_2 y con la peroxidación lipídica. Se ha descrito que la liberación de PGE_2 después de un abuso crónico de alcohol contribuye a la aparición de esteatosis y que el uso de COXIBs atenúa el grado de esteatosis [29]. Sin embargo,

existen resultados preliminares que indican que la expresión constitutiva de COX-2 en el hepatocito ejerce un efecto protector frente a la esteatosis y a la resistencia a la insulina [44]. COX-2 se induce en el hepatocito en otras enfermedades crónicas como la cirrosis hepática. En modelos animales experimentales de cirrosis la expresión de COX-2 favorece la proliferación y recuperación de la masa hepática [42]. Durante el daño hepático crónico aumenta la proliferación y se activan las células hepáticas estrelladas que son las responsables del engrosamiento de la matriz extracelular y de la acumulación de colágeno promoviendo la fibrosis hepática. Las células hepáticas estrelladas expresan COX-2 sugiriendo que esta vía podría estar jugando un papel crucial en el proceso fibrogénico. Sin embargo, existen datos dispares que implican a COX-2 tanto en la exacerbación como en la disminución de la fibrosis e incluso datos que demuestran que COX-2 es irrelevante en este proceso [37, 61]. Modelos experimentales de fibrosis, como el tratamiento con una dieta deficiente en colina y metionina (DCM) o con tetracloruro de carbono (CCl_4) en animales TG que expresan COX-2 ectópicamente en el hepatocito revelaron que la presencia de COX-2 en el hepatocito, no es transcendental en el desarrollo fibrogénico [163]. La inducción de COX-2 se ha descrito en la hipertensión portal que es una complicación de la cirrosis hepática. Además, el uso de AINEs selectivos para COX-2 reduce la hipertensión portal en modelos experimentales de fibrosis con CCl_4 [144]. Asimismo, la expresión de COX-2 también se ha descrito en enfermedades crónicas como el colangiocarcinoma y en el CHC, así como en las líneas celulares de hepatoma [128].

4.2 COX-2 en el carcinoma hepatocelular

No hay una relación clara de la contribución de COX-2 con el CHC. Tan solo los modelos que estudian la implicación de COX-2 en CHC *in vitro* describen de forma más uniforme el papel de esta enzima en determinados procesos relacionados con CHC en líneas de hepatoma. Sin embargo, tanto los estudios de la modulación epigenética de COX-2 en CHC como los análisis *in vivo* en modelos experimentales de CHC indican que la contribución de COX-2 a la iniciación y al desarrollo del CHC es controvertida.

4.2.1 Modulación epigenética del gen de COX-2 en el CHC. En el CHC la influencia de alteraciones en la modulación epigenética de oncogenes o genes supresores de tumores es importante. En el CHC el ADN se encuentra globalmente hipometilado y como consecuencia presenta mayor inestabilidad genómica, lo que promueve la aparición de mutaciones en oncogenes. A pesar de ello, en el CHC también se ha descrito que la hipermetilación de ciertas islas CpG resultan en el silenciamiento de genes supresores de tumores. De hecho, es frecuente la sobre-expresión de DNMTs (DNMT1 y DNMT3b) en el tejido tumoral comparado

con el no tumoral. La hipoacetilación de histonas, que es otro fenómeno epigenético asociado al silenciamiento génico, se relaciona con desarrollo y progresión del CHC [126].

La regulación epigenética del gen de COX-2 es clave en el CHC. Se ha descrito que el gen de COX-2 está hipometilado en pacientes con cirrosis hepática y hepatitis crónica poco propensos a desarrollar CHC. Por el contrario, también se ha descrito que un aumento en la metilación en el gen de COX-2 entre otros genes (APC, GSTP1, RASSF1A, p16, E-cadherina) está relacionado con el desarrollo del CHC [76]. Se sabe que el promotor de COX-2 contiene numerosas islas CpG que cuando se hipermetilan impiden la transcripción del gen en estadios avanzados de CHC [109]. Recientemente, se ha descrito que en la infección por el VHB y como consecuencia de la expresión de la proteína HBx, se induce COX-2, debido a eventos de desmetilación mediados por la disminución en la proteína DNMT3B [164]. Otras alteraciones epigenéticas que influencian la expresión del gen de COX-2 como la modificación de histonas, podrían ser claves en el CHC. En un modelo de formación de tumores con células de CHC tratados con COXIBs se detectaron cambios en la acetilación de histonas y de la HDAC2 [23].

4.2.2 Mecanismos moleculares de contribución de COX-2 al CHC en modelos *in vitro*. Los mecanismos moleculares de contribución de COX-2 al CHC han sido caracterizados principalmente en estudios con líneas de hepatoma. Se ha demostrado *in vitro* que algunas líneas celulares derivadas de CHC expresan constitutivamente COX-2 [60] y se ha descrito que COX-2 participa en los siguientes procesos y vías de señalización en CHC:

- Alteración de vías de señalización: COX-2 participa en la alteración de las vías de IGF/IGF-1R, HGF/c-MET, TGF-α/EGFR y de Wnt/β-catenina. Hay estudios que indican que existe una correlación directa entre la expresión de COX-2 y la activación de la vía de señalización IGF/IGF-1R. Por otro lado, el uso de COXIBs reduce los efectos pro-tumorigénicos en las células HepG2 mediados por la vía de HGF/c-MET. Además, se ha descrito que la activación del receptor EP-1 trans-activa al receptor c-MET mediante convergencia con la vía del EGFR, siendo un proceso crítico en la invasión celular. También se ha descrito que la PGE_2 activa al EGFR que a su vez incrementa los niveles de PGs por lo que es un proceso de retroalimentación positiva, mientras que la inhibición de COX-2 reduce su fosforilación. La convergencia entre las vías de COX-2 y de EGFR señala el posible potencial terapéutico de la combinación de fármacos dirigidos contra ambas dianas. Además, otros estudios en células de CHC relacionan la expresión de COX-2 con alteración de la vía de Wnt/β-catenina por aumentar la expresión de β-catenina y disminuir la propia expresión de COX-2 a través del incremento de la expresión de APC [20].
- Conversión de pro-carcinógenos a carcinógenos: Una gran cantidad de xenobióticos pro-carcinógenos pueden ser bioactivados metabólicamente a carcinógenos por la actividad

HOX de COX-2, aunque en el hígado las reacciones de oxidación son principalmente catalizadas por la citocromo P-450 [153].

- Apoptosis: La expresión de factores anti-apoptóticos y pro-apoptóticos están alterados en el CHC. En numerosas investigaciones *in vitro* se ha descrito que el uso COXIBs reducen la viabilidad de diferentes líneas celulares de CHC. Los COXIBs inducen la vía intrínseca de la apoptosis mediante la activación de las caspasas -3, -9 y -8, a través de una disminución de los niveles de Mcl-1 (anti-apoptótico) favoreciendo la translocación de Bax (pro-apoptótico) a la membrana mitocondrial y alterando su potencial [114]. Los COXIBs también activan la vía extrínseca de la apoptosis promoviendo la expresión de los ligandos de los receptores de muerte [96]. Los estudios de sobre-expresión de COX-2 en células de CHC mediante transfección corroboran este hecho, mostrando una prevención de la apoptosis por una disminución de la actividad de las caspasas -3, -9 y -8 y de la liberación tanto de citocromo c como de poli-ADP-ribosa polimerasa 1 (PARP-1) [43]. La inhibición de la apoptosis mediada por los COXIBs se puede antagonizar con la adición de PGE_2 [78].
- Proliferación celular: Los estudios de expresión constitutiva de COX-2 en líneas celulares hepáticas demuestran que la PGE_2 promueve el crecimiento de las células de CHC mediante la fosforilación de Akt y la disminución de los niveles de p53. Además, se ha demostrado que aumenta el porcentaje de células en fase S [43]. De hecho, los COXIBs disminuyen la fosforilación de Akt, reducen la fase de síntesis de ADN y están implicados con la parada del ciclo celular en las células de CHC [114].
- Angiogénesis: Los productos de COX-2 pueden inducir la angiogénesis [3]. Hay estudios que revelan una correlación positiva entre la expresión de COX-2 y de VEGF. Además, la inhibición de la vía de señalización de COX-2 disminuye la angiogénesis mediante la disminución de factores pro-angiogénicos [167].
- Invasión tumoral: Altos niveles de COX-2 se asocian con invasión tumoral. Se ha descrito que la PGE_2 estimula la migración y adhesión en células de CHC por la inducción de metaloproteasas-2 y -9 (MMP-2 y MMP-9) e integrina β1, mediante la modulación de las vías de MEK/ERK, p38/MAPK, PKA y PKC. Mientras que el uso de COXIBs disminuye la migración a través de la atenuación de la señalización de la vía de MAPK/ERK [96].
- Respuesta inmune: La expresión de COX-2 se ha vinculado con la supresión de la respuesta inmune en el CHC. COX-2 disminuye el número y la proliferación de linfocitos T citotóxicos (CD8+), ejerce efectos supresores en la activación de macrófagos e inhibe la respuesta de los linfocitos cooperadores Th2 inhibiendo la proliferación de células B [137, 149]. Se ha demostrado que la PGE_2 promueve la progresión tumoral mediante la inducción de las células supresoras derivadas de progenitores mieloides (CSDM) [146].

- Inflamación: A pesar de que COX-2 suprime la respuesta inmune, también está relacionada con la inflamación en el CHC [104]. Esto es debido a que muchos metabolitos de la vía de COX-2 favorecen la producción de especies reactivas de oxígeno (ROS), son altamente peroxidativos e interaccionan con los componentes del ambiente tumoral favoreciendo la inflamación. Además en el CHC hay una correlación positiva entre COX-2 e iNOS, de hecho, la inhibición de COX-2 con AINEs reduce los niveles de óxido nitrico [40].
- Resistencia a fármacos terapéuticos: COX-2 está relacionado con la sobre-expresión de numerosos factores implicados en la resistencia a múltiples fármacos como MDR1, MRP1, MRP2, MARP3 y cMOAT [136].

4.2.3 COX-2 en el CHC en modelos *in vivo*. A pesar de todos estos datos, los estudios *in vivo* demuestran que el papel de COX-2 en la carcinogénesis hepática es controvertido y hay varias cuestiones sin resolver referentes al patrón de expresión de COX-2 en el CHC: 1) la frecuencia de expresión de COX-2 en el CHC es muy variable (15-85%), 2) se ha descrito que COX-2 se expresa en estadios tempranos pero no en estadios avanzados de CHC, 3) hay evidencias de que en el CHC bien diferenciado caracterizado por tener mejor pronóstico la expresión de COX-2 es elevada, mientras que en el CHC poco diferenciado con un peor pronóstico la expresión de COX-2 está disminuida [128], 4) la expresión de COX-2 en el tejido no tumoral es mayor que en el tejido tumoral y un aumento de la expresión de COX-2 en el tejido no tumoral se asocia con la presencia de cirrosis, mal pronóstico y recurrencia de la enfermedad en pacientes con CHC [56], 5) se ha descrito una mayor expresión de COX-2 en la EHGNA y en cirrosis que en el CHC [46] 6) en los estudios de análisis de la expresión global de genes para identificar la firma genética de CHC no aparece COX-2 [75]. Este patrón de expresión de COX-2 en CHC es inusual comparando con otros cánceres y hasta la fecha, no existe una explicación satisfactoria. La expresión de COX-2 es gradual desde la hepatitis crónica hasta las lesiones pre-malignas sugiriendo que la expresión de COX-2 puede ser determinante en las primeras fases de la hepatocarcinogénesis [72]. La causa de que el CHC desdiferenciado tenga una expresión disminuida de COX-2 no está bien definida, aunque puede deberse al hecho de la pérdida del fenotipo de los hepatocitos en estadios de CHC avanzado.

A pesar de que la expresión de COX-2 se haya asociado con modelos experimentales *in vitro* de CHC, los modelos animales que sobre-expresan COX-2 de forma constitutiva en el hepatocito no desarrollan espontáneamente CHC [16, 53, 162]. Tan solo un modelo de transgénesis de COX-2 en el hepatocito ha descrito que la expresión de COX-2 favorece el desarrollo de hepatitis [162]. Estos antecedentes indican la necesidad de esclarecer el papel de las PGs derivadas de COX-2 en el desarrollo del CHC.

Objetivos

1. **Estudio del papel de COX-2 en el modelo de fibrosis inducido con una dieta deficiente en colina y metionina.**
2. **Contribución de las PGs derivadas de COX-2 al desarrollo de CHC:**
   - **2.1** Modelo de hepatocarcinogénesis química inducida con DEN en los ratones TG para COX-2 y en células hepatocitarias transfectadas establemente con un vector de expresión de COX-2.
   - **2.2** Modelo de hepatocarcinogenesis genética mediante el desarrollo de un triple ratón TG c-Myc/TGF-α/COX-2.
3. **Estudio de la modulación epigenética del gen de COX-2 en el CHC:**
   - **3.1** Líneas de hepatoma humano.
   - **3.2** Biopsias humanas de CHC.

Resultados

Modelo de animal transgénico para COX-2 en el hepatocito

Con el objetivo de analizar el efecto de las PGs derivadas de COX-2 en el hígado se desarrolló el primer modelo descrito de animal TG para COX-2 en el hepatocito [16]. Los ratones TG que se generaron contienen un gen de fusión LIVhCOX-2 que consiste en un ADNc de COX-2 humana (hCOX-2) cuya expresión en hígado está regulada por el promotor de la apolipoproteína E (ApoE). Para construir el gen de fusión LIVhCOX-2 se clonó el fragmento de ADNc que codifica para el marco de lectura abierto (ORF) de la hCOX-2 en los sitios KpnI-XhoI del vector pLiv-Le6 que contiene el promotor del gen de la ApoE humana y una región de control de expresión hepática. A continuación, el fragmento NotI-SpeI de 6,84 Kb del plásmido TG LIVhCOX-2 se aisló y se inyectó en el pronúcleo masculino de un embrión de una sola célula de ratón de la cepa C57BL/6xDBA2. Las células embrionarias portadoras del transgén se implantaron en los oviductos de ratonas CD1 pseudopreñadas. Después del parto, los ratones TG se identificaron mediante genotipado por PCR y Southern blot con el fin de determinar el número de copias integradas. Se obtuvieron seis líneas de ratón con expresión del transgén LIVhCOX-2 de forma constitutiva en el hepatocito. La línea 4 heterocigota con 55 copias del transgén LIVhCOX-2 se utilizó para el análisis de la expresión del ARNm de hCOX-2 mediante PCR de transcripción inversa en 5 tejidos. Confirmando lo esperado, la expresión del ARNm de hCOX-2 al ser dirigida por el promotor de ApoE siguió el patrón de expresión del promotor detectándose en riñón e hígado. A pesar de que en el riñón haya expresión de ARNm de hCOX-2, la expresión de proteína en este mismo órgano no fue detectable por Western blot. Sin embargo, la expresión de proteína hCOX-2 en hígado fue muy elevada. Se comprobó la funcionalidad de COX-2 en hígado midiendo los niveles de PGE_2 que resultaron ser 5 veces superiores en el animal TG (230 pg/mg de proteína) comparando con el animal WT (40 pg/mg de proteína). Además, mediante el tratamiento de los animales TG con inhibidores selectivos de COX-2 se redujo la expresión de PGE_2 a niveles equiparables a los del animal WT lo que indica que la PGE_2 producida en el modelo TG es debida a la acción de COX-2. En este modelo, los animales TG de 12 semanas de edad presentaron un fenotipo normal [16]. Con el fin de comprobar que los datos anteriormente mencionados eran debidos a la sobre-expresión de COX-2 y no a la alteración del genoma del ratón por la inserción aleatoria del transgén, se realizaron los mismos experimentos en otra línea TG, en la que se obtuvieron los mismos resultados.

Hasta ahora, para estudiar la función de COX-2 en el hígado se han creado tres modelos de animales TG que expresan COX-2 constitutivamente en el hepatocito. Para ello además de utilizar el promotor de ApoE [16] se han utilizado otros promotores también específicos de

hígado como el promotor de la transtirretina [162] y el de la albumina [53]. Estos tres modelos, presentan diferentes niveles intrahepáticos de PGE_2 donde el modelo con el promotor de la transtiterrina expresa los niveles más elevados de PGE_2 (550 pg/mg) mientras que el modelo que emplea el promotor de la albúmina expresa los menores niveles de PGE_2 (58 pg/mg). Estos tres modelos han mostrado diferencias en la respuesta a determinados tratamientos para inducir daño hepático agudo. No obstante, ninguno de los tres modelos desarrolla CHC espontáneamente.

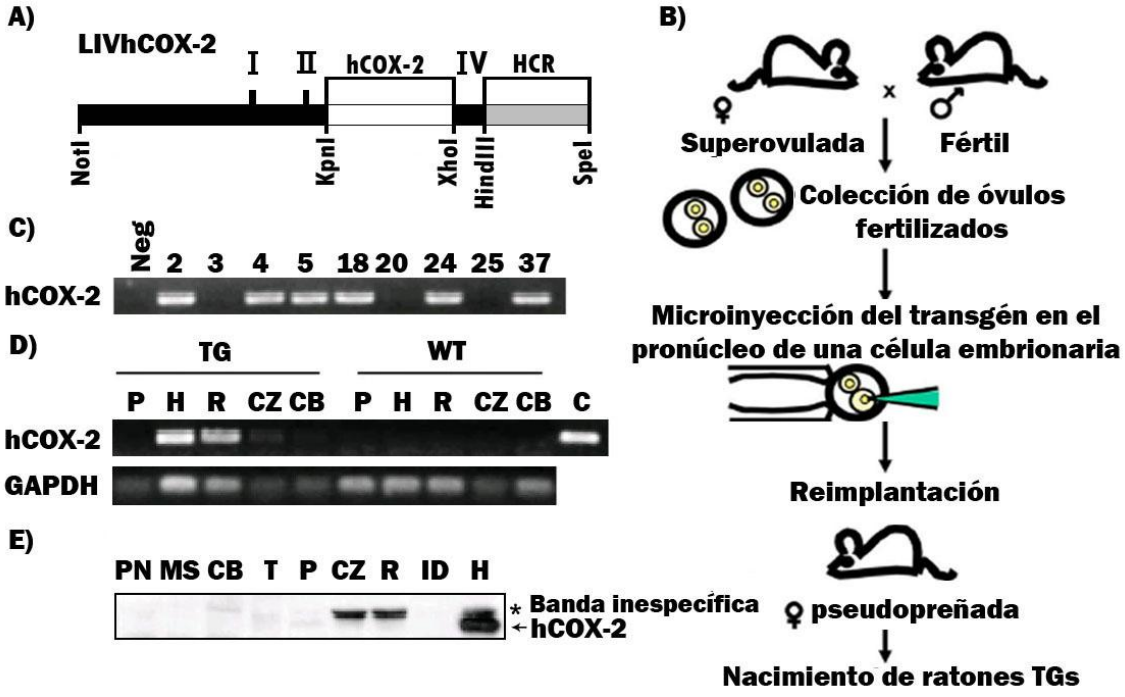

Modelo de ratón transgénico para COX-2 en el hepatocito. *A)Representación del transgén LIVhCOX-2 que consta de una región flanqueante 5' con un tamaño de 3Kb, el primer exón (I), parte del segundo exón (II) y la secuencia de poliadenilación localizada en el cuarto exón del gen humano de la ApoE así como el ADNc de hCOX-2 y la secuencia de control de expresión hepática (HCR) de la ApoE. B) Diagrama esquemático de la construcción ratones TG. C) Detección de la integración del transgén por PCR del ADN de la cola de los ratones usando oligos específicos para hCOX-2. Neg. PCR sin ADN. D) PCR de transcripción inversa para la detección del ARNm de hCOX-2 de ratón TG y (W). Como control interno se utilizó GAPDH. E) Western blot para la detección de la expresión de hCOX-2 en animales TG. Pulmón (P), hígado (H), riñón (R), corazón (CZ), cerebro (CB), páncreas (PN), músculo esquelético (MS), cerebro (CB), testículo (T), intestino delgado (ID). Adaptado de Casado et al. y de Martín Sanz et al. [16, 94].*

Generación de una línea celular con expresión estable de COX-2

Para estudiar *in vitro* el efecto de las PGs derivadas de COX-2, se transfectó establemente a la línea hepatocitaria no tumoral de origen humano CCL-13 [Chang Liver (CHL)] con el vector pPyCAGIP/GFP para la generación de la línea CHL-V con expresión estable de GFP o con el vector pPyCAGIP/hCOX-2/GFP para la generación de la línea CHL-C con expresión estable de hCOX-2/GFP. Para la construcción del vector pPyCAGIP/GFP se obtuvo el fragmento XhoI-NotI del plásmido comercial pEGFP-N1 que contiene la secuencia codificante para la GFP y se insertó en el plásmido pPyCAGIP. Para la construcción del vector pPyCAGIP/hCOX-2/GFP se empleó el ADNc de hCOX-2 clonado en el plásmido pcADN1/Amp cedido por Dr. S. Prescott (Huntsman Cancer Institute, Salt Lake City, UT). Se extrajo y amplificó por PCR el ORF de hCOX-2 sin codón de parada y se insertó en los sitios XhoI-EcoRI del plásmido pEGFP-N1 de tal manera que la secuencia de hCOX-2 está en el marco de lectura de la proteína de fusión GFP. Finalmente, de esta nueva construcción pEGFP-N1/hCOX-2, se extrajo el fragmento XhoI-NotI que contiene la información para la expresión del hCOX-2/GFP y se clonó en el plásmido pPyCAGIP digerido con los enzimas de restricción XhoI-NotI. La orientación y la integridad de las construcciones se determinaron por secuenciación.

Para la generación de la línea CHL-V y CHL-C, células CHL al 50% de confluencia se expusieron durante 24 horas al reactivo de transfección Fugene 6 (Roche Applied Science, Indianapolis, IN) conteniendo el vector pPyCAGIP/GFP o el vector pPyCAGIP/hCOX-2/GFP respectivamente. Después, el medio de transfección fue reemplazado con medio fresco al 10% de suero bovino fetal (FBS). Al segundo día de la transfección, las células fueron plaqueadas al 25% de confluencia en un medio de selección conteniendo puromicina (3 µg/ml). Después de 12 días de selección, se comprobó la expresión de proteína GFP así como la expresión del ARNm de hCOX-2 y de las proteínas hCOX-2/GFP en las líneas transfectadas de manera estable. Además se valoraron los niveles de PGE_2 en el medio de cultivo siendo muy superiores en la línea CHL-C comparada con la línea control CHL-V. La contribución de COX-2 a este proceso fue confirmada con la inhibición de la síntesis de PGE_2 con el uso de un inhibidor selectivo de COX-2 [86].

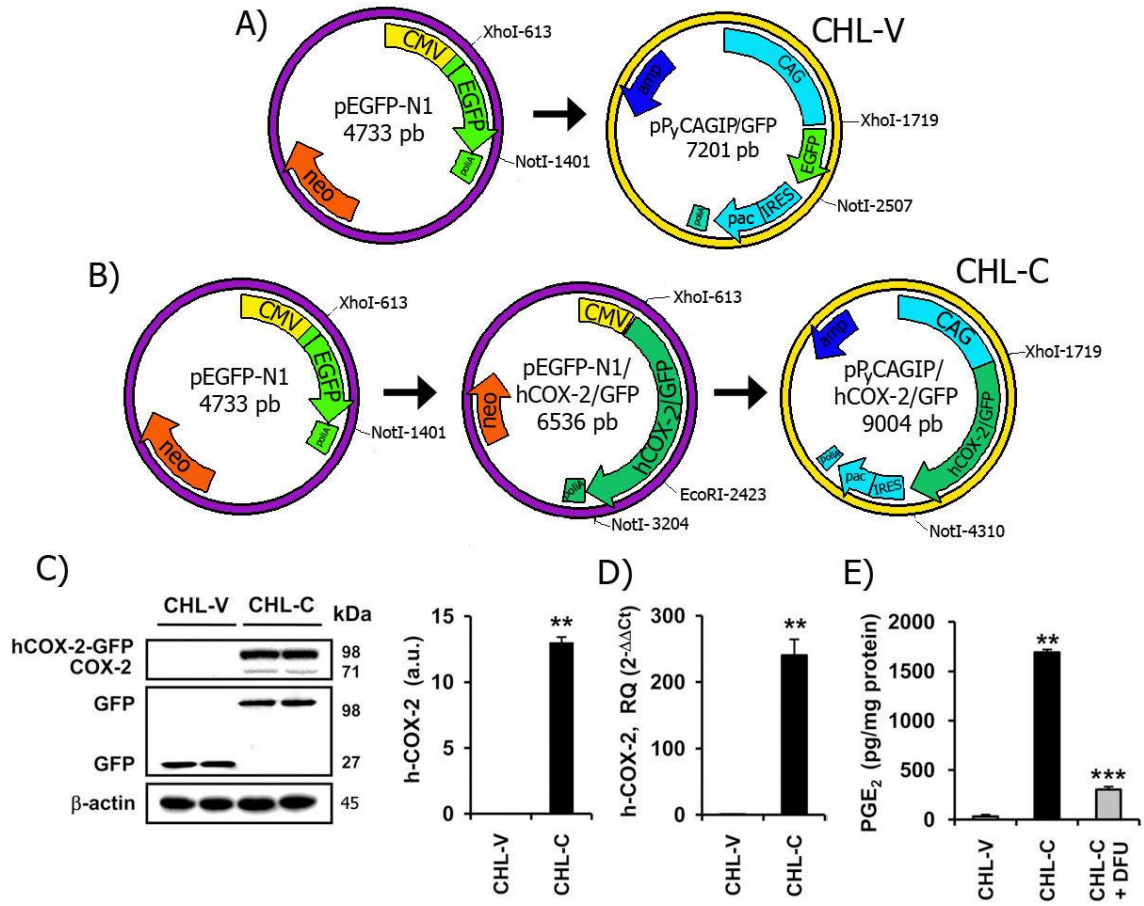

Caracterización de las líneas celulares CHL-V y CHL-C. *A) Generación del vector pPyCAGIP/GFP. B) Generación del vector pPyCAGIP/hCOX-2/GFP.C) Western blot para la detección de la expresión estable de GFP y hCOX-2/GFP en las líneas CHL-V y CHL-C respectivamente. D) Análisis de la expresión del ARNm de hCOX-2 por PCR cuantitativa. Como control interno se utilizó 36b4. E) Determinación de la producción de PGE_2 por enzimo-inmunoensayo en el medio de cultivo de CHL-V, CHL-C y CHL-C tratadas con el inhibidor selectivo de COX-2 5,5-dimetil-3-(3-fluorofenil)-4-(4-metilsulfonil)-fenil-2-(5H)-furanona (DFU). Adaptado de Llorente Izquierdo et al. [86].*

ARTÍCULO I: ***Am J Pathol. 2011; 178(3): 1361-73.***

Ratones transgénicos que expresan ciclooxigenasa-2 en el hepatocito revelan una escasa contribución de esta enzima a la hepatocarcinogénesis química.

Llorente Izquierdo C, Mayoral R, Flores JM, García-Palencia P, Cucarella C, Boscá L, Casado M, Martín-Sanz**. P.**

RESUMEN DEL ARTÍCULO I

Para esclarecer la contribución de COX-2 al desarrollo del CHC se generaron ratones TG que sobre-expresan la enzima COX-2 humana (hCOX-2) de forma constitutiva en el hepatocito bajo el control del promotor de la ApoE. El plan de trabajo consistió en el análisis de la susceptibilidad o protección frente a hepatitis crónica, fibrosis y carcinogénesis por el efecto de las PGs dependientes de COX-2.

En el modelo de ratón TG para COX-2 se analizó la contribución de las PGs a la fisiopatología hepática en relación al envejecimiento y se trataron los animales con una dieta DCM, para la inducción de fibrosis hepática. Tanto en el modelo de edad como en el de DCM se comprobó la expresión de la proteína y del ARNm de hCOX-2 y se valoraron los niveles de PGE_2 intrahepática que resultaron ser tres veces superiores en los animales TG para COX-2 comparados con los animales WT.

En el estudio de la contribución de las PGs a la fisiopatología hepática con la edad, la expresión de hCOX-2, de COX-1 y de PGE_2 fue similar en los ratones TG de 16 y 60 semanas. No se encontraron diferencias significativas en el peso corporal y del hígado entre el animal WT y el TG ni tampoco en la función hepática. El análisis macroscópico e histopatológico de los tejidos mostró nódulos inflamatorios en los ratones TG a las 60 semanas de edad pero no a las 16 semanas sugiriendo que las PGs producidas por la sobre-expresión de COX-2 en el hepatocito promueven una ligera hepatitis a las 60 semanas de edad de manera espontánea.

En el modelo de fibrosis hepática los animales fueron alimentados con la dieta DCM durante 15 semanas, las curvas de supervivencia y la pérdida de peso fueron similares entre los animales WT y los TG. Los niveles de ALT, los ensayos histológicos, el contenido de colágeno y la medida de los niveles de hidroxiprolina para la valoración del estado fibrótico, además de la medida del contenido de α-SMA y de la MMP-9 fueron significativamente superiores en los animales WT y TG alimentados con la dieta DCM comparando con los animales WT y TG alimentados con una dieta normal. Finalmente, los animales tratados con la dieta DCM desarrollaron fibrosis hepática. Sin embargo, dichos ensayos presentan la misma severidad entre los ratones WT y TG tratados con una dieta DCM. Los resultados obtenidos indican que las PGs derivadas de COX-2 no contribuyen al desarrollo de fibrosis hepática.

Para el análisis del papel de COX-2 en modelos experimentales crónicos de CHC se diseñaron tres abordajes: 1) se indujo una hepatocarcinogénesis experimental con DEN en los ratones TG para COX-2, 2) se transfectó establemente la línea hepatocitaria humana CHL de manera estable con un vector de expresión para COX-2 y se trató con DEN/fenobarbital (PB), 3) se hicieron implantes de las mismas líneas celulares tratadas y no tratadas en ratones atímicos

desnudos. En el modelo de hepatocarcinogénesis química los animales se sacrificaron a las 10, 25 y 40 semanas después del tratamiento con DEN. El análisis histopatológico indicó que la incidencia de lesiones pre-neoplásicas es relativamente mayor en los animales TG a las 10 semanas de tratamiento con DEN, aunque estos resultados no alcanzaron significación estadística. Además, el desarrollo de adenomas y carcinomas hepatocelulares a las 25 y 40 semanas de edad fue similar en los animales WT y TG, aunque la incidencia metastásica fue mayor en los ratones TG. El análisis de las vías de señalización molecular en los tumores mostró que a las 25 semanas de edad los niveles de expresión de Ciclina E y de c-Myc fueron significativamente superiores en los tumores de los animales TG, datos que fueron posteriormente confirmados mediante un array de PCR de genes de cáncer y por PCR cuantitativa. A las 40 semanas de tratamiento los tumores de los ratones TG presentaron una disminución significativa en los niveles de p53 y un incremento significativo de PCNA, Ciclina E y c-Jun. Por tanto, este modelo muestra que COX-2 favorece el desarrollo de nódulos pre-neoplásicos y acelera la proliferación inicial de los hepatocitos mediante la modulación de vías implicadas en la regulación del ciclo celular.

En la línea hepática TG y en la control se analizaron múltiples parámetros después de ser tratadas con DEN/PB. La proliferación celular fue mayor a la 48 y 72 h de cultivo, el daño oxidativo al ADN fue superior, los niveles de especies reactivas de oxígeno se encontraron incrementados, los de GSH disminuidos y se detectaron aumentos moderados pero significativos en la expresión de pJNK, p38 y pStat3 en la línea celular que expresa COX-2. A pesar de estos resultados, el ensayo de formación de colonias no presentó diferencias significativas en el número y tamaño de las colonias entre la línea celular TG y su control después del tratamiento con DEN/PB. Finalmente, se siguió y monitorizó el desarrollo de los tumores en ratones desnudos después de haberles implantado un número determinado de células de la línea hepática TG y su control, tratadas con DEN/PB. Este abordaje reveló un incremento significativo en el área del tumor debido al efecto de las PGs dependientes de COX-2. La alteración del estado redox, el incremento al daño oxidativo al ADN en la células TG, así como la alteración de la vías de señalización implicadas en la regulación de la proliferación celular y el crecimiento de los tumores tras el implante de las células en ratones corroboran la contribución de COX-2 al proceso de proliferación inicial de los hepatocitos.

The American Journal of Pathology, Vol. 178, No. 3, March 2011

DOI: 10.1016/j.ajpath.2010.11.074

Tumorigenesis and Neoplastic Progression

Transgenic Mice Expressing Cyclooxygenase-2 in Hepatocytes Reveal a Minor Contribution of This Enzyme to Chemical Hepatocarcinogenesis

Cristina Llorente Izquierdo,* Rafael Mayoral,*† Juana María Flores,‡ Pilar García-Palencia,‡ Carme Cucarella,§ Lisardo Boscá,*† Marta Casado,†§ and Paloma Martín-Sanz*†

From Institute of Biomedical Research Alberto Sols (CSIC-UAM), Madrid; the Biomedical Research Centre Network of Hepatic and Digestive Diseases (CIBERehd),† Barcelona; the Department of Medicine and Animal Surgery,‡ Veterinary Faculty, Complutense University, Madrid; and the Institute of Biomedicine of Valencia (IBV-CSIC),§ Valencia, Spain*

Cyclooxygenase-2 (COX-2) has been associated with cell growth regulation, tissue remodeling, and carcinogenesis. Ectopic expression of COX-2 in hepatocytes constitutes a nonphysiological condition ideal for evaluating the role of prostaglandins (PGs) in liver pathogenesis. The effect of COX-2-dependent PGs in chronic liver disease, hepatitis, fibrosis, and chemical hepatocarcinogenesis, has been investigated in transgenic (Tg) mice that express human COX-2 in hepatocytes and in Tg hepatic human cell lines. We have used three different complementary approaches: i) diethylnitrosamine (DEN)-induced chemical hepatocarcinogenesis in COX-2 Tg mice, ii) DEN/phenobarbital treatment of human COX-2 Tg hepatocyte-like cells, and iii) COX-2 Tg hepatocyte-like cells implants in nude mice. The data suggest that PGs produced by COX-2 in hepatocytes promoted mild hepatitis in 60-week-old mice, as assessed by histological examination, but failed to contribute to the development of liver fibrogenesis after methionine- and choline-deficient diet treatment. Moreover, liver injury, collagen content, and hepatic stellate cell activation were equally severe in wild-type and COX-2 Tg mice. The contribution of COX-2-dependent PGs to the development of DEN-induced hepatocarcinogenesis was evaluated in Tg mice, Tg hepatocyte-like cells, and nude mice and the analysis revealed that COX-2 expression favors the development of preneoplastic foci without affecting malignant transformation. Endogenous COX-2 expression in wild-type mice is a late event in the development of hepatocellular carcinoma. ***(Am J Pathol 2011, 178:1361–1373; DOI: 10.1016/j.ajpath.2010.11.074)***

Hepatocellular carcinoma (HCC) is a neoplasm with increasing incidence worldwide.[1] Epidemiological studies suggest that the major risk factors for HCC are persistent infection with hepatitis B and C virus and exposure to genotoxic and cytotoxic chemicals. All these factors cause chronic liver injury and inflammation, conditions in which hepatocytes die and resident inflammatory cells (Kupffer cells), as well as newly recruited inflammatory cells (macrophages, neutrophils, and natural killer and natural killer T cells), are activated to produce cytokines that conduct the compensatory proliferation of surviving hepatocytes.[2]

Cyclooxygenases 1 and 2 (COX-1 and COX-2) catalyze the first step in prostanoid biosynthesis. COX-1 is constitutively expressed in many tissues; COX-2 is induced by a variety of stimuli such as growth factors, proinflammatory stimuli, hormones, and other cellular stresses.[3] Adult hepatocytes fail to induce COX-2 expression, regardless of the proinflammatory factors used; however, Kupffer, stellate, hepatoma mouse liver cells, and fetal hepatocytes retain the ability to express COX-2 on stimulation with lipopolysaccharide and pro-inflammatory cytokines.[4,5] In the case of hepatocytes, and only under prolonged aggression, COX-2 is expressed as a result of the drop of C/EBPα levels, among other conditions.[6] Thus, ectopic expression of COX-2 in hepatocytes

Supported by grants SAF2007-60551, SAF2009-12602, and BFU2008-02161 from the Ministry of Science and Innovation (MICINN) and grant no. S-BIO-0283/2006 from the Community of Madrid (Comunidad de Madrid). The Biomedical Research Centre Network of Hepatic and Digestive Diseases (CIBERehd) is funded by National Institute of Health Carlos III (Instituto de Salud Carlos III).

Accepted for publication November 23, 2010.

C.L.I. and R.M. contributed equally to the present work.

Address reprint requests to Paloma Martín-Sanz, Ph.D., or Marta Casado, Ph.D., Instituto de Investigaciones Biomédicas Alberto Sols, CSIC-UAM Madrid, Arturo Duperier, 4, 28029 Madrid, Spain. E-mail: pmartins@iib.uam.es or mcasado@ibv.csic.es.

constitutes an ideal condition for evaluating the role of prostaglandins (PGs) in liver pathogenesis. In this regard, we and others demonstrated that partial hepatectomy[7] induced COX-2 in hepatocytes and contributed to the progression of cell cycle after partial hepatectomy.[8,9] In addition to liver regeneration after partial hepatectomy or hepatotoxic agents, expression of COX-2 has been detected in animal models of cirrhosis,[10] in human hepatoma cell lines,[11,12] after hepatitis B virus and hepatitis C virus infection,[13,14] and in human HCC.[15] High levels of COX-2-derived prostaglandin E_2 (PGE_2) lead to a decrease in apoptosis, a modulation of the immune system and a stimulation of cell migration, proliferation, and angiogenesis.[16] Nonetheless, even though COX-2 expression is elevated in the early stages of HCC, many questions remain unsolved regarding the contribution of COX-2-dependent PGs to induce tumorigenesis.

Studies with genetically altered mice have revealed many genes associated with HCC. Such genes fall into two categories: i) those that augment spontaneous HCC and ii) those that increase the susceptibility to chemically induced HCC. The HCC develops spontaneously in transgenic mice overexpressing hepatitis B virus surface antigen (HBsAg), transforming growth factor α the c-*Myc* proto-oncogene,[17] or the IκB kinase (IKK) subunit NEMO/IKKγ.[18] HCC development is also augmented in mice deficient in the Mdr2 P-glycoprotein transporter[19] or carrying a lymphotoxin-transgene.[20] Most of these mouse strains display enhanced susceptibility to chemical carcinogens such as diethylnitrosamine (DEN), although the molecular and cellular mechanisms involved are not well understood.

To clarify the role of COX-2 in liver tumorigenesis, we used transgenic mice expressing human COX-2 constitutively in hepatocytes under the control of the human ApoE promoter (COX-2 Tg)[21] and hepatic human cell lines carrying the COX-2 transgene. We sought to examine the response of the COX-2 transgenic (Tg) mice to the DEN-induced HCC model. Our results show that COX-2 expression in hepatocytes caused mild hepatitis in aged mice, but was not involved in the development of liver fibrosis. COX-2 favored the development of preneoplastic foci and adenomas, but it was not sufficient to significantly increase the malignant transformation induced by DEN. Furthermore, endogenous COX-2 expression in wild-type (WT) mice is a late event in the development of HCC induced by DEN.

Materials and Methods

Chemicals

Antibodies were obtained from Santa Cruz Biotechnology (Santa Cruz, CA), Sigma-Aldrich (St. Louis, MO), Cell Signaling Technology (Danvers, MA), and Cayman Chemical (Ann Arbor, MI). Reagents were from Roche Diagnostics (Mannheim, Germany) or Sigma-Aldrich. DFU [5,5-dimethyl-3(3-fluorophenyl)-4-(4-methylsulfonyl) phenyl-2(5*H*)-furanone] was from Merck (Darmstadt, Germany). Reagents for electrophoresis were obtained from Bio-Rad (Hercules, CA). Tissue culture dishes were from Falcon (Becton Dickinson Labware, Franklin Lakes, NJ). Tissue culture media were from Gibco (Invitrogen, Grand Island, NY).

Cell Culture

The human liver cell line CCL-13 [Chang liver (CHL)], an immortalized nontumor cell line derived from normal liver, was purchased from the American Type Culture Collection (ATCC, Manassas, VA). Cells were grown on Falcon tissue culture dishes in Dulbecco's modified Eagle's medium supplemented with 10% fetal bovine serum (FBS) and antibiotics (50 μg/ml each of penicillin, streptomycin, and gentamicin) at 37°C in a humidified, 5% CO_2-enriched atmosphere.

Characterization of COX-2 Vectors

pEGFP-N1 was obtained from Clontech (Mountain View, CA) and pPyCAGIP was a gift from Dr. I. Chambers (University of Edinburgh, Edinburgh, Scotland). Human COX-2 ORF was amplified by PCR from human full-length COX-2 cDNA cloned into pcDNA1/Amp, a gift from Dr. S. Prescott (Huntsman Cancer Institute, Salt Lake City, UT). The PCR product was cloned into the XhoI-EcoRI restriction site of pEGFP-N1 vector, so that it is in lecture frame with the green fluorescent protein (GFP) coding sequence. We then subcloned the hCOX-2/GFP fusion sequence into the XhoI-NotI restriction site of pPyCAGIP vector. pPyCAGIP-GFP construct was obtained by restriction digestion and subcloning from pEGFP-N1 vector. The orientation and integrity of the constructs were determined by sequencing.

Generation of Stable hCOX-2 Cells

For plasmid transfections, attached CHL cells at 50% confluence were exposed for 24 hours to Fugene 6 reagent (Roche Applied Science, Indianapolis, IN) containing pPyCAGIP-hCOX-2-GFP or control vector pPyCAGIP-GFP. At the end of this period, the transfection medium was replaced with fresh medium containing 10% FBS; on the second day after transfection, the cells were plated at 25% confluence in medium supplemented with 3 μg/ml puromycin. Single colonies of resistant cells were detectable after approximately 12 days and were selected and subcultured for 30 days. Subsequent cultures of selected cells were grown in the presence of puromycin. Cells stably expressing hCOX-2-GFP or GFP proteins were termed CHL-C and CHL-V, respectively. At 18 hours before experiments, the culture medium was replaced with fresh medium containing 1% FBS. For the *in vitro* phenobarbital (PB)/DEN protocol, CHL-C and CHL-V cells were incubated with 1.5 mmol/L PB for 16 hours followed by 15 mmol/L DEN for 24 to 48 hours. These cells were also used for tumorigenesis experiments in nude mice.

Animal Experimentation

Hepatocyte COX-2 transgenic mice (25 to 30 g body weight; 4 months of age) on a C57BL6J × DBA background were used in this study, along with corresponding age-matched WT mice.[21] The animals were housed on a 12-hour light/dark cycle in an air conditioned room at 25°C with food and water available *ad libitum* and were treated according to the Institutional Care Instructions (Bioethical Commission, Spanish National Research Council–CSIC). In some experiments, 60-week-old mice were analyzed. Liver fibrosis was induced by feeding the animals with a diet deficient in methionine and (MCD diet) (TD 90262; Harlan Laboratories, Madison, WI). The animals were sacrificed after 15 weeks of treatment, and their body weights were recorded before the liver tissues were used for analysis ($n = 8$ to 9).

To induce HCC, DEN (25 mg/kg; Sigma-Aldrich) was injected intraperitoneally into 14-day-old mice. Mice were sacrificed at 10, 25, or 40 weeks after DEN treatment. Body and liver weights were recorded, and livers were removed and separated into individual lobes. Externally visible tumors (≥0.5 mm) were counted and measured by stereomicroscopy. It is relevant to note that DEN is a poor carcinogen on its own in mice of a C57BL6 genetic background, but the hybrid genetic background C57BL6J × DBA that we used is much more susceptible to DEN treatment.[22] Liver tissues were snap-frozen in liquid nitrogen, stored at −80°C, and collected in a solution containing 30% sucrose in PBS or fixed in 10% buffered formalin. Plasma was obtained by puncture of the retro-orbital venous plexus.

Female athymic *nu/nu* mice (6 weeks old) were obtained from Charles River Laboratories (Wilmington, MA). The animals were kept under pathogen-free conditions and were given an autoclaved standard diet and water *ad libitum*. CHL-C or CHL-V cells (4×10^6) suspended in PBS were injected in one flank of the *nu/nu* mice, along with the corresponding control, depending on the treatment of the cells in the other flank (4 mice per condition). Tumor growth was monitored weekly by two-dimensional measurements using a vernier caliper. The formula $(L/2) \times (W/2) \times \pi$ (where L is the maximum diameter of each tumor and W is the length at right angles to L) was used to calculate the maximal tumor surface area. After 32 days, mice were sacrificed by cervical dislocation before the tumor burden caused any obvious morbidity. The final tumor size and weights were recorded.[23]

RNA Isolation

Total RNA of liver biopsy samples was extracted by using TRIzol reagent (Invitrogen, Carlsbad, CA). Total RNA (1 μg) was reverse-transcribed using a Transcriptor first strand cDNA synthesis kit according to the manufacturer's instructions (Roche Applied Science). For transcriptional profiling analyses, total RNA was further cleaned using the Qiagen RNeasy mini kit (Valencia, CA; Hilden, Germany) with one step of DNase I digestion according to the manufacturer's instructions. Three micrograms RNA were used for cDNA synthesis with the RT2 First Standard kit (SuperArray Bioscience, Frederick, MD).

Quantitative Real-Time PCR Analysis

The qPCR analysis was performed with a MyiQ real-time PCR system (Bio-Rad) sequence detector using the Sso-Fast EvaGreen polymerase method (Bio-Rad) and d(N)6 random hexamer with the following primers: hCOX-2 F 5′-CGCAGTACAGAAAGTATCACAGGC-3′ and R 5′-GCGTTTGCGGTACTCATTAAAA-3′;36b4 F 5′-ACTGGTCTAGGACCCGAGAAG-3′ and R 5′-TCCCACCTTGTCTCCAGTCT-3′; Ccne1 F 5′-TTCTGCAGCGTCATCCTCT-3′ and R 5′-TGGAGCTTATAGACTTCGCACA-3′; and Myc F 5′-CCTAGTGCTGCATGAGGAGA-3′ and R 5′-TCTTCCTCATCTTCTTGCTCTTC-3′.Specific primers were purchased from Invitrogen. PCR thermocycling parameters were 95°C for 30 seconds, 40 cycles of 95°C for 5 seconds, and 60°C for 10 seconds. Each sample was run in triplicate and was normalized to 36b4 RNA. The replicates were then averaged, and fold induction was determined in a $\Delta\Delta C_T$-based fold-change calculations.

Histochemistry Analysis

Samples of liver were fixed in 10% buffered formalin, embedded in paraffin wax, sectioned at 4-μm thickness, and stained with H&E. Histopathology analysis was performed by the Department of Medicine and Animal Surgery from Faculty of Veterinary, Madrid, Spain. Immunohistochemical staining was performed using the streptavidin-biotin-peroxidase complex method as described previously.[24] Histological sections were stained following standard procedures with an antibody against the active form of caspase 3 (R&D Systems, Minneapolis, MN) or Ki-67 (Novocastra, Newcastle Upon Tyne, UK). Five entire areas of each tissue section (500 cells) were counted.

Western Blot Analysis

Extracts from tissue samples (50 to 100 mg) or cells (2 to 3×10^6) were obtained as previously described.[21] For Western blot analysis, whole-cell extracts were boiled for 5 minutes in Laemmli sample buffer, and equal amounts of protein (20 to 30 μg) were separated by 10% to 15% SDS-polyacrylamide electrophoresis gel. The relative amounts of each protein were determined with the following polyclonal or monoclonal antibodies: COX-2 and COX-1 (from Cayman Chemical and Santa Cruz Biotechnology); cyclin E, PCNA, p53, and c-Jun (Santa Cruz Biotechnology); p38MAPK (Thr180/Tyr182), p38 MAPK, p-Erk (Thr202/Tyr204), Erk, p-JNK (Thr183/Thy185), JNK, p-Stat3 (Tyr705), Stat3, and cleaved caspase-3 (Cell Signaling Technology); MMP-9 (Chemicon International, Temecula, CA); and αSMA (Sigma-Aldrich) After incubation with the corresponding anti-rabbit or anti-mouse horseradish peroxidase conjugated secondary antibody, blots were developed by the enzymatic chemiluminescence protocol (Amersham–GE Healthcare, Chalfont St. Giles, UK). Target protein band densities were normalized with β-actin. The

blots were revealed, and different exposition times were performed for each blot with a charged coupling device camera in a luminescent image analyzer (Gel-Doc; Bio-Rad) to ensure the linearity of the band intensities. Densitometric analysis was expressed in arbitrary units.

Cell Viability

To perform the growth rate analysis, cells were trypsinized and stained with trypan blue at the indicated times, and the cells that excluded trypan blue were counted under the microscope. Cell viability was measured using the MTT assay, 3-(4,5-dimethylthiazol-2-yl)-2,5′-diphenyltetrazolium bromide. Cells (3×10^3) were seeded on 96-well plates in Dulbecco's modified Eagle's medium supplemented with 10% FBS. After incubation with the PB/DEN-protocol, cells were treated with 10 μL of MTT solution (0.3 mg/ml) for 1 hour at 37°C. The medium was removed and dimethyl sulfoxide was added to dissolve the blue formazan residue. The optical density was measured at 550 nm.

Determination of Metabolites

PGE_2 was determined in liver tissue by specific immunoassay (GE Healthcare).[21] Alanine transaminase, aspartate transaminase, alkaline phosphatase, and lactate dehydrogenase were assayed spectrophotometrically in plasma at the School of Clinical Biochemistry, Faculty of Pharmacy, Complutense University, Madrid, Spain. Protein levels were determined with Bradford reagent (Bio-Rad). To quantify collagen content, hepatic hydroxyproline was assayed according to the instructions of a hydroxyproline ELISA kit (Antibodies-online, Aachen, Germany).

Measurement of Oxidative DNA Damage and Intracellular Redox State

Oxidative damage of DNA was analyzed in cultured cells under different treatments by measuring the levels of 8-hydroxy-2-deoxyguanosine (8-OH-dG) by immunoassay according to the manufacturer's instructions (StressMarq Biosciences, Victoria, BC, Canada). The oxidation-sensitive fluorescent probe 2′,7′-dichlorodihydrofluorescein diacetate (H_2DCFDA) and the oxidative-insensitive analog carboxy-DCFH-DA (Invitrogen) were used to analyze the total intracellular content of reactive oxygen species (ROS); the analog is a nonoxidable fluorescent probe that does not change its fluorescence in the presence of ROS. The fluorescent probe monochlorobimane (Sigma-Aldrich) was used to analyze the total intracellular content of reduced glutathione. After treatment and at the indicated times, cells were incubated with 2.5 μmol/L H_2DCFDA (30 minutes, 37°C), 2.5 μmol/L carboxy-DCFH-DA, or 2 mmol/L monochlorobimane (1 hour, 37°C) in Hanks' balanced salt solution without phenol red, lysed with a buffer containing 25 mmol/L HEPES pH 7.5, 60 mmol/L NaCl, 1.5 mmol/L $MgCl_2$, 0.2 mmol/L EDTA, and 0.1% Triton X-100 (10 minutes, 4°C), and then transferred in duplicate into a 96-well plate. Fluorescence was measured in a microplate fluorescence reader and normalized with protein content.

Soft Agar Assays

Cells (3×10^4) were suspended in 1.5 ml of Dulbecco's modified Eagle's medium containing 0.4% of low-melting-point agarose (type VII; Sigma-Aldrich) and 10% FBS, and seeded onto a coating of 1% low-melting-point aga-

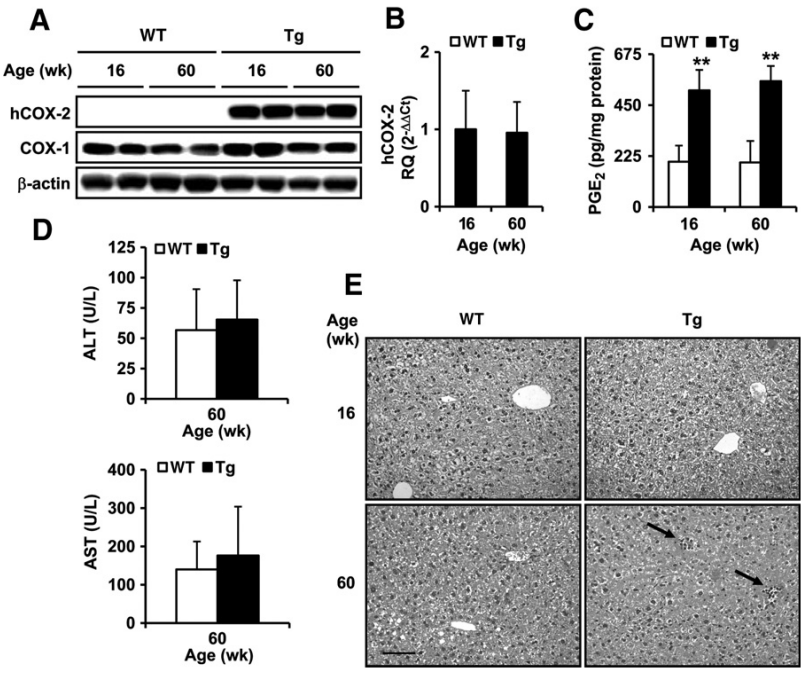

Figure 1. Aged COX-2 Tg mice developed subclinical hepatitis. **A:** Human COX-1 and COX-2 protein expression in liver homogenates from WT and Tg animals at 16 and 60 weeks of age detected by Western blot and normalized with β-actin. **B:** qPCR analysis of COX-2 mRNA expression. COX-2 mRNA amounts were calculated as relative quantity (RQ) and normalized to the expression of 36b4 mRNA. Values represent fold change relative to COX-2 Tg 16 weeks. **C:** Intrahepatic PGE_2 concentration was determined by enzyme immunoassay in liver homogenates. **D:** Plasma levels of aspartate transaminase (AST) and alanine transaminase (ALT) were assayed spectrophotometrically **E:** H&E staining of liver sections of 16- and 60-week-old WT and Tg mice. Inflammatory foci are indicated with **arrows**. Micrographs were taken with a Color View Camera in a Vanox Olympus microscope at 20× magnification. Scale bar = 100 μm (for all images). Data are reported as means ± SD of six animals per condition. $^{**}P < 0.001$ vs the corresponding matched animals. Wk, week.

rose in complete culture medium. Every 4 days, the medium was removed and replaced with fresh medium. Cells were incubated for 21 days; the colonies containing more than 50 cells were counted after stained with 0.5% MTT for 1 hour at room temperature. The number of colonies was quantified by soft agar analysis with the software Analysis auto from Olympus (Wendenstrasse, Hamburg, Germany).

Transcriptional Profiling of COX-2 Tg Liver after DEN Treatment

The mouse cancer PCR array was performed according to the manufacturer's protocol, using the Profiler PCR array system and the SYBR Green/fluorescein qPCR master mix (SuperArray Bioscience) on a MyiQ Real-Time PCR System (Bio-Rad). Gene expression was compared using a Web-based software package for the PCR array system (*http://www.sabiosciences.com/pcr/arrayanalysis.php*); this software automatically performs all $\Delta\Delta C_T$ based fold-change calculations from the specific uploaded raw threshold cycle data.

Data Analysis

Statistical analyses were performed using the SPSS package version 17 (SPSS, Chicago, IL). Data are expressed as means ± SD. Statistical significance of differences between the control and transgenic groups was evaluated by the *U* of the Mann-Whitney *U*-test. The association of histological analysis was assessed using Fisher's exact test. Curves for overall survival were generated using the Kaplan-Meier method. All tests were calculated two-tailed, and the significance level was set at $P < 0.05$.

Results

COX-2 Tg Mice Developed Subclinical Hepatitis

hCOX-2 mRNA and protein were detected in COX-2 Tg mice, and intrahepatic PGE_2 levels were threefold higher compared with WT mice. The expression of hCOX-2, COX-1, and PGE_2 was similar between 16- and 60-week-old COX-2 Tg mice (Figure 1, A–C). No significant differences were observed between old WT and Tg mice in body weight (38.8 ± 2.3 g vs 41.1 ± 1.8 g), liver weight

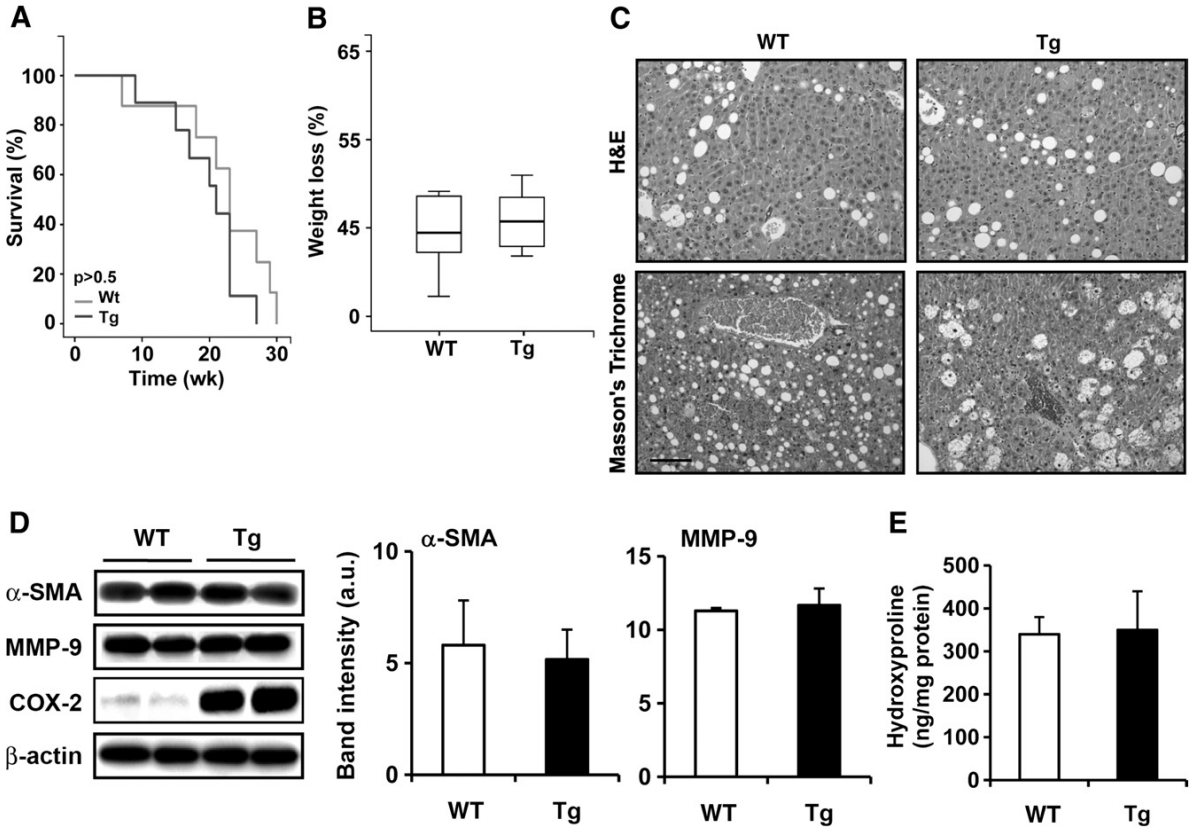

Figure 2. COX-2 expression in hepatocytes did not mediate the development of liver fibrosis. Survival curves (**A**) and the loss of body weight (**B**) of WT (n = 14) and Tg (n = 14) mice after the MCD diet. **C:** H&E and Masson's trichrome staining of liver sections of WT and Tg mice after the MCD diet and sacrificed at 15 weeks. Micrographs were taken with a Color View Camera in a Vanox Olympus microscope at 20× magnification. Scale bar = 100 μm (for all images). **D** and **E:** α-SMA, MMP-9, COX-2 protein expression measured by Western blot (**D**) and hydroxyproline levels analyzed by ELISA (**E**) in WT and Tg liver after the MCD diet. Data are reported as means ± SD of six animals per condition.

(1.9 ± 0.1 g vs 2.1 ± 0.1 g), and alanine transaminase and aspartate transaminase (Figure 1D). Nevertheless, inflammatory foci, composed mainly of lymphocytes, were seen in the livers of 60-week-old Tg mice, compared with WT mice, indicating that the expression of the COX-2 transgene causes subclinical hepatitis at 60 weeks of age (Figure 1E).

COX-2 Expression in Hepatocytes Did Not Mediate the Development of Liver Fibrosis

Similar survival curves and changes in body weight were observed in WT and COX-2 Tg mice fed with the MCD diet (Figure 2, A and B). Feeding with the MCD diet for 15 weeks induced significantly higher plasma alanine transaminase levels than in the corresponding control (320 ± 20 vs 40 ± 7 UI/L and 250 ± 32 vs 25 ± 4 UI/L for WT and Tg mice, respectively). Liver histology of WT and Tg mice fed with the MCD diet (Figure 2C) showed fatty liver degeneration, although Masson's trichrome staining (collagen content) did not show significant differences between WT and Tg mice. To evaluate liver fibrosis in a quantitative manner, the levels of hydroxyproline and the amount of α-smooth muscle actin (α-SMA) and matrix metalloproteinase 9 (MMP-9) were measured as markers of hepatic stellate cell activation and liver fibrotic stage. The MCD diet induced both α-SMA and MMP-9 expression (control levels of α-SMA and MMP-9 without the MCD diet were undetectable; data not shown) and increased hydroxyproline content

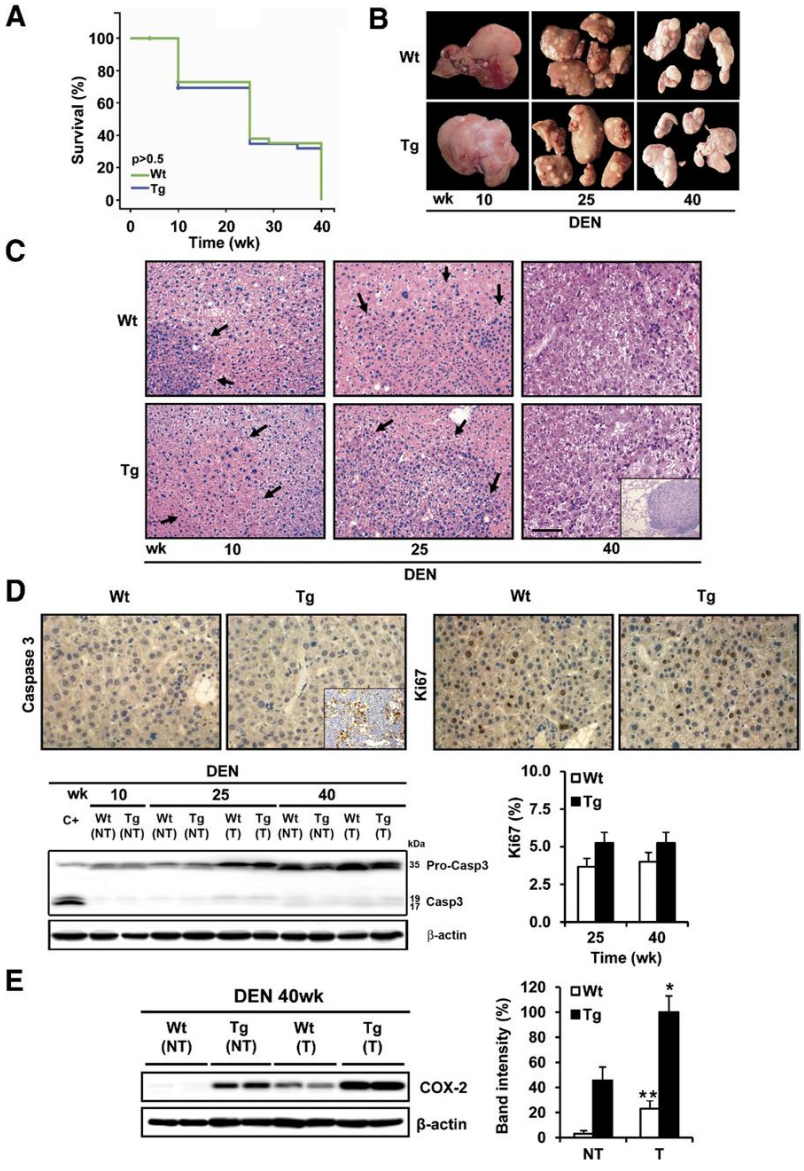

Figure 3. Effects of hepatic COX-2 expression on tumor development. **A:** Survival curves of WT and Tg mice injected with DEN (25 mg/kg) at 2 weeks of age (n = 36). **B:** Gross liver features after 10, 25, and 40 weeks of DEN treatment in WT and Tg mice. **C:** H&E staining of liver sections in WT and Tg mice after 10, 25, and 40 weeks of DEN treatment. Lesions are indicated by **arrows**. **Inset:** Lung metastases. Micrographs were taken with a Color View Camera in a Vanox Olympus microscope at 20× magnification. Scale bar = 100 μm (for all images in **C**). **D:** Cell proliferation and apoptosis were analyzed in liver sections from WT and Tg mice after DEN treatment by Ki-67 and active caspase 3 staining. **Inset**: Positive control of murine thymic lymphoma section. A representative Western blot of cleaved caspase 3 is shown. C+ is a liver extract from WT mice treated with lipopolysaccharide (35 μg/kg)/D-GalN (1g/kg). The percentage of mitotic cells was quantified at 25 and 40 weeks after DEN treatment. Data are reported as means ± SD of five sections per animal (n = 3). **E:** Endogenous COX-2 expression was detected in tumor tissue from WT liver at 40 weeks after DEN treatment. Data are reported as means ± SD of 12 animals per condition. $^{*}P < 0.05$ and $^{**}P < 0.001$ tumor vs paired control tissue.

Table 1. Body and Liver Weight, Tibia Length, and Plasma Levels of Liver Injury Markers in WT and COX-2 Tg Mice after DEN Treatment

Treatment	Body weight (g)	Liver weight (g)	Tibia length (cm)	Liver/body ratio	AST* (UI/L)	ALT* (UI/L)	LDH* (UI/L)
WT							
DEN10	32.6 ± 4.1	1.6 ± 0.2	2.2 ± 0.1	0.05	240 ± 120	95 ± 60	500 ± 260
DEN25	41.8 ± 2.8	2.7 ± 0.7	2.3 ± 0.1	0.07	215 ± 70	100 ± 30	1015 ± 310
DEN40	36.7 ± 0.7	5.3 ± 1.4	2.3 ± 0.1	0.15	160 ± 50	160 ± 30	630 ± 220
Tg							
DEN10	30.5 ± 2.7	1.5 ± 0.1	2.2 ± 0.1	0.05	300 ± 180	83 ± 60	470 ± 290
DEN25	42.7 ± 6.1	2.5 ± 0.7	2.3 ± 0.1	0.06	230 ± 140	97 ± 40	1080 ± 580
DEN40	37.1 ± 9.4	4.2 ± 0.8	2.3 ± 0.1	0.11	210 ± 130	195 ± 140	1140 ± 750

Both WT and Tg mice were given diethylnitrosamine starting at 2 weeks of age for 10, 25, or 40 weeks. Hepatocyte COX-2 Tg mice on a C57BL6J × DBA background were used, along with corresponding age-matched WT mice.[21] Results are reported as mean ± SD of 10 to 12 animals per condition. ALT, alanine transaminase; AST, aspartate transaminase; DEN, diethylnitrosamine; LDH, lactate dehydrogenase; Tg, transgenic; WT, wild type.
*Plasma levels of AST, ALT, and LDH were assayed spectrophotometrically at the indicated times after DEN treatment. The control levels of AST, ALT, and LDH of WT vs Tg mice were 84 ± 16 vs. 71 ± 12 UI/L, 39 ± 7 vs. 22 ± 4 UI/L, and 47 ± 9 vs. 33 ± 6 UI/L, respectively.

(Figure 2, D and E); however, COX-2 expression in Tg mice did not affect liver fibrosis. Endogenous COX-2 expression was slightly induced by the MCD diet in WT mice.

Effects of Hepatic COX-2 Expression on Tumor Development

To determine the role of COX-2 in HCC induction, WT and Tg mice were injected with DEN (25 mg/kg) at postnatal day 14 and were sacrificed at 10, 25, or 40 weeks after treatment. The survival of mice, the liver/body weight ratio, and tibial size are shown in Figure 3A and Table 1. A macroscopic view of representative WT and COX-2 livers is shown in Figure 3B. Analysis of plasma levels of liver injury markers after DEN treatment are given in Table 1. There was an important increase of aspartate transaminase, alanine transaminase, and LDH after DEN treatment in the Tg mice, but liver injury was similar in WT and Tg mice. Morphometric analysis revealed no differences in the number, size, or volume of detectable tumors (Table 2). Histological analysis confirmed that all tumors at 40 weeks after DEN treatment, both in WT and Tg mice, corresponded to liver carcinoma (Figure 3C). The histopathological analysis of the liver biopsies indicated that the incidence of preneoplastic lesions was higher in COX-2 Tg than in WT mice 10 weeks after DEN treatment (25% vs 8%), but these changes did not reach statistical significance ($P = 0.053$). At the end of DEN treatment (40 weeks), similar HCCs were detected in WT and Tg liver, although a high pulmonary metastatic incidence was seen in Tg mice (Table 2).

Next, we measured the apoptotic rate in WT and Tg liver at 25 and 40 weeks after DEN treatment by quantifying the percentage of cells with active caspase 3 and the mitotic index measured by Ki-67 immunohistochemistry. Caspase 3 staining was not detected, nor cleaved caspase 3 (measured by Western blotting), and Ki-67 was similar in both WT and Tg liver (Figure 3D). DEN treatment has been reported to decrease CYP2E1 levels,[25] but in the present study the expression was similar between WT and Tg mice, suggesting that COX-2 does not affect DEN bioactivation (data not shown). Of note, endogenous COX-2 expression was detected in tumors of WT mice at 40 weeks after DEN treatment (Figure 3E).

COX-2 Tg Liver Tumors Showed an Increase in Cyclin E1 and c-Myc

To better understand how COX-2 accelerates the initial events of liver tumorigenesis induced by DEN, cell cycle regulators and tumor suppressors in tumor and nontumor samples were analyzed. No changes were observed in the protein levels of p53, PCNA, cyclin E1, and c-Jun at 10 weeks after treatment (Figure 4A). At 25 weeks, significant differences were observed in cyclin E levels in tumor versus

Table 2. Morphometric Analysis and Incidence of Pathological Signs in Livers of WT and COX-2 Tg Male Mice after DEN Treatment

Treatment	Sample size	Tumors, ≥0.5 mm (no.)	Tumor area (%)	Maximal size (mm)	Preneoplastic lesions, no. (%)	Adenomas, no. (%)	Hepatocellular carcinomas, no. (%)	Lung metastasis, no. (%)
WT								
DEN10	12	0	0	0	1 (8)	0 (0)	0 (0)	0 (0)
DEN25	12	42.5 ± 9.4	8.0 ± 2.6	6.8 ± 1.5	1 (8)	11 (92)	0 (0)	0 (0)
DEN40	12	38.7 ± 0.5	43.7 ± 3.9	19.3 ± 2.4	0 (0)	0 (0)	12 (100)	3 (25)
Tg								
DEN10	12	0	0	0	3 (25)	0 (0)	0 (0)	0 (0)
DEN25	12	59.2 ± 11.8	8.8 ± 2.38	5.5 ± 1.1	0 (0)	12 (100)	0 (0)	0 (0)
DEN40	12	43.0 ± 6.3	43.5 ± 6.0	14.7 ± 0.7	0 (0)	0 (0)	12 (100)	8 (67)*

*$P < 0.05$ vs. WT.

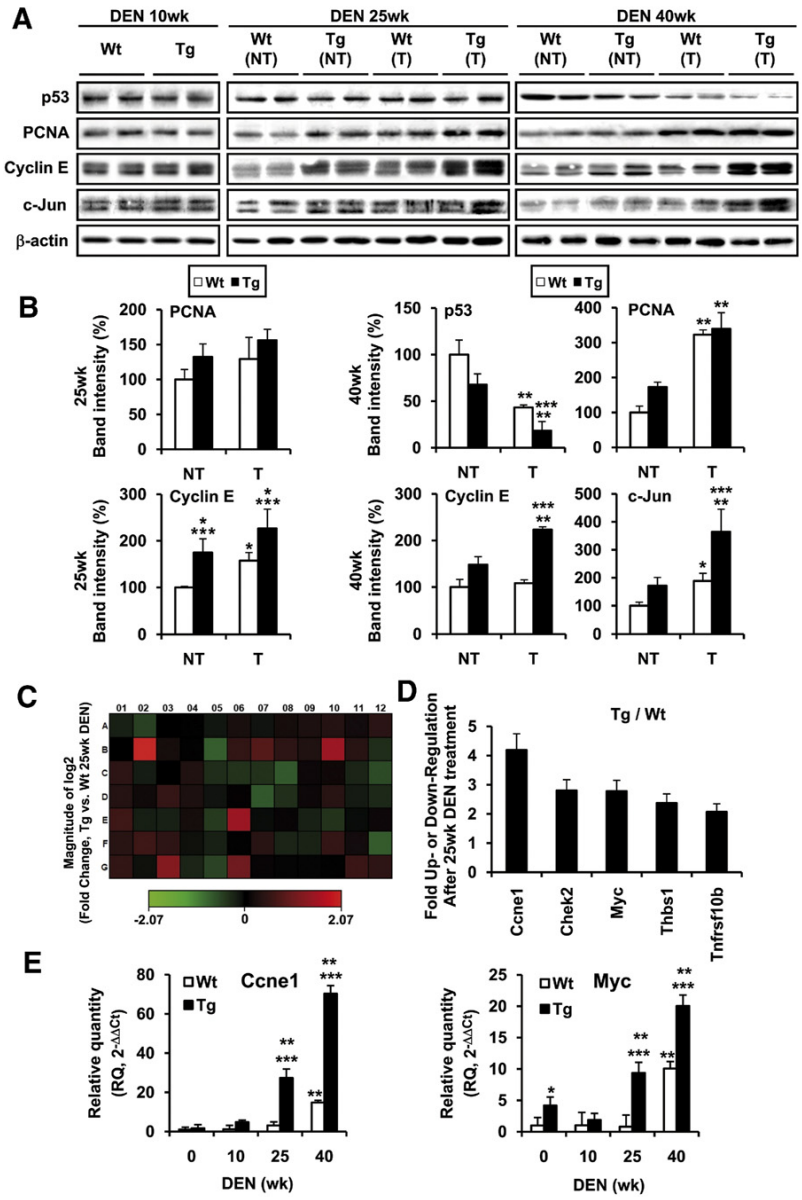

Figure 4. COX-2 Tg liver tumors showed an increase in cyclin E1 and c-Myc. **A:** Nontumor liver (NT) and HCC (T) were analyzed for cell cycle and tumor suppressors associated proteins. Representative Western blots showing the expression of p53, PCNA, cyclin E and c-Jun in WT and Tg mice. **B**: Densitometric analysis of the expression of the proteins in WT and Tg mice after DEN treatment. Data are reported as means ± SD of 12 animals per condition. $^{*}P < 0.05$ and $^{**}P < 0.001$ tumor vs paired control tissue. $^{***}P < 0.05$ COX-2 Tg vs WT mice treated under identical conditions. **C** and **D**: Colorimetric diagram of 84 cancer-related genes (**C**) and fold change (**D**) for genes whose transcription is up- or down-regulated twofold in COX-2 Tg mice at 25 weeks after DEN treatment. Data are reported as means of four animals per condition. **E:** Validated array results from qPCR analysis. mRNA amounts were calculated as RQ and were normalized to the expression of 36b4 mRNA. $^{*}P < 0.05$ and $^{**}P < 0.001$ for COX-2 Tg or WT after DEN treatment vs WT mice without treatment. $^{***}P < 0.001$ for COX-2 Tg vs WT mice treated under identical conditions.

normal tissue. Furthermore, cyclin E levels were significantly increased in Tg versus WT liver. At 40 weeks after DEN treatment, a significant decrease of p53 and a significant increase of PCNA, cyclin E, and c-Jun levels were detected in tumor versus paired control tissue from both WT and Tg liver and in Tg liver versus WT (Figure 4, A and B).

To gain further insight into the response to DEN in WT and Tg liver, a specific mouse cancer microarray was used. The magnitude of changes and the corresponding statistical significance of the 84 genes analyzed are summarized in Figure 4, C and D, and in Table 3. We sorted the candidate genes whose expression threshold after DEN treatment was altered more than twofold (Figure 4D), including *Ccne1* (cyclin E1), *Chek2*, *Myc*, *Tnfrsf10b*, and *Thbs1* in Tg mice at 25 weeks after DEN treatment, all of them related with cell proliferation. These results were validated by qPCR (Figure 4E).

Effect of DEN on CHL Cells Expressing a COX-2 Transgene

To investigate more deeply the molecular mechanisms triggered by COX-2/PGE_2 in the chemical carcinogenesis induced by DEN, a human CHL cell line stably transfected with an hCOX-2-GFP expression vector or control vector and treated with an *in vitro* PB/DEN induction protocol. The hCOX-2 was expressed only in CHL-C cells (Figure 5, A and B). Moreover, CHL-C cells released significantly greater quantities of PGE_2 into the culture

Table 3. Heat Map Data for Gene Expression

Layout	1	2	3	4	5	6	7	8	9	10	11	12
A	*Akt1* −1.16	*Akt2* −1.42	*Angpt1* −1.01	*Apaf1* 1.02	*Atm* −1.09	*Bad* 1.17	*Bax* −1.08	*Bcl2* 1.14	*Bcl2l1* 1.20	*Birc5* 1.27	*Brca1* 1.12	*Casp8* 1.32
B	*Ccnd1* 1.00	*Ccne1* 4.19	*Cdc25a* 1.15	*Cdh1* 1.03	*Cdk2* −1.68	*Cdk4* 1.38	*Cdkn1a* 1.75	*Cdkn2a* 1.36	*Cflar* 1.23	*Chek2* 2.8	*Col18a1* 1.28	*Ctnnb1* −1.27
C	*E2f1* 1.35	*Egfr* −1.13	*Ets2* −1.01	*Fas* 1.22	*Fgf1* −1.26	*Fgfr2* −1.31	*Figf* −1.29	*Fos* −1.64	*Grb2* 1.09	*Hgf* 1.10	*Ifnb1* −1.20	*Igf1* −1.50
D	*Itga2* 1.27	*Itga3* 1.10	*Itga4* 1.43	*Itgav* 1.20	*Itgb1* −1.08	*Itgb3* 1.05	*Jun* −1.61	*Kiss1* −1.28	*Map2k1* 1.08	*Mcam* 1.29	*Mdm2* −1.12	*Met* −1.22
E	*Mmp2* 1.52	*Mmp9* −1.15	*Mta1* −1.18	*Mta2* 1.15	*Muc1* −1.37	*Myc* 2.78	*Ncam1* −1.04	*Nfkb1* 1.07	*Nfkbia* −1.17	*Nme4* −1.31	*Pdgfa* −1.04	*Pdgfb* 1.09
F	*Pik3r1* 1.30	*Plau* 1.52	*Plaur* 1.38	*Pten* −1.07	*Raf1* −1.17	*Rb1* 1.03	*S100a4* 1.30	*Serpinb2* −1.20	*Serpine1* −1.19	*Syk* 1.42	*Tek* 1.12	*Tert* −1.66
G	*Tgfb1* 1.38	*Tgfbr1* −1.06	*Thbs1* 2.37	*Timp1* −1.20	*Tnf* −1.45	*Tnfrsf10b* 2.07	*Tnfrsf1a* 1.05	*Trp53* −1.03	*Twist1* −1.03	*Vegfa* 1.03	*Vegfb* 1.48	*Vegfc* 1.36

Gene expression between Tg and WT mice at 25 weeks after DEN treatment was compared using RT^2 Profiler version 3.2, a Web-based software package for the Profiler PCR array system (SABiosciences-Qiagen, Frederick, MD; *http://www.sabiosciences.com/pcr/arrayanalysis.php*); this software automatically performs all $\Delta\Delta C_T$-based fold-change calculations from the specific uploaded raw threshold cycle data.

medium than did CHL-V (Figure 5C). The contribution of COX-2 to this process was confirmed by the inhibition of PGE_2 synthesis after treating the cells with 5 μmol/L DFU. The CHL-C cell number after 72 hours of culture in 10% (v/v) FBS was greater (150%) than that of CHL-V (Figure 5D). COX-2/PGE_2 levels were not modified by the effect of PB/DEN treatment (data not shown).

Next, we evaluated the contribution of COX-2 activity to cell viability after PB/DEN treatment, assessed by the MTT reduction assay. No significant differences were found between CHL-V and CHL-C cells, although DEN treatment decreased cell survival by approximately 50% (Figure 5E). Similar results were obtained when LDH activity was measured (data not shown). Oxidative damage of DNA was analyzed by measuring the 8-OH-dG levels, and CHL-C cells exhibited a higher content (1.6 fold) of 8-OH-dG than CHL-V after DEN treatment (Figure 5F). ROS production was analyzed in CHL-V and CHL-C cells after DEN treatment, and ROS production was significantly increased in CHL-C cells, compared with CHL-V without DEN treatment (1.5 fold) (Figure 5G). No differences in fluorescence between cells were found when carboxy-DCFH-DA was used (0.52 vs 0.48 fluorescence units/mg protein for CHL-V and CHL-C, respectively). As expected, the levels of glutathione were lower in the CHL-C cells without treatment (Figure 5H). To identify signaling pathways that affect hepatocyte proliferation, we examined the phosphorylation of several protein kinases. An increase in the p-JNK1/JNK1, p-Erk/Erk, p-p38/p-38, and p-Stat3/Stat3 ratios was observed in both CHL-V and CHL-C cells after 2 to 4 hours of PB/DEN treatment, with some significant differences (Figure 6, A and B).

Transforming Activity and Growth of CHL Cells Implants in Nude Mice

The proliferation of CHL-V and CHL-C cells with and without PB/DEN treatment was compared by soft-agar colony formation assays. The number and size of the colonies formed by CHL-C cells treated with PB/DEN were similar to those formed by CHL-V (Figure 7, A–C). Finally, we evaluated the growth of transplanted CHL-V and CHL-C cells with and without PB/DEN treatment in nude mice. PB/DEN treatment increased the tumor area at the end of the treatment by 1.7 and 3.2 fold in CHL-V and CHL-C, respectively (Figure 7D). Of note, a significant increase in tumor area due to the effect of COX-2-dependent PGs was observed (2.2 fold) (Figure 7E).

Discussion

In the present study, we analyzed the role of COX-2 in the development of chronic liver disease, hepatitis, fibrosis, and chemical hepatocarcinogenesis, by using both *in vivo* and *in vitro* models of constitutive COX-2 expression and elevated PGE_2 synthesis in the hepatocyte. Our results demonstrate that aged COX-2 Tg mice develop mild hepatitis, but COX-2 does not appear to mediate the development of liver fibrosis. COX-2 favors early assessment of preneoplastic foci, but it is not sufficient to enhance malignant transformation and HCC induced by DEN.

Ectopic expression of COX-2 in hepatocytes constitutes a nonphysiopathological condition[26] and, therefore, the generation and characterization of COX-2 genetically altered mice models may help to clarify the phenotypic changes related to COX-2 activity in normal hepatocytes and might facilitate the identification of the mechanisms by which COX-2 contributes to liver pathology. In previous work, we generated and partially characterized the first model of Tg mice carrying human hCOX-2 under the control of the human Apo E promoter.[21] Prostaglandin synthesis in hepatocytes exerted an efficient protection against acute liver injury by antiapoptotic/antinecrotic mechanisms and by accelerating early hepatocyte proliferation.[27] Recently, two other models of COX-2 Tg mice have been published, in which COX-2 is expressed under the control of the transthyretin promoter[28] or the albumin enhancer promoter[29]; on challenge with proinflammatory stimuli, the animals behave very differently. Expression of COX-2 under the albumin-enhancer promoter produces very low levels of PGE_2, and animals show increased injury after endotoxin challenge. More-

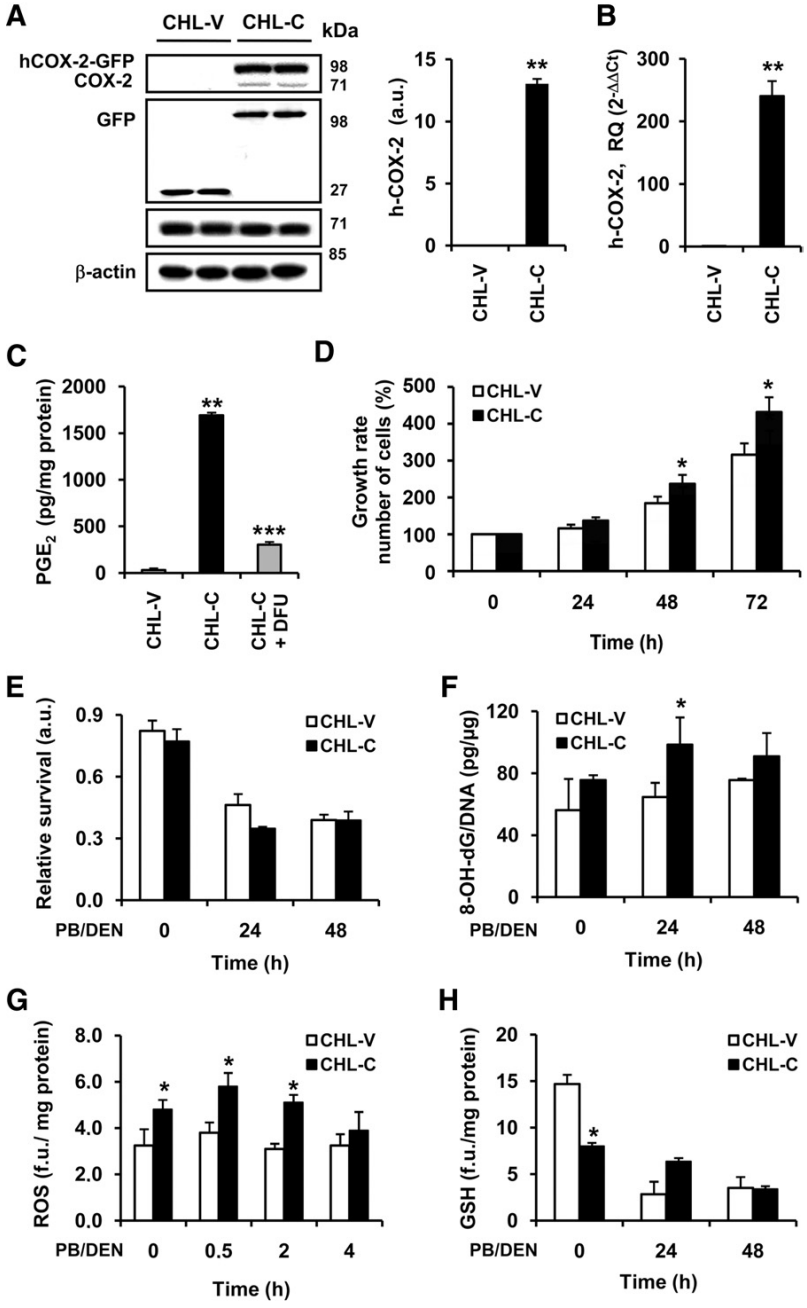

Figure 5. Characterization of CHL cells expressing COX-2 after DEN treatment. CHL cells were stably transfected with empty pPyCAGIP-GFP vector (CHL-V) or pPyCAGIP-hCOX-2-GFP encoding human COX-2 (CHL-C). For *in vitro* PB/DEN protocol, CHL-C and CHL-V cells were incubated with 1.5 mmol/L PB for 16 hours following by 15 mmol/L DEN for 24 to 48 hours. **A:** hCOX-2-GFP and COX-1 expression in whole cell extracts were detected by Western blot and normalized with β-actin. **B:** qPCR analysis of COX-2 mRNA expression. COX-2 mRNA amounts were calculated as RQ and normalized to the expression of 36b4 mRNA. Values represent fold change relative to CHL-V. **C:** PGE_2 production determined by enzyme immunoassay in the culture medium of CHL-V and CHL-C cells. **D:** Growth rate of CHL-V and CHL-C cells. **E:** Cell viability was measured after PB/DEN treatment at 24 and 48 hours as indicated in *Materials and Methods* using the MTT assay. **F:** Oxidative damage of DNA was analyzed in cultured cells under PB/DEN treatment by measuring the levels of 8-OH-dG by immunoassay. Intracellular content of ROS (**G**) and glutathione (GSH) (**H**) were measured by using the fluorescent probes H_2DCFDA and monochlorobimane, respectively. Data are reported as means ± SD of four independent experiments. $^*P < 0.05$ and $^{**}P < 0.001$ vs the CHL-V control cells treated under identical conditions. $^{***}P < 0.05$ vs CHL-C cells without DFU treatment.

over, in the same model, this COX-2 transgene accelerates endotoxin-induced acute liver failure[29] but prevents Fas-induced liver injury.[30] The expression of hCOX-2 under the transthyretin promoter produced the highest levels of intrahepatic PGE_2 and induced hepatitis in animals more than 12 months of age, characterized by the activation of NF-κB, stimulation of the secretion of proinflammatory cytokines, and enhanced macrophage and lymphocyte infiltration.[28] These data are in agreement with the results we observed in aged animals.

Chronic liver injury can promote fibrosis, characterized by proliferation of hepatic stellate cells and their change to myofibroblast-like cells, leading to extracellular matrix and collagen accumulation. Activated hepatic stellate cells but not quiescent hepatic stellate cells express COX-2, suggesting that this pathway has an active role in hepatic fibrogenesis. Nonetheless, data regarding the role of COX-2 on liver fibrotic process are controversial, with reports describing both exacerbation of fibrogenesis[31] and amelioration of fibrogenesis, through the induction of celecoxib-mediated

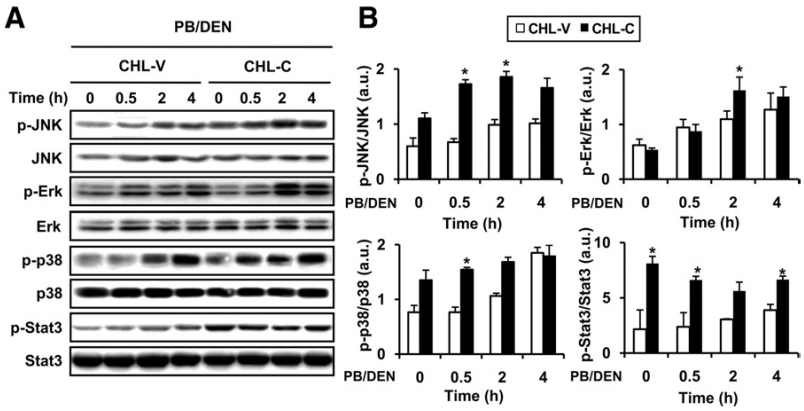

Figure 6. Signaling pathways implicated in proliferation in CHL cells expressing COX-2 after DEN treatment. **A:** Representative Western blots showing the phosphorylation of JNK, Erk, p38, and Stat3 in CHL-V and CHL-C cells after PB/DEN treatment at the indicated times. The expression of target proteins was normalized to that of β-actin. **B:** Densitometric analysis of the expression of the ratios p-JNK/JNK, p-Erk/Erk, p-p38/p38, and p-Stat3/Stat3 in CHL-V and CHL-C cells after DEN treatment. Data are reported as means ± SD of four independent experiments. $^{*}P < 0.05$ vs the CHL-V control cells treated under identical conditions.

apoptosis of hepatic stellate cells.[32] Our results, however, and those of others[33] using COX-2 Tg mice clearly demonstrate that COX-2 expression did not influence liver fibrogenesis even after feeding with the MCD diet.

Several lines of evidence suggest that COX-2 signaling is implicated in hepatocarcinogenesis and that COX-2 inhibitors prevent HCC cell growth *in vitro* and in animal models.[23] Increased COX-2 expression has been found in human HCC, in which COX-2 is highly expressed at early stages but is down-regulated in advanced stages, and with changes in the areas of expression in tumor versus nontumor adjacent tissue.[15] To clarify the contribution of COX-2 to the development of HCC, we used three complementary approaches: i) DEN-induced chemical hepatocarcinogenesis in COX-2 Tg mice, ii) PB/DEN treatment of human COX-2 Tg hepatocyte-like cells, and iii) COX-2 Tg hepatocyte-like cells implants in nude mice.

Both p53 and JNK are well known markers of the genotoxic and cytotoxic effects induced by DEN.[2] Of note, both WT and COX-2 Tg mice exhibited an important decrease of p53 (involved in G1 cell arrest) and an increase of c-Jun levels after DEN treatment. COX-2 has been reported to promote tumorigenesis by functional inactivation of p53 under genotoxic stress,[34] and p53 expression declined notably in hepatocytes expressing COX-2.[35] The levels of p53 declined in our models with DEN treatment, but COX-2 expression did not modify these changes.

Analysis of cell cycle proteins in WT and COX-2 Tg liver showed a significant difference of cyclin E levels. These results suggest that the presence of COX-2 accelerated early hepatocyte proliferation in this *in vivo* model of HCC, corroborating previous results, and that COX-2 expression could be related to its anti-apoptotic

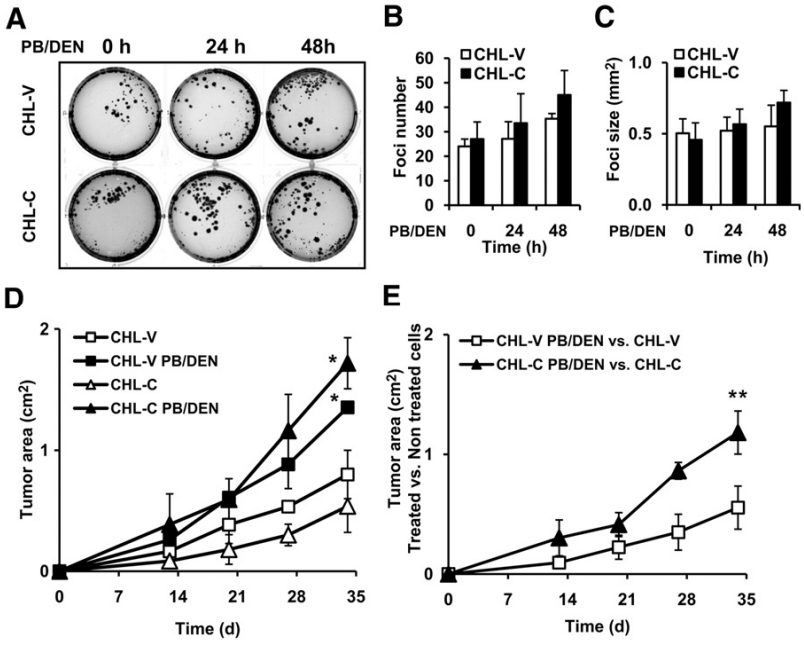

Figure 7. Soft agar colony formation and growth of CHL-V and CHL-C cells implants in nude mice. **A:** CHL-V and CHL-C cells without or with PB/DEN treatment protocol were maintained 72 hours with 10% FBS, plated in soft agar as described in *Materials and Methods* and were incubated for 21 days. A representative experiment is shown. The number (**B**) and size (**C**) of colonies were quantified by soft agar analysis. **D:** CHL-V and CHL-C cells without or with PB/DEN treatment were injected in nude mice as described in experimental procedures and tumor area was measured. **E:** The ratio between treated vs untreated CHL-V or CHL-C cells, related to tumor area. Data are reported as means ± SD of three different experiments or four animals per conditions. $^{*}P < 0.05$ vs the CHL-V or the CHL-C cells without treatment. $^{**}P < 0.05$ vs CHL-V control cells.

effect and inflammatory phenomena in the early phases of HCC.[27]

Enhancement of liver tumorigenesis by DEN administration was seen after hepatocyte-specific ablation in IKKβ, p38α, and IKKγ/NEMO deficient mice.[18] It was proposed that enhanced liver damage and hepatocyte death driven by ROS accumulation could explain augmented HCC development in all these mouse genetic models.[36] In agreement with these data, in the present study COX-2 Tg hepatocyte-like cells exhibited elevated oxidative stress and ROS accumulation after DEN administration, together with an important decrease in the levels of glutathione. Indeed, ROS production may cause oxidative DNA damage, reflected by a higher level of anti-8-OHdG reactivity in COX-2 Tg cells.

The JNKs are activated by stress signals, pro-inflammatory stimuli, and some mitogenic signals and are required for hepatocyte proliferation after partial hepatectomy.[37] JNK1-deficient mice are much less susceptible to DEN-induced HCC development, whereas prolonged activation of JNK1 is a principal mechanism by which the absence of hepatocyte IKKβ results in increased susceptibility to DEN-induced hepatocarcinogenesis.[38] Erk, JNK/SAPK, and p38 contribute to COX-2 expression, and the anti-inflammatory activity of many compounds is a function of COX-2 inhibition via JNK and p38 MAPK inactivation.[39] The effect of COX-2-dependent PGs on these signaling pathways have been recently studied using cell lines stably overexpressing COX-2.[40] Our data in COX-2 Tg hepatocyte-like cells verify moderate activation of JNK, Erk, and p38 in CHL-C cells.

How hepatocyte death promotes HCC development is not clear, but it was proposed that necrotic hepatocytes release IL-1α, which induces IL-6 production by Kupffer cells, and that this response drives the compensatory proliferation of surviving hepatocytes, involving Stat3 activation.[36] He et al,[41] using liver-specific Stat3 knockout mice, found that this transcriptional target for IL-6 is required for HCC development and that hepatocyte NF-κB inhibits tumor promotion and progression by preventing oxidative stress-driven Stat3 activation. Furthermore, expression of IL-6, a major Stat3 activator in the liver, is elevated in cirrhosis and in HCC.[42] Moreover, activation of COX-2/PGE_2 enhances Stat3 phosphorylation through EP-1 receptor-induced activation of c-Src and EGFR in human cholangiocarcinoma cells and in non-small-cell lung cancer.[43] We observed a moderate increase of Stat3 phosphorylation in CHL-C cells, in agreement with an elevated oxidative stress and ROS accumulation, together with a significant decrease in the levels of glutathione even without PB/DEN treatment.

Targets of PGs through their EP receptors are the PI3K and the Akt/PKB (protein kinase B) pathways. Akt improves cellular energy stores by accelerating cell proliferation and size, and induces anti-apoptotic effects by phosphorylation and inactivation of the proapoptotic protein Bad and up-regulation of Bcl-2 and Mcl-1.[44] Our previous studies showed that, in COX-2 Tg hepatocyte-like cells and in COX-2 Tg liver, Akt phosphorylation is enhanced, compared with WT cells, indicating a reinforcement of survival pathways.[27,35] The present data show that COX-2 moderately increased the growth of CHL cell implants in nude mice, which may be due to the modulation of Akt and JNK-c-Jun pathways.[23]

Tumor initiation occurred in the present study through DEN-induced mutagenesis, which induces genetic changes that cause proto-oncogene activation (c-*Myc*) and/or loss of tumor suppressors (p53). After initiation, tumor promotion is needed for expansion of altered cells into premalignant lesions that progress into malignant tumors. Our results show that, although COX-2 induces changes in different signaling pathways implicated in the initiation, promotion, and expansion of liver cells, other genes besides the COX-2 gene are needed to enhance liver tumorigenesis caused by DEN. Furthermore, COX-2 was detected in WT tumor tissue at the end of DEN treatment, indicating that endogenous COX-2 expression is a late event in HCC development. These results, together with the high pulmonary metastatic incidence of HCC in Tg mice and the promotion and migration of HCC cells induced by PGE_2,[12] suggest that COX-2 might be implicated in the expansion and metastatic phase of HCC.

In conclusion, our results demonstrate that COX-2 Tg mice develop subclinical hepatitis, but that COX-2 does not appear to mediate the development of liver fibrosis in the absence of a broad proinflammatory onset. COX-2 expression is not sufficient to enhance malignant transformation induced by DEN, and it is a late event in the development of HCC.

Acknowledgments

We thank Carlos Grau for the morphometric analysis and Verónica Terrón for technical assistance.

References

1. Llovet JM, Bruix J: Molecular targeted therapies in hepatocellular carcinoma. Hepatology 2008, 48:1312–1327
2. Maeda S, Kamata H, Luo JL, Leffert H, Karin M: IKKbeta couples hepatocyte death to cytokine-driven compensatory proliferation that promotes chemical hepatocarcinogenesis. Cell 2005, 121:977–990
3. Simmons DL, Botting RM, Hla T: Cyclooxygenase isozymes: the biology of prostaglandin synthesis and inhibition. Pharmacol Rev 2004, 56:387–437
4. Ledwith BJ, Pauley CJ, Wagner LK, Rokos CL, Alberts DW, Manam S: Induction of cyclooxygenase-2 expression by peroxisome proliferators and non-tetradecanoylphorbol 12,13-myristate-type tumor promoters in immortalized mouse liver cells. J Biol Chem 1997, 272:3707–3714
5. Martín-Sanz P, Callejas NA, Casado M, Díaz-Guerra MJ, Boscá L: Expression of cyclooxygenase-2 in foetal rat hepatocytes stimulated with lipopolysaccharide and pro-inflammatory cytokines. Br J Pharmacol 1998, 125:1313–1319
6. Callejas NA, Boscá L, Williams CS, Du BR, Martín-Sanz P: Regulation of cyclooxygenase 2 expression in hepatocytes by CCAAT/enhancer-binding proteins. Gastroenterology 2000, 119:493–501
7. Pham H, Eibl G, Vincenti R, Chong B, Tai HH, Slice LW: 15-Hydroxyprostaglandin dehydrogenase suppresses K-RasV12-dependent tumor formation in Nu/Nu mice. Mol Carcinog 2008, 47:466–477
8. Casado M, Callejas NA, Rodrigo J, Zhao X, Dey SK, Boscá L, Martín-Sanz P: Contribution of cyclooxygenase 2 to liver regeneration after partial hepatectomy. FASEB J 2001, 15:2016–2018
9. Rudnick DA, Perlmutter DH, Muglia LJ: Prostaglandins are required for CREB activation and cellular proliferation during liver regeneration. Proc Natl Acad Sci USA 2001, 98:8885–8890

10. Yamamoto H, Kondo M, Nakamori S, Nagano H, Wakasa K, Sugita Y, Chang-De J, Kobayashi S, Damdinsuren B, Dono K, Umeshita K, Sekimoto M, Sakon M, Matsuura N, Monden M: JTE-522, a cyclooxygenase-2 inhibitor, is an effective chemopreventive agent against rat experimental liver fibrosis1. Gastroenterology 2003, 125:556–571
11. Kern MA, Haugg AM, Koch AF, Schilling T, Breuhahn K, Walczak H, Fleischer B, Trautwein C, Michalski C, Schulze-Bergkamen H, Friess H, Stremmel W, Krammer PH, Schirmacher P, Müller M: Cyclooxygenase-2 inhibition induces apoptosis signaling via death receptors and mitochondria in hepatocellular carcinoma. Cancer Res 2006, 66:7059–7066
12. Mayoral R, Fernández-Martinez A, Boscá L, Martin-Sanz P: Prostaglandin E2 promotes migration and adhesion in hepatocellular carcinoma cells. Carcinogenesis 2005, 26:753–761
13. Cheng AS, Yu J, Lai PB, Chan HL, Sung JJ: COX-2 mediates hepatitis B virus X protein abrogation of p53-induced apoptosis. Biochem Biophys Res Commun 2008, 374:175–180
14. Núñez O, Fernández-Martínez A, Majano PL, Apolinario A, Gómez-Gonzalo M, Benedicto I, López-Cabrera M, Boscá L, Clemente G, García-Monzón C, Martín-Sanz P: Increased intrahepatic cyclooxygenase 2, matrix metalloproteinase 2, and matrix metalloproteinase 9 expression is associated with progressive liver disease in chronic hepatitis C virus infection: role of viral core and NS5A proteins. Gut 2004, 53:1665–1672
15. Cusimano A, Fodera D, Lampiasi N, Azzolina A, Notarbartolo M, Giannitrapani L, D'Alessandro N, Montalto G, Cervello M: Prostaglandin E2 receptors and COX enzymes in human hepatocellular carcinoma: role in the regulation of cell growth. Ann N Y Acad Sci 2009, 1155:300–308
16. Cha YI, DuBois RN: NSAIDs and cancer prevention: targets downstream of COX-2. Annu Rev Med 2007, 58:239–252
17. Calvisi DF, Factor VM, Ladu S, Conner EA, Thorgeirsson SS: Disruption of beta-catenin pathway or genomic instability define two distinct categories of liver cancer in transgenic mice. Gastroenterology 2004, 126:1374–1386
18. Luedde T, Beraza N, Kotsikoris V, van Loo G, Nenci A, De Vos R, Roskams T, Trautwein C, Pasparakis M: Deletion of NEMO/IKK-gamma in liver parenchymal cells causes steatohepatitis and hepatocellular carcinoma. Cancer Cell 2007, 11:119–132
19. Pikarsky E, Porat RM, Stein I, Abramovitch R, Amit S, Kasem S, Gutkovich-Pyest E, Urieli-Shoval S, Galun E, Ben-Neriah Y: NF-kappaB functions as a tumour promoter in inflammation-associated cancer. Nature 2004, 431:461–466
20. Haybaeck J, Zeller N, Wolf MJ, Weber A, Wagner U, Kurrer MO, Bremer J, Iezzi G, Graf R, Clavien PA, Thimme R, Blum H, Nedospasov SA, Zatloukal K, Ramzan M, Ciesek S, Pietschmann T, Marche PN, Karin M, Kopf M, Browning JL, Aguzzi A, Heikenwalder M: A lymphotoxin-driven pathway to hepatocellular carcinoma. Cancer Cell 2009, 16:295–308
21. Casado M, Mollá B, Roy R, Fernández-Martínez A, Cucarella C, Mayoral R, Boscá L, Martín-Sanz P: Protection against Fas-induced liver apoptosis in transgenic mice expressing cyclooxygenase 2 in hepatocytes. Hepatology 2007, 45:631–638
22. Goldsworthy TL, Fransson-Steen R: Quantitation of the cancer process in C57BL/6J, B6C3F1 and C3H/HeJ mice. Toxicol Pathol 2002, 30:97–105
23. Kern MA, Schoneweiss MM, Sahi D, Bahlo M, Haugg AM, Kasper HU, Dienes HP, Kaferstein H, Breuhahn K, Schirmacher P: Cyclooxygenase-2 inhibitors suppress the growth of human hepatocellular carcinoma implants in nude mice. Carcinogenesis 2004, 25:1193–1199
24. De la Cueva E, García-Cao I, Herranz M, López P, García-Palencia P, Flores JM, Serrano M, Fernández-Piqueras J, Martín-Caballero J: Tumorigenic activity of p21Waf1/Cip1 in thymic lymphoma. Oncogene 2006, 25:4128–4132
25. Freeman JE, Stirling D, Russell AL, Wolf CR: cDNA sequence, deduced amino acid sequence, predicted gene structure and chemical regulation of mouse Cyp2e1. Biochem J 1992, 281:689–695
26. Martín-Sanz P, Mayoral R, Casado M, Boscá L: COX-2 in liver, from regeneration to hepatocarcinogenesis: what we have learned from animal models? World J Gastroenterol 2010, 16:1430–1435
27. Mayoral R, Mollá B, Flores JM, Boscá L, Casado M, Martín-Sanz P: Constitutive expression of cyclo-oxygenase 2 transgene in hepatocytes protects against liver injury. Biochem J 2008, 416:337–346
28. Yu J, Hui AY, Chu ES, Cheng AS, Go MY, Chan HL, Leung WK, Cheung KF, Ching AK, Chui YL, Chan KK, Sung JJ: Expression of a cyclo-oxygenase-2 transgene in murine liver causes hepatitis. Gut 2007, 56:991–999
29. Han C, Li G, Lim K, DeFrances MC, Gandhi CR, Wu T: Transgenic expression of cyclooxygenase-2 in hepatocytes accelerates endotoxin-induced acute liver failure. J Immunol 2008, 181:8027–8035
30. Li G, Han C, Xu L, Lim K, Isse K, Wu T: Cyclooxygenase-2 prevents fas-induced liver injury through up-regulation of epidermal growth factor receptor. Hepatology 2009, 50:834–843
31. Hui AY, Leung WK, Chan HL, Chan FK, Go MY, Chan KK, Tang BD, Chu ES, Sung JJ: Effect of celecoxib on experimental liver fibrosis in rat. Liver Int 2006, 26:125–136
32. Paik YH, Kim JK, Lee JI, Kang SH, Kim DY, An SH, Lee SJ, Lee DK, Han KH, Chon CY, Lee SI, Lee KS, Brenner DA: Celecoxib induces hepatic stellate cell apoptosis through inhibition of Akt activation and suppresses hepatic fibrosis in rats. Gut 2009, 58:1517–1527
33. Yu J, Wu CW, Chu ES, Hui AY, Cheng AS, Go MY, Ching AK, Chui YL, Chan HL, Sung JJ: Elucidation of the role of COX-2 in liver fibrogenesis using transgenic mice. Biochem Biophys Res Commun 2008, 372:571–577
34. Choi EM, Kim SR, Lee EJ, Han JA: Cyclooxygenase-2 functionally inactivates p53 through a physical interaction with p53. Biochim Biophys Acta 2009, 1793:1354–1365
35. Fernández-Martínez A, Mollá B, Mayoral R, Boscá L, Casado M, Martín-Sanz P: Cyclo-oxygenase 2 expression impairs serum-withdrawal-induced apoptosis in liver cells. Biochem J 2006, 398:371–380
36. Sakurai T, He G, Matsuzawa A, Yu GY, Maeda S, Hardiman G, Karin M: Hepatocyte necrosis induced by oxidative stress and IL-1 alpha release mediate carcinogen-induced compensatory proliferation and liver tumorigenesis. Cancer Cell 2008, 14:156–165
37. Schwabe RF, Bradham CA, Uehara T, Hatano E, Bennett BL, Schoonhoven R, Brenner DA: c-Jun-N-terminal kinase drives cyclin D1 expression and proliferation during liver regeneration. Hepatology 2003, 37:824–832
38. Sakurai T, Maeda S, Chang L, Karin M: Loss of hepatic NF-kappa B activity enhances chemical hepatocarcinogenesis through sustained c-Jun N-terminal kinase 1 activation. Proc Natl Acad Sci USA 2006, 103:10544–10551
39. Tanabe T, Tohnai N: Cyclooxygenase isozymes and their gene structures and expression. Prostaglandins Other Lipid Mediat 2002, 68–69:95–114.
40. Kim YM, Park SY, Pyo H: Cyclooxygenase-2 (COX-2) negatively regulates expression of epidermal growth factor receptor and causes resistance to gefitinib in COX-2-overexpressing cancer cells. Mol Cancer Res 2009, 7:1367–1377
41. He G, Yu GY, Temkin V, Ogata H, Kuntzen C, Sakurai T, Sieghart W, Peck-Radosavljevic M, Leffert HL, Karin M: Hepatocyte IKKbeta/NF-kappaB inhibits tumor promotion and progression by preventing oxidative stress-driven STAT3 activation. Cancer Cell 2010, 17:286–297
42. Trikha M, Corringham R, Klein B, Rossi JF: Targeted anti-interleukin-6 monoclonal antibody therapy for cancer: a review of the rationale and clinical evidence. Clin Cancer Res 2003, 9:4653–4665
43. Han C, Demetris AJ, Stolz DB, Xu L, Lim K, Wu T: Modulation of Stat3 activation by the cytosolic phospholipase A2alpha and cyclooxygenase-2-controlled prostaglandin E2 signaling pathway. J Biol Chem 2006, 281:24831–24846
44. Schulze-Bergkamen H, Brenner D, Krueger A, Suess D, Fas SC, Frey CR, Dax A, Zink D, Büchler P, Müller M, Krammer PH: Hepatocyte growth factor induces Mcl-1 in primary human hepatocytes and inhibits CD95-mediated apoptosis via Akt. Hepatology 2004, 39:645–654

ARTÍCULO II: ***Am. J. Pathol. 2012 (Enviado).***

La progresión de la oncogénesis hepática en ratones dobles transgénicos c-Myc/TGF-α no está potenciada por la expresión de ciclooxigenasa-2

Llorente Izquierdo C, Mayoral R, Cucarella C, Grau C, García-Palencia P, Agra N, Castro L, Boscá L, Martín-Sanz P and Casado M.

RESUMEN DEL ARTÍCULO II

Existen pocos modelos TG para COX-2 que evalúen la implicación del efecto de las PGs en la carcinogénesis hepática. Por esta razón, se utilizó un modelo genético de CHC bien establecido de ratones TG que expresan c-Myc bajo el promotor de la albumina y TGF-α bajo el promotor de la metalotioneina. Estos ratones se cruzaron con ratones TG que expresan COX-2 en el hepatocito bajo el promotor de la ApoE. Los animales del modelo doble TG c-Myc/TGF-α (DTG) y triple TG c-Myc/TGF-α/COX-2 (TTG) se sacrificaron a los 5 y 9 meses de edad y se siguió el desarrollo del tumor, displasia, foci, adenoma, carcinoma y metástasis pulmonares así como sus parámetros bioquímicos y moleculares.

Se comprobó la expresión de los transgenes. La presencia de c-Myc y del TGF-α fue verificada en ambos modelos TG mientras que la expresión de COX-2 se detectó solamente en los animales TTG. La expresión de las tres proteínas no se modificó con la edad.

A los 5 meses de edad, alrededor de un 90% de los animales DTG y TTG desarrollaron nódulos pre-neoplásicos. Tan solo se observaron tendencias no significativas en una mayor formación de adenomas en los animales DTG (27%) comparado con los animales TTG (9%). Estos datos fueron coherentes con el incremento significativo en el ratio peso de hígado/peso corporal, con la elevación de los niveles de AST y con el aumento, aunque no significativo, de Ki67 en los ratones DTG comparado con los TTG. A pesar de estas diferencias, no se detectaron cambios en la formación de CHC entre ambos modelos que se produjo con una proporción de alrededor de un 9% en los DTG y un 13% en los TTG. A los 9 meses de edad, los animales DTG y TTG presentaron porcentajes parecidos (90 y 100% respectivamente) en el desarrollo de CHC. Se estudiaron las vías de señalización y los cambios en la expresión génica de marcadores específicos de la progresión tumoral para analizar si la presencia o no del transgén de COX-2 era capaz de alterar rutas alternativas en el desarrollo del CHC a pesar de las pocas diferencias detectadas entre los animales DTG y TTG. Se analizó la expresión de proteínas y supresores tumorales relacionadas con el ciclo celular, apoptosis y vías de transducción de señales implicadas en la proliferación de los hepatocitos. Los animales DTG y TTG mostraron alteradas estas vías comparadas con los animales controles y con los animales mono MTG para COX-2 que no desarrollan CHC. Comparando el modelo DTG y TTG solamente se halló un incremento significativo en la expresión del factor de transcripción E2F1, de p53 y de la proteína anti-apoptótica Bcl-2. A pesar de estos resultados, no se encontraron diferencias significativas en los genes proliferación celular (Ccdn1, Cxcr4, Ccne1) ni en los de apoptosis (Birc5, Tnfrsf10b, Gadd45b) analizados por PCR cuantitativa a los 5 meses entre los ratones D y TTG. Estos datos

sugieren que la presencia de COX-2 no altera las vías de transducción de señales relevantes en el desarrollo del CHC en el modelo genético c-Myc/TGF-α.

Además, se analizaron marcadores de buen o mal pronóstico para comprobar el efecto de la inserción del transgén de COX-2. Está descrito que los ratones c-Myc/TGF-α presentan altos niveles de marcadores de CHC de mal pronóstico. A los 5 meses y a los 9 meses de edad, los genes Inhbc y Slc16a2 que son marcadores de buen pronóstico en el CHC, no presentaron diferencias significativas en su expresión entre los animales TTG comparado con los DTG. Tampoco se hallaron diferencias en los genes de mal pronóstico Ask y Gtse1 que juegan un papel importante en la replicación del ADN y la proliferación celular. Los resultados observados indican que la presencia del transgén de COX-2 no altera el mal pronóstico del modelo genético c-Myc/TGF-α de CHC.

Finalmente, dado que la producción de especies reactivas es uno de los factores primordiales en la carcinogénesis mediada por c-Myc/TGF-α se estudió la expresión de iNOS, HO-1, Nfr-2 y la producción de especies reactivas al ácido tiobarbitúrico (TBARS). El análisis del estado redox indicó que efectivamente tanto el modelo DTG como el TTG presentan alteradas proteínas de estrés oxidativo comparando con el modelo MTG de COX-2 y control. A los 9 meses en los ratones TTG se observó un incremento en la producción de TBARS indicativo de una mayor peroxidación lipídica. Sin embargo, entre los modelos DTG y TTG se hallaron exclusivamente tendencias no significativas de un aumento en las proteínas iNOS, HO-1 y Nfr-2. La contribución oxidativa asociada a COX-2 en este modelo genético resultó ser irrelevante probablemente debido a una saturación del sistema oxidativo en el CHC.

Por tanto, las pocas diferencias halladas vinculadas a la presencia del transgén de COX-2, sugieren que su expresión en el hepatocito a los 5 meses de edad podría estar previniendo la hipertrofia e hiperplasia causada por c-Myc/TGF-α. Sin embargo, con la edad, las pequeñas diferencias desaparecen, indicando, en concordancia con nuestros resultados descritos en el modelo de hepatocarcinogénesis química, que las PGs derivadas de COX-2 juegan un papel poco relevante en el desarrollo de la carcinogénesis mediada por c-Myc/TGF-α.

Progression of liver oncogenesis in the double transgenic mice c-myc/TGFα is not enhanced by cyclooxygenase-2 expression

[1]Cristina Llorente-Izquierdo, [1,2]Rafael Mayoral, [4]Carme Cucarella, [4]Carlos Grau, [3]Juana María Flores, [3]Pilar García-Palencia, [1]Noelia Agra, [1]Luis Castro, [1,2]Lisardo Boscá, [♦1,2]Paloma Martín-Sanz and [♦4,2]Marta Casado.

[1]Instituto de Investigaciones Biomédicas Alberto Sols, CSIC-UAM. Madrid. Arturo Duperier, 4, 28029 Madrid, Spain, [2]Centro de Investigación Biomédica en Red de Enfermedades Hepáticas y Digestivas (CIBERehd), Córcega 180, 08036 Barcelona, Spain, [3]Departamento de Medicina y Cirugía Animal, Facultad de Veterinaria, Universidad Complutense, 28040 Madrid, Spain, [4]Instituto de Biomedicina de Valencia, IBV-CSIC, Jaime Roig 11, 46010 Valencia, Spain.

Running title: COX-2 in genetic hepatocarcinogenesis

Financial support: This work was supported by grants SAF2010-16037, SAF2009-12602 and BFU2011-24760 from MICINN, P2010/BMD-2378 from Comunidad de Madrid. CIBERehd is funded by the Instituto de Salud Carlos III. NA was supported by the Carlos III Health Institute (Red de Centros FIS-RECAVA RD06/0014/0025).

♦Corresponding authors

Dr. Marta Casado or Dr. Paloma Martín Sanz, Instituto de Biomedicina de Valencia, IBV-CSIC, Jaime Roig 11, 46010 Valencia, Spain. Instituto de Investigaciones Biomédicas Alberto Sols, CSIC-UAM. Madrid. Arturo Duperier, 4 28029 Madrid, Spain Tel 34914972746, Fax: 34914972748; e-mail: mcasado@ibv.csic.es or pmartins@iib.uam.es.

ABSTRACT

Cyclooxygenase-2 (COX-2) has been associated with cell growth regulation, tissue remodeling and carcinogenesis. Overexpression of COX-2 in hepatocytes constitutes an ideal condition to evaluate the role of prostaglandins (PGs) in liver pathogenesis. The effect of COX-2-dependent PGs in genetic hepatocarcinogenesis has been investigated in triple c-myc/transforming growth factor α (TGF-α) transgenic mice that express human COX-2 in hepatocytes on a B6CBAxCD1xB6DBA2 background. Analysis of the contribution of COX-2-dependent PGs to the development of hepatocarcinogenesis, evaluated in this model, suggested a minor role of COX-2-dependent prostaglandins to liver oncogenesis as indicated by liver histopathology, morphometric analysis and specific markers of tumor progression. This allows concluding that COX-2 is insufficient for modifying the hepatocarcinogenesis course mediated by c-myc/TGF-α.

Abbreviations: COX-2, cyclooxygenase 2; DEN, diethylnitrosamine; HCC, human hepatocellular carcinoma; PGs, prostaglandins; PGE_2, prostaglandin E_2; Tg, transgenic; TGF-α, transforming growth factor α.

Keywords: c-myc, COX-2, HCC, TGF-α, transgenic mice

Human hepatocellular carcinoma (HCC) is a neoplasia with increasing incidence (1). Epidemiological studies suggest that the major risk factors for HCC are persistent infection with hepatitis B and C virus (HBV and HCV) and exposure to genotoxic and cytotoxic chemicals. All these factors cause chronic liver injury and inflammation, conditions in which hepatocytes die and resident inflammatory cells (Kupffer cells), as well as newly recruited inflammatory cells (macrophages, neutrophils, natural killer (NK) and NKT cells), are activated to produce cytokines that conduct the compensatory proliferation of surviving hepatocytes (2).

Cyclooxygenase-1 (COX-1) and -2 catalyze the first step in prostanoid biosynthesis. COX-1 is constitutively expressed in many tissues, whereas COX-2 is induced by a variety of stimuli such as growth factors, pro-inflammatory stimuli, hormones and other cellular stresses (3). Adult hepatocytes fail to induce COX-2 expression regardless of the pro-inflammatory factors used (4, 5); only under prolonged injury, COX-2 is expressed as a result of the drop of C/EBPα levels among other conditions (6). Therefore, ectopic expression of COX-2 in hepatocytes constitutes an ideal condition to evaluate the role of prostaglandins (PGs) in liver pathogenesis. In this regard, we and others demonstrated that partial hepatectomy (PH) induced COX-2 in hepatocytes and contributed to the progression of cell cycle after PH (7, 8). In addition to liver regeneration after PH or hepatotoxic agents, expression of COX-2 has been detected in animal models of cirrhosis (9), in human hepatoma cell lines (10, 11), in human HCC (12) and after HBV and HCV infection (13, 14). However, although COX-2 expression is elevated in the early stages of HCC, many questions remain unsolved regarding the contribution of COX-2-dependent PGs to induce tumorigenesis.

Studies with genetically altered mice have identified many genes associated with HCC. HCC develops spontaneously in transgenic mice overexpressing HBV surface antigen (HBsAg), in mice lacking the methionine adenosyltransferase (MAT) gene *MAT1A* (15), the overexpression of the transforming growth factor α (TGF-α) or the c-Myc protooncogene (16) or the deletion of the IκB kinase (IKK) subunit NEMO/IKKγ (17). HCC development is also increased in mice deficient in the Mdr2P-glycoprotein transporter (18) or carrying a lymphotoxin-transgene (19). The c-myc/TFG-α double transgenic mice develop HCCs with different incidence, kinetics and histopathological features. Co-expression of c-myc and TFG-α transgenes results in a dramatic synergistic effect on liver tumor development when compared with their respective single transgenic lines, including a shorter latency period and a more aggressive phenotype (20).

Our previous work (21) demonstrated that COX-2 expression is not sufficient to enhance malignant transformation induced by diethylnitrosamine (DEN) in a model of transgenic mice expressing COX-2 in hepatocytes. To evaluate whether COX-2 has a prone role in genetic liver tumorigenesis, mice carrying a hepatic human COX-2 transgene were crossed with the c-myc/ transforming growth factor α (TFG-α) double-transgenic mice. The analysis of these triple-transgenic c-myc/TFG-α/COX-2 mice evidenced a minor role of COX-2-dependent prostaglandins to the tumor onset and progression of HCC in a mouse model of aggressive human liver cancer, in agreement with the data obtained in the chemically-induced carcinogenesis model.

MATERIAL AND METHODS

Chemicals.

Antibodies were from Santa Cruz Laboratories (Santa Cruz, CA, USA), Sigma Chemical Co. (St. Louis, MO, USA), Cell Signaling (Boston, MA, USA), Millipore (Bilerica, MA, USA) and Leica Microsystems (Wetzlar, Germany). Reagents were from Roche Diagnostics (Mannheim, Germany) or Sigma Chemical Co (St. Louis, MO, USA). Reagents for electrophoresis were obtained from Bio-Rad (Hercules, CA, USA).

Animal experimentation.

Alb-c-myc (c-myc) and MT-TGF-α (TGF-α) single-transgenic mice were kindly obtained from Dr. S.S. Thorgeirsson at the National Cancer Institute (NCI), Bethesda, Maryland. Hepatocyte COX-2 transgenic mice, generated by pronuclear microinjection on B6DBA2 background, have been described previously (22). Generation of c-myc/TGF-α double transgenic mice (D) was achieved by crossing homozygous B6CBA c-myc and CD-1 TGFα mice as described previously (23). Female heterozygous c-myc/TGF-α transgenic mice were mated to male heterozygous COX-2 mice to generate the wild type, c-myc and TGF-α single transgenic, c-myc/COX-2, TGF-α/COX-2 and c-myc/TGF-α (D) double transgenic mice and c-myc/TGF-α/COX-2 (T) triple animal model, all in a hybrid (B6CBAxCD1xDBA2) background. Expression of TGF-α driven by metallothionein I promoter was maintained by giving mice 50 mM $ZnCl_2$ in drinking water starting at weaning. All the experiments were performed in accordance with the animal care guidelines of the European Union (2010/63/EU), and approved by the Bioethical Committee from Consejo Superior de Investigaciones Científicas (reference projet SAF2010/16037). The animals were given diet and water *ad libitum* and treated according to the

Institutional Care Instructions (Bioethical Commission from Consejo Superior de Investigaciones Científicas, CSIC, Spain).

Male were sacrificed after 5 and 9 months of age and their body and liver weights were recorded before the liver tissues were used for analysis. Livers were photographed and externally visible tumors (≥ 0.5mm) were analyzed using the Metamorph software (Universal Imaging Corp, West Chester, PA, USA). Liver tissues were snap frozen in liquid nitrogen and stored at -80ºC or fixed in 10% buffered formalin. Plasma was obtained by puncture of the retro-orbital venous plexus.

RNA extraction and quantitative real-time PCR analysis.

Total RNA of liver biopsy samples was extracted by using TRIzol reagent (Invitrogen™, Grand Island, NY, USA). Total RNA (1µg) was reverse transcribed using a Transcriptor First Strand cDNA Synthesis Kit following manufacturer's indications (Roche Applied Science). The cDNA was used as template for real-time PCR. qPCR was performed with a MyiQ Real-Time PCR System (Bio-Rad) sequence detector using the SsoFast EvaGreen polymerase method (Bio-Rad) and d(N)6 random hexamer with the primers described in Supplementary Table S1. Specific primers were purchased from Invitrogen. PCR thermocycling parameters were 95°C for 30 s, 40 cycles of 95°C for 5 s, and 60°C for 10 s. Each sample was run in triplicate and was normalized to 36b4 RNA. The replicates were then averaged, and fold induction was determined in a ΔΔCt based fold-change calculations.

Histochemistry analysis.

Samples of liver were fixed in 10% buffered formalin, embedded in paraffin wax, sectioned at 4 µm and stained with hematoxylin and eosin (H&E). Histopathology analysis was carried out by the Department of Medicine and Animal Surgery from

Faculty of Veterinary, Madrid, Spain. Immunohistochemical staining was performed using the streptavidin-biotin-peroxidase complex method as described previously (24). Histological sections were stained following standard procedures with an antibody against the active form of caspase 3 (R&D Systems, Minneapolis, USA) or Ki67 (Novocastra, Newcastle, UK). Five entire areas of each tissue sections (500 cells) were counted.

Western blot analysis.

Extracts from tissue samples (50-100 mg) were obtained as previously described (22). For Western blot analysis, whole-cell extracts were boiled for 5 minutes in Laemmli sample buffer, and equal amounts of protein (20-30 μg) were separated by 10-15% SDS-polyacrylamide electrophoresis gel (SDS-PAGE). The relative amounts of each protein were determined with the polyclonal or monoclonal antibodies described in Supplementary Table 4. After incubation with the corresponding anti-rabbit or anti-mouse horseradish peroxidase conjugated secondary antibody, blots were developed by the ECL protocol (GE Healthcare, Chalfont St Giles, UK). Target protein band densities were normalized with β-actin. The blots were revealed, and different exposition times were performed for each blot with a charged coupling device camera in a luminescent image analyzer (Gel-Doc, Bio-Rad) to ensure the linearity of the band intensities. Densitometric analysis was expressed in arbitrary units.

Determination of metabolites.

Prostaglandin E_2 (PGE_2) was determined in liver tissue by specific immunoassay (Arbor Assays, Ann Arbor, MI, USA) following the instruction of the manufacturer. Amino transferases, ALT and ASP, alkaline phosphatase, ALP, and lactate dehydrogenase, were assayed spectrophotometrically in plasma in the School of Clinic

Biochemistry, Faculty of Pharmacy, Complutense University, Madrid, Spain. Lipid peroxidation was determined by the reaction of TBA with malondialdehyde (MDA), a product formed by lipid peroxidation. Extracts from liver tissue (30 mg) were homogenized with 300 µl of 0.15 M KCl. 50 µl of liver homogenate were incubated for 60 min at 95 ºC with 0.3% TBA pH 3-3.5, 0.5% SDS and 7,5% acetic acid. The mixture was centrifuged at 4000g for 10 min. The amount of TBA reactive substances (TBARS) was expressed in terms of 1,1,3,3-tetramethoxypropane (TMP) as standard. Levels of MDA equivalents were determined by absorbance at 532nm and the results were expressed as nmol of MDA per mg of protein. Protein levels were determined with Bradford reagent (Bio-Rad).

Data analysis.

Data are expressed as means ± standard deviation (SD). Individual pair-wise comparisons were performed with Mann-Whitney U test for ordinal variables. A p value of ≤ 0.05 was considered significant.

RESULTS

Effects of hepatic COX-2 expression on tumor development in c-myc/TGF-α transgenic mice.

First we confirmed the presence of the transgenes human COX-2, c-myc and TGF-α in c-myc/TGF-α (D) and c-myc/TGF-α/COX-2 (T) livers. c-myc and TGF-α proteins were detected in both models whereas human COX-2 was only detected in the triple transgenic mice as expected. The expression of the three proteins did not change with the age of the animals (Fig. 1A). The intrahepatic PGE_2 levels were tenfold higher in c-myc/TGF-α/COX-2 mice *vs.* c-myc/TGF-α animals (Fig. 1B). The liver/body

weight ratio and plasma levels of liver injury markers are given in Table 1. There was a significant decrease of liver and body weight and the liver/body weight ratio in T mice at 5 months-old-age as well as in aspartate transaminase (AST) *vs.* D mice.

Macroscopic view of c-myc/TGF-α and c-myc/TGF-α/COX-2 representative livers showed some D and T mice with abnormal masses at 5-months-old-age whereas all the animals presented tumoral abscess at 9-months-old-age (Fig. 1C). An extensive morphometric analysis revealed no significant differences in the number, size and tumor area of detectable tumors (Fig. 1D-F). Most of the c-myc/TGF-α double (93.3%) and c-myc/TGF-α/COX-2 triple (90.9%) transgenic mice sacrificed at 5-months-old-age had preneoplasic foci (Table 1). Furthermore, the histological analysis of liver biopsies revealed that D mice showed a tendency to develop more adenomas than T mice (26.7 *vs.* 9.1%) without any significant differences in the percentage of hepatocellular carcinomas (13.3 *vs* 9.1%). After 9 months, 89-100% of both D and T Tg mice developed HCC (Table 1). At 5 months the incidence of adenomas in c-myc/TGF-α mice (C57BL/6xCBAxCD1xDBA2) was lower than the double transgenic mice in the original background (C57BL/6xCBAxCD1; 26.7 *vs* 60%) (23).

The ratio of liver/body weight provided the first indication of the abnormal liver growth in the transgenic mice. As we had observed a significant difference in the liver/body weight ratio between T and D transgenic mice, we measured the apoptotic rate in D and T Tg mice by quantifying the percentage of cells with active caspase 3 and the mitotic index measured by Ki67 immunohistochemistry. Caspase 3 staining was scarcely detected and Ki67 staining was lower, although not significant, in T Tg mice at 5 months-old-age indicating that at this stage the presence of COX-2 might inhibit the proliferation induced by c-myc/TGF-α (Fig. 2B-C).

We also analyzed the corresponding monogenic, c-myc and TGF-α, and the double transgenic, c-myc/COX-2 and TGF-α/COX-2 lines, and the results given in supplementary Table S3 showed no significant differences in plasma injury levels and in the histological analysis because the presence or absence of COX-2.

COX-2 Tg liver tumors showed no differences in several signaling pathways comparing with* c-myc/TGF-α *Tg liver.

To further deepen in the potential role of overexpression of COX-2 in the liver tumorigenesis induced by c-myc/TGF-α proto-oncogenes, cell cycle regulators and tumor suppressors were analyzed in liver samples. As shown in Fig. 3A-B, an important increase in several proteins was measured in D and T liver *vs.* wild-type (C) or COX-2 monogenic (M) mice. However, no changes were observed in the protein levels of pRb, PCNA, cyclin D1, cyclin E and p21 between T and D at 5 or 9 months-old-age transgenic liver. E2F1 and p53 protein levels were up-regulated in T mice at 9 months-old-age. To identify signalling pathways that affect hepatocyte proliferation, we examined the phosphorylation of several protein kinases. As expected the pErk/Erk, pJNK/JNK, p-p38/p38 and pStat3/Stat3 ratios were increased in D and T mice compared with C or M but no changes were found in the ratios in T liver *vs.* D (Fig. 4A-B). Next, we analyzed survival signals such as the levels of p-Akt (Ser^{473}) and p-p70S6K. Again no differences were found in the presence or absence of COX-2, except for an increase of Bcl-2 protein levels observed in T mice at 9 months-old-age (Fig. 5A-B). To gain further insight into the response of c-myc/TGF-α/COX-2 Tg vs. c-myc/TGF-α liver, several genes related with cell proliferation (Ccnd1, Cxcr4, Ccne1) and apoptosis (Bir5, Tnfrsf10b, Gadd45b) were analyzed by real-time PCR (Fig. 6A). The results confirm the data obtained by Western blot and suggest that the presence of

COX-2 did not modulate the cell proliferation and apoptosis at 5 months-old age observed in c-myc/TGF-α transgenic mice.

c-myc/TGF-α transgenic mice have higher expression of poor prognostic markers similar to those of the poorer survival group of human HCC (Subclass A) (25). We measured the expression of some genes in liver tissue from 5 and 9 months-old-age c-myc/TGF-α/COX-2 (T) *vs.* c-myc/TGF-α (D) transgenic mice. As shown in Fig. 6B, mRNA levels of Ask (Activator of S phase kinase), Gtse1 (G-2 and S-phase expressed 1), both genes playing a central role in DNA replication and cell proliferation, Slc16a2 (Solute carrier family 16, member 2, monocarboxylate transporter 8), which is the transporter of thyroid hormone, and Inhbc (Inhibin beta C chain), a member of TGF-β superfamily involved in growth and differentiation of various cell types, did not change between D and T mice.

Finally, as previous data indicated ROS as the primary carcinogenic agent in the c-myc/TGF-α over expressing livers (26), genes related with ROS production such as inducible nitric oxide synthase (15), heme oxygenase-1 (HO-1), the nuclear transcription factor (erythroid-derived 2) like 2 (Nrf-2) and thiobarbituric acid reactive substances (TBARS) levels were measured (Fig. 7A-C). We found a significant increase in the protein levels of iNOS, HO-1 and Nrf-2 in D and T Tg liver compared with wild type (C) and COX-2 transgenic mice without detecting changes between D and T mice. MDA levels were increased in the presence of COX-2 at 9 months-old-age.

DISCUSSION

Hepatocellular carcinoma remains a disease with a poor prognosis despite recent advances in the pathophysiology and treatment. COX-2 expression in hepatocytes is

restricted to those situations in which dedifferentiation or proliferation occur, suggesting an important role for PGs in the onset of liver pathologies including HCC (27). In this study, we have analyzed the role of COX-2 in the development of HCC by using *in vivo* models of constitutive COX-2 expression and elevated PGE_2 synthesis in the hepatocyte together with a well-established mouse model of genetic liver cancer, the double-transgenic c-myc/TGF-α mice. Our results demonstrate that COX-2 dependent PGs do not contribute to acceleration or differential tumor onset and progression of HCC.

During the last years, different models of transgenic (Tg) mice over expressing COX-2 have been published and all of them exhibited some kind of neoplasia or preneoplastic conditions offering the rationale for a therapeutic intervention via COX-2 pharmacologic targeting. Abnormal differentiation of epidermis and an increase in mouse skin carcinogenesis have been described in keratinocytes (28). However, Bol et al. reported that COX-2 over expression in the skin results in suppression of tumor development (29). Moreover, cognitive deficits and neuronal apoptosis were reported in Tg mice that overexpressed COX-2 in neurons (30). Tg mice over expressing COX-2 gene in mammary glands developed tumorigenesis (31). Double COX-2/mPGES-1 Tg mice, developed hyperplasic gastric tumors induced by activated macrophages; moreover this pathway contributes to the helicobacter-associated gastric tumorigenesis (32). Dysplastic changes and preinvasive duct-derived neoplasms have been described in pancreas and urinary bladder respectively of transgenic mice with keratin 5 promoter-driven COX-2 over expression (33, 34). Concerning liver, several lines of evidence suggest that COX-2 signaling is implicated in hepatocarcinogenesis and that COX-2 inhibitors prevent cell growth in hepatoma cells (35).

To clarify the role of COX-2 in liver tumorigenesis, we used transgenic mice expressing human COX-2 constitutively in hepatocytes under the control of the human ApoE promoter (COX-2 Tg). PGs exert an efficient protection against acute liver injury by an antiapoptotic/antinecrotic effect and by accelerated early hepatocyte proliferation (22, 36). When chronic liver injury was studied in COX-2 Tg mice, mild hepatitis was developed in 60-week-old-mice but COX-2 failed to contribute to the development of liver fibrogenesis after methionine and choline deficient diet (21).

We have crossed these COX-2 Tg mice with a mouse model of aggressive human liver cancer. Co-expression of c-myc and TGF-α proto-oncogenes has been frequently detected in HCC, suggesting a crucial role for these genes in the malignant growth of the liver. TGF-α/c-myc mice not only developed tumors more rapidly than either of the parental lines, but the multiplicity and tumor size were significantly increased, indicating escalation of both initiation and promotion stages of cancer development. Thus, combined up-regulation of c-myc and TGF-α resulted in a rapid progression from early preneoplastic focal lesions to HCC in 4 months with 100% frequency of HCC before 8 months and survival reduced to 1 year (23). Interestingly, this model appears to be independent of COX-2 expression, as confirmed by the low COX-2 expression and, hence, the levels of PGs, therefore offering an unique approach to validate the view of COX-2 as a regulator of liver oncogenic processes. Surprisingly, hepatic COX-2 overexpression did not modify significantly the time-dependent development of liver oncogenesis in the c-myc/TGF-α transgenic mice, although there was a significant decrease of liver/body weight ratio in c-myc/TGF-α/COX-2 mice at 5 months-old-age *vs.* c-myc/TGF-α mice. This observation suggested that COX-2 overexpression in hepatocytes prevents the hepatocyte hypertrophy and hyperplasia

caused by the co-expression of c-myc/TGF-α transgenes. This could be related with the tendency of a lower incidence of the adenomas and Ki67 staining in the triple mouse model.

Tumour development and progression depend on the disruption of normal tissue homeostatic mechanisms that shift the balance between cell proliferation and cell death toward cell accumulation (37). The presence of COX-2 together with c-myc/TGF-α did not change the expression of different genes related with cell proliferation and apoptosis. A comparative functional genomics to identify the best-fit mouse models to study human cancer by using 70 HCCs from seven different mouse models and 91 human HCCs from predefined subclasses revealed that gene expression patterns in HCCs from c-myc, E2F1 and c-myc/E2F1 transgenic were similar to those of the better survival group of human HCCs (subclass B-like), whereas the expression patterns in HCCs from c-myc/TGF-α transgenic mice and in diethylnitrosamine-induced mouse HCC were more similar to those of poorer survival group of human HCC (subclass A-like) (25). We have analyzed some of these markers in order to determine whether the presence of COX-2 influences the better/poorer survival scores and, interestingly, we could not observe significant differences between both mouse models.

c-myc/TGF-α mice-driven hepatocarcinogenesis leads to tumors of low-grade differentiation, high malignancy and reduced survival with an early disruption of growth control including cell cycle progression and apoptosis (20). Increased COX-2 expression has been found in human HCC, however, although COX-2 expression is elevated in the early stages of HCC, there is an inverse correlation with the differentiation grade of the tumor and the mechanisms regulating COX-2 expression at specific stages of HCC development remain unknown. In this line, our recent results

have demonstrated a relantioship between a reduction of overall survival of the patients and a decreased COX-2 expression by promoter hypermethylation and histone H3 hypoacetylation (38).

In the same line of reasoning, chemical carcinogenesis has been widely used to analyse multistep hepatocarcinogenesis to generate useful animal models. Genotoxic chemicals, such as DEN, may act as tumor initiators by directly activating oncogenes through mutagenesis (39). Our previous work (21) demonstrated that COX-2 expression is not sufficient to enhance malignant transformation in a model of chemical hepatocarcinogenesis induced by DEN. COX-2 expression favoured the development of preneoplastic foci and this could be related to its anti-apoptotic effect and inflammatory phenomena in the early phases of HCC. Furthermore, our data reported moderate activation of JNK, Erk and p38 in COX-2Tg cells treated with PB/DEN (Phenobarbital/diethylnitrosamine) and COX-2 moderately increased the growth of cell implants in nude mice, which may be due to the modulation of Akt and JNK-c-Jun pathways (21). However, we did not find these changes in c-myc/TGF-α/COX-2 liver compared to c-myc/TGF-α which suggest that COX-2 differently modulate specific markers of tumor progression in chemical that in genetic carcinogenesis.

Factor et al. (26) demonstrated that the production of reactive oxygen species (ROS) was significantly elevated in c-myc/TGF-α mice when compared with wild type or c-myc lesions in parallel with increases in lipid peroxidation. It is known that Vitamin E, a potent free radical scavenging antioxidant, promotes chromosomal and mitochondrial DNA stability in c-myc/TGF-α mice. These data indicate ROS as the primary carcinogenic agent and chromosomal instability as the underlying mechanisms in this model of liver cancer. iNOS, NADPH oxidase and HO-1 are involved in ROS

generation during c-myc/TGF-α hepatocarcinogenesis (40). Our previous data (21) by using COX-2 Tg hepatocyte-like cells showed elevated oxidative stress and ROS accumulation after DEN administration, together with an important decrease in the levels of glutathione and a higher level of anti-8-OHdG reactivity. The present data show an increase in lipid peroxidation (TBARS) by the presence of COX-2; however no significant differences were found in the levels of iNOS, HO-1β and in the transcription factor Nrf-2 between c-myc/TGF-α double and c-myc/TGF-α/COX-2 triple transgenic mice which suggest that the injury associated to this mechanism looks like 'a saturated' signal.

In conclusion, our results, by using the chemical or genetic models of HCC, provide a consistent support to the fact that the presence of COX-2 in liver does not contribute significantly to enhance HCC development and onset; however, the studies based on the analysis of the COX-2 promoter activity might reflect broad epigenetic changes that have a further impact on HCC than the COX-2 activity by itself. The present results, although negative in the common view of COX-2 as a gene contributing to carcinogenesis, give support to the fact that this enzyme is of minor relevance in HCC.

ACKNOWLEDGMENTS

TGF-α/c-myc mice were kindly obtained from Dr. S.S. Thorgeirsson at the National Cancer Center (NCI), Bethesda, Maryland.

DISCLOSURE/DUALITY OF INTEREST

The authors declare no conflict of interest.

REFERENCES

1. Llovet JM, Bruix J. Molecular targeted therapies in hepatocellular carcinoma. Hepatology. 2008 Oct;48(4):1312-27.

2. Maeda S, Kamata H, Luo JL, Leffert H, Karin M. IKKbeta couples hepatocyte death to cytokine-driven compensatory proliferation that promotes chemical hepatocarcinogenesis. Cell. 2005 Jul 1;121(7):977-90.

3. Simmons DL, Botting RM, Hla T. Cyclooxygenase isozymes: the biology of prostaglandin synthesis and inhibition. Pharmacol Rev. 2004 Sep;56(3):387-437.

4. Ledwith BJ, Pauley CJ, Wagner LK, Rokos CL, Alberts DW, Manam S. Induction of cyclooxygenase-2 expression by peroxisome proliferators and non-tetradecanoylphorbol 12,13-myristate-type tumor promoters in immortalized mouse liver cells. J Biol Chem. 1997 Feb 7;272(6):3707-14.

5. Martin-Sanz P, Callejas NA, Casado M, Diaz-Guerra MJ, Bosca L. Expression of cyclooxygenase-2 in foetal rat hepatocytes stimulated with lipopolysaccharide and pro-inflammatory cytokines. Br J Pharmacol. 1998 Nov;125(6):1313-9.

6. Callejas NA, Bosca L, Williams CS, Du BR, Martin-Sanz P. Regulation of cyclooxygenase 2 expression in hepatocytes by CCAAT/enhancer-binding proteins. Gastroenterology. 2000 Aug;119(2):493-501.

7. Casado M, Callejas NA, Rodrigo J, Zhao X, Dey SK, Bosca L, et al. Contribution of cyclooxygenase 2 to liver regeneration after partial hepatectomy. FASEB J. 2001 Sep;15(11):2016-8.

8. Rudnick DA, Perlmutter DH, Muglia LJ. Prostaglandins are required for CREB activation and cellular proliferation during liver regeneration. Proc Natl Acad Sci U S A. 2001 Jul 17;98(15):8885-90.

9. Yamamoto H, Kondo M, Nakamori S, Nagano H, Wakasa K, Sugita Y, et al. JTE-522, a cyclooxygenase-2 inhibitor, is an effective chemopreventive agent against rat experimental liver fibrosis1. Gastroenterology. 2003 Aug;125(2):556-71.

10. Kern MA, Haugg AM, Koch AF, Schilling T, Breuhahn K, Walczak H, et al. Cyclooxygenase-2 inhibition induces apoptosis signaling via death receptors and mitochondria in hepatocellular carcinoma. Cancer Res. 2006 Jul 15;66(14):7059-66.

11. Mayoral R, Fernandez-Martinez A, Bosca L, Martin-Sanz P. Prostaglandin E2 promotes migration and adhesion in hepatocellular carcinoma cells. Carcinogenesis. 2005 Apr;26(4):753-61.

12. Cusimano A, Fodera D, Lampiasi N, Azzolina A, Notarbartolo M, Giannitrapani L, et al. Prostaglandin E2 receptors and COX enzymes in human hepatocellular carcinoma: role in the regulation of cell growth. Ann N Y Acad Sci. 2009 Feb;1155:300-8.

13. Cheng AS, Yu J, Lai PB, Chan HL, Sung JJ. COX-2 mediates hepatitis B virus X protein abrogation of p53-induced apoptosis. Biochem Biophys Res Commun. 2008 Sep 19;374(2):175-80.

14. Nunez O, Fernandez-Martinez A, Majano PL, Apolinario A, Gomez-Gonzalo M, Benedicto I, et al. Increased intrahepatic cyclooxygenase 2, matrix metalloproteinase 2, and matrix metalloproteinase 9 expression is associated with progressive liver disease in chronic hepatitis C virus infection: role of viral core and NS5A proteins. Gut. 2004 Nov;53(11):1665-72.

15. Martinez-Lopez N, Varela-Rey M, Fernandez-Ramos D, Woodhoo A, Vazquez-Chantada M, Embade N, et al. Activation of LKB1-Akt pathway independent of phosphoinositide 3-kinase plays a critical role in the proliferation of hepatocellular carcinoma from nonalcoholic steatohepatitis. Hepatology. [Research Support, N.I.H., Extramural

Research Support, Non-U.S. Gov't]. 2010 Nov;52(5):1621-31.

16. Calvisi DF, Factor VM, Ladu S, Conner EA, Thorgeirsson SS. Disruption of beta-catenin pathway or genomic instability define two distinct categories of liver cancer in transgenic mice. Gastroenterology. 2004 May;126(5):1374-86.

17. Luedde T, Beraza N, Kotsikoris V, van Loo G, Nenci A, De Vos R, et al. Deletion of NEMO/IKKgamma in liver parenchymal cells causes steatohepatitis and hepatocellular carcinoma. Cancer Cell. 2007 Feb;11(2):119-32.

18. Pikarsky E, Porat RM, Stein I, Abramovitch R, Amit S, Kasem S, et al. NF-kappaB functions as a tumour promoter in inflammation-associated cancer. Nature. 2004 Sep 23;431(7007):461-6.

19. Haybaeck J, Zeller N, Wolf MJ, Weber A, Wagner U, Kurrer MO, et al. A lymphotoxin-driven pathway to hepatocellular carcinoma. Cancer Cell. 2009 Oct 6;16(4):295-308.

20. Calvisi DF, Thorgeirsson SS. Molecular mechanisms of hepatocarcinogenesis in transgenic mouse models of liver cancer. Toxicol Pathol. 2005;33(1):181-4.

21. Llorente Izquierdo C, Mayoral R, Flores JM, Garcia-Palencia P, Cucarella C, Bosca L, et al. Transgenic mice expressing cyclooxygenase-2 in hepatocytes reveal a minor contribution of this enzyme to chemical

hepatocarcinogenesis. The American journal of pathology. [Research Support, Non-U.S. Gov't]. 2011 Mar;178(3):1361-73.

22. Casado M, Molla B, Roy R, Fernandez-Martinez A, Cucarella C, Mayoral R, et al. Protection against Fas-induced liver apoptosis in transgenic mice expressing cyclooxygenase 2 in hepatocytes. Hepatology. 2007 Mar;45(3):631-8.

23. Santoni-Rugiu E, Jensen MR, Thorgeirsson SS. Disruption of the pRb/E2F pathway and inhibition of apoptosis are major oncogenic events in liver constitutively expressing c-myc and transforming growth factor alpha. Cancer Res. 1998 Jan 1;58(1):123-34.

24. De la Cueva E, Garcia-Cao I, Herranz M, Lopez P, Garcia-Palencia P, Flores JM, et al. Tumorigenic activity of p21Waf1/Cip1 in thymic lymphoma. Oncogene. 2006 Jul 6;25(29):4128-32.

25. Lee JS, Chu IS, Mikaelyan A, Calvisi DF, Heo J, Reddy JK, et al. Application of comparative functional genomics to identify best-fit mouse models to study human cancer. Nat Genet. 2004 Dec;36(12):1306-11.

26. Factor VM, Kiss A, Woitach JT, Wirth PJ, Thorgeirsson SS. Disruption of redox homeostasis in the transforming growth factor-alpha/c-myc transgenic mouse model of accelerated hepatocarcinogenesis. J Biol Chem. 1998 Jun 19;273(25):15846-53.

27. Kondo M, Yamamoto H, Nagano H, Okami J, Ito Y, Shimizu J, et al. Increased expression of COX-2 in nontumor liver tissue is associated with shorter disease-free survival in patients with hepatocellular carcinoma. Clinical cancer research : an official journal of the American Association for Cancer Research. [Research Support, Non-U.S. Gov't]. 1999 Dec;5(12):4005-12.

28. Neufang G, Furstenberger G, Heidt M, Marks F, Muller-Decker K. Abnormal differentiation of epidermis in transgenic mice constitutively expressing cyclooxygenase-2 in skin. Proc Natl Acad Sci U S A. 2001 Jun 19;98(13):7629-34.

29. Bol DK, Rowley RB, Ho CP, Pilz B, Dell J, Swerdel M, et al. Cyclooxygenase-2 overexpression in the skin of transgenic mice results in suppression of tumor development. Cancer Res. 2002 May 1;62(9):2516-21.

30. Andreasson KI, Savonenko A, Vidensky S, Goellner JJ, Zhang Y, Shaffer A, et al. Age-dependent cognitive deficits and neuronal apoptosis in cyclooxygenase-2 transgenic mice. J Neurosci. 2001 Oct 15;21(20):8198-209.

31. Chang SH, Liu CH, Conway R, Han DK, Nithipatikom K, Trifan OC, et al. Role of prostaglandin E2-dependent angiogenic switch in cyclooxygenase 2-induced breast cancer progression. Proc Natl Acad Sci U S A. 2004 Jan 13;101(2):591-6.

32. Oshima H, Oshima M, Inaba K, Taketo MM. Hyperplastic gastric tumors induced by activated macrophages in COX-2/mPGES-1 transgenic mice. EMBO J. 2004 Apr 7;23(7):1669-78.

33. Colby JK, Klein RD, McArthur MJ, Conti CJ, Kiguchi K, Kawamoto T, et al. Progressive metaplastic and dysplastic changes in mouse pancreas induced by cyclooxygenase-2 overexpression. Neoplasia. 2008 Aug;10(8):782-96.

34. Muller-Decker K, Furstenberger G, Annan N, Kucher D, Pohl-Arnold A, Steinbauer B, et al. Preinvasive duct-derived neoplasms in pancreas of keratin 5-promoter cyclooxygenase-2 transgenic mice. Gastroenterology. 2006 Jun;130(7):2165-78.

35. Kern MA, Schoneweiss MM, Sahi D, Bahlo M, Haugg AM, Kasper HU, et al. Cyclooxygenase-2 inhibitors suppress the growth of human hepatocellular carcinoma implants in nude mice. Carcinogenesis. 2004 Jul;25(7):1193-9.

36. Mayoral R, Molla B, Flores JM, Bosca L, Casado M, Martin-Sanz P. Constitutive expression of cyclo-oxygenase 2 transgene in hepatocytes protects against liver injury. Biochem J. 2008 Dec 15;416(3):337-46.

37. Vail ME, Pierce RH, Fausto N. Bcl-2 delays and alters hepatic carcinogenesis induced by transforming growth factor alpha. Cancer research. [Research Support, Non-U.S. Gov't

Research Support, U.S. Gov't, P.H.S.]. 2001 Jan 15;61(2):594-601.

38. Fernández-Alvarez A, Izquierdo CL, Mayoral R, Agra N, Boscá L, Casado M, et al. Evaluation of epigenetic modulation of cyclooxygenase-2 as a prognostic marker for hepatocellular carcinoma. Oncogenesis. 2012.

39. Takagi H, Sharp R, Takayama H, Anver MR, Ward JM, Merlino G. Collaboration between growth factors and diverse chemical carcinogens in hepatocarcinogenesis of transforming growth factor alpha transgenic mice. Cancer research. [Research Support, U.S. Gov't, P.H.S.]. 1993 Sep 15;53(18):4329-36.

40. Calvisi DF, Ladu S, Hironaka K, Factor VM, Thorgeirsson SS. Vitamin E down-modulates iNOS and NADPH oxidase in c-Myc/TGF-alpha transgenic mouse model of liver cancer. J Hepatol. 2004 Nov;41(5):815-22.

TITLES AND LEGENDS TO FIGURES

Figure 1.- Effects of hepatic COX-2 expression on tumor development in c-myc/TGF-α transgenic mice. **(A)** Human COX-2, c-myc and TGF-α protein expression in liver homogenates from c-myc/TGF-α (D) and c-myc/TGF-α/COX-2 (T) mice at 5 and 9 months-old-age detected by Western blot and normalized with β-actin. **(B)** Intrahepatic PGE_2 concentration was determined by EIA in liver homogenates. **(C)** Photographs of gross liver features at 5 and 9 months from D and T mice. **(D,E,F)** Morphometric analysis of Tumor foci number, Maximal size and Tumor area at 5 and 9 months-old-age D and T mice. Data are the means ± SD of the number of animals indicated in Table 1 per condition. $^{**}P<0.001$ *vs*. the corresponding matched animals.

Figure 2.- Histological analysis and Ki67 staining in liver from c-myc/TGF-α and c-myc/TGF-α/COX-2 transgenic mice. **(A)** Hematoxylin and eosin (H&E) staining of liver sections showing hepatocellular carcinoma with trabecular pattern, cytological atypias and nuclear polimorphisms in both c-myc/TGF-α (D) and c-myc/TGF-α/COX-2 (T) mice at 9 months-old-age. A sharply demarcated hepatocellular adenoma with enlarged eosinophilic hepatocytes is shown in D mice at 5 months-old-age whereas T mice exhibits a foci of hepatocyte hyperplasia with granular cytoplasm and condensed nuclei. Lesions are indicated with arrows. The bar corresponds to 100μm. Figures were taken with a Color View Camera in a Vanox Olympus microscope at 20X magnification. **(B)** Caspase 3 and Ki67 staining were analyzed in liver sections from D and T transgenic mice at 5 months-old-age. **(C)** The percentage of apoptotic and mitotic cells was quantified and results show the mean ± SD of the five sections per animal (n=3).

Figure 3.- Rb/E2F1 pathway and cell cycle protein analysis in c-myc/TGF-α and c-myc/TGF-α/COX-2 transgenic mice. **(A)** Tumor liver HCC was analyzed for Rb, E2F1, cell cycle and tumor suppressors associated proteins. Representative Western blots showing the expression of p-Rb, Rb, E2F1, PCNA, cyclin E, cyclin D1, p53 and p21 in livers from wild-type (C), monogenic COX-2 transgenic mice (M), c-myc/TGF-α (D) and c-myc/TGF-α/COX-2 (T) mice at 5 and 9 months-old age. **(B)** Densitometric analysis of the protein expression normalized to that of β-actin. Data are the means ± SD of the number of animals indicated in Table 1 per condition. *$p<0.05$ T *vs*. D. *a.u.*, arbitrary units.

Figure 4.- Signaling pathways implicated in proliferation in c-myc/TGF-α and c-myc/TGF-α/COX-2 transgenic mice. **(A)** Representative Western blots showing the phosphorylation of JNK, Erk, p38 and Stat3 in in livers from wild-type (C), monogenic COX-2 transgenic mice (M), c-myc/TGF-α (D) and c-myc/TGF-α/COX-2 (T) mice at 5 and 9 months-old age. The expression of β-actin was used as load control **(B)** Densitometric analysis of the expression of the ratios p-JNK/JNK, p-Erk/Erk, p-p38/p38 and p-Stat3/Stat3. Data are the means ± SD of the number of animals indicated in Table 1 per condition. *a.u.*, arbitrary units.

Figure 5.- Signaling pathways implicated in survival and apoptosis in c-myc/TGF-α and c-myc/TGF-α/COX-2 transgenic mice. **(A)** Representative Western blots showing the phosphorylation of Akt (Ser^{473}) and p70S6K and the protein levels of Bcl-2 and Mcl-1. The expression of β-actin was used as load control. **(B)** Densitometric analysis of the expression of the ratios p-Akt/Akt and p-p70S6K/p70S6K. Data are the means ± SD of the number of animals indicated in Table 1 per condition. *$p<0.05$ T *vs*. D. *a.u.*, arbitrary units.

Figure 6.- Gene expression pattern of proliferation, apoptosis and poor survival genes in c-myc/TGF-α/COX-2 vs. c-myc/TGF-α transgenic mice. **(A)** Expression of several genes related with cell proliferation (Ccnd1, Cxcr4, Ccne1) and apoptosis (Bir5, Tnfrsf10b, Gadd45b) were analyzed by real-time PCR. **(B)** Gene expression of poor survival genes analyzed by real-time PCR. mRNA amounts were calculated as RQ and normalized to the expression of 36b4 mRNA.

Figure 7.- iNOS and HO-1 expression in c-myc/TGF-α and c-myc/TGF-α/COX-2 transgenic mice. **(A)** Representative Western blots of HO-1, iNOS and Nrf-2. The expression of target proteins was normalized to that of β-actin. **(B)** Densitometric analysis of the protein expression. **(C)** Intracellular content of ROS was measured by using the TBARs assay as described in Methods. Data are the means ± SD of the number of animals indicated in Table 1 per condition. *$p<0.05$ T *vs*.D. a.u., arbitrary units.

TABLE 1: Body and liver weight, plasma levels of liver injury markers and frequency (percentage) of lesions in c-myc/TGF-α double (D) transgenic or c-myc/TGF-α/COX-2 (T) triple transgenic mice. The control levels of alkaline phosphatase (ALP), aspartate transaminase (AST), alanine transaminase (ALT) and lactate dehydrogenase (LDH) of wild-type mice in a same background (C57BL/6JxCBAxDBAxFVB) were at 5 months liver weight (LW, g) 1.70±0.21, body weight (BW, g) 42.42±4.68; LW/BW ratio 4.01±0.40; ALP (U/L) 109.7±32.6, AST (U/L) 64.4±10.6; ALT (U/L) 32.3±7.8; LDH (U/L) 145.0±53.2 and at 9 months LW (g) 2.55±0.45, BW (g) 54.19±4.33; LW/BW ratio 4.70±0.72; ALP (U/L) 101.0±29.6, AST (U/L) 65.6±12; ALT (U/L) 40.1±9.7; LDH (U/L) 145.0±53.2. *p<0.05.

Age (months)	Genotype	Number of mice	LW (g)	BW (g)	LW/BW ratio (%)	ALP (U/L)	AST (U/L)	ALT (U/L)	LDH	Foci	Adenoma	HCC
5	D	15	3.24±0.91	41.26±5.73	7.81±1.68	149.1±84.7	177.7±51.1	133.7±65.4	295.4±161.2	14/15 (93.3)	4/15 (26.7)	2/15 (13.3)
	T	11	2.40±0.74*	36.87±3.22*	6.47±1.75*	96.8±21.4	126.4±44.6*	74.4±23.9	176.0±40.1	10/11 (90.9)	1/11 (9.1)	1/11 (9.1)
9	D	9	5.51±1.69	37.31±4.36	15.11±5.50	1508.4±1401.6	201.8±63.1	176.0±67.7	384.0±165.8	0/9 (0)	9/9 (100)	8/9 (89)
	T	10	5.78±1.51	36.80±5.58	16.02±4.52	1424.8±819.4	263.2±126.2	222.8±125.2	572.8±265.8	1/10 (10)	10/10 (100)	10/10 (100)

Numbers in parentheses are percentages

Figure 1

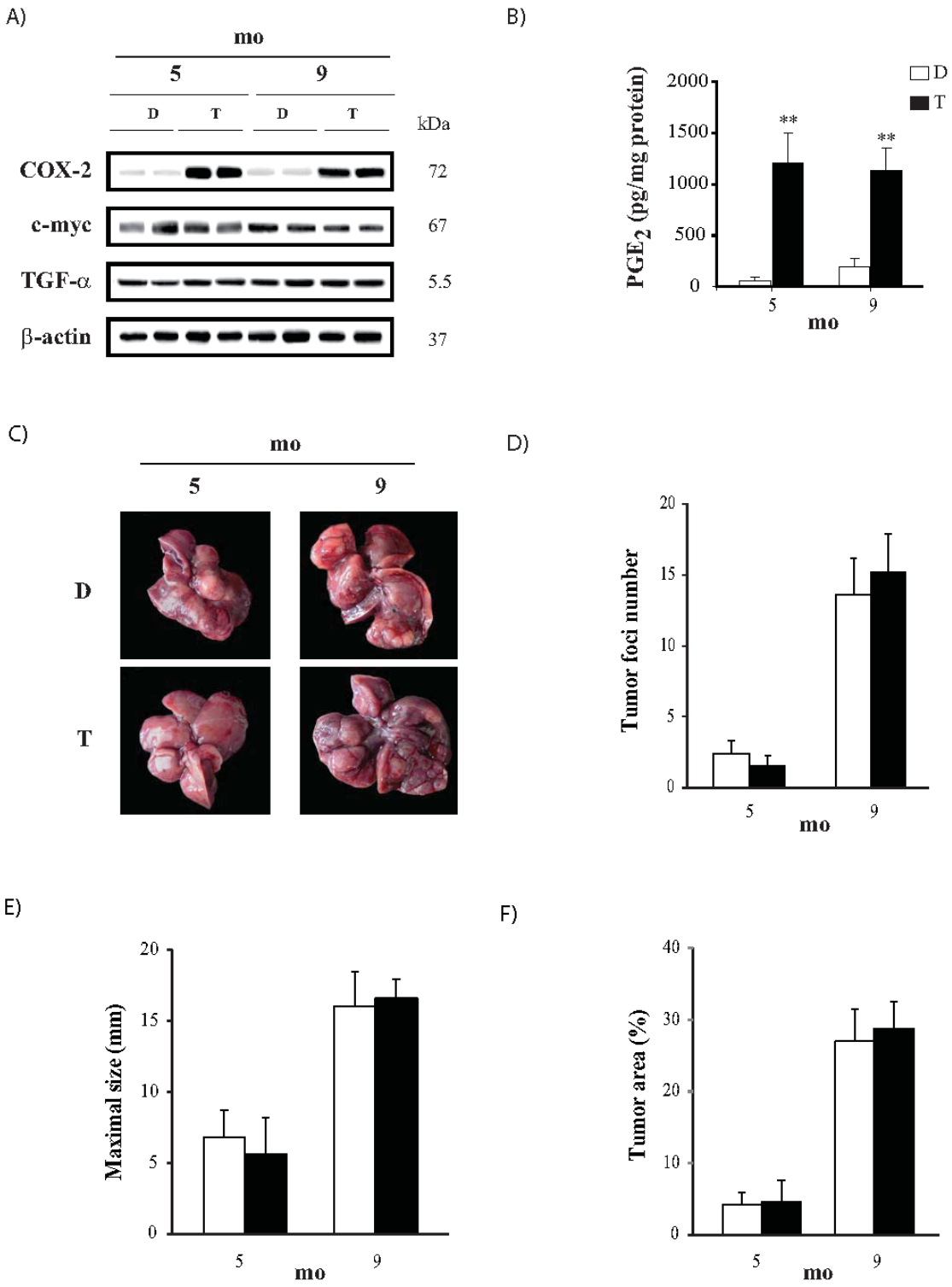
A)
mo
5
9
D
T
D
T
kDa
COX-2
c-myc
TGF-α
β-actin
72
67
5.5
37
B)
D
T
PGE_2 (pg/mg protein)
2000
1500
1000
500
0
**
**
5
9
mo
C)
mo
5
9
D
T
D)
Tumor foci number
20
15
10
5
0
5
9
mo
E)
Maximal size (mm)
20
15
10
5
0
5
9
mo
F)
Tumor area (%)
40
30
20
10
0
5
9
mo

Figure 2

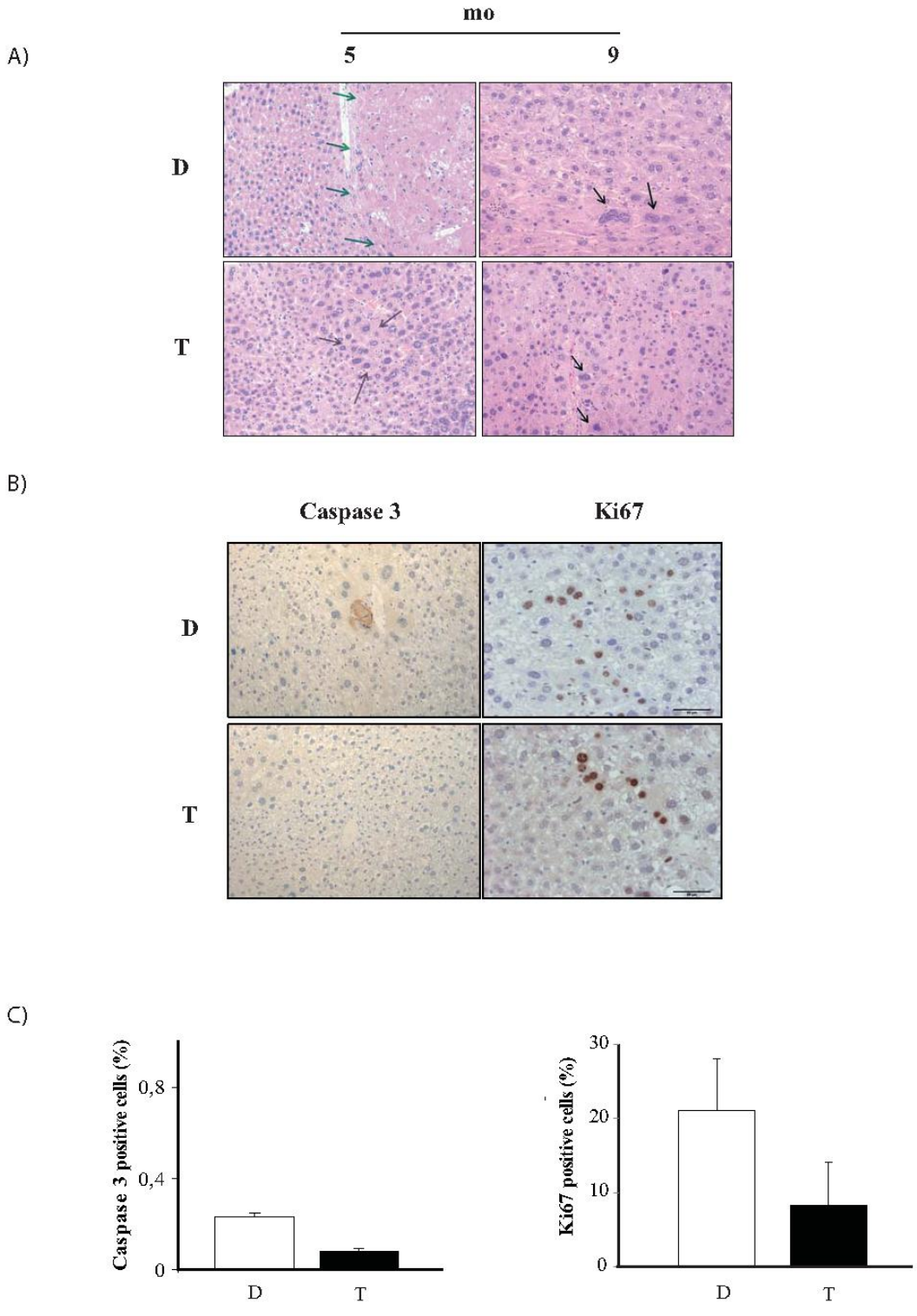
A)
mo
5
9
D
T
B)
Caspase 3
Ki67
D
T
C)
Caspase 3 positive cells (%)
0,8
0,4
0
D
T
Ki67 positive cells (%)
30
20
10
0
D
T

Figure 3

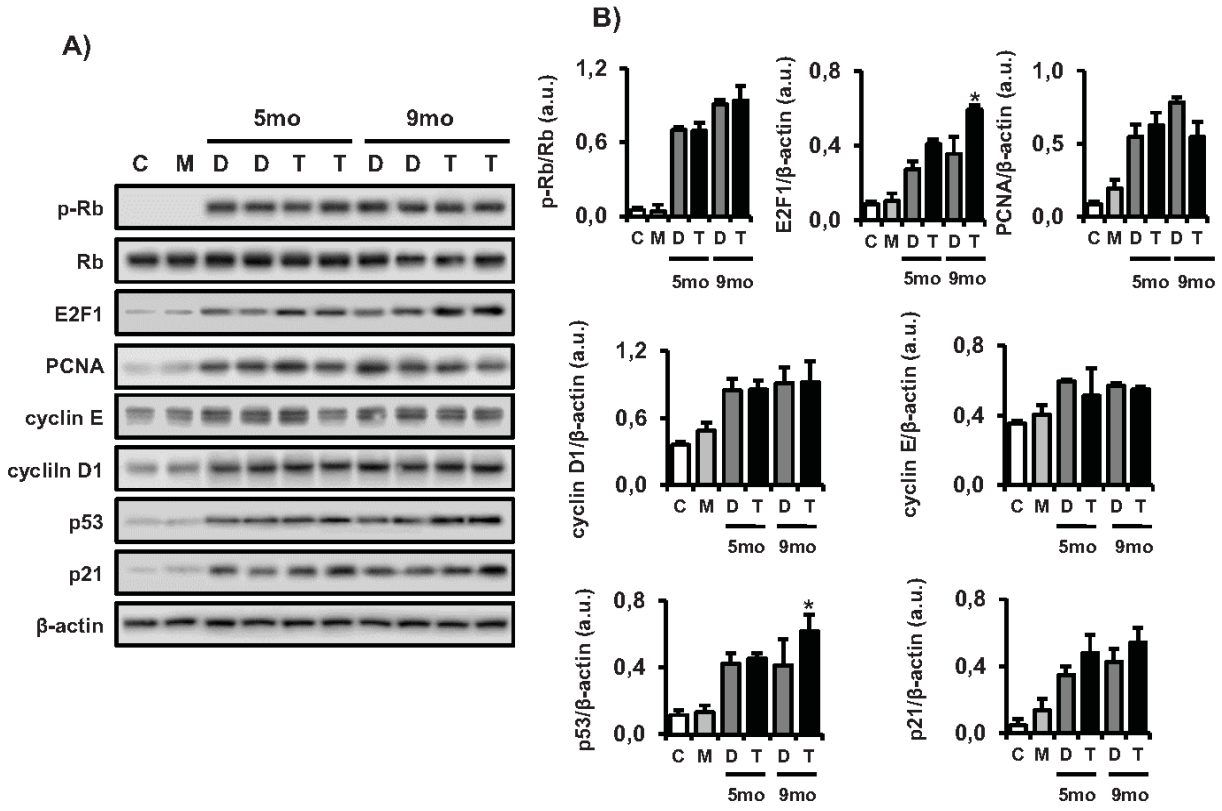
A)
5mo
9mo
C M D D T T D D T T
p-Rb
Rb
E2F1
PCNA
cyclin E
cycliln D1
p53
p21
β-actin
B)
p-Rb/Rb (a.u.)
E2F1/β-actin (a.u.)
PCNA/β-actin (a.u.)
cyclin D1/β-actin (a.u.)
cyclin E/β-actin (a.u.)
p53/β-actin (a.u.)
p21/β-actin (a.u.)
C M D T D T
5mo 9mo
*

Figure 4

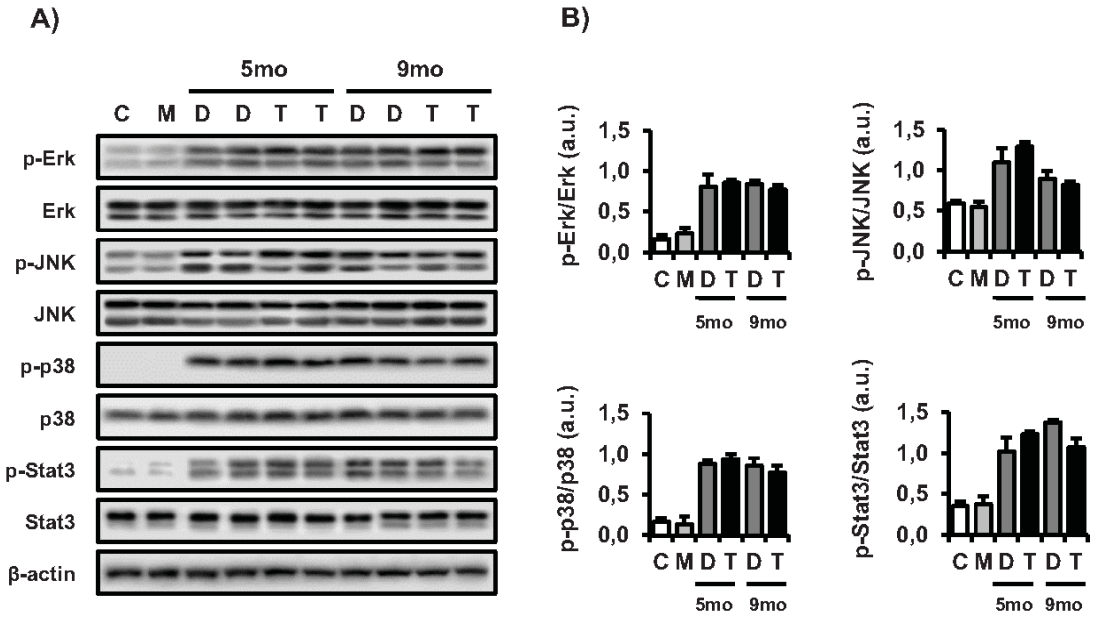
A)
5mo
9mo
C M D D T T D D T T
p-Erk
Erk
p-JNK
JNK
p-p38
p38
p-Stat3
Stat3
β-actin
B)
p-Erk/Erk (a.u.)
p-JNK/JNK (a.u.)
p-p38/p38 (a.u.)
p-Stat3/Stat3 (a.u.)
1,5
1,0
0,5
0,0
C M D T D T
5mo 9mo

Figure 5

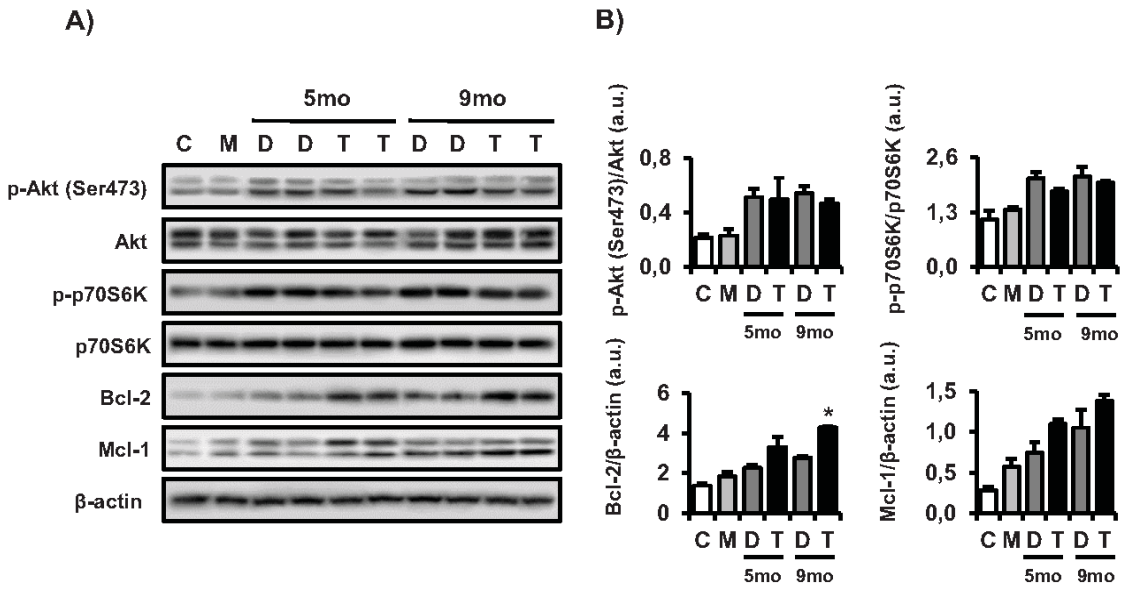
A)
B)
5mo
9mo
C M D D T T D D T T
p-Akt (Ser473)
Akt
p-p70S6K
p70S6K
Bcl-2
Mcl-1
β-actin
p-Akt (Ser473)/Akt (a.u.)
0,8
0,4
0,0
p-p70S6K/p70S6K (a.u.)
2,6
1,3
0,0
Bcl-2/β-actin (a.u.)
6
4
2
0
*
Mcl-1/β-actin (a.u.)
1,5
1,0
0,5
0,0
C M D T D T
5mo 9mo

Figure 6

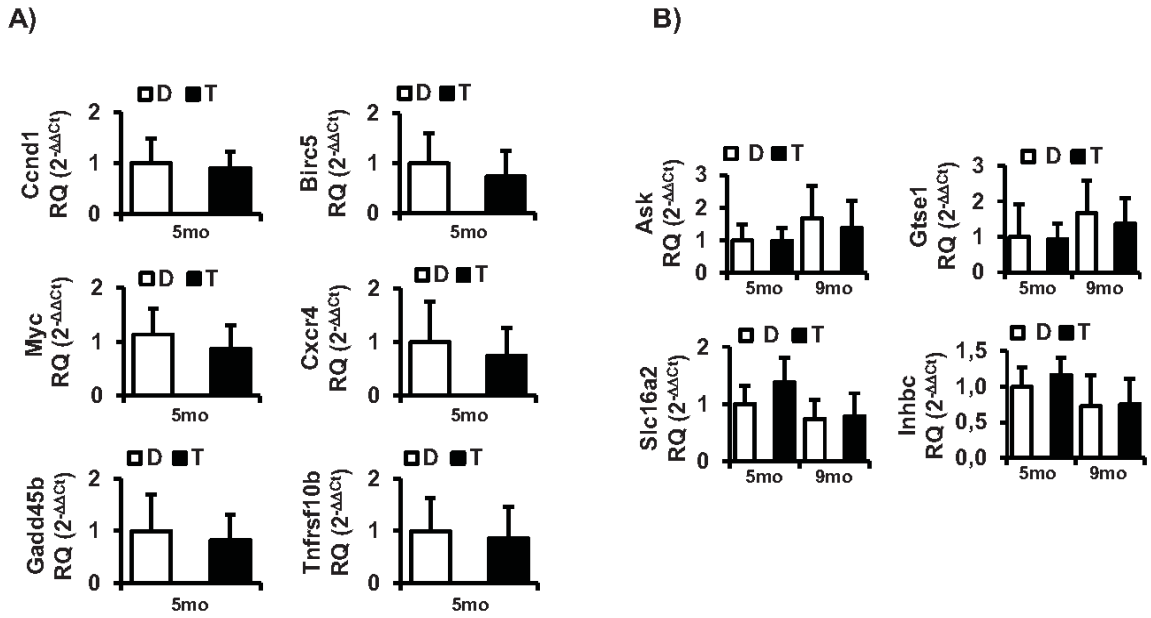
A)
B)
D T
Ccnd1 RQ (2-ΔΔCt)
Birc5 RQ (2-ΔΔCt)
Myc RQ (2-ΔΔCt)
Cxcr4 RQ (2-ΔΔCt)
Gadd45b RQ (2-ΔΔCt)
Tnfrsf10b RQ (2-ΔΔCt)
Ask RQ (2-ΔΔCt)
Gtse1 RQ (2-ΔΔCt)
Slc16a2 RQ (2-ΔΔCt)
Inhbc RQ (2-ΔΔCt)
5mo
9mo

Figure 7

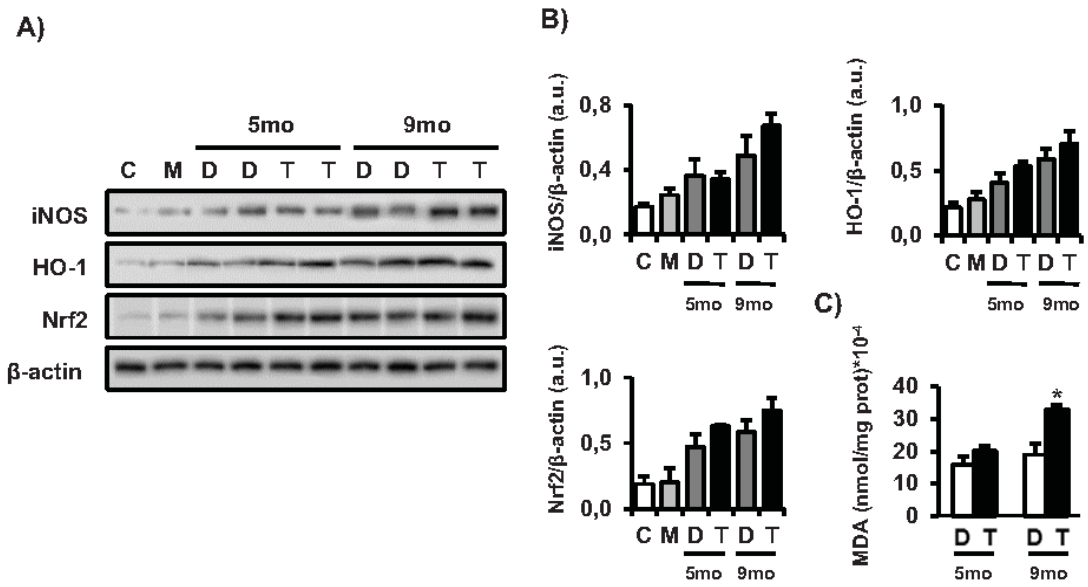
A)
5mo
9mo
C M D D T T D D T T
iNOS
HO-1
Nrf2
β-actin
B)
iNOS/β-actin (a.u.)
0,8
0,4
0,0
C M D T D T
5mo 9mo
HO-1/β-actin (a.u.)
1,0
0,5
0,0
C M D T D T
5mo 9mo
Nrf2/β-actin (a.u.)
1,0
0,5
0,0
C M D T D T
5mo 9mo
C)
MDA (nmol/mg prot)*10⁻⁴
40
30
20
10
0
*
D T D T
5mo 9mo

TABLA S1: List of primers used in the quantitative real-time PCR analysis

Gene	Forward primer sequence	Reverse primer sequence
Ask	CAGTGCTTCTGGGAAGGATGCG	AAGGCTTCTTGAGTCTCCCTGTTCT
Birc5	CTCAAGAACTACCGCATCGCCACT	CTCCGCCATTCGCTCTGGGG
Ccnd1	GCGTGCAGAAGGAGATTGTGCCA	GCACTTCTGCTCCTCACAGACCTCC
Cxcr4	ACCGCCTTTACCCCGATAGCCT	ATGACGATGCCGGGCAGGAC
Gadd45b	GGGGATCTTCCGTGGGGGTCC	CCTGCATCTTCTGAACCGCGTTGTC
Gtse1	AGTGACGTGCTCCAGGACAAACC	AGCCCCAACTTGCCAGGAATGG
Inhbc	GACACAGACCTCTCCAGCATCAACC	TCTGGGTGGCATTGTGGGGGAA
Myc	CCAGCAGCGACTCTGAAGAAGAGC	TCCGACCTCTTGGCAGGGGTTT
Slc16A2	GCTCTTGGTGTGCATTGGGGCT	GGAGCAGGAATGAGAGGACCTGCAA
Tnfrsf10b	GTCCAGCTGGCCTACAGC	GCTTGCAGTTCCCTTCTGAC
36b4	ACTGGTCTAGGACCCGAGAAG	TCCCACCTTGTCTCCAGTCT

TABLA S2: List of the polyclonal or monoclonal antibodies used in the Western blot analysis

	Antibody	Reference number
Cell Signaling Technology	Akt	#9272
	Bcl-2	#2876
	c-Myc	#5605
	Erk	#9102
	JNK	#9252
	p38	#9212
	p-Erk	#9101
	p-JNK	#9251
	p-p38	#9211
	p-Stat3	#9138
	Stat3	#0132
Leica Microsystems	p53	NCL-p53-CM5p
Millipore	HO-1	AB1284
Santa Cruz Biotechnology	COX-2	sc-1747
	cyclin D1	sc-718
	cyclin E	sc-25303
	E2F1	sc-22820
	iNOS	sc-650
	Mcl-1	sc-819
	Nrf2	sc-13032
	p21	sc-397
	p70S6K	sc-8418
	p-Akt (Ser473)	sc-7985-R
	PCNA	sc-7907
	p-p70S6K	sc-11759
	p-Rb (Ser 780)	sc-12901
	Rb	sc-50
	TGF-α	sc-36
Sigma-Aldrich	β-Actin	A5441

TABLE S3: Body and liver weight, plasma levels of liver injury markers and frequency (percentage) of lesions in mono (c-myc or TGF-α) or double (c-myc/COX-2; TGF-α/COX-2) transgenic mice. The control levels of alkaline phosphatase (ALP), aspartate transaminase (AST), alanine transaminase (ALT) and lactate dehydrogenase (LDH) of wild-type mice in a same background (C57BL/6JxCBAxDBAxFVB) were at 5 months liver weight (LW, g) 1.70±0.21, body weight (BW, g) 42.42±4.68; LW/BW ratio 4.01±0.40; ALP (U/L) 109.7±32.6, AST (U/L) 64.4±10.6; ALT (U/L) 32.3±7.8; LDH (U/L) 145.0±53.2 and at 9 months LW (g) 2.55±0.45, BW (g) 54.19±4.33; LW/BW ratio 4.70±0.72; ALP (U/L) 101.0±29.6, AST (U/L) 65.6±12; ALT (U/L) 40.1±9.7; LDH (U/L) 145.0±53.2.

Age (months)	Genotype	Number of mice	LW (g)	BW (g)	LW/BW ratio (%)	ALP (U/L)	AST (U/L)	ALT (U/L)	LDH (U/L)	Foci	Adenoma	HCC
5	TFG-α	9	1,96±0,27	40,58±4,77	4,82±0,41	112,6±16,7	128±86,8	51.3±20.9	197.3±133.8	3/9 (33)	2/9 (22)	2/9 (22)
	TGF-α/ COX-2	9	1,91±0,26	40,54±5,53	4,73±0,50	98.7±16.7	98.6±26.6	49.3±25.4	218.7±154.2	0/9 (0)	0/9 (0)	0/9 (0)
	c-myc	9	1,97±0,35	39,51±5,35	4,87±0,84	108.0±18.3	64.7±15.1	24.5±5.6	96.0±34.8	0/9 (0)	0/9 (0)	0/9 (0)
	c-myc/ COX-2	15	1,75±0,25	36,43±3,49	4,81±0,53	112.0±29.4	126.1±65.8	79.0±15.9	124.0±44.9	1/15 (7)	1/15 (7)	0/15 (0)
9	TFG-α	5	3.7±1.3	47.7±8.2	7.8±3.4	169.6±90.7	140.8±51.4	61.6±36.4	262.4±53.9	2/5 (40)	3/5 (60)	3/5 (60)
	TGF-α/ COX-2	8	3.5±1.7	44.6±9.2	8.3±5.0	363.0±422.1	164.5±92.8	82.1±56.3	375.0±26.6	3/8 (38)	6/8 (75)	6/8 (75)
	c-myc	3	2.3±0.5	42.7±4.7	5.3±0.6	96.0±24.0	125.3+36.1	69.3±14.3	130.7±88.6	1/3 (33)	2/3 (67)	1/3 (33)
	c-myc/ COX-2	4	2.4±0.1	49.0±5.4	4.9±0.8	78.0±2.8	100.0±50.9	84.1±45.2	206.0±56.0	0/4 (0)	1/4 (25)	1/4 (25)

Numbers in parentheses are percentages

Líneas celulares

Las características de las líneas celulares empleadas se detallan a continuación.

Línea celular	Origen	Especie
CHL	Tejido hepático adulto normal	Humana
HuH-6	Hepatoblastoma	Humana
HuH-7	Carcinoma hepatocelular bien diferenciado	Humana
HepG2	Carcinoma hepatocelular bien diferenciado	Humana
Hep3B	Carcinoma hepatocelular bien diferenciado	Humana
WRL68	Hígado embrionario	Humana

Descripción del origen y la especie de las líneas celulares usadas.

Biopsias Humanas de CHC

Los parámetros clínico-patológicos de los pacientes con CHC están resumidos a continuación. Las muestras proceden del Banco de Tumores del Centro Nacional de Investigaciones Oncológicas (CNIO).

Características	Tipo	Nº de pacientes
Sexo	**Masculino**	**18**
	Femenino	**5**
Edad		**66.8**
Etiología	**VHB**	**2**
	VHC	**8**
	Etanol	**4**
	Hemocromatosis	**1**
	No asignado	**8**
Cirrosis	**Positivo**	**8**
	Negativo	**15**
Talla del tumor	**>5**	**8**
	<5	**12**
	No asignado	**3**
Grado histológico	**Bien diferenciado**	**14**
	Moderadamente diferenciado	**6**
	Indiferenciado	**1**
	No asignado	**2**

Características clínico-patológicas de 23 pacientes con CHC.

ARTÍCULO III: ***Oncogenesis, 2012; 1, e23:1-11.***

Evaluación de la modulación epigenética de ciclooxigenasa-2 como marcador pronóstico del carcinoma hepatocelular

Ana Fernández-Alvarez*, ***Llorente Izquierdo C****, Mayoral R, Agra N, Boscá L, Casado M, and Martín-Sanz P.

RESUMEN DEL ARTÍCULO III

En este trabajo se abordó el estudio de la modulación epigenética del gen de COX-2, su influencia sobre cambios en la expresión de la enzima y su utilidad como marcador pronóstico del CHC humano. Con este fin, se analizaron los cambios en la metilación del promotor de COX-2 y en la acetilación de histonas en células humanas de hepatoma y en biopsias humanas de CHC.

Se evaluaron los niveles de proteína y ARN de COX-2 así como los niveles de PGE_2 en líneas celulares de CHC humano (HepG2, HuH-7 y Hep3B), de hepatoblastoma (HuH-6), derivadas de hígado embrionario (WRL68) y de hepatocitos humanos (CHL). Los niveles de expresión de COX-2 y PGE_2 fueron máximos en la línea WRL68 y los niveles más bajos correspondieron a las líneas HepG2 y HuH-7.

En estas mismas líneas celulares se analizó la metilación del promotor por metilación sensible a enzimas de restricción (MSRA) y pirosecuenciación en tres islas CpGs de COX-2. Las dos primeras islas CpG están incluidas en el promotor y la última cubre el dominio de unión a CRE, el primer exón y la parte inicial del primer intrón. Los datos no muestran correlación entre la expresión de COX-2 y su metilación en las islas CpGs en las líneas celulares analizadas. En las mismas líneas se examinó el efecto del tratamiento con el agente demetilante 5'-aza-2'-deoxicitidina (AzadC) en las islas CpG del gen de COX-2 y se estudiaron los cambios en la expresión de COX-2 por PCR cuantitativa. El porcentaje de metilación global cayó un 21% en HuH-6 y un 10% en Hep3B, líneas que en el análisis previo presentaron un perfil hipermetilado. Además, en estas líneas celulares, la expresión de COX-2 se elevó 5 y 78 veces respectivamente después del tratamiento con AzadC. Estos resultados sugieren que el estado de metilación del promotor puede regular la expresión de COX-2. Por el contrario, a pesar de que después del tratamiento con el agente demetilante el perfil de metilación de HuH-7 no varió, la expresión de COX-2 fue 5 veces superior. Este último resultado refleja la posible existencia de mecanismos de regulación alternativos.

Para analizar el efecto de la modificación de histonas en la expresión de COX-2 se examinó el efecto de los inhibidores de HDAC, butirato sódico (NaB) y ácido hidroxámico suberoilanilida (SAHA) en la expresión de COX-2 en las líneas celulares hepáticas. El tratamiento con los inhibidores causó un marcado incremento en la expresión del ARNm de COX-2 en todas las líneas celulares analizadas a excepción de la línea WRL68. Estos datos concuerdan con el incremento en la expresión de proteína y con los niveles de PGE_2. A pesar de que las expresiones de la HDAC1, 2, 3 y SIRT1 no variaron por el tratamiento con los iHDAC, la actividad global de las HDACs se mostró inhibida y los niveles de histona H3 y H4 acetilada

(Ac-H3 y Ac-H4) incrementaron. Estos resultados sugieren que la acetilación de histonas puede regular la expresión de COX-2 en algunas líneas de CHC. Para definirlo, se analizaron los efectos del NaB en la acetilación de histonas reclutadas en el promotor de COX-2 mediante ensayos de inmunoprecipitación de cromatina y posterior PCR cuantitativa. Los resultados manifestaron un incremento de la Ac-H3 en el promotor de COX-2 en HuH-6 y HuH-7 aunque el incremento de la Ac-H4 solo se observó en HuH-6.

Para investigar si la acetilación de histonas está asociada con el CHC, se valoró la Ac-H3 en biopsias de tejido tumoral por inmunohistoquímica. En un 67% de los CHCs se detectaron altos niveles de expresión de Ac-H3. Los análisis de la supervivencia de estos pacientes evidenciaron que altos niveles en la acetilación de H3 están significativamente vinculados tanto con la expresión de COX-2 como con el buen pronóstico de los pacientes.

El tratamiento de las líneas de celulares combinando el agente demetilante con los iHDAC mostró un sinergismo en el incremento de los niveles de COX-2 comparado con el incremento de los iHDAC por si solos y una disminución en la DNMT1.

Para concluir el trabajo, se analizó la metilación del promotor y la expresión de COX-2 en CHCs de biopsias de muestras humanas. Comparando con el hígado humano control no tumoral, los niveles de COX-2 fueron más elevados en las biopsias de CHC. Además, un 86% de los pacientes presentó una expresión significativa incrementada de COX-2 en el tejido no tumoral comparado con el tejido tumoral de la misma biopsia. Se determinó si la expresión de COX-2 estaba o no relacionada con la metilación aberrante de su promotor. Para ello, se analizó la metilación mediante modificación con bisulfito y pirosecuenciación de las tres islas CpG del promotor de COX-2 en 23 biopsias de CHC tanto en la zona tumoral como en su pareado no tumoral. Un 57% de las biopsias presentó un perfil de hipermetilación en la zona tumoral comparada con su respectiva región no-tumoral (31% vs 7.6%). El incremento de metilación en el promotor resultó estar significativamente correlacionado con la disminuida expresión de COX-2 en las biopsias humanas. Además, la supervivencia global de los pacientes mostró ser significativamente diferente dependiendo del estado de metilación del promotor de COX-2. Los resultados sugieren, que la hipermetilación del promotor de COX-2 está estrechamente asociada con la menor supervivencia de los pacientes. Así que, a pesar de que el efecto anti-apoptótico de COX-2 generalmente favorece el desarrollo del crecimiento celular en cáncer, la disminución de la expresión de COX-2 en el CHC avanzado está vinculada con una menor supervivencia de los pacientes con CHC.

Citation: Oncogenesis (2012) **1**, e23; doi:10.1038/oncsis.2012.23

www.nature.com/oncsis

ORIGINAL ARTICLE

Evaluation of epigenetic modulation of cyclooxygenase-2 as a prognostic marker for hepatocellular carcinoma

A Fernández-Alvarez[1,4], C Llorente-Izquierdo[2,4], R Mayoral[2,3], N Agra[2], L Boscá[2,3], M Casado[1,3] and P Martín-Sanz[2,3]

Cyclooxygenases (COX-1 and 2) catalyze the first step in prostanoid biosynthesis. They are implicated in homeostatic processes with an important role in inflammation and carcinogenesis. In the liver, COX-2 expression is restricted to proliferation or dedifferentiation situations. The COX-2 promoter contains numerous CpG islands that, when hypermethylated, result in transcriptionally silencing thus regulating the growth of carcinoma cells. In this work, we investigated whether a correlation exists between COX-2 expression and methylation signatures at the 5′region of the gene in hepatoma cell lines and human hepatocellular carcinoma (HCC). We also examined the acetylation status of the COX-2 promoter and the effects of histone deacetylase (HDAC) inhibitors on COX-2 expression. Our results suggest a significant association between reduced COX-2 expression and promoter hypermethylation of COX-2 and histone deacetylation in some hepatoma cell lines and in HCC. Treatment with demethylating agents or HDAC inhibitors restored the expression of COX-2. Moreover, in an HCC cohort, a statistically significant inverse association was observed between COX-2 mRNA levels and promoter methylation. In agreement with these data, a reduction of overall survival of the patients was observed after decreased COX-2 expression by promoter hypermethylation and histone H3 hypoacetylation.

Oncogenesis (2012) **1,** e23; doi:10.1038/oncsis.2012.23; published online 9 July 2012

Subject Category: molecular oncology

Keywords: COX-2; promoter methylation; HCC; histone acetylation; survival

INTRODUCTION

Cyclooxygenases (COX-1 and -2) are the key enzymes in prostanoid biosynthesis. COX-1 is constitutively expressed in many tissues, whereas COX-2 is induced by a variety of stimuli such as growth factors, pro-inflammatory stimuli, hormones and other cellular stresses.[1] Adult hepatocytes fail to induce COX-2 expression regardless of the pro-inflammatory factors used; however, Kupffer, stellate, hepatoma mouse cells and fetal hepatocytes retain the ability to express COX-2 upon stimulation with lipopolysaccharide (LPS) and pro-inflammatory cytokines.[2,3] In this regard, we and others demonstrated that partial hepatectomy (PH) induced COX-2 in hepatocytes and contributed to the progression of cell cycle after PH.[4,5] In addition to liver regeneration after PH or hepatotoxic agents, expression of COX-2 has been detected in animal models of cirrhosis,[6] in human hepatoma cell lines,[7,8] in human hepatocellular carcinoma (HCC)[9] and after hepatitis B or C virus infection.[10,11] Nevertheless, recent data reported that COX-2 mRNA levels were significantly higher in the adjacent liver than in HCC[12] and there was an inverse correlation between COX-2 expression and the differentiation grade and poor prognosis of HCC.[13] Therefore, although the antiapoptotic feature of COX-2 generally supports cancer cell growth, COX-2 downregulation in advanced HCC may be advantageous and specific for HCC development. The mechanisms regulating the expression of COX-2 at specific stages of HCC development remain unknown.

COX-2 is widely regarded as a potential pharmacological target for preventing and treating cancer disease mainly in colorectal cancer. Thus far, therapeutic strategies have focused on selective inhibitors of COX-2 activity; however, less attention has been paid to identifying anticancer agents that suppress the expression of COX-2. The 5′-untranslated region of the *COX-2* gene contains binding sites for numerous regulatory transcription factors including two nuclear factor-κB motifs, two activator protein 1 sites and two cAMP-response elements (CREs) among other.[14] However, the regulation of the expression of COX-2 is much more complex; it is known that COX-2 expression is also regulated by genomic DNA and chromatin modifications and by post-transcriptional regulation via its 3′-untranslated region.[15]

DNA methylation and histone modifications represent the major epigenetic mechanisms implicated in the regulation of gene transcription in mammals. COX-2 promoter contains numerous CpG islands that, when hypermethylated, result in transcriptional silencing and this regulates the survival of carcinoma cells and affects clinical outcomes in gastric cancer.[16,17] The COX-2 promoter activation by inflammatory mediators in human fibroblasts and mouse macrophages is mediated by the histone acetyltransferase p300/CBP-associated factor.[18] Diminished COX-2 expression in fibroblasts due to epigenetic abnormality in the form of histone hypoacetylation has a key role in the pathogenesis of idiopathic pulmonary fibrosis.[19] Recently, it has been reported that induction of COX-2 by hepatitis B virus depends on the demethylation of the COX-2 promoter by downregulating the DNA methyltransferase 3B and the increased binding of transcription factors.[20]

In this work, we have monitored the epigenetic marks (that is, DNA methylation and histone acetylation) at the COX-2 promoter in hepatoma cells lines and HCC biopsies. The results shown in this study suggest that the reduced COX-2 expression in some hepatoma cell lines and HCC is closely associated with the

[1]Instituto de Biomedicina de Valencia, IBV-CSIC, Valencia, Spain; [2]Instituto de Investigaciones Biomédicas Alberto Sols, CSIC-UAM, Madrid, Spain and [3]Centro de Investigación Biomédica en Red de Enfermedades Hepáticas y Digestivas (CIBERehd), Barcelona, Spain. Correspondence: Dr M Casado, Instituto de Biomedicina de Valencia, IBV-CSIC, Jaime Roig 11, 46010 Valencia, Spain or Dr P Martín-Sanz, Instituto de Investigaciones Biomédicas Alberto Sols, CSIC-UAM Arturo Duperier, 4 28029 Madrid, Spain.
E-mail: mcasado@ibv.csic.es or pmartins@iib.uam.es
[4]These authors contributed equally to this work.
Received 30 March 2012; revised 11 June 2012; accepted 14 June 2012

methylation status and histone deacetylation. Treatment with demethylating agents or histone deacetylase (HDAC) inhibitors restored the expression of COX-2. In agreement with these data, a reduction of overall survival (OS) of the patients was observed after decreased COX-2 expression by promoter hypermethylation and histone H3 hypoacetylation.

RESULTS

COX-2 expression and protein levels in HCC cell lines

COX-2 mRNA and protein levels were analyzed in six human cell lines using human hepatocytes as control. WRL68, which is derived from the human liver embryo, exhibited the highest COX-2 mRNA expression whereas HepG2 and HuH-7 liver carcinomas showed low levels of COX-2 mRNA and protein (Figures 1a and b). Prostaglandin E_2 levels, measured in cell supernatants, correlate with COX-2 protein levels (Figure 1c).

Methylation analysis of COX-2 promoter in hepatic cell lines

It has been suggested that hypermethylation of certain CpG sites on COX-2 promoter results in transcriptionally silencing and this regulates the growth of carcinoma cells.[17,21,22] The MethPrimer analysis of the COX-2 genomic region organizes the CpG sites in the 5′region into three CpG islands (Figure 2a). The first two islands (A and B) are located in the promoter region and they do not overlap with previously identified binding sites (C/EBP, nuclear factor of activated T-cells or AP1).[23] The third one (C) covers a domain including the CRE-binding site with a main function in transcriptional regulation, the first exon, including both the coding and noncoding regions, and the initial part of the first intron.

We analyzed first by methylation-sensitive restriction assay (MSRA) the methylation state in several CpG sites to asses if there was a correlation between methylation signatures and COX-2 expression in different hepatic cell lines as compared with the human liver. HuH-7 and CHL cells, as well as the human liver, presented a non-methylation pattern along the studied region. Although different patterns were found in all the cell lines analyzed, no correlation between CpG methylation and the COX-2 mRNA levels was observed, even considering separately each CpG site (Figure 2b). We further quantified the methylation size by sequencing 6, 8 and 20 CpGs on the CpG islands A, B and C, respectively (Figure 2c). The pyrosequencing data are in accordance with the MSRA results. The first two CpG islands were remarkably hypermethylated in Hep3B and HuH-6, while they remained unmethylated in CHL and WRL68 cells. Moreover, HepG2 and HuH-6 but not HuH-7 cells presented a hypermethylation pattern in CpG island C. In this region, Hep3B and CHL presented a low methylation profile. The analysis of a pool of control human liver DNA showed that normal liver presents unmethylated CpGs all along this region. The results obtained by both assays indicate that it is not possible to predict the basal expression of COX-2 from the methylation data. The WRL68 cell line, which presents the highest levels of COX-2 expression, showed the same methylation profile than the human liver or HuH-7 cells, both with negative expression levels.

We then analyzed by pyrosequencing the effect of the demethylating agent 5-aza-2′-deoxycytidine (AzadC) on COX-2 CpG islands. The percentage of COX-2 global CpG islands methylation decreased from 80 to 59% in HuH-6, and from 43 to 33% in Hep3B cells after AzadC treatment (Figure 3a). No decrease was observed in HuH-7 cells that presented a low

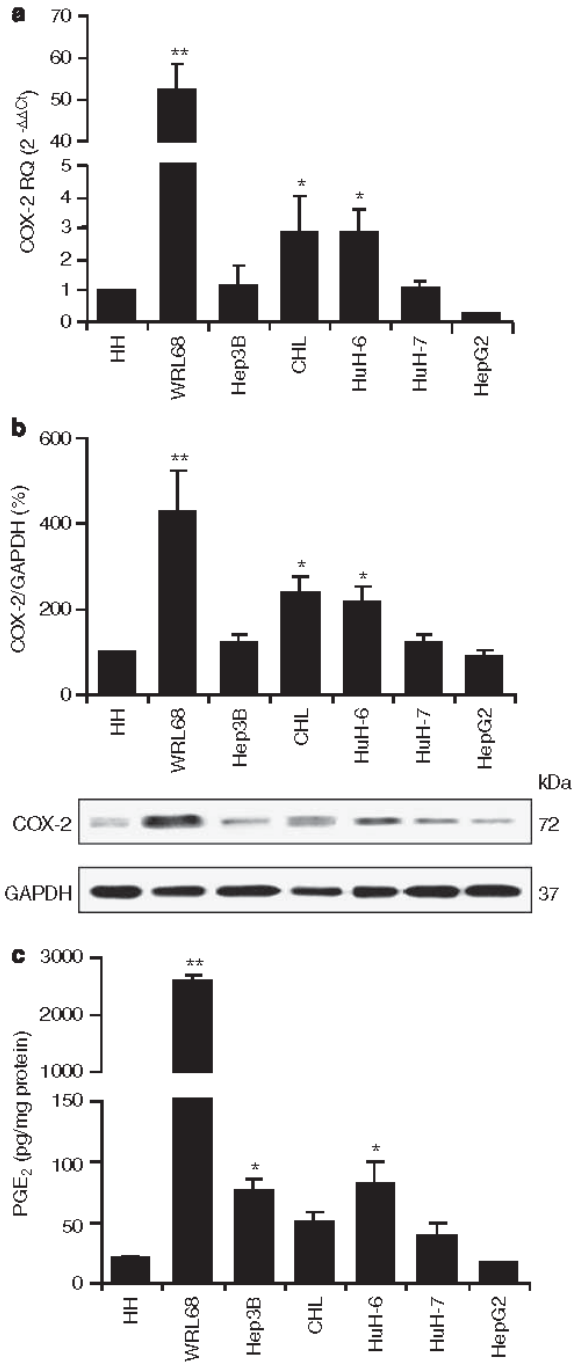

Figure 1. COX-2 expression and protein levels in HCC cell lines. Cells were plated in 100-mm dishes and grown to 60–70% confluence in a culture medium supplemented with 10% fetal bovine serum. (**a**) Total RNA was prepared from hepatic cell lines and COX-2 mRNA was analyzed by quantitative PCR. COX-2 mRNA amounts were calculated as relative quantitation (RQ) and normalized to the expression of 18S levels. Values represent fold change relative to human hepatocytes (HH). (**b**) Total cellular extracts were prepared from hepatic cells and protein (50 μg per lane) was analyzed by western blot. A representative western blot out of four is shown. The expression of target protein was normalized to that of GAPDH. Densitometric analysis of COX-2 expression using HH as reference control (100%) is also shown (**c**) Prostaglandin E_2 (PGE_2) concentration was determined by enzyme immunoassay in the supernatant of the cells. Data are reported as means ± s.d. of four independent experiments. $^*P<0.05$ and $^{**}P<0.01$ vs HH.

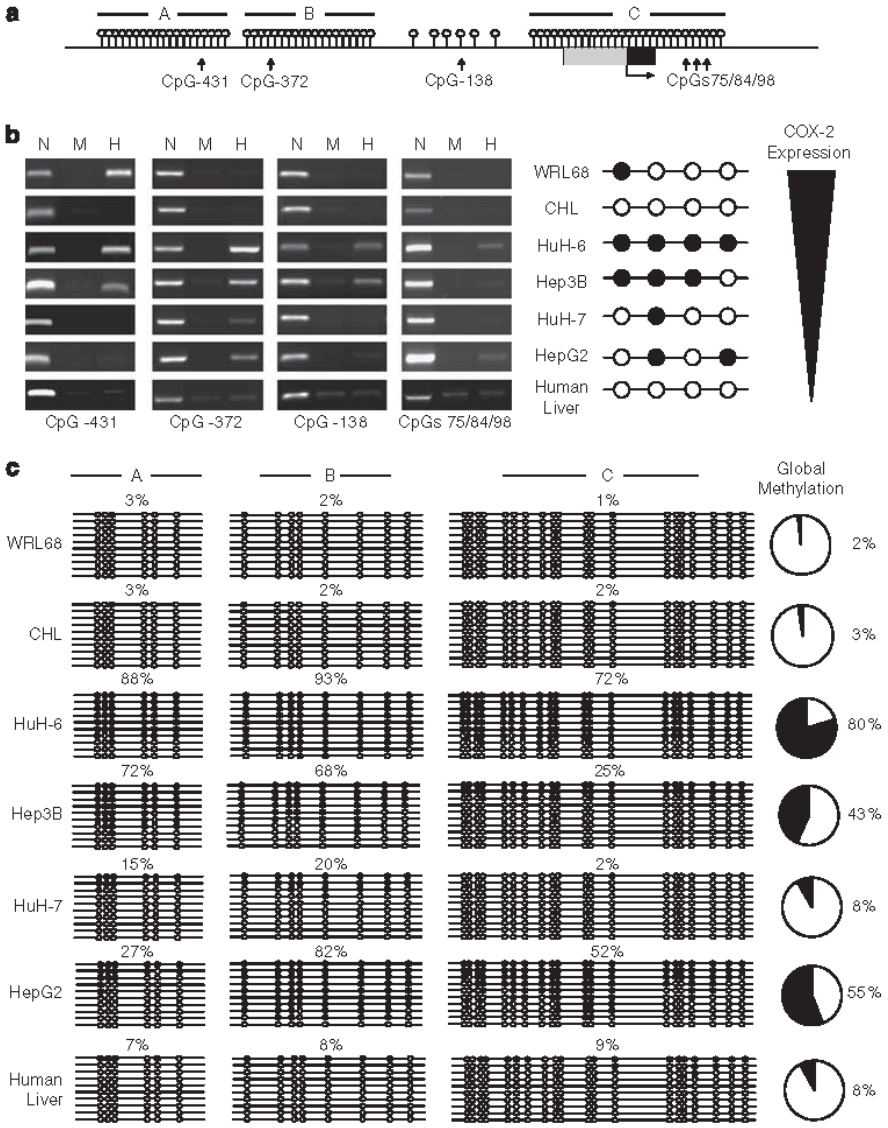

Figure 2. Methylation analysis of CpG islands at *COX-2* gene in HCC cells. (**a**) Representative scheme of putative CpG islands (A, B, C) identified by bioinformatic analysis and CpG dinucleotides detected by MSRA (black arrows) in the 5′ upstream region of *COX-2* gene. The non-coding (gray rectangle) and coding (black rectangle) regions of the first exon are also shown. (**b**) The MSRA technique was used to analyze the methylation profile of CpG sites in the COX-2 promoter region using DNA from the human liver and six liver derived cell lines. DNA digested with *Msp*I (M), *Hpa*II (H) or no restriction enzyme (N) was amplified by PCR using primers recognizing the − 431, − 372, − 138 or 75/84/98 CpG sites. A representative ethidium bromide-stained agarose gel is shown for each PCR reaction. A scheme of methylation state is represented using white balls (non-methylated) or black balls (methylated). The COX2 expression levels in the cell lines are represented with a black triangle. (**c**) Profiles of the percentage of methylation in the each CpG (A, B, C) islands of COX-2 promoter in the human liver and hepatic cell lines analyzed by bisulfite pyrosequencing. The global promoter methylation percentage for each sample is shown in the right panel.

methylation percentage in basal conditions. In the same conditions, COX-2 mRNA levels were analyzed by reverse transcription-quantitative PCR. HuH-6 and Hep3B presented a 5- and 78-fold induction of COX-2 expression, respectively. Furthermore, HuH-7 cells presented a fourfold induction of COX-2 expression after treatment with AzadC despite the absence of changes in the methylation pattern (Figure 3b), highlighting the relevance of promoter demethylation in the regulation of COX-2, although other alternative mechanisms may coexist. To asses if this differential response is a specific mechanism related to COX-2 regulation, we determined the amount of glyceraldehyde-3-phosphate dehydrogenase (GAPDH) mRNA normalized to the expression of 18S in all cell lines used. AzadC produced a minor reduce in GAPDH expression, with an effect that was quantitatively comparable in the three cell lines analyzed.

Role of histone acetylation on COX-2 transcription in HCC cells

To evaluate the effect of histone modifications on COX-2 expression, we first examined the effects of two HDAC inhibitors (HDACis), sodium butyrate (NaB) and suberoylanilide hydroxamic acid (SAHA), on COX-2 mRNA and protein levels in hepatic cell lines. Treatment of cells with the inhibitors promoted a marked increase of COX-2 mRNA levels at 16 h (no changes were found at

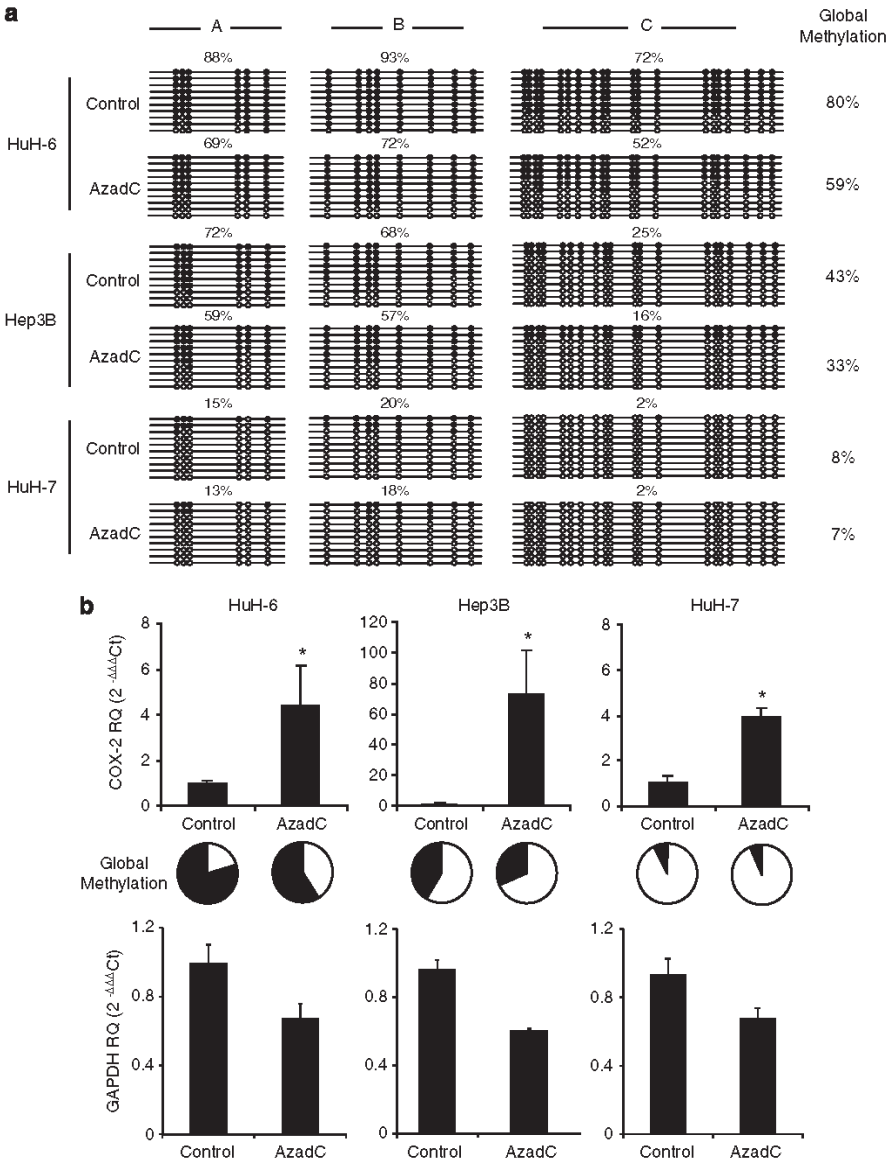

Figure 3. Effect of the demethylating agent, AzadC, on the methylation state in COX-2 CpG islands. (**a**) Methylation percentage profiles of each COX-2 promoter CpG (A,B,C) islands in HuH-6, Hep3B and HuH-7 cells in control or 5 μM AzadC-treated cells analyzed by bisulfite pyrosequencing. The global promoter methylation percentage for each condition is shown in the right panel. (**b**) COX-2 mRNA in HuH-6, Hep3B and HuH-7 control and AzadC-treated cells by quantitative PCR. COX-2 and GAPDH mRNA amounts were calculated as RQ and normalized to the expression of ribosomal 18S. Values represent fold change relative to control condition in each cell line. The global CpG methylation for each cell line and condition is also shown. $^*P<0.05$ vs the corresponding cell line without treatment.

6 h) except for WRL68 (Supplementary Figure S1). A significant increase in COX-2 was observed in Hep3B, HuH-6 and HuH-7 hepatoma cells by the effect of both NaB and SAHA after 24 h of treatment (Figure 4a). Prostaglandin E_2 levels well correlated with COX-2 protein (Figure 4b). No changes were detected in HDAC1, 2, 3 and SIRT1 protein levels by the effect of HDACis in HCC cells. The acetylation status of histone H3 and histone H4 was evaluated (Figure 4a) and a significant increase in acetylated histones H3 and H4 was observed in HCC cells. Moreover, when global HDAC activity was measured by using a colorimetric detection assay, the highest activity corresponded to Hep3B and HuH-6 cells. As expected, global HDAC activity was inhibited by treatment of the cells with NaB and SAHA (Figure 4c). These results suggest that histone acetylation regulates COX-2 expression in some HCC cells.

We determined whether there was a direct link between the increased H3 and H4 acetylation and COX-2 expression, analyzing the effects of NaB on acetylated histones recruitment at the COX-2 promoter. We ascertained the interaction of Ac-H3 and Ac-H4 all along the 5′ region of the *COX-2* human gene using a standard chromatin immunoprecipitation assay followed by real-time PCR. The α-RNA polymerase antibody was used as a control of gene activity. Four different primer pairs were used to cover the complete regulatory sequence starting on a distal promoter region, and ending on the first intronic region. We found an

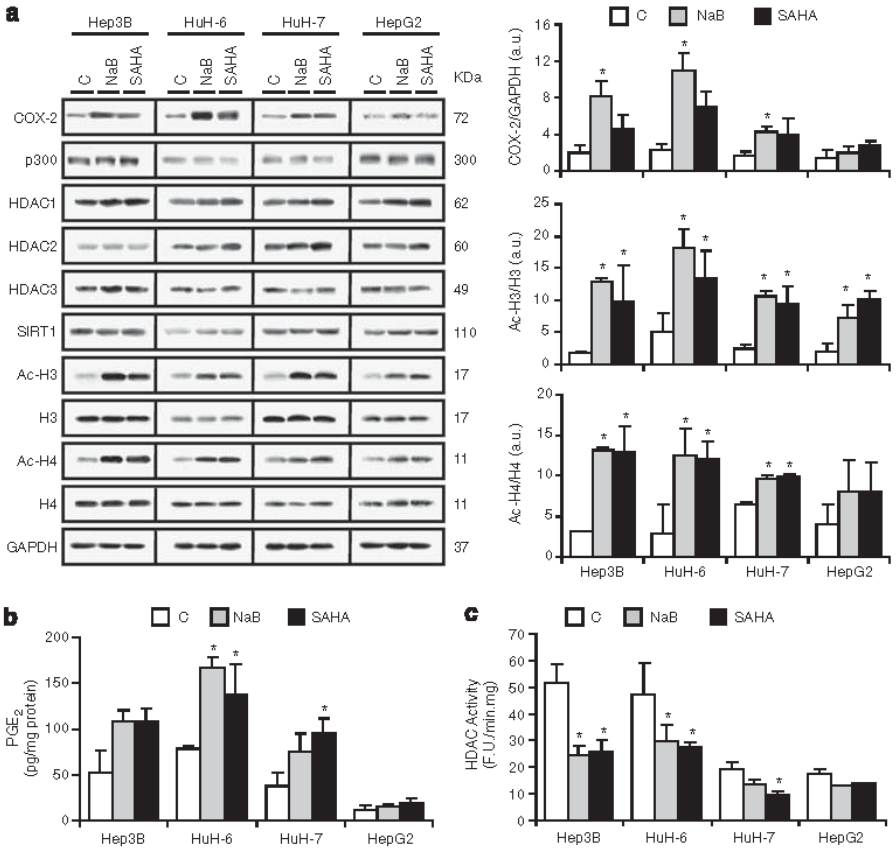

Figure 4. COX-2, HDACs and acetylated H3 and H4 protein levels after treatment of HCC cells with HDACis. (**a**) HCC cells in 1% fetal bovine serum were incubated without (white) or with 2.5 mM NaB (gray) or 2.5 μM SAHA (black) for 24 h. Cellular extracts were prepared and protein was analyzed by western blot. Left panel shows a representative western blot analyzing COX-2, p300, HDAC1, 2, 3, SIRT1 and acetylated (Ac) or total histones H3 y H4 protein levels. Each panel has an optimal exposition time. Results are expressed as arbitrary units after densitometric analysis of COX-2 expression or the expression of the ratios Ac-H3/H3 and Ac-H4/H4 normalized to GAPDH (right panel). (**b**) Prostaglandin E_2 (PGE_2) concentration was determined by enzyme immunoassay in the supernatant of the cells. (**c**) Global HDAC activity was measured by using a fluorimetric detection assay as described in Materials and Methods and the results are expressed as fluorescence units (FU) per minute and mg of protein. Data are expressed as means ± s.d. of three independent experiments. *$P < 0.05$ vs the corresponding cell line without treatment.

increased Ac-H3 association both in HuH-6 and HuH-7 cells, with a higher signal in HuH-6 cells after treatment with NaB. The increased association is higher in the proximal promoter and the noncoding part of the first exon, which includes the CRE regulatory site. An increased Ac-H4 association was only seen on HuH-6 cells chromatin (Figure 5a).

To investigate whether histone acetylation is associated with HCC, we determined the COX-2, histone H3 and aceylated-H3 immunoreactivity in tumor tissue samples. Ac-H3 staining was observed primarily in the cell nuclei (Figure 5b). Immunoreactivity of Ac-H3 protein ranged from 138% to 34% vs a positive control tissue (amygdala) considered as 100%.[24] In the study cohort, high expression of Ac-H3/H3 ratio was detected in 67% of HCCs. Assessment of survival in these patients revealed that high Ac-H3/H3 ratio was correlated with a favorable disease-specific survival ($P = 0.021$; Figure 5c). Moreover, an increased COX-2 immunoreactivity was observed in the tumors with a major Ac-H3/H3 ratio (Figure 5b).

It has been described that demethylating agents and HDACis function in synergy by depleting methyltransferase activity and reversing the formation of transcriptionally repressive chromatin structure.[25,26] Combined treatment with AzadC and NaB or SAHA induced a higher increase of functional COX-2 protein levels than the HDACis alone. Moreover, both drugs decreased DNMT1 protein levels in HCC cells (Supplementary Figure S2).

Methylation analysis of COX-2 promoter in primary HCCs

Quantitative real-time RT–PCR analysis of HCC samples revealed significantly higher COX-2 mRNA levels vs normal human liver. Moreover, 86% patients showed a higher COX-2 expression in the non-tumoral biopsies compared with their paired tumoral sections (Figure 6b), as it has been described previously.[12] To determine whether aberrant methylation of COX-2 is associated with HCCs, we performed bisulfite sequencing of CpG islands A, B and C at COX-2 locus from 23 tumor and non-tumor clinical samples of HCC patients. Consistent with the expression levels, the COX-2 promoter was methylated extensively in tumor tissues compared with the corresponding nontumor sections (Figure 6c). However, the hypermethylation of COX-2 promoter was exclusively found in 57% of the tumor tissues with respect to their non-tumor counterparts (Figure 6a). The average global methylation in these samples was 31% and 7.6% of tumor and non-tumor tissues, respectively. In all cases, the altered methylation pattern was clearly seen in the CpG islands B and C but not in the A. Next, we investigated whether this differential methylation status was

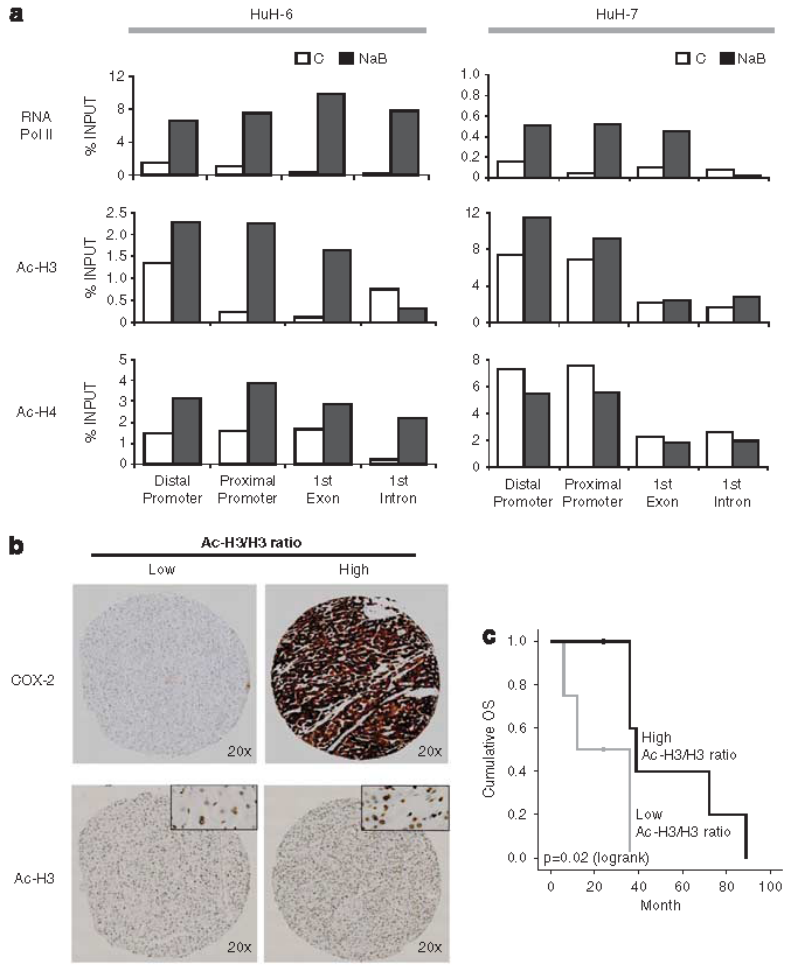

Figure 5. Effect of HDACis on histone H3 and H4 acetylation at the human COX-2 promoter in HCC cells. Role of acetylation in primary HCCs. (**a**) Chromatin immunoprecipitation assay was performed with HuH-6 and HuH-7 cells in control (white bars) or NaB (black bars)-treated conditions. Immunoprecipitation of samples was performed with anti-acetylated histone antibodies. The histone binding was analyzed using oligonucleotides that recognize different parts of the 5′regulatory region of the *COX-2* gene. A positive control of transcriptionally active genes was performed using anti-RNA-polymerase II antibody and a negative control with no antibody. The results are representative of three quantitative PCR independent experiments. (**b**) Immunohistochemical staining of COX-2, acetylated histone H3 (Ac-H3) in HCCs. Original magnification $\times 20$. Expression of COX-2 and Ac-H3 was shown in representative HCC patients according immunoreactivity levels. Inset: Positive staining of Ac-H3 in nuclei ($\times 80$). (**c**) Kaplan–Meier survival analysis of Ac-H3/H3 ratio in subsets of HCC patients with a different percentage ratio: $\leqslant 50\%$ (low; gray line) or $>50\%$ (high; black line) relative to the ratio in the positive control tissue (100%).

correlated with COX-2 expression in clinical samples of HCC. A statistically significant inverse association was observed between the COX-2 mRNA levels and methylation status in HCC (Figure 6d). Moreover, OS was significantly different according to the methylation status without significant differences in disease-free survival rates (Figure 6e). A hypermethylation of COX-2 promoter was significantly associated with a poor OS ($P = 0.04$). We did not observe any significant association with other clinical signs (Table 1).

DISCUSSION

Increased COX-2 expression has been found in the early stages, but is lost in advanced HCC.[13] Moreover, COX-2 mRNA levels were significantly higher in the adjacent healthy liver than in HCC and lower in HCC than in nonalcoholic steatohepatitis disease.[27] Therefore, many questions remain unsolved regarding the contribution of COX-2 to induce/regulate tumorigenesis. As the mechanisms regulating COX-2 expression at specific stages of HCC progression remain unknown, we hypothesize that COX-2 expression could be regulated by epigenetic changes such as DNA methylation and histone acetylation. Here, we show that the low COX-2 expression in some HCC lines and in HCC biopsies is associated with COX-2 promoter hypermethylation and histone deacetylation. Conversely, treatment with HDACis or demethylating agents increased the expression of COX-2.

DNA methylation is a predominant mechanism used to inactivate relevant genes during HCC tumorigenesis. Recent findings support the hypothesis that hypomethylation of the DNA surrounding the proximal promoter region is a prerequisite for activation of oncogenes, whereas hypermethylation leads to gene silencing of putative tumor-suppressor genes.[28] The therapeutic and chemopreventive significance of methylation patterns in human HCC have been reported; Lee *et al*,[29] showed

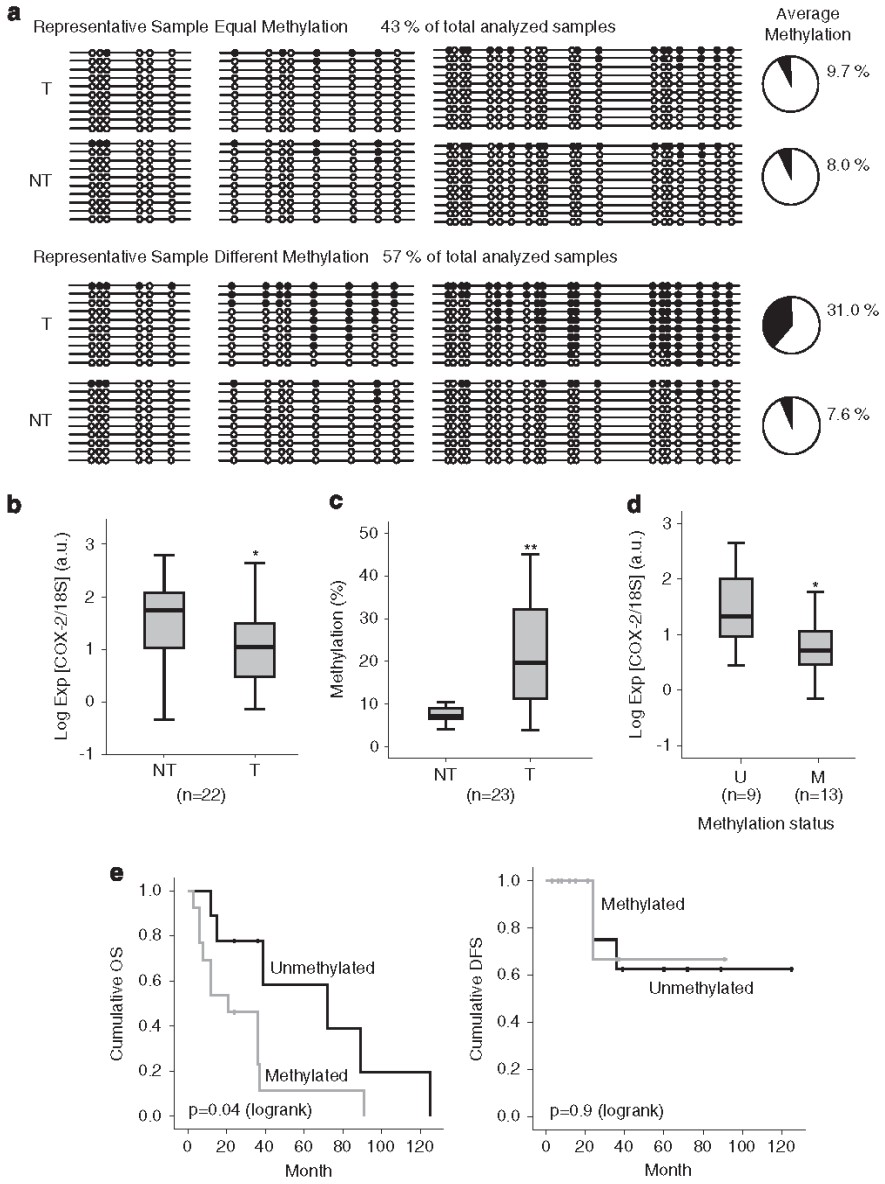

Figure 6. Methylation analysis of COX-2 promoter in primary HCCs. (**a**) DNA methylation status of the COX-2 promoter in HCC tumor (T) and non-tumor (NT) samples determined by bisulfite pyrosequencing. A representative scheme of equal or altered methylation status between tumor (T) and non-tumor (NT) biopsies is shown. The global promoter methylation percentage for each group is shown in the right panel. (**b**) COX-2 mRNA levels in liver tissue from 23 patients were determined by quantitative real-time RT–PCR using 18S as the normalization control. NT, T ($n=22$). *$P<0.05$ vs NT samples; (**c**) Methylation quantities were determined by pyrosequencing ($n=23$). **$P<0.01$ vs NT samples (**d**) Box plots showing the analysis of the association between COX-2 mRNA levels and methylation status. The samples were classified according the average methylation of COX-2 promoter between tumor and their non-tumor counterparts. U, samples exhibited a low percentage of COX-2 promoter methylation without differences between the tumoral and non-tumoral tissue ($n=9$); M, patients showed a higher percentage of COX-2 promoter methylation in the tumoral tissue ($n=13$). (**e**) OS and disease-free survival (DFS) curves according to COX-2 methylation status using Kaplan–Meier survival plots. OS is significantly associated with the methylation status of COX-2 ($P=0.04$). Gray line, patients with a hypermethylation status in the tumoral tissue; black line, patients without alteration in percentage of methylation of COX-2 promoter between tumor and their non-tumor counterparts.

that the *APC, GSTP1 RASSF1A, p16, COX-2* and *E-cadherin* genes were frequently methylated in HCC. Moreover, COX-2, p16, RASSF1A and TIMP-3 were not methylated in liver cirrhosis and chronic hepatitis from patients without concurrent HCC. To date, frequent and aberrant methylation of *Ras* and Janus kinase/signal transducer and activator of transcription inhibitors in HCC resulted in persistent activation of the *Ras* and Janus kinase/signal transducer and activator of transcription pathways.[30] The same group[31] has investigated the global levels of DNA methylation as well as the methylation status of 105 putative tumor-suppressor

Table 1. Clinicopathological features of 23 HCC patients

	Methylation status of tumor biopsies		P
	Unmethylated	*Methylated*	
Sex			0.339
Male	9	9	
Female	1	4	
Age	70.2 ± 7.2	63.46 ± 15.6	0.284
Etiology			0.709
HBV	1	1	
HCV	4	4	
Ethanol	1	3	
HCT	1	0	
NA	3	5	
Cirrhosis			0.673
Positive	3	5	
Negative	7	8	
Tumor size			0.372
>5	2	6	
<5	6	6	
NA	2	1	
Histological grade			0.282
WD	5	9	
MD	3	3	
UD	0	1	
NA	2	0	

Abbreviations: HBV, hepatitis B infection; HCC, human hepatocellular carcinoma; HCT, Hemochromatosis; HCV, hepatitis C infection; MD; moderate differentiated; NA, not assigned; UD, undifferentiated; WD, well differentiated.

genes and found that the extent of genome-wide hypomethylation and CpG hypermethylation correlates with biological features and clinical outcomes of HCC patients. Furthermore, methylation also appears to be an early event, suggesting that this may precede cirrhosis. The more aggressive subclass A of HCC displayed a very high frequency of gene promoter hypermethylation, a condition similar to the CpG island methylator phenotype described in human colorectal cancer.[32] Recently, Yang *et al.*[33] have identified genes whose methylation and mRNA levels are associated with recurrence after resection for HCC using integrated analysis by whole-genome DNA methylation and mRNA expression data. They suggest that potential novel oncogenes (*PSRC1*, *MYO1E*), tumor-suppressor genes (*CFH*, *MYRIP*) and TGF, Wnt and cytoskeletal remodeling were the major pathways enriched with the recurrence predicting genes. Regarding COX-2, it has been reported that epigenetic silencing of COX-2 affects clinical outcome in gastric cancer.[16]

To clarify the methylation status of the COX-2 promoter in HCC three CpG islands, identified through bioinformatic analysis, were examined by pyrosequencing in six hepatic cell lines exhibiting different COX-2 expression levels. Furthermore, CpG sites located at −431, −372, −138 and +75/84/98 were analyzed by the MSRA analysis. We observed a broad range of methylation from 2% in WRL68 to 43% in Hep3B cell line, without a correlation between these percentages and COX-2 expression. Nevertheless, we could demonstrate that treatment with a demethylating agent, AzadC, readily induced COX-2 expression in HCC cells. These results suggest that the methylation status of the promoter can regulate COX-2. However, we could not discard indirect mechanisms regulating COX-2 expression, as observed in HuH-7 cells, in which the treatment with demethylating agent increased the COX-2 mRNA levels despite the permanent hypomethylation status of the promoter in this cell line. In fact, it has been suggested that in colorectal cancer cells, AzadC is capable of influencing other factors involved in gene expression such as proteins with a methyl-binding domain or histone modifications.[34]

Prostaglandin E_2 promotes intestinal tumor growth via DNA methylation of certain tumor-suppressor and DNA-repair genes by enhancing their promoter methylation.[35] Moreover, hypermethylation of *COX-2* gene promoter has been identified as an independent prognostic factor in gastric cancer patients.[16] These results prompted us to study whether the methylation of COX-2 promoter was related with the COX-2 expression in HCC. In agreement with previous work,[9,36] COX-2 mRNA levels were higher in the adjacent liver tissue than in HCC in the 86% of the studied biopsies. When we analyzed the methylation profile at three CpG islands, we could classify the samples in two groups: 43% of samples exhibited a low percentage of COX-2 promoter methylation without differences between the tumoral and non-tumoral tissue, whereas the remaining 57% showed a higher percentage of COX-2 promoter methylation in the tumoral tissue. This methylation status was associated with COX-2 expression as suggested by the significant differences in the levels of COX-2 between both groups. These results suggest that the promoter hypermethylation is an important regulatory mechanism of COX-2 expression in HCC.

The long-term survival of patients with HCC is unsatisfactory, in part because of the high rate of recurrence after curative surgical resection of hepatocellular carcinoma. There have been many reports on the prognostic significance of epigenetic alterations at the promoter region of genes associated with HCC. For example, patients with E-cadherin or GSTP1 methylation showed poorer survival than those without.[29] In this study, COX-2 methylation was associated with poor prognosis in HCC. Although it remains unclear how COX-2 methylation affects prognosis in these cases, methylation of COX-2 may occur concordant with other methylation alterations and could be part of the genome-wide methylation defect in these cancers.[37] Thus, COX-2 may integrate a CpG island methylator phenotype associated with poor prognosis.

NaB, a short-chain fatty acid that is normally present in the human colon as a product of the metabolic degradation of complex carbohydrates, was the first compound found to possess histone deacetyltransferase-inhibiting activity.[38] Different preclinical studies with NaB showed its ability to inhibit HCC cell growth. Beside NaB, hydroxamic acids including trichostatin A and SAHA are undergoing phase I and II clinical trials to validate their potential use as anticancer drugs for solid and hematological tumor treatment either as monotherapies or in combination with other cytotoxic agents. Our data demonstrate that treatment of HCC cells with NaB or SAHA increased COX-2 expression and restored acetylation of histones H3 and H4 around COX-2 promoter in some hepatoma cell lines. An interesting finding in our study was that HCC patients with a major percentage of histone H3 acetylation had a better survival. Thus, it is speculated that epigenetic mechanism that implies a less expression of COX-2 are linked to poor prognosis of patients with hepatocarcinoma.

There are some different results concerning the effect of HDACis on COX-2 expression. To date, butyrate and trichostatin A suppress COX-2 expression in HT-29 cells by inhibition of RNA polymerase II elongation on the *COX-2* gene and the same occurs for c-myc.[39] In KYSE450 (esophageal squamous cell carcinoma) and in 184B5/HER (Neu-transformed breast cells), HDACis suppress PMA-mediated induction of COX-2[40] and in human non-small cell lung cancer cells, trichostatin A-induced apoptosis and decreased the levels of COX-2 mRNA and protein expression.[41] However, NaB and trichostatin A accentuated LPS-induced *COX-2* gene expression through mitogen-activated protein kinase-dependent increase of phosphorylation and acetylation of histone H3 at the COX-2 promoter and by decreasing C/EBPδ levels.[42,43] These

results and our data suggest that the effect of HDACis on COX-2 activation does not appear to be common to all the cell types and even not related with their anti-tumoral activity.

In conclusion, COX-2 expression appears to be regulated at first instance by promoter methylation and histone acetylation in hepatoma cell lines and HCC. Our results indicate that alterations in promoter methylation of COX-2 occur exclusively in hepatic tumor regions of HCC and that aberrant methylation of COX-2 in HCC leads to poor prognosis after surgical resection. Primary tumor COX-2 methylation status may therefore be used as a signature to decide a more aggressive treatment in HCC. Our data suggest that epigenetic mechanisms that imply reduced COX-2 expression are linked to poor prognosis of HCC patients. The identification of the crosstalk between epigenetic signatures and transcription factors activity appears to be relevant for the implementation of new HCC therapeutic approaches.

MATERIALS AND METHODS

Cell lines and tissue samples

A total of 23 individual tumoral and paired non-tumoral frozen HCC tumors were obtained from the de Spanish Tumor Bank Network of the Centro Nacional de Investigaciones Oncológicas. Institutional Review Board approval was obtained for these studies and all participants provided written informed consent. All tissues were evaluated by pathologists by means of hematoxylin/eosin staining. Histological graded as well (WD), moderate (MD) or undifferentiated (UD) was determined according to the Edmondson and Steiner classification, following World Health Organization recommendations. Clinicopathological parameters of HCC patients are summarized in Table 1. This retrospective cohort study used a prospective database during 8-year period (partial liver resection from 2001 to 2009, follow-up data until 2011). Death from any cause was used to determine the OS rate. Disease-free survival was defined as a patient who was alive at the end of the follow-up period. All specimens examined in this study were collected at primary surgery. At the time of the last follow-up 5 (21.7%) patients were alive and 18 (78.3%) patients had died of disease (median OS 44.2 months, confidence interval 95% = 27–61%).

The human liver cell lines WRL68, Chang liver (CHL) and the hepatoma cell lines HepG2 and Hep3B were purchased from the American Type Culture Collection (ATCC, Manassas, VA, USA). All these cells lines were authenticated by ATCC and were expanded twice, and stored in liquid N_2. Expansions from these clones were used up to 6 months in culture. HuH-6 and HuH-7 cell lines were kindly provided by Dr Perret (Institut Cochin, CNRS UMR8104, University Paris-Descartes, Paris, France) and Dr Kern (Department of General Pathology, University Hospital Heidelberg, Heidelberg, Germany), respectively. Cells were grown on Eagle's Minimal Essential Medium or Dulbecco's modified Eagle's medium (Sigma Chemical Co. St Louis, MO, USA) supplemented with 10% fetal bovine serum and antibiotics (50 μg each of penicillin, streptomycin and gentamicin per ml). The cells were treated with the following drugs alone or in combination: 2.5 mM NaB (Sigma), 2.5 μM SAHA (Sigma) and 5 μM 5-aza-2′-deoxycytidine (AzadC; Sigma). Timing and concentration curves were performed previously to determine the optimal concentrations.

RNA extraction and quantitative real-time PCR analysis

Total RNA from single-freeze cryopreserved pooled human hepatocytes (HPCH10 CryostaX, XenoTech, Lenexa, KS, USA), cell lines and liver biopsy samples was extracted by using TRIzol reagent (Life Technologies, NY, USA). RNA (1 μg) was reverse transcribed using a Transcriptor First Strand cDNA Synthesis Kit following the manufacturer's indications (Roche Applied Science, Indianapolis, IN, USA). The cDNA was used as template for real-time PCR through Taqman probes. COX-2 (Hs00153133_m1), GAPDH (Hs99999905_m1) or 18S (Hs99999901_m1) assay on demand gene expression products were used (Life Technologies). Real-time PCR was performed using a MyiQ detection system (Bio-Rad Laboratories, Hemel Hempstead, UK) and thermocycling parameters were 95 °C for 10 min, 50 cycles of 95C for 15 s followed for 60 °C for 1 min. Each sample was run in triplicate and was normalized to 18S levels. Three replicates were then averaged, and fold induction was determined in a ΔΔCt based fold-change calculations.

Western blot analysis

Extracts from cells ($2–3 \times 10^6$) or cryopreserved pooled human hepatocytes were obtained as described previously.[44] The relative amounts of each protein were determined with the following polyclonal or monoclonal antibodies: COX-2 (sc-1747, Santa Cruz Biotechnology, Santa Cruz, CA, USA); HDAC 1, 2, 3 (Santa Cruz and Cell Signaling, Boston, MA, USA); sirtuin 1 (SIRT1; Millipore, Billerica, MA, USA); anti-histone 3 (H3), anti-histone 4 (H4) and anti-acetylated H4 (Ac-H4; Abcam, Cambridge, UK); anti-acetylated H3 (Ac-H3; Millipore) and DNA (cytosine-5) methyltransferase 1 (DNMT1; Imgenex, San Diego, CA, USA). After incubation with the corresponding anti-rabbit or anti-mouse horseradish peroxidase-conjugated secondary antibody, blots were developed by the ECL protocol (GE Healthcare, Chalfont St Giles, UK). Target protein band densities were normalized with the expression of GAPDH (Life Technologies). The blots were revealed, and different exposition times were performed for each blot with a charged coupling device camera in a luminescent image analyzer (Chemi-Doc XRS, Bio-Rad) to ensure the linearity of the band intensities. Densitometric analysis was expressed in arbitrary units.

Immunohistochemical staining

Two- to four-micrometer thick paraffin-embedded tissue microarrays and complete sections were cut onto Dako slices (Dako, Glostrup, Denmark) by Immunohistochemistry unit of the Centro Nacional de Investigaciones Oncológicas, and subsequently dewaxed, rehydrated and subjected to antigen retrieval by heating in PTLink with 50 mM Tris/EDTA pH 9.0. The slides were cooled and treated with peroxidase-blocking solution (Dako) for 5 min. Sections were immunostained with a COX-2 antibody (NeoMarkers, Suffolk, UK), anti-histone H3 (Abcam) and acetyl-histone H3 (K9; Abcam) in a Autostainer Plus (Dako). In parallel, each tissue section was also incubated with a rabbit anti-mouse antiserum and was used as a negative control. Microphotographs were taken with an EnVision FLEX system (Dako). The images were processed with the Image J software developed at the National INstitutes of Health (Bethesda, MD, USA). Integrated density was calculated for each image after background substraction. The background corresponds to the immunoreactivity in the negative control tissue (normal liver). The percentage of the ratio between acetyl histone H3 and histone H3 immunoreactivity was calculated considering 100% the ratio of a positive control tissue (amygdala) added to tissue microarray slides.[24]

Determination of metabolites and enzymatic activities

Prostaglandin E_2 was determined in culture media by specific immunoassay (Arbor Assays, Ann Arbor, MI, USA).[44] HDAC total activity was analyzed in cell extracts by a fluorimetric detection method (HDAC Assay Kit, Upstate, Billerica, MA, USA).

Genomic DNA isolation, bisulfite treatment and methylation-specific analysis

Genomic DNAs were isolated from cells or resected specimens using the Maxwell 16 DNA purification Kit (Promega, Madison, WI, USA) and DNA samples were treated with bisulfite using the EZ DNA Methylation-Gold Kit (Zymo Research, Irvine, CA, USA) to convert cytosine to uracil, according to the manufacturer's instructions. A two steps nested-PCR strategy was used to amplify COX-2 CpG islands starting with 1 μl of bisulfate-treated DNA in a final volume of 25 μl. In the first step, a 412-bp fragment was amplified for CpG islands A and B, and a 476-bp fragment for the CpG island C. The PCR cycle used was as follows: 95 °C for 10 min, 40 cycles at 95 °C for 30 s, 58 °C (islands A and B) or 56 °C (island C) for 30 s and 72 °C for 45 s and a final extension at 72 °C for 10 min. A 2.6 μl volume of the first PCR product was used as a template for a new round of amplification in a final volume of 65 μl using a pair of internal primers, one of them a biotin-5′-modified oligonucleotide. A fragment of 368 bp for CpG islands A and B or a 290-bp fragment for CpG island C was amplified using the PCR cycle described above. The final product was purified and pyrosequenced for methylation analysis by the DNA Analysis Facility of the Instituto de Biomedicina de Valencia, Spain. All used primers are detailed in the Supplementary Table 1.

The methylation status was also evaluated by MSRA. After isolation genomic DNA samples were treated with restriction enzymes *Msp*I and *Hpa*II and amplified by PCR as follows: 95 °C for 10 min and then 30 cycles at 95 °C for 15 s, 58 °C for 30 s and 72 °C for 30 s and a final extension at 72 °C for 7 min. A non-digested sample was used as the positive control. PCR products were visualized on a 2% agarose gels stained with ethidium

bromide. Specific primers used for amplification of each CpG site are shown in the Supplementary Table 2.

Chromatin immunoprecipitation analysis

Evaluation of histone acetylation levels was performed by chromatin immunoprecipitation analysis as described previously,[45] using isolated nuclei from formaldehyde-cross-linked HuH-6 and HuH-7 cells. Chromatin obtained from untreated (control) or 16 h NaB-treated cells was immunoprecipitated using antibodies against: RNA polymerase II (sc-899, Santa Cruz), Ac-H3 (K9, K14) (06-599, Millipore) and Ac-H4 (K12) (07-595, Millipore). The amount of DNA in each chromatin immunoprecipitated was quantified by real time–PCR on a 7500 Fast System (Life Technologies) using the SYBR Green PCR reagent. The oligonucleotides used for each PCR reaction are listed in the Supplementary Table 3.

Data analysis

Data are expressed as mean ± s.d. (*n* ranged from three to five independent experiments). The Mann–Whitney *U* test was used for ordinal variables. Survival length was determined from the day of primary tumor surgery to the date of death or last clinical follow-up. The Kaplan–Meier method was used for survival analysis grouping with COX-2 methylation or acetylation status. Differences between curves were analyzed using the log-rank test. The statistical software SPSS Statistics 20 (IBM, Armonk, NY, USA) was used; a *P*-value of <0.05 was considered significant.

CONFLICT OF INTEREST

The authors declare no conflict of interest.

ACKNOWLEDGEMENTS

We thank Beatriz Agueda, Silvia Aparicio and Benito Alarcón for their technical assistance. This work was supported by the Ministry of Science and Innovation (SAF2010-16037, SAF2009-12602 and BFU2011-24760) and by Comunidad de Madrid (P2010/BMD-2378). CIBERehd is funded by the Instituto de Salud Carlos III. AF-A and NA were supported by the Carlos III Health Institute (Red de Centros FIS-RECAVA RD06/0014/0025).

REFERENCES

1 Simmons DL, Botting RM, Hla T. Cyclooxygenase isozymes: the biology of prostaglandin synthesis and inhibition. *Pharmacol Rev* 2004; **56**: 387–437.
2 Ledwith BJ, Pauley CJ, Wagner LK, Rokos CL, Alberts DW, Manam S. Induction of cyclooxygenase-2 expression by peroxisome proliferators and non-tetradecanoylphorbol 12,13-myristate-type tumor promoters in immortalized mouse liver cells. *J Biol Chem* 1997; **272**: 3707–3714.
3 Martin-Sanz P, Callejas NA, Casado M, Diaz-Guerra MJ, Bosca L. Expression of cyclooxygenase-2 in foetal rat hepatocytes stimulated with lipopolysaccharide and pro-inflammatory cytokines. *Br J Pharmacol* 1998; **125**: 1313–1319.
4 Casado M, Callejas NA, Rodrigo J, Zhao X, Dey SK, Bosca L *et al.* Contribution of cyclooxygenase 2 to liver regeneration after partial hepatectomy. *FASEB J* 2001; **15**: 2016–2018.
5 Rudnick DA, Perlmutter DH, Muglia LJ. Prostaglandins are required for CREB activation and cellular proliferation during liver regeneration. *Proc Natl Acad Sci USA* 2001; **98**: 8885–8890.
6 Yamamoto H, Kondo M, Nakamori S, Nagano H, Wakasa K, Sugita Y *et al.* JTE-522, a cyclooxygenase-2 inhibitor, is an effective chemopreventive agent against rat experimental liver fibrosis1. *Gastroenterology* 2003; **125**: 556–571.
7 Kern MA, Haugg AM, Koch AF, Schilling T, Breuhahn K, Walczak H *et al.* Cyclooxygenase-2 inhibition induces apoptosis signaling via death receptors and mitochondria in hepatocellular carcinoma. *Cancer Res* 2006; **66**: 7059–7066.
8 Mayoral R, Fernandez-Martinez A, Bosca L, Martin-Sanz P. Prostaglandin E2 promotes migration and adhesion in hepatocellular carcinoma cells. *Carcinogenesis* 2005; **26**: 753–761.
9 Cusimano A, Fodera D, Lampiasi N, Azzolina A, Notarbartolo M, Giannitrapani L *et al.* Prostaglandin E2 receptors and COX enzymes in human hepatocellular carcinoma: role in the regulation of cell growth. *Ann NY Acad Sci* 2009; **1155**: 300–308.
10 Cheng AS, Yu J, Lai PB, Chan HL, Sung JJ. COX-2 mediates hepatitis B virus X protein abrogation of p53-induced apoptosis. *Biochem Biophys Res Commun* 2008; **374**: 175–180.
11 Nunez O, Fernandez-Martinez A, Majano PL, Apolinario A, Gomez-Gonzalo M, Benedicto I *et al.* Increased intrahepatic cyclooxygenase 2, matrix metalloproteinase 2, and matrix metalloproteinase 9 expression is associated with progressive liver disease in chronic hepatitis C virus infection: role of viral core and NS5A proteins. *Gut* 2004; **53**: 1665–1672.
12 Cervello M, Foderaa D, Florena AM, Soresi M, Tripodo C, D'Alessandro N *et al.* Correlation between expression of cyclooxygenase-2 and the presence of inflammatory cells in human primary hepatocellular carcinoma: possible role in tumor promotion and angiogenesis. *World J Gastroenterol* 2005; **11**: 4638–4643.
13 Koga H, Sakisaka S, Ohishi M, Kawaguchi T, Taniguchi E, Sasatomi K *et al.* Expression of cyclooxygenase-2 in human hepatocellular carcinoma: relevance to tumor dedifferentiation. *Hepatology* 1999; **29**: 688–696.
14 Kang YJ, Mbonye UR, DeLong CJ, Wada M, Smith WL. Regulation of intracellular cyclooxygenase levels by gene transcription and protein degradation. *Prog Lipid Res* 2007; **46**: 108–125.
15 Harper KA, Tyson-Capper AJ. Complexity of COX-2 gene regulation. *Biochem Soc Trans* 2008; **36**(Pt 3): 543–545.
16 de Maat MF, van de Velde CJ, Umetani N, de Heer P, Putter H, van Hoesel AQ *et al.* Epigenetic silencing of cyclooxygenase-2 affects clinical outcome in gastric cancer. *J Clin Oncol* 2007; **25**: 4887–4894.
17 Murata H, Tsuji S, Tsujii M, Sakaguchi Y, Fu HY, Kawano S *et al.* Promoter hypermethylation silences cyclooxygenase-2 (Cox-2) and regulates growth of human hepatocellular carcinoma cells. *Lab Invest* 2004; **84**: 1050–1059.
18 Deng WG, Zhu Y, Wu KK. Role of p300 and PCAF in regulating cyclooxygenase-2 promoter activation by inflammatory mediators. *Blood* 2004; **103**: 2135–2142.
19 Coward WR, Watts K, Feghali-Bostwick CA, Knox A, Pang L. Defective histone acetylation is responsible for the diminished expression of cyclooxygenase 2 in idiopathic pulmonary fibrosis. *Mol Cell Biol* 2009; **29**: 4325–4339.
20 Yue X, Yang F, Yang Y, Mu Y, Sun W, Li W *et al.* Induction of cyclooxygenase-2 expression by hepatitis B virus depends on demethylation-associated recruitment of transcription factors to the promoter. *Virol J* 2011; **8**: 118.
21 Hur K, Song SH, Lee HS, Ho Kim W, Bang YJ, Yang HK. Aberrant methylation of the specific CpG island portion regulates cyclooxygenase-2 gene expression in human gastric carcinomas. *Biochem Biophys Res Commun* 2003; **310**: 844–851.
22 Song SH, Jong HS, Choi HH, Inoue H, Tanabe T, Kim NK *et al.* Transcriptional silencing of Cyclooxygenase-2 by hyper-methylation of the 5′ CpG island in human gastric carcinoma cells. *Cancer Res* 2001; **61**: 4628–4635.
23 Callejas NA, Bosca L, Williams CS, Du BR, Martin-Sanz P. Regulation of cyclooxygenase 2 expression in hepatocytes by CCAAT/enhancer-binding proteins. *Gastroenterology* 2000; **119**: 493–501.
24 Uhlen M, Bjorling E, Agaton C, Szigyarto CA, Amini B, Andersen E *et al.* A human protein atlas for normal and cancer tissues based on antibody proteomics. *Mol Cell Proteomics* 2005; **4**: 1920–1932.
25 Baylin SB, Herman JG, Graff JR, Vertino PM, Issa JP. Alterations in DNA methylation: a fundamental aspect of neoplasia. *Adv Cancer Res* 1998; **72**: 141–196.
26 Marks PA, Richon VM, Miller T, Kelly WK. Histone deacetylase inhibitors. *Adv Cancer Res* 2004; **91**: 137–168.
27 Giannitrapani L, Ingrao S, Soresi M, Florena AM, La Spada E, Sandonato L *et al.* Cyclooxygenase-2 expression in chronic liver diseases and hepatocellular carcinoma: an immunohistochemical study. *Ann NY Acad Sci* 2009; **1155**: 293–299.
28 Esteller M. Cancer epigenomics: DNA methylomes and histone-modification maps. *Nat Rev Genet* 2007; **8**: 286–298.
29 Lee S, Lee HJ, Kim JH, Lee HS, Jang JJ, Kang GH. Aberrant CpG island hypermethylation along multistep hepatocarcinogenesis. *Am J Pathol* 2003; **163**: 1371–1378.
30 Calvisi DF, Ladu S, Gorden A, Farina M, Conner EA, Lee JS *et al.* Ubiquitous activation of Ras and Jak/Stat pathways in human HCC. *Gastroenterology* 2006; **130**: 1117–1128.
31 Calvisi DF, Ladu S, Gorden A, Farina M, Lee JS, Conner EA *et al.* Mechanistic and prognostic significance of aberrant methylation in the molecular pathogenesis of human hepatocellular carcinoma. *J Clin Invest* 2007; **117**: 2713–2722.
32 Weisenberger DJ, Siegmund KD, Campan M, Young J, Long TI, Faasse MA *et al.* CpG island methylator phenotype underlies sporadic microsatellite instability and is tightly associated with BRAF mutation in colorectal cancer. *Nat Genet* 2006; **38**: 787–793.
33 Yang JD, Seol SY, Leem SH, Kim YH, Sun Z, Lee JS *et al.* Genes associated with recurrence of hepatocellular carcinoma: integrated analysis by gene expression and methylation profiling. *J Korean Med Sci* 2011; **26**: 1428–1438.
34 Mossman D, Kim KT, Scott RJ. Demethylation by 5-aza-2′-deoxycytidine in colorectal cancer cells targets genomic DNA whilst promoter CpG island methylation persists. *BMC Cancer* 2010; **10**: 366.
35 Xia D, Wang D, Kim SH, Katoh H, Dubois RN. Prostaglandin E(2) promotes intestinal tumor growth via DNA methylation. *Nat Med* 2012; **18**: 224–226.
36 Morinaga S, Yamamoto Y, Noguchi Y, Imada T, Rino Y, Akaike M *et al.* Cyclooxygenase-2 mRNA is up-regulated in cirrhotic or chronic hepatitis liver adjacent to hepatocellular carcinoma. *J Gastroenterol Hepatol* 2002; **17**: 1110–1116.
37 Um TH, Kim H, Oh BK, Kim MS, Kim KS, Jung G *et al.* Aberrant CpG island hypermethylation in dysplastic nodules and early HCC of hepatitis B virus-related human multistep hepatocarcinogenesis. *J Hepatol* 2011; **54**: 939–947.

38 Vidali G, Boffa LC, Bradbury EM, Allfrey VG. Butyrate suppression of histone deacetylation leads to accumulation of multiacetylated forms of histones H3 and H4 and increased DNase I sensitivity of the associated DNA sequences. *Proc Natl Acad Sci USA* 1978; **75**: 2239–2243.
39 Tong X, Yin L, Joshi S, Rosenberg DW, Giardina C. Cyclooxygenase-2 regulation in colon cancer cells: modulation of RNA polymerase II elongation by histone deacetylase inhibitors. *J Biol Chem* 2005; **280**: 15503–15509.
40 Yamaguchi K, Lantowski A, Dannenberg AJ, Subbaramaiah K. Histone deacetylase inhibitors suppress the induction of c-Jun and its target genes including COX-2. *J Biol Chem* 2005; **280**: 32569–32577.
41 Choi YH. Induction of apoptosis by trichostatin A, a histone deacetylase inhibitor, is associated with inhibition of cyclooxygenase-2 activity in human non-small cell lung cancer cells. *Int J Oncol* 2005; **27**: 473–479.
42 Liu YW, Wang SA, Hsu TY, Chen TA, Chang WC, Hung JJ. Inhibition of LPS-induced C/EBP delta by trichostatin A has a positive effect on LPS-induced cyclooxygenase 2 expression in RAW264.7 cells. *J Cell Biochem* 2010; **110**: 1430–1438.
43 Park GY, Joo M, Pedchenko T, Blackwell TS, Christman JW. Regulation of macrophage cyclooxygenase-2 gene expression by modifications of histone H3. *Am J Physiol Lung Cell Mol Physiol* 2004; **286**: L956–L962.
44 Casado M, Molla B, Roy R, Fernandez-Martinez A, Cucarella C, Mayoral R *et al.* Protection against Fas-induced liver apoptosis in transgenic mice expressing cyclooxygenase 2 in hepatocytes. *Hepatology* 2007; **45**: 631–638.
45 Fernandez-Alvarez A, Soledad Alvarez M, Cucarella C, Casado M. Characterization of the human insulin-induced gene 2 (INSIG2) promoter: the role of Ets-binding motifs. *J Biol Chem* 2010; **285**: 11765–11774.

Supplementary Information accompanies the paper on the Oncogenesis website (http://www.nature.com/oncsis)

Supplementary Table 1 - Primers for Pyrosequencing

	Forward	Reverse
1st/2nd CpG Island First Step	AGTTATGTATGTATGTGTTGTATATAGAGT	AAAAAATAATCCCCACTCTCCTATC
1st/2nd CpG Island Second Step	[Btn]TATATAGAGTAGATATATAGTTTATTAAG	CTATCTAATCCCTCCCTCTC
1st/2nd CpG Island Sequencing A	----------	CTTCCTCTCCAAAAATCTAA
1st/2nd CpG Island Sequencing B	----------	TTTCTTCTTCCCAATCTTTACC
1st/2nd CpG Island Sequencing C	----------	CCTCTCCTCCCCCAATTCCA
1st/2nd CpG Island Sequencing D	----------	CCAAATATCTTTTCTTCT
3rd CpG Island First Step	GAGGTGAGAGTGTTTTAGAT	CATAAACTTAATTTTCAATCTTAT
3rd CpG Island Second Step	GTTTATAATGATTAGTGTTTGTGGGAAAG	[Btn] AACCAAACCCCCTCAAACAACAAAACCTA
3rd CpG Island Sequencing A	AGGTTAGAGAGGAAATTTTG	----------
3rd CpG Island Sequencing B	GGTTGAGAGTTAGGAT	----------

Supplementary Table 2 - Primers for methylation-sensitive restriction assay (MSRA)

	Forward	Reverse
CpG -431	CTTAACCTTACTCGCCCCAGTCT	AGAAGGACACTTGGCTTCCTC
CpG -372	GGAAGCCAAGTGTCCTTCTGC	GGGCAGGGTTTTTTACCCAC
CpG -138	AGCTTCCTGGGTTTCCGATT	CCCCCACAAATTTTTCCCTC
CpG +75/84/98	GCCCTCAGACAGCAAAGCCTA	GGGAAAGCTGGAATATCCACG

Supplementary Table 3 - Primers for Chromatin immunoprecipitation

	Forward	Reverse
Distal Promoter	GGAAGCCAAGTGTCCTTCTGC	TGATCGCCTTGGATGGGATA
Proximal Promoter	AGCTTCCTGGGTTTCCGATT	GGGCAGGGTTTTTTACCCAC
First Exon	CTCGGTTAGCGACCAATTGTC	CGTGCTCCTGACGCTCACT
First intron	AGCTTGGACCGCTAGAGTTCG	GGGAAAGCTGGAATATCCACG

Figure. S1- Expression of COX-2 increases after treatment of HCC cells with HDAC inhibitors. Eight hours before the experiment HCC cells were change to 1% FBS and they were incubated without (white bars) or with 2.5 mM NaB or 2.5 μM SAHA for 16 h. Total RNA was then isolated and mRNA levels for COX-2 and the internal control 18S were determined by qPCR. COX-2 mRNA amounts were calculated as RQ and normalized to the expression of ribosomal levels. Values represent fold change relative to each cell line without treatment. Data are reported as means ± SD of three independent experiments. $**p<0.01$ and $*p<0.05$

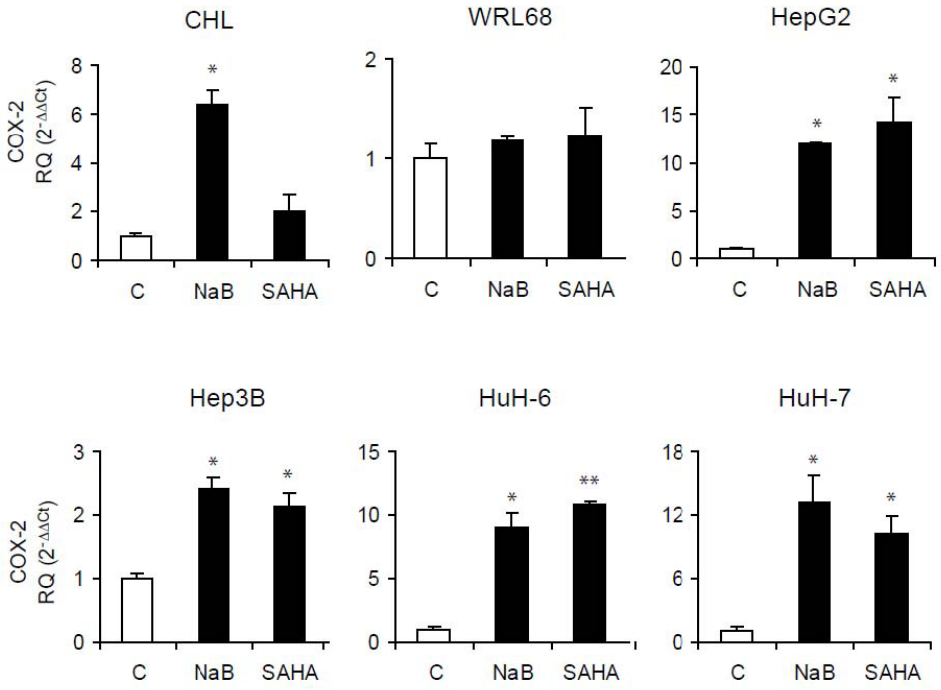

Figure. S2- Synergistic effect of HDAC inhibitors and AzadC on COX-2 expression.

(A) HCC cells in 1% FBS were incubated without (white) or with 5 μM AzadC and 2.5 mM NaB (A+N, grey) or AzadC and 2.5 μM SAHA (A+S, black) for 48 h. Cellular extracts were prepared and protein was analyzed by Western blot. A representative Western blot analyzing COX-2 and DNMT1 protein levels is shown. The expression of target proteins was normalized to GAPDH. Each panel has an optimal exposition time. Densitometric analysis of COX-2 and DNMT1 protein levels is shown. Results are expressed as arbitrary units. **(B)** PGE_2 concentration was determined by enzyme immunoassay in the supernatant of the cells. Data are expressed as means $\pm$ SD of three independent experiments. $*p<0.05$ *vs.* the corresponding cell line without treatment

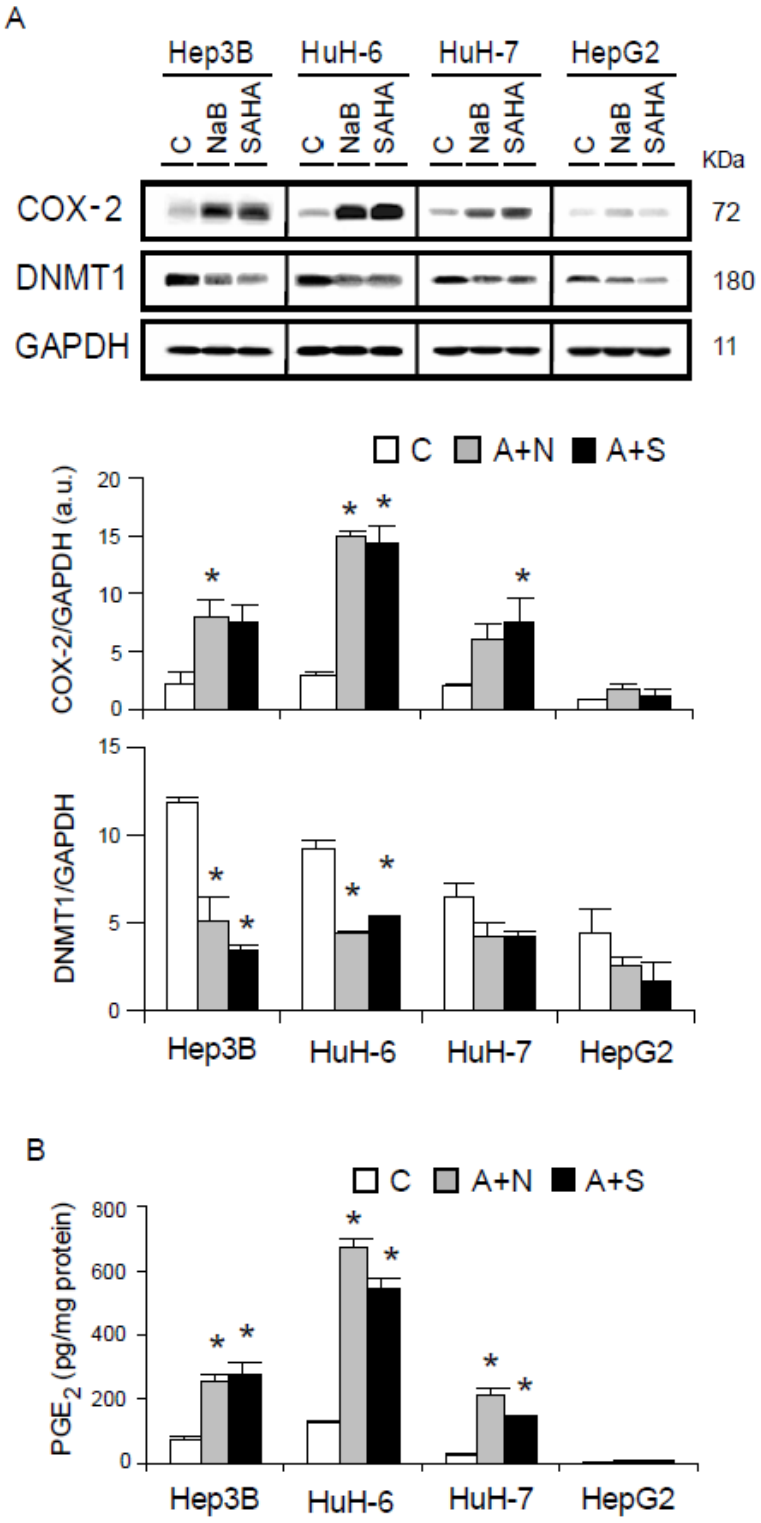
A
Hep3B
HuH-6
HuH-7
HepG2
C
NaB
SAHA
KDa
COX-2
DNMT1
GAPDH
72
180
11
C
A+N
A+S
COX-2/GAPDH (a.u.)
DNMT1/GAPDH
Hep3B
HuH-6
HuH-7
HepG2
B
PGE2 (pg/mg protein)

Discusión

En el hepatocito adulto, COX-2 no se expresa ni se induce por estimulación con factores pro-inflamatorios como LPS, IL-1β, TNF-α etc. Sin embargo, COX-2 si se expresa en las células no parenquimales, en el hepatocito fetal que tiene un fenotipo menos diferenciado que el hepatocito adulto y en algunas líneas celulares hepáticas [92]. La expresión de COX-2 en el hepatocito adulto se restringe a determinados procesos de des-diferenciación y proliferación como en respuesta a una hepatectomía parcial, a un daño hepático agudo y a enfermedades hepáticas crónicas (cirrosis, VHB, VHC, EHGN, colangiosarcoma y CHC) por lo que la expresión ectópica de COX-2 en los hepatocitos constituye una condición experimental, no fisiológica, ideal para el estudio de la contribución de las PGs derivadas de COX-2 a la patología hepática [93, 94].

En trabajos previos de nuestro grupo se generó y caracterizó parcialmente el primer modelo de animal TG para hCOX-2 cuya expresión está regulada bajo el promotor de la ApoE [16]. Se han descrito otros dos modelos animales TG para COX-2 con expresión específica en el hepatocito bajo el promotor de la transtirretina [162] y de la albúmina [53]. Estos tres modelos, presentan diferentes niveles intrahepáticos de PGE_2 donde el modelo con el promotor de la transtiterrina expresa los niveles más elevados de PGE_2, mientras que el modelo que emplea el promotor de la albúmina expresa los menores niveles de PGE_2. Estos tres modelos han mostrado diferencias en la respuesta a determinados inductores de daño hepático agudo. Esta diversidad en la respuesta puede ser debida a las diferencias en los niveles de expresión de PGE_2, a variaciones en la disponibilidad del sustrato de COX-2, a la disparidad en el tiempo de activación de los promotores o incluso puede ser causa de los distintos fondos genéticos empleados en los modelos animales [93].

Los estudios realizados en estos modelos TG para COX-2 en el hepatocito revelaron que las PGs ejercen en el hígado un efecto anti-apoptótico en modelos de daño hepático agudo [16, 79, 97] y que aceleran el inicio de la proliferación de los hepatocitos durante la regeneración hepática después de una hepatectomía parcial [97]. Existen otros estudios que también apoyan el efecto protector de las PGs frente a apoptosis en modelos de daño hepático agudo usando animales deficientes en COX-2 así como en modelos quirúrgicos de isquemia/reperfusión en el corazón [8, 63, 160].

Estos antecedentes, junto con los análisis que indican una alta frecuencia de expresión de COX-2 en enfermedad hepática crónica, el hecho de que los inhibidores de COX-2 previenen el crecimiento de las células de CHC *in vitro* e *in vivo* y que la transgénesis de COX-2 en líneas celulares hepatocitarias promueve la proliferación y protege frente a apoptosis indican que la expresión de COX-2 podría tener cierta implicación en el desarrollo del CHC. Para analizar la contribución de la expresión de COX-2 en la progresión del CHC, analizamos las características

fenotípicas hepáticas, llevamos a cabo un modelo de fibrosis y un modelo de hepatocarcinogénesis química inducida con DEN en nuestro modelo de ratón TG para COX-2 cuya expresión está regulada por el promotor de la ApoE.

El análisis de las características fenotípicas hepáticas en nuestro modelo de ratón TG para COX-2 mostró que a las 60 semanas de edad, los animales TG presentaban focos inflamatorios compuestos principalmente por linfocitos indicando que la expresión constitutiva del transgén de COX-2 con la edad, origina una hepatitis leve [86]. Estos resultados son coherentes con los ya descritos en el modelo TG para COX-2 que usa el promotor de transtirretina para dirigir la expresión de COX-2 en el hepatocito, donde se detectó infiltración de células inflamatorias y hepatitis mediante un mecanismo que implica la activación persistente de la vía de NF-κB [162]. No obstante, ningún modelo TG para COX-2 en el hepatocito desarrolló CHC de forma espontánea indicando que por sí sola COX-2 no induce CHC [16, 53, 162].

El daño hepático crónico puede promover fibrosis. La fibrosis está caracterizada por la activación de las células hepáticas estrelladas que incrementan su proliferación y adquieren un fenotípico miofibroblástico promoviendo el engrosamiento de la matriz extracelular, la acumulación de colágeno y la inducción de COX-2 sugiriendo un posible papel fibrogénico para COX-2. No obstante, los datos concernientes al papel de COX-2 en el proceso fibrogénico hepático son controvertidos, implicándola tanto en la exacerbación como en la atenuación del proceso [61, 112]. Previamente, el análisis de la contribución de las PGs derivadas de COX-2 en la fibrosis hepática solo había sido analizado en el modelo con el promotor de transtirretina. Este modelo reveló que la presencia constitutiva de COX-2 en el hepatocito es irrelevante en el proceso fibrogénico mediado por el tratamiento con una dieta DCM y con CCl_4 [163]. La dieta DCM es un modelo donde el daño hepático crónico se atribuye a la depleción del mecanismo antioxidante, como la reducción del GSH, que termina con la producción de daño oxidativo al ADN, inflamación y cirrosis [45, 158]. Nuestros resultados, usando el tratamiento con una dieta DCM en ratones TG para COX-2, en coherencia con los resultados publicados, demostraron que la expresión de COX-2 en el hepatocito no favorece ni promueve la fibrogénesis hepática.

La sobre-expresión de COX-2 se ha detectado en muchos tipos de cánceres sugiriendo su implicación en la iniciación y/o el desarrollo tumoral. COX-2 se ha relacionado con inducción de tumorigénesis en glándula mamaria, empleando el promotor del virus del tumor de mama de ratón y en la célula gástrica, usando ratones TG que expresan simultáneamente COX-2 y mPGES-1 bajo el promotor de Ck19 [28, 111]. No obstante, numerosos estudios de sobre-expresión de COX-2 en colon, en piel y en la lámina basal del epitelio de varios órganos (glándula mamaria, vejiga urinaria y páncreas) han demostrado que la expresión de COX-2 es

incapaz de inducir tumorigénesis espontáneamente y el desarrollo del tumor solo tiene lugar tras el uso de agentes iniciadores y/o promotores tumorales [2, 21, 64, 82, 90, 107, 117, 151]. Incluso Bol y colaboradores describieron que la sobre-expresión de COX-2 en la piel está implicada en la supresión del desarrollo tumoral [7].

El análisis histopatológico en nuestro modelo indicó que la incidencia de lesiones pre-neoplásicas es relativamente mayor en los animales TG a las 10 semanas de tratamiento con DEN, aunque estos resultados no alcanzaron significación estadística. El desarrollo de adenomas y carcinomas hepatocelulares a las 25 y 40 semanas de edad fue similar en los animales WT y TG, aunque la incidencia metastásica pulmonar fue mayor en los ratones TG.

DEN es un carcinógeno que se metaboliza a un agente alquilante que produce citotoxicidad, muerte de los hepatocitos, genotoxicidad, formación de aductos de ADN, alteraciónes fenotípicas, mutaciones y proliferación celular [147]. La apoptosis y necrosis de los hepatocitos mediada por el tratamiento con DEN está correlacionada con la activación de IKK en la células de Kupffer resultando en la secreción de IL-6, TNF-α, y HGF que actúan induciendo la proliferación compensatoria de los hepatocitos y la hepatocarcinogénesis [132]. Está descrito que tanto p53 (implicada en la parada en la fase G1 del ciclo celular) como JNK (implicada en la proliferación de los hepatocitos) son marcadores del efecto genotóxico y citotóxico inducido por DEN [87]. Nuestros resultados muestran que tanto los ratones WT como los TG presentan disminuidos los niveles de expresión de p53 e incrementados los niveles de expresión de c-Jun, cuya activación depende de JNK, a las 40 semanas después del tratamiento con DEN comparando la zona tumoral con la zona no tumoral adyacente. Por otra parte, se ha descrito que el mecanismo molecular por el cual COX-2 promueve tumorigénesis en algunos modelos implica la inactivación de p53 en condiciones de estrés genotóxico [30]. Asimismo, se ha descrito que la sobre-expresión de COX-2 en los hepatocitos disminuye los niveles de expresión de p53 [43]. Nuestros análisis tan solo muestran diferencias significativas en la expresión de p53 a las 40 semanas después del tratamiento con DEN y exclusivamente en la zona tumoral donde los resultados macroscópicos e histológicos determinaron que no hay diferencias entre los ratones WT y TG. Por lo tanto, la implicación de COX-2 en el proceso tumorigénico mediado por la señalización de p53 es irrelevante. Por esta misma razón, las diferencias significativas en la expresión de c-Jun a las 40 semanas de tratamiento con DEN no son relevantes en el desarrollo de CHC.

El efecto mutagénico de DEN que promueve la iniciación tumoral, además de ser una consecuencia de la pérdida del supresor tumoral p53, es debido a la activación del proto-oncogén c-Myc. Se ha descrito que los inhibidores selectivos de COX-2 inhiben la proliferación celular en varias líneas celulares de cáncer hematopoyético mediante la

disminución de los niveles de c-Myc [135]. Además, en cánceres de tipo gastrointestinal, PGE_2 puede activar c-Myc a través de la activación de múltiples vías de transducción de señales [156]. Nuestros resultados confirman que la expresión de COX-2 promueve la activación del proto-oncogén c-Myc pudiendo favorecer el desarrollo leve de nódulos pre-neoplásicos, no obstante esta diferencia carece de relevancia a la 40 semanas de tratamiento con DEN, ya que no se observan diferencias en la progresión tumoral debidas a la expresión de COX-2. El proto-oncogén c-Myc es un factor de transcripción implicado en la regulación del ciclo celular, apoptosis, diferenciación celular, adhesión celular, regulación del metabolismo y senescencia celular. Se ha confirmado que c-Myc coopera en la transición de la fase G1 a S promoviendo la expresión de Ciclina D1, que a su vez activa a quinasas como Cdk2 y Cdk4 que controlan la fosforilación de Rb, de manera que el factor de transcripción E2F1 se libera activando la transcripción de genes como Ciclina E y PCNA [156]. Los análisis de las proteínas de ciclo celular mostraron que la expresión del transgén de COX-2 promueve un incremento en la expresión de Ciclina E a las 25 y 40 semanas después del tratamiento con DEN, sugiriendo que la sobre-expresión del transgén de COX-2 está implicada en la aceleración de la proliferación temprana de los hepatocitos en este modelo experimental de hepatocarcinogénesis. Estos resultados son coherentes con los análisis previos donde la expresión de COX-2 está relacionada con un efecto anti-apoptótico en daño hepático agudo [97]. El hecho de que COX-2 favorezca la proliferación temprana de los hepatocitos en nuestro modelo es coherente con la tendencia al aumento en la formación de nódulos pre-neoplásicos en el animal TG. Por otra parte, COX-2 podría estar favoreciendo la transformación tumoral en estadios tempranos mediante la producción de ROS y la peroxidación lipídica, que junto con la inflamación crónica inducen genotoxicidad, inestabilidad génica y mutaciones en el ADN determinantes para la iniciación tumoral [77]. No obstante, se ha descrito que los efectos de iniciación tumoral de COX-2 están determinados por su relación con la red de señalización molecular del entorno tumoral. De hecho, la expresión de COX-2 *per se* no tiene un potencial tumorigénico en muchos de los modelos experimentales, ni en los tejidos normales que en condiciones fisiológicas expresan constitutivamente COX-2. Numerosos estudios señalan al daño oxidativo como un factor clave en la transformación tumoral en el CHC. Los modelos animales deficientes para IKKβ, p38α, IKKγ/NEMO y β-catenina han mostrado potenciación de hepatocarcinogénesis inducida con DEN como consecuencia de la acumulación de daño oxidativo debido a la producción continuada de ROS en respuesta a la ausencia de estos genes [85, 119]. De hecho, el tratamiento con antioxidantes reduce la incidencia de CHC en ratones con deleción en IKKβ y β-catenina [87, 166]. Se ha descrito que la expresión de COX-2 aumenta la producción de ROS y la depleción de GSH en los hepatocitos [122]. Para estudiar si la

expresión de COX-2 alteraba el estado oxidativo en el modelo de DEN, se analizó el estado redox de la línea hepatocitaria humana CHL-C, que expresa establemente COX-2-GFP, y de su control CHL-V, que expresa GFP, ambas tratadas con DEN/PB. Debido a que las líneas celulares en cultivo tienden a presentar bajos niveles de proteínas del sistema citocromo P450 (CYP450), y que la metabolización de DEN requiere de ellas, de CYP2E1 principalmente en hígado, para bioactivarse a un ión etildiazonio que produce aductos en el ADN, se trataron las células con PB que es un inductor del sistema CYP450 [81, 139]. El PB se utiliza como promotor tumoral de forma generalizada. En concordancia con los resultados observados, la línea CHL-C comparada con la línea CHL-V ambas tratadas con DEN/PB, presentó niveles de estrés oxidativo superiores reflejados en una elevada acumulación de ROS y una disminución de los niveles de GSH. Además, esta alteración del estado redox tuvo efectos genotóxicos demostrados por los elevados niveles de 8-hidroxi-2'-deoxiguanosina (8-OHdG) detectados en la línea CHL-C.

Se ha descrito que las proteínas JNK, que se activan en respuesta a estrés, estímulos pro-inflamatorios y por algunas señales mitogénicas, participan en la proliferación de los hepatocitos después de una hepatectomía parcial [131]. Los ratones con disrupción de JNK-1 son menos susceptibles al desarrollo de CHC inducido con DEN, mientras que la deleción de IKKβ, que promueve la activación prolongada de JNK1, resulta en un incremento de la susceptibilidad a la hepatocarcinogénesis inducida por DEN [120]. Una de las principales vías de señalización implicadas en la inducción de la expresión del gen de COX-2 es la vía de las MAPK (ERK, JNK/SAPK y p38). De hecho, el mecanismo de acción de muchos compuestos con actividad anti-inflamatoria se basa en la inhibición de la señalización de JNK y p38 con la consecuente inhibición de COX-2 [140]. Por otra parte, los análisis en la línea CHL-C demostraron que las PGs derivadas de COX-2 a su vez activan las vías de señalización de las MAPK que participan en la proliferación de los hepatocitos [71]. Además hay estudios *in vitro* que demuestran que la adición de PGE_2 induce la migración de células de CHC mientras que el uso del COXIBs disminuye su migración mediante la modulación de las vías MEK/ERK, p38/MAPK, PKA y PKC [19, 96]. La vía de Raf/Ras/MEK/ERK se encuentra globalmente activada en cáncer hepático [10, 98]. Nuestros datos verifican una activación moderada de JNK, ERK y p38 debida a la expresión del transgén de COX-2 en la línea CHL-C comparada con la línea CHL-V, ambas tratadas con DEN/PB.

La muerte celular incrementa la proliferación compensatoria de los hepatocitos, fenómeno que favorece la progresión tumoral. De hecho, se suelen encontrar células con gran capacidad proliferativa alrededor de los focos de células apoptóticas en lesiones hepáticas después de la exposición a DEN [87]. La deleción de FADD, la molécula adaptadora de los receptores de muerte, reduce el exceso de apoptosis, inflamación y esteatosis en el modelo deficiente para

NEMO, resultando en una disminución de la tumorigénesis [85]. Se ha propuesto que los hepatocitos necróticos liberan IL-1α, activando a las células de Kupffer con un aumento en la producción de IL-6, y que esta respuesta conduce a la proliferación compensatoria de los hepatocitos supervivientes implicado la activación de Stat3 [119]. La implicación de IL-6 y de Stat3 ha sido corroborada en CHC [47, 55, 150]. La elevada producción de PGE_2 por la acción enzimática de COX-2 conduce a la estimulación del receptor EP1 promoviendo la activación de c-Src y EGFR que finalmente conduce a la fosforilación de Stat3 en células de colangiocarcinoma humano y en cáncer de pulmón no microcítico [52]. Los resultados obtenidos reflejan un incremento moderado de la fosforilación de Stat3 en las células CHL-C que son coherentes con la acumulación de ROS, la disminución de GSH y el aumento del estrés oxidativo observado incluso en ausencia del tratamiento con DEN/PB.

La producción de PGs, a través la activación de los receptores EPs conduce a la activación de las vías de PI3K y de la vía Akt/PKB. Akt favorece el almacenaje de energía, regula el ciclo celular y promueve la supervivencia por inducir la fosforilación e inactivación de la proteína pro-apoptótica Bad y el aumento de los niveles de proteinas anti-apoptóticas como Bcl-2 y Mcl-1 [129]. Estudios previos de nuestro grupo, mostraron que tanto las células hepatocitarias con expresión estable de COX-2 como los ratones TG para COX-2 en el hepatocito presentan elevados niveles de proteína Akt fosforilada comparados con las células control y los ratones WT indicando que la expresión de COX-2 estimula estas vías de supervivencia [43, 97]. Se ha descrito que la vía de PI3K/PTEN/Akt/mTOR se encuentra alterada en CHC [41]. La activación de estas vías conlleva a la resistencia a la apoptosis, proliferación celular, estimulación de la angiogénesis, invasividad y metástasis. La regulación negativa de la vía está mediada por el supresor tumoral PTEN y la deleción específica en hígado de PTEN resulta en hepatomegalia, esteatohepatitis y finalmente en CHC [57, 152]. Nuestros resultados muestran que las células CHL-C tratadas con DEN/PB implantadas en ratones desnudos crecen moderadamente más rápido que sus controles CHL-V, lo que puede ser debido a la modulación de las vías de Akt y de JNK/c-Jun [69].

La iniciación tumoral en el modelo estudiado ocurre mediante la mutagénesis producida por DEN, por la activación del proto-oncogén c-Myc y la pérdida del supresor tumoral p53. Después de la iniciación, es necesario que se produzca la progresión del tumor donde las células alteradas tengan ventajas proliferativas, se expandan y produzcan lesiones pre-malignas que con el tiempo se acumulen y deriven en una transformación tumoral. Se ha descrito que la expresión de COX-2 es gradual desde la hepatitis crónica hasta las lesiones pre-malignas sugiriendo que la expresión de COX-2 puede ser determinante en las primeras fases de la hepatocarcinogénesis [72]. Nuestros resultados muestran que en la inducción de

una hepatocarcinogénesis química experimental con DEN en el modelo TG para COX-2 en el hepatocito, la expresión de COX-2 favorece el desarrollo leve de nódulos pre-neoplásicos mediante la modulación de vías de señalización implicadas en la regulación del ciclo celular. Además, los análisis tras el tratamiento de la línea CHL-V y CHL-C con DEN/PB indicaron que la contribución de COX-2 al proceso de proliferación inicial de los hepatocitos es consecuencia de su participación en el incremento del daño oxidativo y en la alteración de vías de proliferación celular. Asimismo, el estudio de la formación de tumores mediante la implantación de células CHL-V y CHL-C tratadas con DEN/PB en ratones atímicos desnudos confirmó la contribución moderada de COX-2 al crecimiento de los tumores. Hay estudios que demuestran que la PGE_2 favorece la migración y la invasión tumoral mediante la activación de la vía de Akt/PI3K. La activación de Akt por la PGE_2 implica la trans-activación de EGFR mediante c-Src y esta trans-activación es la responsable de la estimulación de la migración y la invasión [9]. La alta incidencia de metástasis pulmonares observadas en el animal TG y el hecho de que la elevada producción de PGE_2 favorezca la progresión y la migración de las células de CHC [96] indican una implicación de COX-2 en la fase de expansión y metástasis de CHC en nuestro modelo de hepatocarcinogénesis química con DEN.

En resumen COX-2 favorece el desarrollo leve de nódulos pre-neoplásicos, sin afectar a la transformación maligna ni al progreso del tumor, y también podría estar contribuyendo a la fase de expansión y metástasis del CHC.

Debido a la escasez de modelos que evalúen la implicación del efecto de las PGs en la carcinogénesis hepática y a la controversia existente en la implicación de COX-2 en la iniciación y progresión tumoral tanto en CHC como en otros tipos de tumores, se utilizó un modelo genético de CHC de ratones DTG que expresan c-Myc/TGF-α, caracterizados con una prognosis similar a los CHC del modelo de DEN. Con este fin, ratones DTG se cruzaron con ratones TG para COX-2 en el hepatocito. Los animales DTG desarrollan CHC de forma más acentuada y más agresiva que los animales de los modelos MTG para TGF-α o MTG para c-Myc [12]. La co-expresión de ambos genes en CHC es frecuente [141]. El TGF-α es un miembro de la familia EGF que interacciona con los receptores de la familia ErbB. El animal TG para TGF-α desarrolla CHC por favorecer pérdidas cromosómicas que alteran la expresión de genes como el retinoblastoma (Rb) y la disrupción de la vía de señalización del TGF-β1 [108, 125]. La expresión constitutiva del proto-oncogen c-Myc promueve el desarrollo de CHC por inducir genes implicados en el ciclo celular, proliferación, diferenciación, adhesión, regulación del metabolismo, senescencia celular y por inducir genes implicados en la biogénesis de ribosomas y en el control de la traducción [22, 95]. La transgénesis de c-Myc/TGF-α en conjunto tiene un efecto sinérgico en el desarrollo de CHC. Ambos genes participan en la proliferación

persistente de los hepatocitos, alterando el silenciamiento mitótico normal durante las primeras semanas de vida [108]. La alta replicación de los hepatocitos, sumada a la reducción de la apoptosis y el incremento en los niveles de uPA, promueven la alteración displásica de los hepatocitos favoreciendo su expansión y progresión a lesiones de tipo neoplásicas [125]. Los ratones DTG no solo desarrollan tumores de forma más rápida sino que además los tumores son superiores en número y tamaño, indicando su implicación en la iniciación y el progreso del tumor [124]. A pesar de la existencia de datos *in vitro* que relacionan la expresión de COX-2 con CHC, así como que el uso de COXIB previenen *in vivo* e *in vitro* la proliferación de células de CHC sugiriendo que COX-2 podría estar implicada en la iniciación y desarrollo de CHC, la co-expresión de COX-2 con c-Myc/TGF-α no aceleró de manera significativa el desarrollo de CHC. Tan solo se observaron tendencias no significativas a una mayor formación de adenomas en los animales DTG comparado con los animales TTG a los 5 meses de edad. Estos datos fueron coherentes con el incremento significativo en el ratio peso de hígado/peso corporal, con la elevación de los niveles de AST y con el aumento, aunque no significativo, de Ki67 en los ratones DTG comparado con los TTG a los 5 meses de edad. Esta observación sugiere que la sobre-expresión de COX-2 en los hepatocitos podría estar previniendo la hipertrofia y la hiperplasia causada por c-Myc/TGF- α.

La progresión del tumor depende de la disrupción de la homeostasis del tejido hepático normal, desregulando el balance entre la proliferación celular y la muerte celular hacia la proliferación celular. El análisis de la expresión de proteínas del ciclo celular, junto con el estudio de la apoptosis y de las vías de transducción de señales implicadas en la proliferación de los hepatocitos indicó que la presencia de COX-2 tan solo tuvo consecuencias en el incremento significativo de la expresión del factor de transcripción E2F1, de p53 y de la proteína anti-apoptótica Bcl-2 en los animales TTG de 9 meses de edad. E2F1 tiene un papel dual controvertido ya que en determinadas situaciones actúa como supresor tumoral participando en la respuesta frente al daño al ADN e induciendo la apoptosis, que puede ser vía dependiente o independiente de p53, y en otras situaciones E2F1 actúa como proto-oncogén favoreciendo la progresión del ciclo celular [138]. E2F1 se expresa activamente en los tejidos proliferantes durante la transición de la fase G1 a S del ciclo celular [50]. A pesar de que en los animales TTG se detectó un incremento significativo en la expresión de E2F1, de p53 y de Bcl-2, no se encontraron diferencias significativas en los genes de proliferación celular (Ccdn1, Cxcr4, Ccne1) ni en los de apoptosis (Birc5, Tnfrsf10b, Gadd45b) a los 5 meses entre los ratones DTG y TTG. De hecho, no se detectaron cambios en la formación de CHC entre ambos modelos ni a los 5 meses ni a los 9 meses de edad. Estos datos sugieren que la

presencia de COX-2 no altera rutas de señalización relevantes en el desarrollo del CHC en el modelo genético c-Myc/TGF-α.

Dado que la producción ROS y la peroxidación lipídica son factores primordiales en la carcinogénesis mediada por c-Myc/TGF-α, se estudió el estado redox en los animales DTG y TTG [39]. Se ha descrito que en el modelo de DTG c-Myc/TGF-α, las proteínas iNOS, NADPH oxidasa (NOX) y HO-1 están implicadas en la producción de ROS. Además, existen análisis que indican que COX-2 y NOX inducen su expresión recíprocamente favoreciendo la producción de ROS y la depleción de GSH en los hepatocitos [122]. En nuestro estudio, los animales TTG mostraron un incremento en la producción de TBARS indicando que la presencia de COX-2 en este modelo es responsable de una mayor peroxidación lipídica. Sin embargo, entre los animales TTG y DTG no se encontraron diferencias significativas en la expresión de iNOS, HO-1 y Nfr-2. Nuestros datos indican que la expresión de COX-2 tiene distinto potencial en la alteración del estado redox en el modelo de CHC químico y genético. Aunque se ha descrito que tanto DEN como la transgénesis c-Myc/TGF-α alteran el estado redox y producen genotoxicidad, los resultados del modelo de DEN demostraron que COX-2 puede incrementar aún más la producción de ROS, disminuir los niveles de GSH y aumentar el daño oxidativo al ADN reflejado en un aumento en los niveles de 8-OHdG. Sin embargo, en el modelo de c-Myc/TGF-α aunque se observó una mayor peroxidación lipídica, la expresión de COX-2 es irrelevante en la alteración del estado redox probablemente debida a una saturación del sistema oxidativo.

La clasificación genómica es de gran importancia para la determinación de marcadores moleculares y para un tratamiento personalizado de los pacientes [74]. Los resultados de múltiples arrays han permitido discernir y clasificar a los CHC en base a su expresión génica. Aunque aún no se dispone de una clasificación definitiva de CHC, un meta-análisis recientemente publicado ha evidenciado tres subclases moleculares homogéneas denominadas S1, S2 y S3 (Figura1) [59].

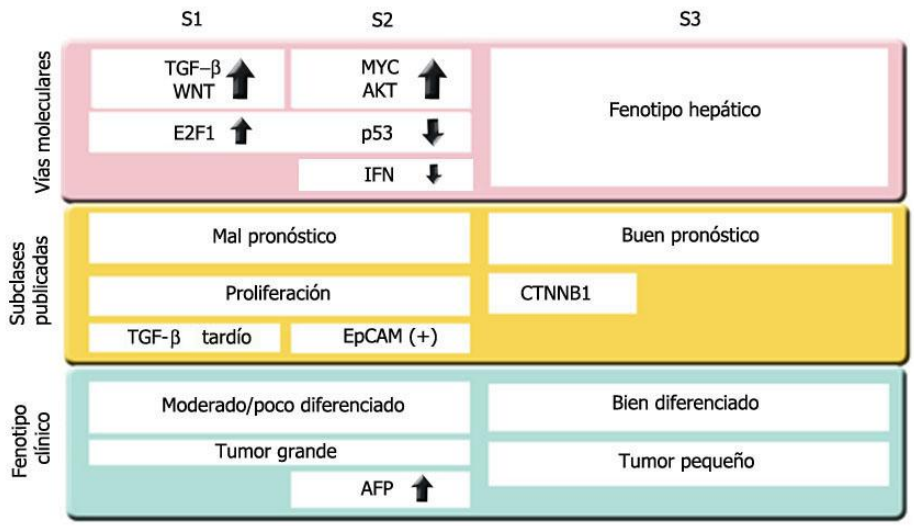

Figura 1. Resumen esquemático de las características de las subclases de CHC. *En un meta-análisis que incluyó 603 pacientes con CHC de 9 estudios diferentes se identificaron tres subclases (S1, S2 y S3) caracterizadas por sus datos clínicos y moleculares. Los tumores de comportamiento más agresivo, con mayor tamaño y menor diferenciación histológica se agruparon en las subclases S1 y S2. La subclase S1 se caracterizó por tener activada la vía de Wnt como consecuencia de la sobreexpresión de TGF-β. La subclase S2 presentó activada la vía de Akt, altos niveles de expresión de c-Myc y de alfa fetoproteína (AFP) y mostró niveles disminuidos de IFN y de p53. La subclase S3 comprende los tumores menos agresivos, con una mayor diferenciación histológica y se caracterizan por preservar la expresión de p53 y tener mutaciones en β-catenina. Adaptado de Hoshida et al. [59].*

Esta clasificación es extrapolable a otros estudios, por ejemplo, el grupo de Thorgeirsson y colaboradores clasificaron siete modelos de CHC murinos comparándolos con 91 biopsias de CHC humanos analizando los perfiles de expresión génica [73]. Los modelos TG para c-Myc, E2F1 y c-Myc/E2F1 mostraron un patrón génico comparable a CHC de pacientes con buen pronóstico mientras que el modelo TG c-Myc/TGF-α y el modelo de hepatocarcinogénesis química inducida con DEN presentaron perfiles genéticos similares a pacientes con CHC de mal pronóstico. Esta clasificación es importante para poder comparar de manera adecuada modelos de CHC murinos con humanos. Los ratones DTG presentan tumores de bajo grado de diferenciación, alta malignidad, reducida supervivencia, elevados niveles de marcadores de CHC de mal pronóstico y una disrupción temprana del control de la proliferación [12]. Para estudiar si el efecto de la expresión de COX-2 podría variar el valor pronóstico del modelo c-Myc/TGF-α se estudiaron marcadores específicos. Los resultados indicaron que el mal pronóstico de los tumores que expresan c-Myc/TGF-α no varía con la expresión de COX-2. A pesar de que tanto el modelo de DEN como el modelo de c-Myc/TGF-α presentan un perfil de mal pronóstico sugiriendo que podrían tener perfiles génicos con cierta similitud, hemos observado distintos comportamientos en la alteración de vías de señalización como consecuencia de la expresión de COX-2. Las vías de las MAPK (JNK, ERK y p38), que se encuentran moderadamente activadas en el modelo de DEN, así como el incremento en la expresión de Ciclina E, no se observaron en el modelo de los TTG c-Myc/TGF-α/COX-2. Además

en el modelo de DEN el desarrollo moderado de nódulos pre-neoplásicos favorecido por la expresión de COX-2 podría ser debido a la inducción de c-Myc en estadios tempranos de CHC. Sin embargo, en el modelo de los TTG y DTG donde los niveles de expresión de c-Myc están igualados, la expresión de COX-2 podría estar previniendo la hipertrofia e hiperplasia. Estos resultados indican que la expresión de COX-2 modula de manera diferente marcadores de progresión tumoral en la hepatocarcinogénesis química y genética. La expresión de COX-2 es incapaz de potenciar la inducción y la progresión de CHC en el modelo de hepatocarcinogénesis genética y se podría pensar que esta falta de efecto de COX-2 se debe a la agresividad *per se* del modelo. No obstante, también se analizaron los DTG de TGF-α/COX-2 y de c-Myc/COX-2 y tampoco se encontraron diferencias significativas en el desarrollo de CHC por efecto de COX-2.

Nuestros resultados son coherentes con los análisis de la expresión global de genes para identificar la firma genética de CHC en los que no se describe la expresión del gen de COX-2 [75]. De hecho, la expresión de COX-2 en CHC es muy variable. En el CHC bien diferenciado, caracterizado por tener mejor pronóstico, la expresión de COX-2 es elevada, mientras que en el CHC poco diferenciado, con un peor pronóstico, la expresión de COX-2 está disminuida [128]. Se ha descrito que COX-2 está incrementada en estadios tempranos pero que disminuye en estadios avanzados de CHC y que su expresión es superior en la zona no tumoral comparada con la tumoral [104]. Además la expresión de COX-2 es mayor en la EHGNA y en cirrosis que en el CHC [46]. Todos estos datos en conjunto indican que la expresión de COX-2 en el CHC sigue un patrón de expresión complejo. Con el objetivo de entender la regulación de la expresión de COX-2 en el CHC humano y dado que en el CHC ocurren numerosas alteraciones epigenéticas, nos propusimos estudiar si la expresión del gen de COX-2 podía ser regulada por cambios en la metilación del gen de COX-2 y la modificación de histonas.

Se ha descrito en CHC que la hipometilación global del ADN promueve la aparición de mutaciones en oncogenes y que la metilación en ciertas islas CpG que se localizan frecuentemente en la región 5’ de los genes, en elementos de repetición dentro del promotor, promueven el silenciamento génico de supresores tumorales [38]. Lee y colaboradores estudiaron la significación terapéutica y quimiopreventiva de los patrones de metilación en CHC humanos describiendo que un aumento en la metilación en el gen de COX-2 entre otros genes (APC, GSTP1, RASSF1A, p16, E-cadherina) está relacionado con el desarrollo del CHC [76]. Se ha demostrado que la metilación de genes inhibidores de Ras y de genes inhibidores de la vía de Jak/Stat3 en CHC resulta en una activación permanente de la vía de Ras y de Jak/Stat y que la inhibición de estas vías o el uso de agentes demetilantes inducen la apoptosis en células de CHC [10]. Este mismo grupo analizó la hipometilación global del genoma y el

estado de metilación de 105 genes supresores tumorales en CHC. La inactivación por hipermetilación en islas CpG de promotores de genes como SPRY-1 y -2, DAB2, SOCS-4/-5, implicados en diversas funciones como la inhibición de la señalización de la vía de FGF, de Ras y de citoquinas respectivamente, así como de genes inhibidores de la angiogénesis como BNIP3, BNIP3L, IGFBP3, y EGLN2 se asoció con mal pronóstico de CHC confirmando que el estado de metilación se correlaciona con el estado clínico, de los pacientes con CHC. Sus resultados indican que la caracterización del perfil de metilación de CHC, al estar relacionado con el estado clínico permite determinar marcadores moleculares de buen o mal pronóstico de CHC abriendo la posibilidad de nuevas dianas terapéuticas [11]. Además, la metilación parece ser un evento temprano sugiriendo que puede preceder a la cirrosis. Recientemente se han analizado genes cuya metilación y niveles de ARNm están asociados con recurrencia al CHC. Los datos sugieren que oncogenes como PSRC1 y MYO1E, genes supresores de tumores como CFH y MYRIP así como genes de la vía de TGF, Wnt y genes implicados en la remodelación del citoesqueleto tienen un elevado potencial de recurrencia tumorigénica, señalándolos como marcadores pronóstico de CHC [159]. Concerniente a COX-2, se ha descrito que el silenciamiento epigenético de COX-2 está relacionado con el estado clínico de los pacientes con cáncer gástrico [31].

Para esclarecer la regulación de la expresión del gen de COX-2 por metilación de su promotor en CHC se analizó el estado de metilación de tres islas CpG del promotor de COX-2 por pirosecuenciación en seis líneas hepáticas que presentaban diferentes niveles de expresión de COX-2. Además, por MSRA se analizaron determinados dinucleótidos CpG localizados en la zona promotora. El porcentaje de metilación de las líneas de CHC analizadas no mostró correlación con la expresión de COX-2. A pesar de esto, se demostró que el tratamiento con el agente demetilante AzadC era capaz de inducir la expresión de COX-2 en las células de CHC. Estos resultados sugieren que el estado de metilación del promotor puede regular la expresión del gen COX-2. No obstante, no podemos descartar que existan mecanismos indirectos en la regulación de la expresión de COX-2, dado que después del tratamiento con AzadC, a pesar de que la línea HuH7 presentó un perfil hipometilado permanente, los niveles del ARNm de COX-2 se incrementaron. De hecho, se ha sugerido, que en células de cáncer colorrectal el AzadC puede regular la expresión de otros factores como proteínas MBDs y proteínas implicadas en la modificación de histonas que regulan la expresión génica [105].

Análisis recientes describen que la PGE_2 promueve el crecimiento de los tumores intestinales por potenciar la metilación de los promotores de ciertos supresores tumorales y de genes implicados en la reparación al ADN [157]. También se ha descrito que en la infección por el VHB y como consecuencia de la expresión de la proteína HBx, se induce COX-2 debido a

eventos de demetilación mediados por la disminución en la proteína DNMT3b [164] Estos resultados junto con el hecho de que la hipermetilación del promotor del gen de COX-2 tenga valor pronóstico en pacientes con cáncer gástrico [31] nos indujeron a estudiar si la metilación del promotor de COX-2 estaba relacionada con la expresión de COX-2 en CHC humano. En concordancia con resultados previos [24, 104], los niveles del ARNm de COX-2 se mostraron incrementados en el tejido hepático adyacente al CHC en un 86% de las biopsias estudiadas. El análisis del perfil de metilación de las tres islas CpG, mostró dos grupos de CHC: el primer grupo formado por un 43% de las muestras mostró un porcentaje bajo de metilación del promotor sin diferencias significativas entre la zona tumoral y su pareado no tumoral, mientras que el otro grupo formado por un 57% de las muestras presentó un perfil hipermetilado en la zona tumoral. Este estado de hipermetilación se correlacionó con una disminución en la expresión de COX-2. Estos resultados sugieren que la hipermetilación del promotor de COX-2 juega un papel importante en la regulación de su propia expresión.

Los pacientes con CHC tienen un mal pronóstico de supervivencia, en parte, debido a la alta tasa de recurrencia de CHC después de su resección. Hay muchos estudios que caracterizan el pronóstico del CHC mediante el análisis de las alteraciones epigenéticas de la región promotora de ciertos genes asociados con CHC [76]. Nuestros análisis mostraron que la hipermetilación del promotor del gen de COX-2 en CHC está correlacionada con un mal pronóstico de superviviencia. No obstante, el mecanismo por el cual la hipermetilación del gen de COX-2 se relaciona con una mala prognosis permanece desconocido.

El NaB es un ácido graso de cadena corta que normalmente se encuentra en el colon humano como producto de la degradación metabólica de carbohidratos complejos. Este fue el primer compuesto descrito con actividad inhibitoria de HDACs [148]. Diferentes estudios preclínicos con NaB han mostrado su capacidad en la inhibición del crecimiento de células de CHC. Además del NaB, otros ácidos hidroxámicos como la tricostatina A (TSA) y el SAHA están en fase I y II de estudios clínicos para validar su potencial como fármacos anticancerígenos dirigidos para el tratamiento de tumores sólidos y hematológicos, bien por si solos o en combinación con otros agentes citotóxicos. Existe un estudio que indica que el tratamiento con COXIBs en un modelo de formación de tumores con células de CHC modifica la acetilación de histonas y de la HDAC2, aunque no determinan si es vía dependiente o independiente de la inhibición de COX-2 [23]. Nuestros datos demuestran que el tratamiento de células de CHC con NaB o SAHA incrementa la expresión de COX-2 y restablece la acetilación de las histonas H3 y H4 localizadas en el promotor de COX-2 en algunas líneas de hepatoma. De hecho, nuestro análisis mostró que los pacientes con CHC y un mayor porcentaje de histona H3 acetilada presentaban mejores pronósticos de supervivencia. El hecho de que un incremento

en los niveles de expresión de COX-2 esté relacionado con un aumento en los niveles de acetilación de histona H3 y que este a su vez se relacione con un mejor pronóstico de los pacientes de CHC sugiere que la expresión de COX-2 en CHC está vinculada con un mejor pronóstico.

Hay una cierta controversia con respecto al efecto de los inhibidores de HDAC sobre la expresión de COX-2. Algunos estudios indican que el NaB y el TSA suprimen la expresión de COX-2 en la línea celular HT-29 mediante la inhibición de la elongación de la ARN polimerasa II en el gen de COX-2 y de c-Myc [140]. En células de carcinoma escamoso esofágico (KYSE450) y en células de mama transformadas (18B5/HER) el tratamiento con iHDAC suprimió la inducción de la expresión de COX-2 mediada por PMA [142], y en células de cáncer de pulmón microcítico el tratamiento con TSA indujo apoptosis y disminuyó los niveles de expresión del ARNm y de la proteína de COX-2. Sin embargo, otros estudios indican que el tratamiento con NaB y TSA incrementan la inducción del gen de COX-2 por LPS en macrófagos mediante el aumento en la fosforilación y acetilación de la histona H3 en el promotor de COX-2 mediado por la activación de la vía de las MAPK y mediante un incremento de los niveles de C/EBPδ [84, 113]. En cáncer gástrico, el tratamiento con TSA solo o combinado con AzadC restaura sinérgicamente la expresión de COX-2 y está correlacionado con la acetilación de histonas en su promotor [70]. Estos resultados y nuestros datos muestran que el efecto de los iHDAC en la activación de la expresión de COX-2 puede variar en función del tipo celular y que incluso puede no estar relacionado con actividad anti-tumoral.

Por tanto, la expresión de COX-2 está regulada por la metilación de su promotor y por la acetilación de histonas en algunas líneas de hepatoma y en CHC humano. Nuestros resultados indican que la alteración en la metilación del promotor de COX-2 ocurre exclusivamente en el tejido tumoral hepático en CHC y que la metilación aberrante de COX-2 en CHC está relacionada con un peor pronóstico. También podrían explicar la disminución en la expresión de COX-2 en los tumores indiferenciados y con peor pronóstico. Estos datos sugieren que el análisis del estado de metilación de COX-2 en tumores primarios podría ser empleado como marcador pronóstico del CHC permitiendo un tratamiento quimioterapéutico más adecuado.

Conclusiones

1. Las PGs producidas por la sobre-expresión de COX-2 en el hepatocito promueven una ligera hepatitis a las 60 semanas de edad en los ratones TG para COX-2. Sin embargo, no contribuyen al proceso de fibrogenesis hepática después de la inducción de un daño hepático crónico con una dieta deficiente en colina y metionina.

2. En el contexto de una hepatocarcinogénesis química inducida con DEN, los modelos TG para COX-2 revelaron que las PGs dependientes de COX-2 aceleran la proliferación inicial de los hepatocitos y favorecen el desarrollo moderado de nódulos pre-neoplásicos sin que estén directamente vinculadas con la transformación tumoral. COX-2 está implicada en el proceso temprano de proliferación de los hepatocitos mediante la modulación de rutas moleculares relativas al ciclo celular y a la proliferación celular

3. En el modelo de animales dobles TG para c-Myc/TGF-α que desarrollan una hepatocarcinogénesis genética, la inserción del transgén de COX-2 y su expresión constitutiva en el hepatocito, mostró que a los 5 meses de edad, la sobre-producción de PGs podría estar previniendo levemente la hipertrofia e hiperplasia causada por c-Myc/TGF-α. No obstante, con la edad, la ausencia de diferencias en el desarrollo de CHC y la falta de alteración de rutas metabólicas alternativas en el proceso de carcinogénesis, mostró la insuficiencia contributiva de las PGs al desarrollo de la carcinogénesis mediada por c-Myc/TGF-α.

4. La expresión reducida de COX-2 en algunas de las líneas celulares de hepatoma y en biopsias humanas de CHC está correlacionada con la hipermetilación de su promotor y con la deacetilación de histonas. El tratamiento con agentes demetilantes o con inhibidores de HDACs aumenta la expresión de COX-2 y la unión de Ac-H3 a su promotor en células de CHC.

5. Los cambios epigenéticos en el promotor de COX-2 que implican una disminución en la expresión de COX-2, como la metilación del promotor y la hipoacetilación de H3, están relacionados con una peor prognosis en pacientes con CHC.

Bibliografía

1. Accioly, M. T., P. Pacheco, C. M. Maya-Monteiro, N. Carrossini, B. K. Robbs, S. S. Oliveira, C. Kaufmann, J. A. Morgado-Diaz, P. T. Bozza, and J. P. Viola. 2008. Lipid bodies are reservoirs of cyclooxygenase-2 and sites of prostaglandin-E2 synthesis in colon cancer cells. Cancer research 68:1732-1740.
2. Al-Salihi, M. A., A. Terrece Pearman, T. Doan, E. C. Reichert, D. W. Rosenberg, S. M. Prescott, D. M. Stafforini, and M. K. Topham. 2009. Transgenic expression of cyclooxygenase-2 in mouse intestine epithelium is insufficient to initiate tumorigenesis but promotes tumor progression. Cancer letters 273:225-232.
3. Amano, H., I. Hayashi, H. Endo, H. Kitasato, S. Yamashina, T. Maruyama, M. Kobayashi, K. Satoh, M. Narita, Y. Sugimoto, T. Murata, H. Yoshimura, S. Narumiya, and M. Majima. 2003. Host prostaglandin E(2)-EP3 signaling regulates tumor-associated angiogenesis and tumor growth. The Journal of experimental medicine 197:221-232.
4. Bannister, A. J., and T. Kouzarides. 2011. Regulation of chromatin by histone modifications. Cell research 21:381-395.
5. Bergstroem, S., H. Danielsson, and B. Samuelsson. 1964. The Enzymatic Formation of Prostaglandin E2 from Arachidonic Acid Prostaglandins and Related Factors 32. Biochimica et biophysica acta 90:207-210.
6. Bird, A. 2007. Perceptions of epigenetics. Nature 447:396-398.
7. Bol, D. K., R. B. Rowley, C. P. Ho, B. Pilz, J. Dell, M. Swerdel, K. Kiguchi, S. Muga, R. Klein, and S. M. Fischer. 2002. Cyclooxygenase-2 overexpression in the skin of transgenic mice results in suppression of tumor development. Cancer research 62:2516-2521.
8. Bolli, R., K. Shinmura, X. L. Tang, E. Kodani, Y. T. Xuan, Y. Guo, and B. Dawn. 2002. Discovery of a new function of cyclooxygenase (COX)-2: COX-2 is a cardioprotective protein that alleviates ischemia/reperfusion injury and mediates the late phase of preconditioning. Cardiovascular research 55:506-519.
9. Buchanan, F. G., D. Wang, F. Bargiacchi, and R. N. DuBois. 2003. Prostaglandin E2 regulates cell migration via the intracellular activation of the epidermal growth factor receptor. The Journal of biological chemistry 278:35451-35457.
10. Calvisi, D. F., S. Ladu, A. Gorden, M. Farina, E. A. Conner, J. S. Lee, V. M. Factor, and S. S. Thorgeirsson. 2006. Ubiquitous activation of Ras and Jak/Stat pathways in human HCC. Gastroenterology 130:1117-1128.
11. Calvisi, D. F., S. Ladu, A. Gorden, M. Farina, J. S. Lee, E. A. Conner, I. Schroeder, V. M. Factor, and S. S. Thorgeirsson. 2007. Mechanistic and prognostic significance of aberrant methylation in the molecular pathogenesis of human hepatocellular carcinoma. The Journal of clinical investigation 117:2713-2722.
12. Calvisi, D. F., and S. S. Thorgeirsson. 2005. Molecular mechanisms of hepatocarcinogenesis in transgenic mouse models of liver cancer. Toxicologic pathology 33:181-184.
13. Callejas, N. A., L. Bosca, C. S. Williams, B. R. Du, and P. Martin-Sanz. 2000. Regulation of cyclooxygenase 2 expression in hepatocytes by CCAAT/enhancer-binding proteins. Gastroenterology 119:493-501.
14. Callejas, N. A., A. Castrillo, L. Bosca, and P. Martin-Sanz. 1999. Inhibition of prostaglandin synthesis up-regulates cyclooxygenase-2 induced by lipopolysaccharide and peroxisomal proliferators. The Journal of pharmacology and experimental therapeutics 288:1235-1241.
15. Casado, M., N. A. Callejas, J. Rodrigo, X. Zhao, S. K. Dey, L. Bosca, and P. Martin-Sanz. 2001. Contribution of cyclooxygenase 2 to liver regeneration after partial hepatectomy. FASEB J 15:2016-2018.
16. Casado, M., B. Molla, R. Roy, A. Fernandez-Martinez, C. Cucarella, R. Mayoral, L. Bosca, and P. Martin-Sanz. 2007. Protection against Fas-induced liver apoptosis in transgenic mice expressing cyclooxygenase 2 in hepatocytes. Hepatology 45:631-638.

17. Cebola, I., and M. A. Peinado. 2012. Epigenetic deregulation of the COX pathway in cancer. Progress in lipid research 51:301-313.
18. Cervello, M., D. Bachvarov, A. Cusimano, F. Sardina, A. Azzolina, N. Lampiasi, L. Giannitrapani, J. A. McCubrey, and G. Montalto. 2011. COX-2-dependent and COX-2-independent mode of action of celecoxib in human liver cancer cells. Omics : a journal of integrative biology 15:383-392.
19. Cervello, M., D. Foderaa, A. M. Florena, M. Soresi, C. Tripodo, N. D'Alessandro, and G. Montalto. 2005. Correlation between expression of cyclooxygenase-2 and the presence of inflammatory cells in human primary hepatocellular carcinoma: possible role in tumor promotion and angiogenesis. World journal of gastroenterology : WJG 11:4638-4643.
20. Cervello, M., J. A. McCubrey, A. Cusimano, N. Lampiasi, A. Azzolina, and G. Montalto. 2012. Targeted therapy for hepatocellular carcinoma: novel agents on the horizon. Oncotarget 3:236-260.
21. Colby, J. K., R. D. Klein, M. J. McArthur, C. J. Conti, K. Kiguchi, T. Kawamoto, P. K. Riggs, A. I. Pavone, J. Sawicki, and S. M. Fischer. 2008. Progressive metaplastic and dysplastic changes in mouse pancreas induced by cyclooxygenase-2 overexpression. Neoplasia 10:782-796.
22. Coulouarn, C., L. E. Gomez-Quiroz, J. S. Lee, P. Kaposi-Novak, E. A. Conner, T. A. Goldina, G. E. Onishchenko, V. M. Factor, and S. S. Thorgeirsson. 2006. Oncogene-specific gene expression signatures at preneoplastic stage in mice define distinct mechanisms of hepatocarcinogenesis. Hepatology 44:1003-1011.
23. Cui, W., S. X. Hu, Z. Y. Tang, and K. Q. Hu. 2008. In-vivo effects and mechanisms of celecoxib-reduced growth of cyclooxygenase-2 (COX-2)-expressing versus COX-2-deleted human HCC xenografts in nude mice. Anti-cancer drugs 19:891-897.
24. Cusimano, A., D. Fodera, N. Lampiasi, A. Azzolina, M. Notarbartolo, L. Giannitrapani, N. D'Alessandro, G. Montalto, and M. Cervello. 2009. Prostaglandin E2 receptors and COX enzymes in human hepatocellular carcinoma: role in the regulation of cell growth. Ann N Y Acad Sci 1155:300-308.
25. Cha, Y. I., and R. N. DuBois. 2007. NSAIDs and cancer prevention: targets downstream of COX-2. Annual review of medicine 58:239-252.
26. Chandrasekharan, N. V., and D. L. Simmons. 2004. The cyclooxygenases. Genome biology 5:241.
27. Chang, M. C., H. H. Chang, C. P. Chan, H. Y. Chou, B. E. Chang, S. Y. Yeung, T. M. Wang, and J. H. Jeng. 2012. Antiplatelet effect of phloroglucinol is related to inhibition of cyclooxygenase, reactive oxygen species, ERK/p38 signaling and thromboxane A(2) production. Toxicology and applied pharmacology 263:287-295.
28. Chang, S. H., C. H. Liu, R. Conway, D. K. Han, K. Nithipatikom, O. C. Trifan, T. F. Lane, and T. Hla. 2004. Role of prostaglandin E2-dependent angiogenic switch in cyclooxygenase 2-induced breast cancer progression. Proceedings of the National Academy of Sciences of the United States of America 101:591-596.
29. Chen, J., D. Liu, Q. Bai, J. Song, J. Guan, J. Gao, B. Liu, X. Ma, and Y. Du. 2011. Celecoxib attenuates liver steatosis and inflammation in non-alcoholic steatohepatitis induced by high-fat diet in rats. Molecular medicine reports 4:811-816.
30. Choi, E. M., S. R. Kim, E. J. Lee, and J. A. Han. 2009. Cyclooxygenase-2 functionally inactivates p53 through a physical interaction with p53. Biochimica et biophysica acta 1793:1354-1365.
31. de Maat, M. F., C. J. van de Velde, N. Umetani, P. de Heer, H. Putter, A. Q. van Hoesel, G. A. Meijer, N. C. van Grieken, P. J. Kuppen, A. J. Bilchik, R. A. Tollenaar, and D. S. Hoon. 2007. Epigenetic silencing of cyclooxygenase-2 affects clinical outcome in gastric cancer. Journal of clinical oncology : official journal of the American Society of Clinical Oncology 25:4887-4894.

32. Dennis, E. A., S. G. Rhee, M. M. Billah, and Y. A. Hannun. 1991. Role of phospholipase in generating lipid second messengers in signal transduction. FASEB journal : official publication of the Federation of American Societies for Experimental Biology 5:2068-2077.
33. Dey, I., M. Lejeune, and K. Chadee. 2006. Prostaglandin E2 receptor distribution and function in the gastrointestinal tract. British journal of pharmacology 149:611-623.
34. Dixon, D. A., N. D. Tolley, P. H. King, L. B. Nabors, T. M. McIntyre, G. A. Zimmerman, and S. M. Prescott. 2001. Altered expression of the mRNA stability factor HuR promotes cyclooxygenase-2 expression in colon cancer cells. The Journal of clinical investigation 108:1657-1665.
35. Dore, S., T. Otsuka, T. Mito, N. Sugo, T. Hand, L. Wu, P. D. Hurn, R. J. Traystman, and K. Andreasson. 2003. Neuronal overexpression of cyclooxygenase-2 increases cerebral infarction. Annals of neurology 54:155-162.
36. Edmondson, H. A., and P. E. Steiner. 1954. Primary carcinoma of the liver: a study of 100 cases among 48,900 necropsies. Cancer 7:462-503.
37. Ekor, M., A. O. Odewabi, O. E. Kale, O. A. Adesanoye, and T. O. Bamidele. 2011. Celecoxib, a selective cyclooxygenase-2 inhibitor, lowers plasma cholesterol and attenuates hepatic lipid peroxidation during carbon-tetrachloride-associated hepatotoxicity in rats. Drug and chemical toxicology.
38. Esteller, M. 2007. Cancer epigenomics: DNA methylomes and histone-modification maps. Nature reviews. Genetics 8:286-298.
39. Factor, V. M., A. Kiss, J. T. Woitach, P. J. Wirth, and S. S. Thorgeirsson. 1998. Disruption of redox homeostasis in the transforming growth factor-alpha/c-myc transgenic mouse model of accelerated hepatocarcinogenesis. The Journal of biological chemistry 273:15846-15853.
40. Fantappie, O., E. Masini, I. Sardi, L. Raimondi, D. Bani, M. Solazzo, A. Vannacci, and R. Mazzanti. 2002. The MDR phenotype is associated with the expression of COX-2 and iNOS in a human hepatocellular carcinoma cell line. Hepatology 35:843-852.
41. Farazi, P. A., and R. A. DePinho. 2006. Hepatocellular carcinoma pathogenesis: from genes to environment. Nature reviews. Cancer 6:674-687.
42. Fernandez-Martinez, A., N. A. Callejas, M. Casado, L. Bosca, and P. Martin-Sanz. 2004. Thioacetamide-induced liver regeneration involves the expression of cyclooxygenase 2 and nitric oxide synthase 2 in hepatocytes. Journal of hepatology 40:963-970.
43. Fernandez-Martinez, A., B. Molla, R. Mayoral, L. Bosca, M. Casado, and P. Martin-Sanz. 2006. Cyclo-oxygenase 2 expression impairs serum-withdrawal-induced apoptosis in liver cells. The Biochemical journal 398:371-380.
44. Frances, D. E., P. I. Ingaramo, R. Mayoral, P. Traves, M. Casado, A. M. Valverde, P. Martin-Sanz, and C. E. Carnovale. 2012. Cyclooxygenase-2 over-expression inhibits liver apoptosis induced by hyperglycemia. Journal of cellular biochemistry.
45. Ghoshal, A. K., M. Ahluwalia, and E. Farber. 1983. The rapid induction of liver cell death in rats fed a choline-deficient methionine-low diet. The American journal of pathology 113:309-314.
46. Giannitrapani, L., S. Ingrao, M. Soresi, A. M. Florena, E. La Spada, L. Sandonato, N. D'Alessandro, M. Cervello, and G. Montalto. 2009. Cyclooxygenase-2 expression in chronic liver diseases and hepatocellular carcinoma: an immunohistochemical study. Ann N Y Acad Sci 1155:293-299.
47. Giannitrapani, L., M. Soresi, A. Giacalone, M. E. Campagna, M. Marasa, M. Cervello, S. Marasa, and G. Montalto. 2011. IL-6 -174G/C polymorphism and IL-6 serum levels in patients with liver cirrhosis and hepatocellular carcinoma. Omics : a journal of integrative biology 15:183-186.
48. Goll, M. G., and T. H. Bestor. 2005. Eukaryotic cytosine methyltransferases. Annual review of biochemistry 74:481-514.

49. Greenhough, A., H. J. Smartt, A. E. Moore, H. R. Roberts, A. C. Williams, C. Paraskeva, and A. Kaidi. 2009. The COX-2/PGE2 pathway: key roles in the hallmarks of cancer and adaptation to the tumour microenvironment. Carcinogenesis 30:377-386.
50. Hallstrom, T. C., and J. R. Nevins. 2003. Specificity in the activation and control of transcription factor E2F-dependent apoptosis. Proceedings of the National Academy of Sciences of the United States of America 100:10848-10853.
51. Hamberg, M., and B. Samuelsson. 1973. Detection and isolation of an endoperoxide intermediate in prostaglandin biosynthesis. Proceedings of the National Academy of Sciences of the United States of America 70:899-903.
52. Han, C., A. J. Demetris, D. B. Stolz, L. Xu, K. Lim, and T. Wu. 2006. Modulation of Stat3 activation by the cytosolic phospholipase A2alpha and cyclooxygenase-2-controlled prostaglandin E2 signaling pathway. The Journal of biological chemistry 281:24831-24846.
53. Han, C., G. Li, K. Lim, M. C. DeFrances, C. R. Gandhi, and T. Wu. 2008. Transgenic expression of cyclooxygenase-2 in hepatocytes accelerates endotoxin-induced acute liver failure. J Immunol 181:8027-8035.
54. Harper, K. A., and A. J. Tyson-Capper. 2008. Complexity of COX-2 gene regulation. Biochemical Society transactions 36:543-545.
55. He, G., G. Y. Yu, V. Temkin, H. Ogata, C. Kuntzen, T. Sakurai, W. Sieghart, M. Peck-Radosavljevic, H. L. Leffert, and M. Karin. 2010. Hepatocyte IKKbeta/NF-kappaB inhibits tumor promotion and progression by preventing oxidative stress-driven STAT3 activation. Cancer cell 17:286-297.
56. He, Y. F., J. Jin, W. Wei, Y. Chang, B. Hu, C. S. Ji, W. D. Jia, X. Q. Wang, K. Chen, and J. Chen. 2010. Overexpression of cyclooxygenase-2 in noncancerous liver tissue increases the postoperative recurrence of hepatocellular carcinoma in patients with hepatitis B virus-related cirrhosis. Canadian journal of gastroenterology = Journal canadien de gastroenterologie 24:435-440.
57. Horie, Y., A. Suzuki, E. Kataoka, T. Sasaki, K. Hamada, J. Sasaki, K. Mizuno, G. Hasegawa, H. Kishimoto, M. Iizuka, M. Naito, K. Enomoto, S. Watanabe, T. W. Mak, and T. Nakano. 2004. Hepatocyte-specific Pten deficiency results in steatohepatitis and hepatocellular carcinomas. The Journal of clinical investigation 113:1774-1783.
58. Hortelano, S., M. Zeini, M. Casado, P. Martin-Sanz, and L. Bosca. 2007. Animal models for the study of liver regeneration: role of nitric oxide and prostaglandins. Frontiers in bioscience : a journal and virtual library 12:13-21.
59. Hoshida, Y., S. M. Nijman, M. Kobayashi, J. A. Chan, J. P. Brunet, D. Y. Chiang, A. Villanueva, P. Newell, K. Ikeda, M. Hashimoto, G. Watanabe, S. Gabriel, S. L. Friedman, H. Kumada, J. M. Llovet, and T. R. Golub. 2009. Integrative transcriptome analysis reveals common molecular subclasses of human hepatocellular carcinoma. Cancer Res 69:7385-7392.
60. Hu, K. Q., C. H. Yu, Y. Mineyama, J. D. McCracken, D. J. Hillebrand, and M. Hasan. 2003. Inhibited proliferation of cyclooxygenase-2 expressing human hepatoma cells by NS-398, a selective COX-2 inhibitor. International journal of oncology 22:757-763.
61. Hui, A. Y., W. K. Leung, H. L. Chan, F. K. Chan, M. Y. Go, K. K. Chan, B. D. Tang, E. S. Chu, and J. J. Sung. 2006. Effect of celecoxib on experimental liver fibrosis in rat. Liver international : official journal of the International Association for the Study of the Liver 26:125-136.
62. Hung, J. H., I. J. Su, H. Y. Lei, H. C. Wang, W. C. Lin, W. T. Chang, W. Huang, W. C. Chang, Y. S. Chang, C. C. Chen, and M. D. Lai. 2004. Endoplasmic reticulum stress stimulates the expression of cyclooxygenase-2 through activation of NF-kappaB and pp38 mitogen-activated protein kinase. The Journal of biological chemistry 279:46384-46392.

63. Inserte, J., B. Molla, R. Aguilar, P. G. Traves, I. Barba, P. Martin-Sanz, L. Bosca, M. Casado, and D. Garcia-Dorado. 2009. Constitutive COX-2 activity in cardiomyocytes confers permanent cardioprotection Constitutive COX-2 expression and cardioprotection. Journal of molecular and cellular cardiology 46:160-168.
64. Ishikawa, T. O., and H. R. Herschman. 2010. Tumor formation in a mouse model of colitis-associated colon cancer does not require COX-1 or COX-2 expression. Carcinogenesis 31:729-736.
65. Iyer, N. G., H. Ozdag, and C. Caldas. 2004. p300/CBP and cancer. Oncogene 23:4225-4231.
66. Jones, P. A., and D. Takai. 2001. The role of DNA methylation in mammalian epigenetics. Science 293:1068-1070.
67. Kanel, G. C. 2009. Liver: Anatomy, Microscopic Structure, and Cell Types, p. 615-622, Atlas of Gastroenterology. Wiley-Blackwell.
68. Kang, Y. J., U. R. Mbonye, C. J. DeLong, M. Wada, and W. L. Smith. 2007. Regulation of intracellular cyclooxygenase levels by gene transcription and protein degradation. Progress in lipid research 46:108-125.
69. Kern, M. A., M. M. Schoneweiss, D. Sahi, M. Bahlo, A. M. Haugg, H. U. Kasper, H. P. Dienes, H. Kaferstein, K. Breuhahn, and P. Schirmacher. 2004. Cyclooxygenase-2 inhibitors suppress the growth of human hepatocellular carcinoma implants in nude mice. Carcinogenesis 25:1193-1199.
70. Kikuchi, T., F. Itoh, M. Toyota, H. Suzuki, H. Yamamoto, M. Fujita, M. Hosokawa, and K. Imai. 2002. Aberrant methylation and histone deacetylation of cyclooxygenase 2 in gastric cancer. International journal of cancer. Journal international du cancer 97:272-277.
71. Kim, Y. M., S. Y. Park, and H. Pyo. 2009. Cyclooxygenase-2 (COX-2) negatively regulates expression of epidermal growth factor receptor and causes resistance to gefitinib in COX-2-overexpressing cancer cells. Molecular cancer research : MCR 7:1367-1377.
72. Koga, H., S. Sakisaka, M. Ohishi, T. Kawaguchi, E. Taniguchi, K. Sasatomi, M. Harada, T. Kusaba, M. Tanaka, R. Kimura, Y. Nakashima, O. Nakashima, M. Kojiro, T. Kurohiji, and M. Sata. 1999. Expression of cyclooxygenase-2 in human hepatocellular carcinoma: relevance to tumor dedifferentiation. Hepatology 29:688-696.
73. Lee, J. S., I. S. Chu, A. Mikaelyan, D. F. Calvisi, J. Heo, J. K. Reddy, and S. S. Thorgeirsson. 2004. Application of comparative functional genomics to identify best-fit mouse models to study human cancer. Nature genetics 36:1306-1311.
74. Lee, J. S., and S. S. Thorgeirsson. 2005. Genetic profiling of human hepatocellular carcinoma. Seminars in liver disease 25:125-132.
75. Lee, J. S., and S. S. Thorgeirsson. 2004. Genome-scale profiling of gene expression in hepatocellular carcinoma: classification, survival prediction, and identification of therapeutic targets. Gastroenterology 127:S51-55.
76. Lee, S., H. J. Lee, J. H. Kim, H. S. Lee, J. J. Jang, and G. H. Kang. 2003. Aberrant CpG island hypermethylation along multistep hepatocarcinogenesis. The American journal of pathology 163:1371-1378.
77. Lee, S. H., M. V. Williams, R. N. Dubois, and I. A. Blair. 2005. Cyclooxygenase-2-mediated DNA damage. The Journal of biological chemistry 280:28337-28346.
78. Leng, J., C. Han, A. J. Demetris, G. K. Michalopoulos, and T. Wu. 2003. Cyclooxygenase-2 promotes hepatocellular carcinoma cell growth through Akt activation: evidence for Akt inhibition in celecoxib-induced apoptosis. Hepatology 38:756-768.
79. Li, G., C. Han, L. Xu, K. Lim, K. Isse, and T. Wu. 2009. Cyclooxygenase-2 prevents fas-induced liver injury through up-regulation of epidermal growth factor receptor. Hepatology 50:834-843.
80. Li, Y., Z. Y. Tang, and J. X. Hou. 2012. Hepatocellular carcinoma: insight from animal models. Nature reviews. Gastroenterology & hepatology 9:32-43.

81. Lin, H., and P. F. Hollenberg. 2001. N-nitrosodimethylamine-mediated formation of oxidized and methylated dna bases in a cytochrome P450 2E1 expressing cell line. Chemical research in toxicology 14:562-566.
82. Liu, C. H., S. H. Chang, K. Narko, O. C. Trifan, M. T. Wu, E. Smith, C. Haudenschild, T. F. Lane, and T. Hla. 2001. Overexpression of cyclooxygenase-2 is sufficient to induce tumorigenesis in transgenic mice. The Journal of biological chemistry 276:18563-18569.
83. Liu, K. G., X. L. Shao, H. H. Xie, L. Xu, H. Zhao, Z. H. Guo, L. Li, and J. Liu. 2010. [The expression of hepatitis B virus X protein and cyclooxygenase-2 in hepatitis B virus-related hepatocellular carcinoma: correlation with microangiogenesis and metastasis, and what is the possible mechanism]. Zhonghua gan zang bing za zhi = Zhonghua ganzangbing zazhi = Chinese journal of hepatology 18:831-836.
84. Liu, Y. W., S. A. Wang, T. Y. Hsu, T. A. Chen, W. C. Chang, and J. J. Hung. 2010. Inhibition of LPS-induced C/EBP delta by trichostatin A has a positive effect on LPS-induced cyclooxygenase 2 expression in RAW264.7 cells. Journal of cellular biochemistry 110:1430-1438.
85. Luedde, T., N. Beraza, V. Kotsikoris, G. van Loo, A. Nenci, R. De Vos, T. Roskams, C. Trautwein, and M. Pasparakis. 2007. Deletion of NEMO/IKKgamma in liver parenchymal cells causes steatohepatitis and hepatocellular carcinoma. Cancer cell 11:119-132.
86. Llorente Izquierdo, C., R. Mayoral, J. M. Flores, P. Garcia-Palencia, C. Cucarella, L. Bosca, M. Casado, and P. Martin-Sanz. 2011. Transgenic mice expressing cyclooxygenase-2 in hepatocytes reveal a minor contribution of this enzyme to chemical hepatocarcinogenesis. The American journal of pathology 178:1361-1373.
87. Maeda, S., H. Kamata, J. L. Luo, H. Leffert, and M. Karin. 2005. IKKbeta couples hepatocyte death to cytokine-driven compensatory proliferation that promotes chemical hepatocarcinogenesis. Cell 121:977-990.
88. Maldve, R. E., Y. Kim, S. J. Muga, and S. M. Fischer. 2000. Prostaglandin E(2) regulation of cyclooxygenase expression in keratinocytes is mediated via cyclic nucleotide-linked prostaglandin receptors. Journal of lipid research 41:873-881.
89. Mancini, A. D., and J. A. Di Battista. 2011. The cardinal role of the phospholipase A(2)/cyclooxygenase-2/prostaglandin E synthase/prostaglandin E(2) (PCPP) axis in inflammostasis. Inflammation research : official journal of the European Histamine Research Society ... [et al.] 60:1083-1092.
90. Marks, F., G. Furstenberger, and K. Muller-Decker. 2007. Tumor promotion as a target of cancer prevention. Recent results in cancer research. Fortschritte der Krebsforschung. Progres dans les recherches sur le cancer 174:37-47.
91. Marks, P., R. A. Rifkind, V. M. Richon, R. Breslow, T. Miller, and W. K. Kelly. 2001. Histone deacetylases and cancer: causes and therapies. Nature reviews. Cancer 1:194-202.
92. Martin-Sanz, P., N. A. Callejas, M. Casado, M. J. Diaz-Guerra, and L. Bosca. 1998. Expression of cyclooxygenase-2 in foetal rat hepatocytes stimulated with lipopolysaccharide and pro-inflammatory cytokines. Br J Pharmacol 125:1313-1319.
93. Martin-Sanz, P., R. Mayoral, M. Casado, and L. Bosca. 2010. COX-2 in liver, from regeneration to hepatocarcinogenesis: what we have learned from animal models? World journal of gastroenterology : WJG 16:1430-1435.
94. Martin Sanz, P., S. Hortelano, L. Bosca, and M. Casado. 2006. Cyclooxygenase 2: understanding the pathophysiological role through genetically altered mouse models. Frontiers in bioscience : a journal and virtual library 11:2876-2888.
95. Matsumura, I., H. Tanaka, and Y. Kanakura. 2003. E2F1 and c-Myc in cell growth and death. Cell Cycle 2:333-338.

96. Mayoral, R., A. Fernandez-Martinez, L. Bosca, and P. Martin-Sanz. 2005. Prostaglandin E2 promotes migration and adhesion in hepatocellular carcinoma cells. Carcinogenesis 26:753-761.
97. Mayoral, R., B. Molla, J. M. Flores, L. Bosca, M. Casado, and P. Martin-Sanz. 2008. Constitutive expression of cyclo-oxygenase 2 transgene in hepatocytes protects against liver injury. Biochem J 416:337-346.
98. McCubrey, J. A., L. S. Steelman, S. L. Abrams, W. H. Chappell, S. Russo, R. Ove, M. Milella, A. Tafuri, P. Lunghi, A. Bonati, F. Stivala, F. Nicoletti, M. Libra, A. M. Martelli, G. Montalto, and M. Cervello. 2010. Emerging MEK inhibitors. Expert opinion on emerging drugs 15:203-223.
99. Melnikova, T., A. Savonenko, Q. Wang, X. Liang, T. Hand, L. Wu, W. E. Kaufmann, A. Vehmas, and K. I. Andreasson. 2006. Cycloxygenase-2 activity promotes cognitive deficits but not increased amyloid burden in a model of Alzheimer's disease in a sex-dimorphic pattern. Neuroscience 141:1149-1162.
100. Menter, D. G., R. L. Schilsky, and R. N. DuBois. 2010. Cyclooxygenase-2 and cancer treatment: understanding the risk should be worth the reward. Clinical cancer research : an official journal of the American Association for Cancer Research 16:1384-1390.
101. Miremadi, A., M. Z. Oestergaard, P. D. Pharoah, and C. Caldas. 2007. Cancer genetics of epigenetic genes. Human molecular genetics 16 Spec No 1:R28-49.
102. Miyamoto, T., N. Ogino, S. Yamamoto, and O. Hayaishi. 1976. Purification of prostaglandin endoperoxide synthetase from bovine vesicular gland microsomes. The Journal of biological chemistry 251:2629-2636.
103. Miyashita, M., T. Ito, M. Sakaki, A. Kajiwara, H. Nozawa, K. Hiroishi, M. Kobayashi, H. Kumada, and M. Imawari. 2012. Genetic polymorphism in cyclooxygenase-2 promoter affects hepatic inflammation and fibrosis in patients with chronic hepatitis C. Journal of viral hepatitis 19:608-614.
104. Morinaga, S., Y. Yamamoto, Y. Noguchi, T. Imada, Y. Rino, M. Akaike, Y. Sugimasa, S. Takemiya, Y. Kameda, and Y. Takanashi. 2002. Cyclooxygenase-2 mRNA is up-regulated in cirrhotic or chronic hepatitis liver adjacent to hepatocellular carcinoma. Journal of gastroenterology and hepatology 17:1110-1116.
105. Mossman, D., K. T. Kim, and R. J. Scott. 2010. Demethylation by 5-aza-2'-deoxycytidine in colorectal cancer cells targets genomic DNA whilst promoter CpG island methylation persists. BMC cancer 10:366.
106. Mottet, D., and V. Castronovo. 2008. Histone deacetylases: target enzymes for cancer therapy. Clinical & experimental metastasis 25:183-189.
107. Muller-Decker, K., and G. Furstenberger. 2007. The cyclooxygenase-2-mediated prostaglandin signaling is causally related to epithelial carcinogenesis. Molecular carcinogenesis 46:705-710.
108. Murakami, H., N. D. Sanderson, P. Nagy, P. A. Marino, G. Merlino, and S. S. Thorgeirsson. 1993. Transgenic mouse model for synergistic effects of nuclear oncogenes and growth factors in tumorigenesis: interaction of c-myc and transforming growth factor alpha in hepatic oncogenesis. Cancer research 53:1719-1723.
109. Murata, H., S. Tsuji, M. Tsujii, Y. Sakaguchi, H. Y. Fu, S. Kawano, and M. Hori. 2004. Promoter hypermethylation silences cyclooxygenase-2 (Cox-2) and regulates growth of human hepatocellular carcinoma cells. Laboratory investigation; a journal of technical methods and pathology 84:1050-1059.
110. Nunez, O., A. Fernandez-Martinez, P. L. Majano, A. Apolinario, M. Gomez-Gonzalo, I. Benedicto, M. Lopez-Cabrera, L. Bosca, G. Clemente, C. Garcia-Monzon, and P. Martin-Sanz. 2004. Increased intrahepatic cyclooxygenase 2, matrix metalloproteinase 2, and matrix metalloproteinase 9 expression is associated with progressive liver disease in

chronic hepatitis C virus infection: role of viral core and NS5A proteins. Gut 53:1665-1672.
111. Oshima, H., M. Oshima, K. Inaba, and M. M. Taketo. 2004. Hyperplastic gastric tumors induced by activated macrophages in COX-2/mPGES-1 transgenic mice. The EMBO journal 23:1669-1678.
112. Paik, Y. H., J. K. Kim, J. I. Lee, S. H. Kang, D. Y. Kim, S. H. An, S. J. Lee, D. K. Lee, K. H. Han, C. Y. Chon, S. I. Lee, K. S. Lee, and D. A. Brenner. 2009. Celecoxib induces hepatic stellate cell apoptosis through inhibition of Akt activation and suppresses hepatic fibrosis in rats. Gut 58:1517-1527.
113. Park, G. Y., M. Joo, T. Pedchenko, T. S. Blackwell, and J. W. Christman. 2004. Regulation of macrophage cyclooxygenase-2 gene expression by modifications of histone H3. American journal of physiology. Lung cellular and molecular physiology 286:L956-962.
114. Park, J. W., J. E. Park, J. A. Lee, C. W. Lee, and C. M. Kim. 2006. Cyclooxygenase-2 (COX-2) is directly involved but not decisive in proliferation of human hepatocellular carcinoma cells. Journal of cancer research and clinical oncology 132:184-192.
115. Popovic, R., and J. D. Licht. 2012. Emerging epigenetic targets and therapies in cancer medicine. Cancer discovery 2:405-413.
116. Rouzer, C. A., and L. J. Marnett. 2009. Cyclooxygenases: structural and functional insights. Journal of lipid research 50 Suppl:S29-34.
117. Rundhaug, J. E., A. Pavone, E. Kim, and S. M. Fischer. 2007. The effect of cyclooxygenase-2 overexpression on skin carcinogenesis is context dependent. Molecular carcinogenesis 46:981-992.
118. Sakaguchi, S., S. Takahashi, T. Sasaki, T. Kumagai, and K. Nagata. 2011. Progression of alcoholic and non-alcoholic steatohepatitis: common metabolic aspects of innate immune system and oxidative stress. Drug metabolism and pharmacokinetics 26:30-46.
119. Sakurai, T., G. He, A. Matsuzawa, G. Y. Yu, S. Maeda, G. Hardiman, and M. Karin. 2008. Hepatocyte necrosis induced by oxidative stress and IL-1 alpha release mediate carcinogen-induced compensatory proliferation and liver tumorigenesis. Cancer cell 14:156-165.
120. Sakurai, T., S. Maeda, L. Chang, and M. Karin. 2006. Loss of hepatic NF-kappa B activity enhances chemical hepatocarcinogenesis through sustained c-Jun N-terminal kinase 1 activation. Proceedings of the National Academy of Sciences of the United States of America 103:10544-10551.
121. Samuelsson, B., R. Morgenstern, and P. J. Jakobsson. 2007. Membrane prostaglandin E synthase-1: a novel therapeutic target. Pharmacological reviews 59:207-224.
122. Sancho, P., P. Martin-Sanz, and I. Fabregat. 2011. Reciprocal regulation of NADPH oxidases and the cyclooxygenase-2 pathway. Free radical biology & medicine 51:1789-1798.
123. Sandoval, J., and M. Esteller. 2012. Cancer epigenomics: beyond genomics. Current opinion in genetics & development 22:50-55.
124. Santoni-Rugiu, E., M. R. Jensen, and S. S. Thorgeirsson. 1998. Disruption of the pRb/E2F pathway and inhibition of apoptosis are major oncogenic events in liver constitutively expressing c-myc and transforming growth factor alpha. Cancer research 58:123-134.
125. Santoni-Rugiu, E., P. Nagy, M. R. Jensen, V. M. Factor, and S. S. Thorgeirsson. 1996. Evolution of neoplastic development in the liver of transgenic mice co-expressing c-myc and transforming growth factor-alpha. The American journal of pathology 149:407-428.
126. Sceusi, E. L., D. S. Loose, and C. J. Wray. 2011. Clinical implications of DNA methylation in hepatocellular carcinoma. HPB : the official journal of the International Hepato Pancreato Biliary Association 13:369-376.

127. Scher, J. U., and M. H. Pillinger. 2009. The anti-inflammatory effects of prostaglandins. Journal of investigative medicine : the official publication of the American Federation for Clinical Research 57:703-708.
128. Schmitz, K. J., J. Wohlschlaeger, H. Lang, G. C. Sotiropoulos, G. M. Kaiser, K. W. Schmid, and H. A. Baba. 2009. Cyclo-oxygenase-2 overexpression is a feature of early and well-differentiated hepatocellular carcinoma with a favourable prognosis. Journal of clinical pathology 62:690-693.
129. Schulze-Bergkamen, H., D. Brenner, A. Krueger, D. Suess, S. C. Fas, C. R. Frey, A. Dax, D. Zink, P. Buchler, M. Muller, and P. H. Krammer. 2004. Hepatocyte growth factor induces Mcl-1 in primary human hepatocytes and inhibits CD95-mediated apoptosis via Akt. Hepatology 39:645-654.
130. Schutte, K., J. Bornschein, and P. Malfertheiner. 2009. Hepatocellular carcinoma--epidemiological trends and risk factors. Dig Dis 27:80-92.
131. Schwabe, R. F., C. A. Bradham, T. Uehara, E. Hatano, B. L. Bennett, R. Schoonhoven, and D. A. Brenner. 2003. c-Jun-N-terminal kinase drives cyclin D1 expression and proliferation during liver regeneration. Hepatology 37:824-832.
132. Schwabe, R. F., and D. A. Brenner. 2006. Mechanisms of Liver Injury. I. TNF-alpha-induced liver injury: role of IKK, JNK, and ROS pathways. American journal of physiology. Gastrointestinal and liver physiology 290:G583-589.
133. Shim, M., J. Foley, C. Anna, Y. Mishina, and T. Eling. 2010. Embryonic expression of cyclooxygenase-2 causes malformations in axial skeleton. The Journal of biological chemistry 285:16206-16217.
134. Simmons, D. L., D. B. Levy, Y. Yannoni, and R. L. Erikson. 1989. Identification of a phorbol ester-repressible v-src-inducible gene. Proceedings of the National Academy of Sciences of the United States of America 86:1178-1182.
135. Sobolewski, C., C. Cerella, M. Dicato, and M. Diederich. 2011. Cox-2 inhibitors induce early c-Myc downregulation and lead to expression of differentiation markers in leukemia cells. Cell Cycle 10:2978-2993.
136. Sorokin, A. 2004. Cyclooxygenase-2: potential role in regulation of drug efflux and multidrug resistance phenotype. Current pharmaceutical design 10:647-657.
137. Sreeramkumar, V., M. Fresno, and N. Cuesta. 2012. Prostaglandin E2 and T cells: friends or foes? Immunology and cell biology 90:579-586.
138. Stevens, C., and N. B. La Thangue. 2004. The emerging role of E2F-1 in the DNA damage response and checkpoint control. DNA repair 3:1071-1079.
139. Swenberg, J. A., D. G. Hoel, and P. N. Magee. 1991. Mechanistic and statistical insight into the large carcinogenesis bioassays on N-nitrosodiethylamine and N-nitrosodimethylamine. Cancer research 51:6409-6414.
140. Tanabe, T., and N. Tohnai. 2002. Cyclooxygenase isozymes and their gene structures and expression. Prostaglandins & other lipid mediators 68-69:95-114.
141. Thorgeirsson, S. S., and J. W. Grisham. 2002. Molecular pathogenesis of human hepatocellular carcinoma. Nature genetics 31:339-346.
142. Tong, X., L. Yin, S. Joshi, D. W. Rosenberg, and C. Giardina. 2005. Cyclooxygenase-2 regulation in colon cancer cells: modulation of RNA polymerase II elongation by histone deacetylase inhibitors. The Journal of biological chemistry 280:15503-15509.
143. Tsatsanis, C., A. Androulidaki, M. Venihaki, and A. N. Margioris. 2006. Signalling networks regulating cyclooxygenase-2. The international journal of biochemistry & cell biology 38:1654-1661.
144. Tu, C. T., J. S. Guo, M. Wang, and J. Y. Wang. 2007. Antifibrotic activity of rofecoxib in vivo is associated with reduced portal hypertension in rats with carbon tetrachloride-induced liver injury. Journal of gastroenterology and hepatology 22:877-884.
145. Vane, J. R. 1971. Inhibition of prostaglandin synthesis as a mechanism of action for aspirin-like drugs. Nature: New biology 231:232-235.

146. Veltman, J. D., M. E. Lambers, M. van Nimwegen, R. W. Hendriks, H. C. Hoogsteden, J. G. Aerts, and J. P. Hegmans. 2010. COX-2 inhibition improves immunotherapy and is associated with decreased numbers of myeloid-derived suppressor cells in mesothelioma. Celecoxib influences MDSC function. BMC cancer 10:464.
147. Verna, L., J. Whysner, and G. M. Williams. 1996. N-nitrosodiethylamine mechanistic data and risk assessment: bioactivation, DNA-adduct formation, mutagenicity, and tumor initiation. Pharmacology & therapeutics 71:57-81.
148. Vidali, G., L. C. Boffa, E. M. Bradbury, and V. G. Allfrey. 1978. Butyrate suppression of histone deacetylation leads to accumulation of multiacetylated forms of histones H3 and H4 and increased DNase I sensitivity of the associated DNA sequences. Proceedings of the National Academy of Sciences of the United States of America 75:2239-2243.
149. Wang, D., and R. N. Dubois. 2010. Eicosanoids and cancer. Nature reviews. Cancer 10:181-193.
150. Wang, H., F. Lafdil, L. Wang, O. Park, S. Yin, J. Niu, A. M. Miller, Z. Sun, and B. Gao. 2011. Hepatoprotective versus oncogenic functions of STAT3 in liver tumorigenesis. The American journal of pathology 179:714-724.
151. Wang, X., J. K. Colby, R. C. Rengel, S. M. Fischer, S. K. Clinton, and R. D. Klein. 2009. Overexpression of cyclooxygenase-2 (COX-2) in the mouse urinary bladder induces the expression of immune- and cell proliferation-related genes. Molecular carcinogenesis 48:1-13.
152. Watanabe, S., Y. Horie, E. Kataoka, W. Sato, T. Dohmen, S. Ohshima, T. Goto, and A. Suzuki. 2007. Non-alcoholic steatohepatitis and hepatocellular carcinoma: lessons from hepatocyte-specific phosphatase and tensin homolog (PTEN)-deficient mice. Journal of gastroenterology and hepatology 22 Suppl 1:S96-S100.
153. Wiese, F. W., P. A. Thompson, and F. F. Kadlubar. 2001. Carcinogen substrate specificity of human COX-1 and COX-2. Carcinogenesis 22:5-10.
154. Williams, C. S., and R. N. DuBois. 1996. Prostaglandin endoperoxide synthase: why two isoforms? The American journal of physiology 270:G393-400.
155. Woodward, D. F., R. L. Jones, and S. Narumiya. 2011. International Union of Basic and Clinical Pharmacology. LXXXIII: classification of prostanoid receptors, updating 15 years of progress. Pharmacological reviews 63:471-538.
156. Wu, W. K., J. J. Sung, C. W. Lee, J. Yu, and C. H. Cho. 2010. Cyclooxygenase-2 in tumorigenesis of gastrointestinal cancers: an update on the molecular mechanisms. Cancer letters 295:7-16.
157. Xia, D., D. Wang, S. H. Kim, H. Katoh, and R. N. DuBois. 2012. Prostaglandin E2 promotes intestinal tumor growth via DNA methylation. Nature medicine 18:224-226.
158. Yamamoto, H., M. Kondo, S. Nakamori, H. Nagano, K. Wakasa, Y. Sugita, J. Chang-De, S. Kobayashi, B. Damdinsuren, K. Dono, K. Umeshita, M. Sekimoto, M. Sakon, N. Matsuura, and M. Monden. 2003. JTE-522, a cyclooxygenase-2 inhibitor, is an effective chemopreventive agent against rat experimental liver fibrosis1. Gastroenterology 125:556-571.
159. Yang, J. D., S. Y. Seol, S. H. Leem, Y. H. Kim, Z. Sun, J. S. Lee, S. S. Thorgeirsson, I. S. Chu, L. R. Roberts, and K. J. Kang. 2011. Genes associated with recurrence of hepatocellular carcinoma: integrated analysis by gene expression and methylation profiling. Journal of Korean medical science 26:1428-1438.
160. Yin, H., L. Cheng, R. Langenbach, and C. Ju. 2007. Prostaglandin I(2) and E(2) mediate the protective effects of cyclooxygenase-2 in a mouse model of immune-mediated liver injury. Hepatology 45:159-169.
161. Young, L. E., and D. A. Dixon. 2010. Posttranscriptional Regulation of Cyclooxygenase 2 Expression in Colorectal Cancer. Current colorectal cancer reports 6:60-67.

162. Yu, J., A. Y. Hui, E. S. Chu, A. S. Cheng, M. Y. Go, H. L. Chan, W. K. Leung, K. F. Cheung, A. K. Ching, Y. L. Chui, K. K. Chan, and J. J. Sung. 2007. Expression of a cyclo-oxygenase-2 transgene in murine liver causes hepatitis. Gut 56:991-999.
163. Yu, J., C. W. Wu, E. S. Chu, A. Y. Hui, A. S. Cheng, M. Y. Go, A. K. Ching, Y. L. Chui, H. L. Chan, and J. J. Sung. 2008. Elucidation of the role of COX-2 in liver fibrogenesis using transgenic mice. Biochemical and biophysical research communications 372:571-577.
164. Yue, X., F. Yang, Y. Yang, Y. Mu, W. Sun, W. Li, D. Xu, J. Wu, and Y. Zhu. 2011. Induction of cyclooxygenase-2 expression by hepatitis B virus depends on demethylation-associated recruitment of transcription factors to the promoter. Virology journal 8:118.
165. Zeini, M., S. Hortelano, P. G. Traves, P. Martin-Sanz, and L. Bosca. 2004. Simultaneous abrogation of NOS-2 and COX-2 activities is lethal in partially hepatectomised mice. Journal of hepatology 40:926-933.
166. Zhang, X. F., X. Tan, G. Zeng, A. Misse, S. Singh, Y. Kim, J. E. Klaunig, and S. P. Monga. 2010. Conditional beta-catenin loss in mice promotes chemical hepatocarcinogenesis: role of oxidative stress and platelet-derived growth factor receptor alpha/phosphoinositide 3-kinase signaling. Hepatology 52:954-965.
167. Zhao, Q. T., S. Q. Yue, Z. Cui, Q. Wang, X. Cui, H. H. Zhai, L. H. Zhang, and K. F. Dou. 2007. Potential involvement of the cyclooxygenase-2 pathway in hepatocellular carcinoma-associated angiogenesis. Life sciences 80:484-492.

Anexo

THE JOURNAL OF BIOLOGICAL CHEMISTRY VOL. 285, NO. 6, pp. 3633–3642, February 5, 2010

Impairment of Transforming Growth Factor β Signaling in Caveolin-1-deficient Hepatocytes

*ROLE IN LIVER REGENERATION**

Received for publication, October 5, 2009, and in revised form, December 4, 2009 Published, JBC Papers in Press, December 5, 2009, DOI 10.1074/jbc.M109.072900

Rafael Mayoral[‡§], Ángela M. Valverde[‡¶], Cristina Llorente Izquierdo[‡], Águeda González-Rodríguez[‡¶], Lisardo Boscá[‡§], and Paloma Martín-Sanz[‡§1]

From the [‡]Instituto de Investigaciones Biomédicas "Alberto Sols," Consejo Superior de Investigaciones Científicas, Arturo Duperier 4, 28029 Madrid, the [§]Centro de Investigación Biomédica en Red de Enfermedades Hepáticas y Digestivas, Villarroel 170, 08036 Barcelona, and the [¶]Centro de Investigación Biomédica en Red de Diabetes y Enfermedades Metabólicas Asociadas, Mallorca 183, 08036 Barcelona, Spain

Caveolin-1 (Cav-1) is the main structural protein of caveolae and plays an important role in various cellular processes such as vesicular transport, cholesterol homeostasis, and signal transduction pathways. The expression and functional role of Cav-1 have been reported in liver and in hepatocyte cell lines, in human cirrhotic liver, and in hepatocellular carcinomas. Previous studies demonstrated that Cav-1 was dispensable for liver regeneration, because Cav-1$^{-/-}$ animals survived and fully regenerated liver function and size after partial hepatectomy. In this study, we have investigated the mechanisms by which the lack of Cav-1 accelerates liver regeneration after partial hepatectomy. The data show that transforming growth factor β (TGF-β) signaling is impaired in regenerating liver of Cav-1$^{-/-}$ mice and in hepatocytes derived from these animals. TGF-β receptors I and II do not colocalize in the same membrane fraction in the hepatocytes derived from Cav-1$^{-/-}$ mice, as Smad2/3 signaling decreased in the absence of Cav-1 at the time that the transcriptional corepressor SnoN accumulates. Accordingly, the expression of TGF-β target genes, such as plasminogen activator inhibitor-1, is decreased due to the presence of the high levels of SnoN. Moreover, hepatocyte growth factor inhibited TGF-β signaling in the absence of Cav-1 by increasing SnoN expression. Taken together, these data might help to unravel why Cav-1-deficient mice exhibit an accelerated liver regeneration after partial hepatectomy and add new insights on the molecular mechanisms controlling the initial commitment to hepatocyte proliferation.

Caveolae are non-clathrin, flask-shaped invaginations of the plasma membrane enriched in sphingolipids, cholesterol, and caveolin, a multifunctional scaffolding protein (1). Three Cavs[2] have been identified in differentiated cells with specific patterns of distribution. Cav-1 and -2 are found in adipocytes and endothelial cells, whereas Cav-3 is selectively expressed in muscle cells (2). Although caveolae participate in many cellular processes, including vesicular transport, cholesterol homeostasis, regulation of signal transduction, integrin signaling, and cancer-associated cell growth (3–7), it is rather surprising that all Cav-null mice are viable, including the complete caveolae-less mouse. However, the combined loss of Cav-1 and -3 has profound effects on the cardiovascular function (2). Cav-1 is a potent inhibitor of proliferative pathways, such as the Ras-p42/p44 MAPK cascades (8), and Cav-1 expression negatively regulates cell cycle progression via p53/p21-dependent pathway (9).

In liver and in different hepatocyte cell lines, the internalization of specific ligands through caveolae has been reported (10). Indeed, changes in the expression of Cav-1 in human cirrhotic liver, HCC, and in hepatoma cells and in regenerating liver have been described (11–15). Cav-1 increases in liver after PH. However, regarding the function of Cav-1 in liver regeneration, our data indicate that animals lacking Cav-1 restore liver mass to the same extent as the wild-type counterparts but with an accelerated hepatocyte proliferation after PH (16).

Although many cytokines are involved in the onset of liver regeneration, TGF-β participates in growth arrest once the liver has gained its appropriate functional mass (17). Interestingly, TGF-β is up-regulated during the early regenerative response to PH (18); however, during regeneration, hepatocytes become refractory to TGF-β signals, and the liver grows despite its presence (19). TGF-β signaling occurs when TGF-β binds to and assembles type I and type II serine/threonine kinase receptors (TβRs). TβR-II phosphorylates TβR-I, and this phosphorylation is both essential and sufficient for TGF-β signaling. The activated TβR-I then phosphorylates and acti-

* This work was supported by Grants SAF2007-60551 and BFU2008-02161 from MICINN, S-BIO-0283/2006 from Comunidad de Madrid, and FIS-RECAVA RD06/0014/0025. Red temática Enfermedades Cardiovasculares, Centro de Investigación Biomédica en Red de Enfermedades Hepáticas y Digestivas, and Centro de Investigación Biomédica en Red de Diabetes y Enfermedades Metabólicas Asociadas are funded by the Instituto de Salud Carlos III.

[1] To whom correspondence should be addressed: Instituto de Investigaciones Biomédicas Alberto Sols, Consejo Superior de Investigaciones Científicas, Arturo Duperier 4, 28029 Madrid, Spain. Tel.: 34914972746; Fax: 34914972748; E-mail: pmartins@iib.uam.es.

[2] The abbreviations used are: Cav, caveolin; Cav-1$^{-/-}$, caveolin-deficient mice; TGF-β, transforming growth factor β; PH, partial hepatectomy; TβR, TGF-β receptor; SnoN, Ski-related novel protein; HGF, hepatocyte growth factor; DRM, detergent-resistant membrane; MES, 4-morpholineethanesulfonic acid; Ab, antibody; NCL, immortalized neonatal cell line; PAI-1, plasminogen activator inhibitor-1; NDRM, nondetergent-resistant membrane; RT, reverse transcription; FBS, fetal bovine serum; CHAPS, 3-[(3-cholamidopropyl)dimethylammonio]-1-propanesulfonic acid; siRNA, small interfering RNA; GFP, green fluorescent protein; qPCR, quantitative PCR; CHL, Chang liver; HCC, hepatocellular carcinoma.

vates Smad2/3, which form oligomers with Smad4 that translocate to the nucleus to regulate the expression of target genes (20). The *ski/snon* family of proto-oncogenes has been shown to inhibit TGF-β/Smad signaling by disrupting heteromeric Smad complexes and blocking recruitment of coactivators. Both Ski and SnoN are highly expressed in cancer cell lines and repress the growth inhibitory function of the Smads (21). In regenerating liver, the induction of SnoN/Ski might explain the hepatocyte resistance to TGF-β signaling during the proliferative phase (22).

It is known that TβRs localize to caveolae; however, the functional consequences differ depending on the receptor and the cell type (23–25). Indeed, it has been recently proposed that TβR endocytosis via clathrin-coated pit-dependent internalization promotes TGF-β signaling; in contrast, the lipid raft-caveolar internalization pathway facilitates the degradation of TGF-β receptors (26). In view of these data, we have investigated the mechanisms by which the lack of Cav-1 accelerated liver regeneration after PH. Our results show that the TGF-β pathway is attenuated in hepatocytes derived from Cav-$1^{-/-}$ mice. We also demonstrated that TβR-I and -II colocalize with Cav-1 in the caveolar fraction, that Smad2/3 signaling decreases in the absence of Cav-1, and that significant up-regulation of the Smad transcriptional corepressor SnoN occurs. Moreover, HGF inhibits TGF-β signaling in the absence of Cav-1 by increasing SnoN expression. These mechanisms might explain why Cav-$1^{-/-}$ mice exhibit an accelerated liver regeneration after PH and provide a model of pathophysiological alteration of the hepatocyte response to TGF-β.

EXPERIMENTAL PROCEDURES

Chemicals—Antibodies were from Santa Cruz Biotechnology (Santa Cruz, CA), BD Transduction Laboratories, Cell Signaling (Boston, MA), Upstate (Upstate Biotechnology, Inc., Lake Placid, NY), Abcam (Cambridge, UK), and Invitrogen. TGF-β1 and other reagents were from Roche Applied Science or Sigma. siRNA-SnoN and scrambled sequences were from Santa Cruz Biotechnology. Tissue culture dishes were from Falcon (Lincoln Park, NJ). Tissue culture media were from BioWhittaker (Walkersville, MD).

Animals—C57BL/6J Cav-$1^{+/+}$ (The Jackson Laboratory, Bar Harbor, ME) and Cav-1 knock-out mice (cav-$1^{-/-}$, strain Cav-1^{tm1Mls}/J, genetic background 129/Sv, C57BL/6J, and SJL) aged 2 months (20–25 g) were cared for by following Institutional Care Instructions (Bioethical Commission from Consejo Superior de Investigaciones Científicas) and underwent 70% PH as described (16).

Isolation and Immortalization of Neonatal Hepatocytes—Pools of 4–6 livers from Cav-$1^{+/+}$ and Cav-$1^{-/-}$ neonates (3–5 days old) were submitted to collagenase dispersion for the isolation of hepatocytes and preparation of primary cultures as described previously (27). To obtain immortalized neonatal cell lines (NCLs), viral BOSC 23 packaging cells were transfected at 70% confluence with 3 μg/6-cm dish of the puromycin-resistance retroviral vector pBabe encoding SV40 large T antigen as described previously (28). Primary neonatal hepatocytes were infected at 60% confluence with Polybrene-supplemented virus (4 μg/ml) for 48 h and maintained in culture medium for 72 h before selection with puromycin (0.5–1 μg/ml) for 1 week. Pools of infected cells, rather than individual clones, were selected to avoid potential clone-to-clone variations. Immortalized cell lines were further cultured for at least 2 weeks with arginine-free medium supplemented with 10% FBS and ornithine to avoid growth of nonparenchymal cells.

Cell Culture, Transient and Stable Cell Transfections, and Treatments—Cell lines were grown in Dulbecco's modified Eagle's medium supplemented with 10% (v/v) FBS and antibiotics (50 μg/ml each of penicillin, streptomycin, and gentamicin) at 37 °C in a humidified 5% CO_2 atmosphere. THLE-2 (derived from normal liver), CCL-13 (Chang liver, CHL), and HepG2 cells were purchased from the ATCC, and the hepatoma cell line HuH-7 (JCRB0403) was purchased from Health Science Research Resources Bank (Osaka, Japan). For transient transfections assays, HuH-7 or NCL cells at 60% of confluence were exposed for 12 h to FuGENE-6 (Roche Applied Science) containing pEGF-N1 (encoding Cav-1-WT-GFP or GFP) (16) and 3TP-lux (luciferase reporter gene that contains the activin/TGFβ-responsive promoter element) (29) vectors following the manufacturer's instructions. For stable transfections, HuH-7 cells at 50% of confluence were exposed for 24 h to FuGENE-6 containing Cav-1-GFP expression vector or GFP control vector. The cells that express Cav-1-GFP or GFP were fluorescence-activated cell sorter-subcloned, and subsequent cultures of selected cells were grown in the presence of G418. At 18 h before experiments, the culture medium was replaced with fresh medium containing 1% (v/v) FBS. Luciferase activity was measured using the luciferase assay system (Promega, Madison, WI).

Isolation of Low Density, Triton-insoluble Caveolae-enriched Fractions—Isolation of caveolin-enriched membrane fractions (detergent-resistant membrane, DRMs) was done using a Triton X-100-based method (16). The samples were ultracentrifuged at 200,000 × *g* for 18–20 h at 4 °C in an SW60Ti rotor. Twelve fractions of 0.375 ml were collected from the top of the gradient after the centrifugation and mixed 1:1 with cold acetone for 4 h at −20 °C. The precipitated proteins were centrifuged at 16,000 × *g* for 10 min and dried. The resulting pellets were resuspended in 25 mM MES buffer, pH 6.5, and stored at −20 °C.

Protein Analysis—Total extracts were prepared from Cav-$1^{+/+}$ and Cav-$1^{-/-}$ remnant liver (50 mg) after PH or cells ($2–3 \times 10^6$) at different times. Samples were homogenized in a medium containing 10 mM Tris/HCl, pH 7.5, 1 mM $MgCl_2$, 1 mM EGTA, 10% (v/v) glycerol, 0.5% (w/v) CHAPS, 1 mM β-mercaptoethanol, 0.1 mM phenylmethylsulfonyl fluoride, Protease Inhibitor Mixture (Sigma) and Phosphatase Inhibitor Mixture 1 and 2 (Sigma). The extracts were vortexed for 30 min at 4 °C, and after centrifuging for 20 min at 13,000 × *g*, the supernatants were stored at −20 °C. For cytosolic extracts, NCL Cav-$1^{+/+}$ and NCL Cav-$1^{-/-}$ cells ($2–3 \times 10^6$) were harvested into ice-cold phosphate-buffered saline, resuspended in ice-cold buffer A (10 mM HEPES, pH 7.9, 10 mM KCl, 0.1 mM EDTA, 0.1 mM EGTA, 1 mM dithiothreitol), and left to swell on ice for 15 min.

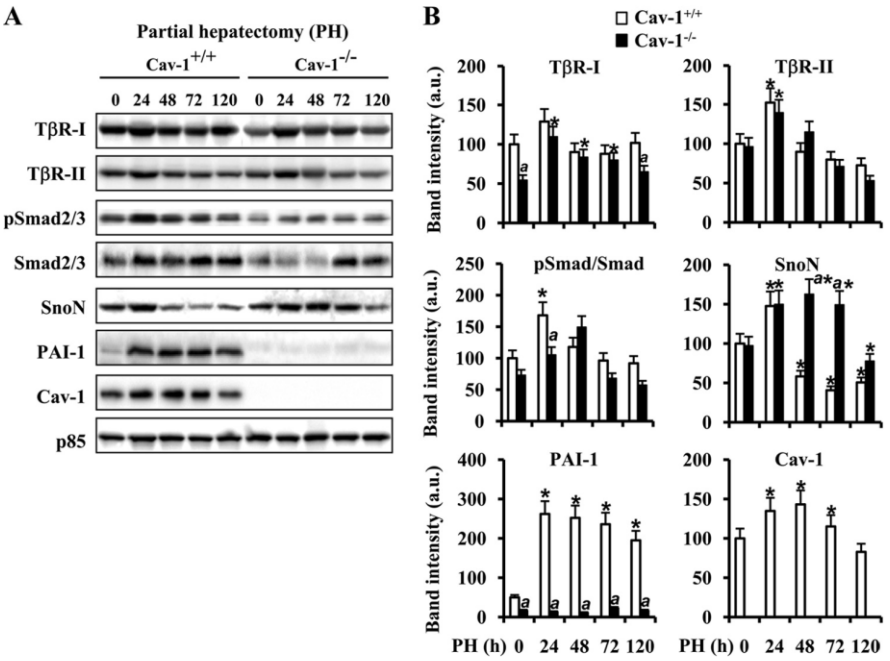

FIGURE 1. **Cav-1 and TGF-β-signaling molecule expression in regenerating liver after PH.** Total tissue extracts were prepared from Cav-1$^{+/+}$ and Cav-1$^{-/-}$ remnant liver after PH at different times. *A*, protein levels of TβR-I and -II, total and pSmad2/3, Cav-1, SnoN, and PAI-1 were determined by Western blot. Representative blots are shown. *B*, densitometric analysis of the immunoblots. Data are presented as the means ± S.D. of five independent experiments (animals). *, $p < 0.01$ *versus* the corresponding value at 0 time. ^{a}, $p < 0.01$ *versus* the corresponding value at the indicated time in Cav-1$^{+/+}$ mice. Blots were normalized with p85 for total extracts.

Nonidet P-40 was added to 0.5%, and the cells were vortexed and centrifuged at 12,000 × *g* for 30 s. The supernatants (cytosolic fraction) were collected and maintained at −20 °C. The pellet (nuclear fraction) was resuspended in ice-cold buffer B (20 mM HEPES, pH 7.9, 0.4 M NaCl, 1 mM EDTA, 1 mM EGTA) and left on ice for 15 min with intermittent mixing, followed by centrifugation at 12,000 × *g* for 15 min at 4 °C. Equal amounts of protein (10–50 μg) from each extract or 50 μl of the fractions obtained from the gradient were size-fractionated in 8–12% SDS-PAGE, transferred to a HybondP membrane (GE Healthcare), and after blocking with 5% nonfat dry milk were incubated with the corresponding Abs. The amounts of Cav-1, GFP, pSmad2/3, Smad2/3, TβR-I, TβR-II, SnoN (sc-9141), PAI-1, c-Met, GM130, calregulin, annexin VI, 5′-nucleotidase, and p85 were determined using commercial Abs. After incubation with the corresponding anti-rabbit or anti-mouse horseradish peroxidase-conjugated secondary Ab, blots were developed by the ECL protocol (GE Healthcare). The blots were revealed, and different exposure times were used for each blot with a CCD camera in a luminescent image analyzer (Gel-Doc, Bio-Rad) to ensure the linearity of the band intensities.

RNA Isolation and RT-PCR Analysis—1 μg of total RNA, extracted with TRIzol reagent (Invitrogen), was reverse-transcribed using SuperScript™ III first-strand synthesis system following the indications of the manufacturer (Invitrogen). Real time PCR was conducted with SYBR Green (Applied Biosystems) on a MyiQ real time PCR system (Bio-Rad). The primers used were as follows: PAI-1, FP, 5′-CGGCAGATCCAAGATGCTATG-3′, and RP, 5′-GACCAGCTCTAGGTCCCGCT-3′; Cav-1, FP, 5′-AGCCCAACAACAAGGCCAT-3′, and RP, 5′-GCAATCACATCTTCAAAGTCAATCTT-3′; 36B4, FP, 5′-AGATGCAGCAGATCCGCAT-3′, and RP, 5′-GTTCTTGCCCATCAGCACC-3′; and for 18 S rRNA, FP 5′-GCAATTATTCCCCATGAACGA-3′, and RP, 5′-CAAAGGGCAGGGACTTAATCAA-3′. PCR thermocycling parameters were 94 °C for 3 min, 40 cycles of 94 °C for 20 s, 60 °C for 20 s, 72 °C 20 s, and a final cycle of 72 °C 5 min for qPCR and 95 °C for 10 min, 40 cycles of 95 °C for 15 s, and 60 °C for 1 min for semiquantitative RT-PCR. Each sample was run in duplicate and was normalized with the expression of 36B4 for qPCR or 18 S for semiquantitative RT-PCR. The fold induction was determined in a $\Delta\Delta Ct$-based fold change calculations (Relative Quantity (*RQ*) is $2\wedge-\Delta\Delta Ct$).

Data Analysis—Data are expressed as mean ± S.D. Statistical significance was estimated with Student's *t* test for unpaired observation. The results were considered significant at $p < 0.05$. Data were analyzed by SPSS for Windows statistical package version 9.0.1.

RESULTS

TGF-β/Smad Signaling Pathway Is Impaired in Cav-1-deficient Mice after PH—Despite the controversy on the requirement of Cav-1 for liver regeneration after PH, accelerated hepatocyte proliferation was observed in Cav-1-deficient mice, exhibiting a higher liver mass recovery at 80 h after PH (15, 16). To gain insight on this process, we focused on the early TGF-β signaling in regenerating liver. When the protein levels of the TGF-β signalosome, TβR-I, TβR-II, Smad2/3, SnoN, PAI-1, and Cav-1, were analyzed in liver samples from Cav-1$^{+/+}$ and Cav-1$^{-/-}$ mice after PH, TβR-I and TβR-II exhibited equivalent profiles of changes, except for the consistent observation of a 46% reduction in TβR-I in Cav-1$^{-/-}$ mice before PH (Fig. 1, *A* and *B*). However, the phosphorylation of Smad2/3 following TβR-I and TβR-II activation (20), which exhibits a significant increase at 24 h after PH in Cav-1$^{+/+}$ mice, showed a lesser modification at this time in Cav-1$^{-/-}$ mice. Moreover, the up-regulation of Smad2/3 was delayed up to 72 h after PH in Cav-1$^{-/-}$ animals. Regarding the levels of SnoN and PAI-1, two genes induced by TGF-β (30), SnoN levels increased transiently at 24 h after PH, returning to basal levels at 48 h. However, they remained overexpressed in Cav-1$^{-/-}$ mice livers up to 72 h. The levels of PAI-1, which inhibits the urokinase-type plasminogen activator/plasminogen and blocks the processing of pro-HGF into active HGF, increased significantly at 24 h after PH in Cav-1$^{+/+}$ mice, but the levels were almost undetectable up to

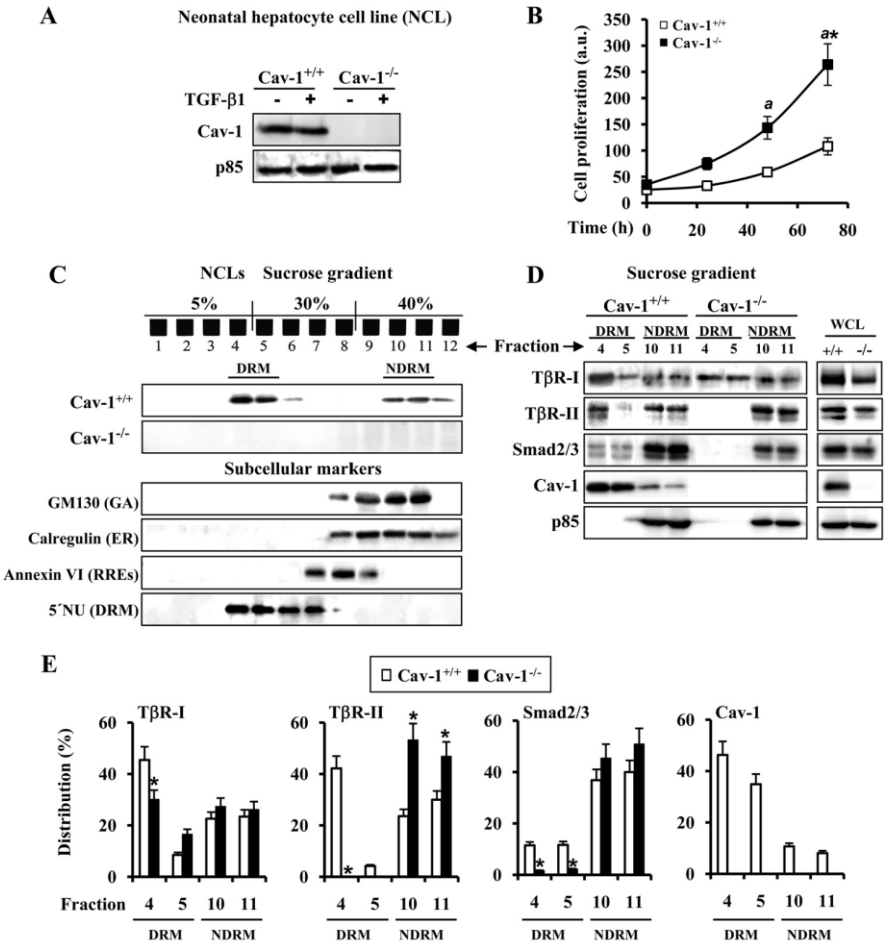

FIGURE 2. **TβR-I/TβR-II interaction is decreased in the absence of Cav-1.** *A*, protein levels of Cav-1 in NCL lines after treatment with 5 ng/ml TGF-β1 for 30 min. *B*, time-dependent proliferation of NCL Cav-$1^{+/+}$ and NCL Cav-$1^{-/-}$ cells. Cells were seeded in medium containing 10% (v/v) FBS and, after the indicated times in culture, were trypsinized, stained with trypan blue, and counted. *a.u.*, arbitrary units. *C*, sucrose discontinuous (5–30-40%) gradients were performed using a Triton X-100-based method to isolate DRM or NDRM fractions from the NCL cells as described under "Experimental Procedures." Cav-1 is mainly localized in the fractions 4–5 in NCL Cav-$1^{+/+}$ cells. GM130 (*GA*), calregulin (*ER*), annexin VI (*RREs*), and 5′-nucleotides (*5′NU*) (DRM) were used as subcellular markers. *D*, Western blot detection of TβR-I and II, Smad2/3, and Cav-1 in 50 μl from fractions 4 to 5 for DRM and fractions 10 to 11 for NDRM from NCL cells. Whole cell lysates (*WCL*) (50 μg) were used as reference for total content and blotted with the same Abs. *E*, quantification (%) of the distribution of the corresponding protein analyzed in *D*. The results are expressed as the band intensity of the protein in DRM (fractions 4 to 5) and NDRM (fractions 10 to 11) fractions with respect to the total protein levels. Representative blots are shown. Results are the means ± S.D. of four independent experiments. *, $p < 0.01$ *versus* the corresponding value at 0 time (*B*) or the corresponding value in NCL Cav-$1^{+/+}$ (*E*). ^{a}, $p < 0.01$ *versus* the corresponding value at the indicated time in NCL Cav-$1^{+/+}$. Blots were normalized with p85 for total extracts.

120 h after PH in Cav-$1^{-/-}$ mice. The changes in Cav-1, with an increase at 24–72 h, after PH were similar to those reported previously (16).

TβR-I/TβR-II Interaction Is Reduced in the Absence of Caveolae—Previous reports described that TβR-I, TβR-II, and Smad-2 cofractionate with Cav-1 in caveolae-enriched microdomains and that Cav-1 directly interacts with TβR-I (23). To better study TβRs-Cav-1 cross-signaling in liver, we generated hepatocyte cell lines (NCL) from neonatal liver of Cav-$1^{+/+}$ and Cav-$1^{-/-}$ mice. Cav-1 was found only in NCLs from Cav-$1^{+/+}$ mice (Fig. 2*A*), and interestingly, cell proliferation of NCL Cav-$1^{-/-}$ clones was always higher (2.5-fold) than the Cav-$1^{+/+}$ counterparts (Fig. 2*B*), in agreement with previous work using Cav-$1^{-/-}$ mouse embryo fibroblasts (9). As expected, Cav-1 was present mainly in DRMs and slightly in NDRM fractions of the discontinuous sucrose gradient (Fig. 2*C*). To identify the subcellular localization in which Cav-1 accumulates, we used different markers as follows: GM130 and calregulin for Golgi and endoplasmic reticulum, respectively, and annexin VI for recycling receptor endosomes and 5′-nucleotidase for the DRM fraction. As shown in Fig. 2*C*, fractions 4–6, in which Cav-1 is located, correspond mainly to the DRM fraction. Fig. 2, *D* and *E*, shows the protein levels and distribution of the TβRs in DRM and NDRM fractions of Cav-$1^{+/+}$ and Cav-$1^{-/-}$ NCL cells. Whereas the main accumulation of TβR-I in NCL Cav-$1^{+/+}$ cells was detected in the DRM fraction, this receptor was equally distributed between the DRM and NDRM fractions in NCL Cav-$1^{-/-}$. Moreover, TβR-II was undetectable in the DRM fraction of NCL Cav-$1^{-/-}$ cells. Smad2/3 were detected in the DRM fraction of NCL Cav-$1^{+/+}$, accumulating in both cell types in the NDRM fraction.

SnoN Accumulates in NCL Cav-$1^{-/-}$ Cells—To evaluate the contribution of Cav-1 to TβR signaling, NCL Cav-$1^{+/+}$ and Cav-$1^{-/-}$ cells were stimulated with TGF-β1, and the activation of Smad2/3 and the expression levels of PAI-1 and SnoN were determined in cytosolic and nuclear extracts. As Fig. 3, *A* and *B*, shows, Smad2/3 proteins were detected in both compartments, although the levels were higher in NCL Cav-$1^{+/+}$ cells. TGF-β1 treatment increased pSmad2/3 in the nucleus, and the phosphorylation was higher in NCL Cav-$1^{+/+}$ cells (Fig. 3, *B* and *D*). The cytosolic levels of PAI-1 increased significantly after 2 h of TGF-β1 treatment in NCL Cav-$1^{+/+}$ but were lower and TGF-β1-insensitive in Cav-$1^{-/-}$ cells. However, SnoN basal levels were significantly higher in NCL Cav-$1^{-/-}$ and were modulated by TGF-β1 in Cav-$1^{+/+}$ cells (Fig. 3*B*). Immunofluorescence analysis of SnoN showed a clear nuclear staining in NCL Cav-$1^{-/-}$, whereas in NCL Cav-$1^{+/+}$ the localization of SnoN was mainly cytoplasmic and lesser expressed (Fig. 3*C*).

Induction of PAI-1 by TGF-β1 Is Impaired in the Absence of Cav-1—To evaluate further the cross-regulation between Cav-1 and TGF-β signaling, NCL cells were transfected with a

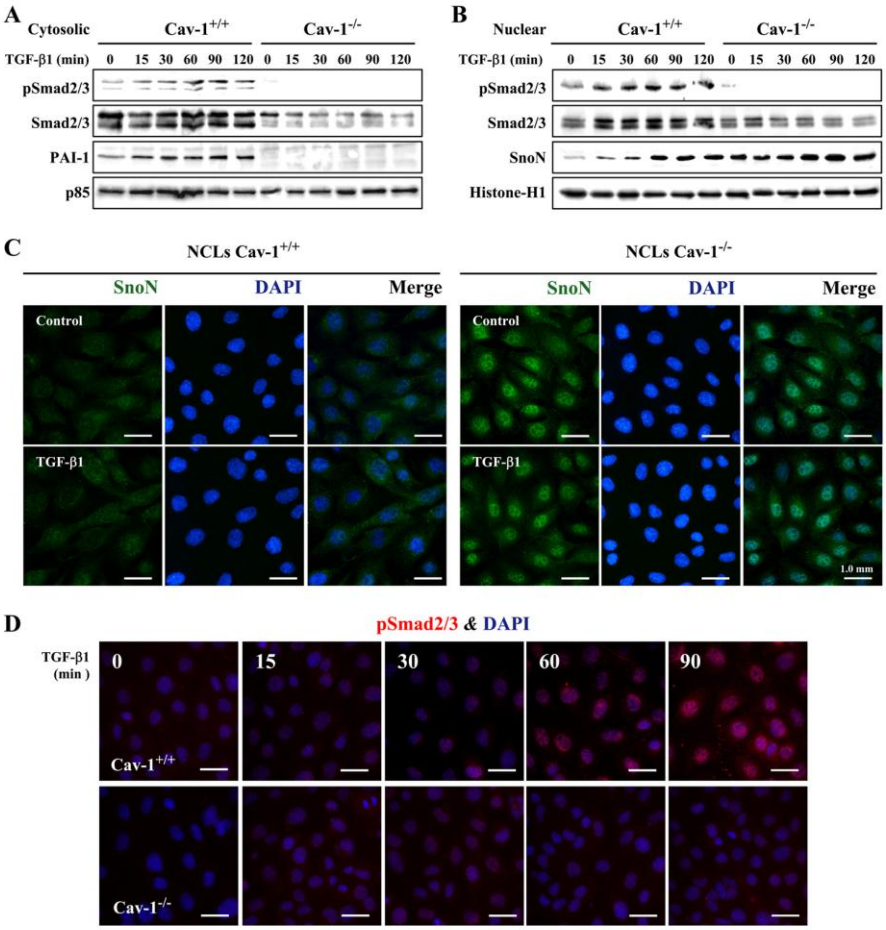

FIGURE 3. **SnoN accumulates in NCL Cav-1$^{-/-}$ cells.** NCL Cav-1$^{+/+}$ and NCL Cav-1$^{-/-}$ cells (2–3 × 10^6) were treated with 5 ng/ml TGF-β1 at the indicated times. Cytosolic (50 μg) (*A*) and nuclear extracts (10 μg) (*B*) were obtained, and protein levels of total and pSmad2/3, PAI-1, and SnoN were analyzed. A representative blot is shown. Blots were normalized with p85 for cytosolic extracts and with histone-H1 for nuclear extracts. *C*, immunofluorescence analysis of SnoN in NCL cells after 1 h of TGF-β1 stimulation. *DAPI*, 4′,6-diamidino-2-phenylindole. *D*, immunofluorescence analysis of pSmad2/3 in NCL cells after TGF-β1 stimulation at the indicated times. Neonatal Cav-1$^{+/+}$ or Cav-1$^{-/-}$ cells (5 × 10^4) were cultured in 24-multiwell plates on glass coverslips and maintained overnight with 1% FBS. After that period, the cells were fixed for 15 min with 4% paraformaldehyde, pH 7.2, washed with phosphate-buffered saline, and permeabilized with 1% Tween 20 in phosphate-buffered saline for 15 min at room temperature. After blocking with 3% bovine serum albumin for 1 h at room temperature, the cells were incubated 2 h with the corresponding Abs diluted 1:150 in 1% bovine serum albumin, washed several times, and incubated for 2 h with fluorochrome-conjugated Abs (Invitrogen) raised against Fc of primary Abs and treated with 4′,6-diamidino-2-phenylindole for 30 min at room temperature. The glass coverslips were mounting with Vectashield (Vector Laboratories, Burlingame, CA) on microscope slides. The images were acquired in a fluorescence Eclipse E400 microscope (Nikon).

TGF-β-responsive promoter (3TP-lux) and with a Cav-1-GFP expression vector (pEGFPN1). Upon TGF-β1 treatment, the activation of the 3TP-lux reporter was 3-fold lower in NCL Cav-1$^{-/-}$ compared with NCL Cav-1$^{+/+}$. When these cells were cotransfected with 3TP-lux and pEGFPN1-Cav-1 and stimulated with TGF-β1, the activation of 3TP-lux was reduced 50% in both cell lines, suggesting that the transient expression of Cav-1 was unable to restore TGF-β1 responsiveness probably due to the elevated levels of SnoN (Fig. 4*A*). Fig. 4*B* shows the expression of Cav-1 (20 kDa), Cav-1-GFP (50 kDa), and GFP (27 kDa) in NCL Cav-1$^{+/+}$ and Cav-1$^{-/-}$ as a control of the transfection extent. Fig. 4*C* shows that the induction of PAI-1 by TGF-β1 analyzed by qPCR was significantly lower in NCL Cav-1$^{-/-}$. From these results, we can suggest that Cav-1 is necessary for the correct signaling of TGF-β; however, and in agreement with previous data reporting Cav-1 as an inhibitor of TGF-β signaling in NIH-3T3 cells (23), the elevated transient expression of Cav-1 down-regulated TGF-β signaling.

To gain further insight into this differential response of the neonatal cells to TGF-β, we used a specific mouse TGF-β-signaling microarray to compare the expression profile in NCL cells after TGF-β1 treatment. Fig. 4, *D* and *E*, summarizes the fold up- or down-regulation of the 84 TGF-β-regulated genes analyzed. We sorted the candidate genes whose expression threshold after TGF-β1 treatment was altered more than 2-fold. The down-regulated genes in NCL Cav-1$^{-/-}$ are those implicated in TGF-β signaling (*i.e. acvrl1, inhba, inhbb, smad4, tgfbl1l*, and *tgfbr1*) or cell cycle (*cdkn1a*), and the majority of the up-regulated genes are implicated in proliferation (*amhr2, fst, igfbp3, il6, ltbp2, Myc*, and *nbl1*).

SnoN Protein Levels Are Increased in HCC Human Cells That Lack Cav-1 Expression—The absence of Cav-1 in well differentiated human HCC has been recently reported to be a specific signature of these cells (31). Accordingly, Cav-1 levels were analyzed in various hepatic cell lines, and although the hepatocyte-like THLE-2 or CHL cells showed a significant expression of Cav-1 mRNA and protein, the HCC lines, such as HepG2 or HuH-7, failed to express this gene (Fig. 5*A*). Moreover, in HuH-7 cells stably transfected with the pEGFPN1-Cav-1 expression vector, the high SnoN levels observed in the parental cells or after transfection with the GFP vector decreased in the presence of Cav-1 (Fig. 5, *B* and *C*). Analysis of TβR-I, TβR-II, pSmad2/3, Smad2/3, and SnoN in wild type or Cav-1-expressing HuH-7 cells stimulated with TGF-β1 showed similar levels of TβRs, although the phosphorylation of Smad2/3 was higher in HuH-7-Cav-1-expressing cells compared with HuH-7-WT cells (Fig. 5, *D* and *E*). When HuH-7-WT cells were transiently cotransfected with 3TP-lux and pEGFPN1-Cav-1 vectors and stimulated with TGF-β1, an inhibition of the activation of 3TP-lux was observed. Moreover, and in agreement with the data obtained with NCLs in Fig. 4*A*, HuH-7-Cav-1 cells showed a tendency to up-regulate luciferase activity *versus* HuH-7 parental cells (Fig. 5*F*).

Hepatocyte Proliferation Is Enhanced in the Absence of Cav-1

TGF-β and HGF Signaling Cooperate through SnoN Expression to Increase the Proliferation of Cav-1$^{-/-}$ Liver Cells after PH—HGF, a potent inducer of DNA synthesis and cell scatter in cultured hepatocytes, promotes the expression of SnoN (32). In addition to this, the interaction of Cav-1 with c-Met (HGF receptor) has been described (33). After PH, a 75% increase of c-Met at 24 h in Cav-1$^{-/-}$ mice was measured without noticeable changes in Cav-1$^{+/+}$ mice (Fig. 6*A*). This situation was partially reproduced in NCLs after HGF challenge (Fig. 6*B*). Moreover, when the levels of SnoN were determined in NCLs stimulated with HGF, a rise from almost negligible levels to a peak value at 4 h was observed in NCL Cav-1$^{+/+}$; however, NCL Cav-1$^{-/-}$ cells exhibited significant basal levels, reaching the same peak value at 1 h after HGF administration (Fig. 6*C*). The

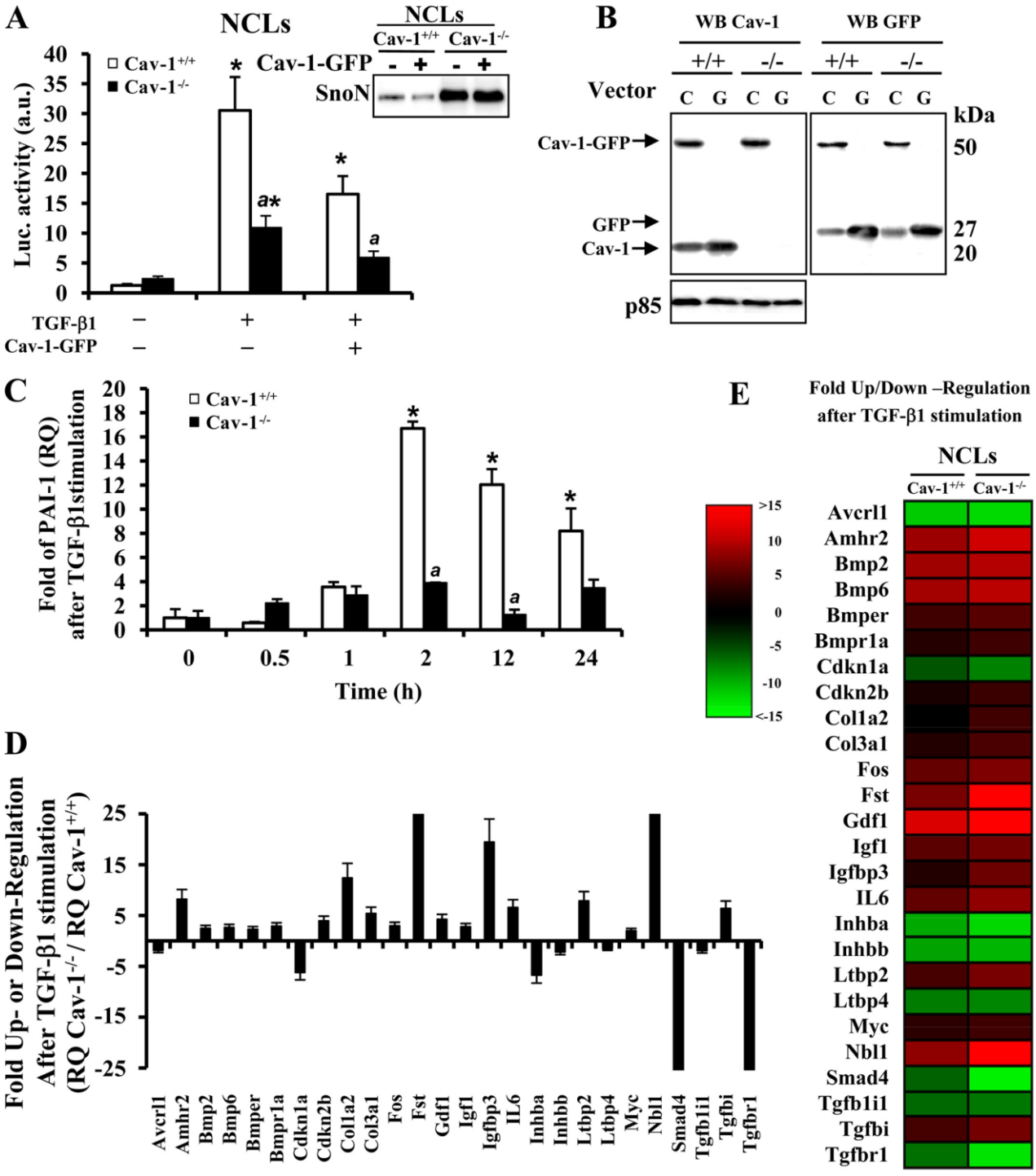

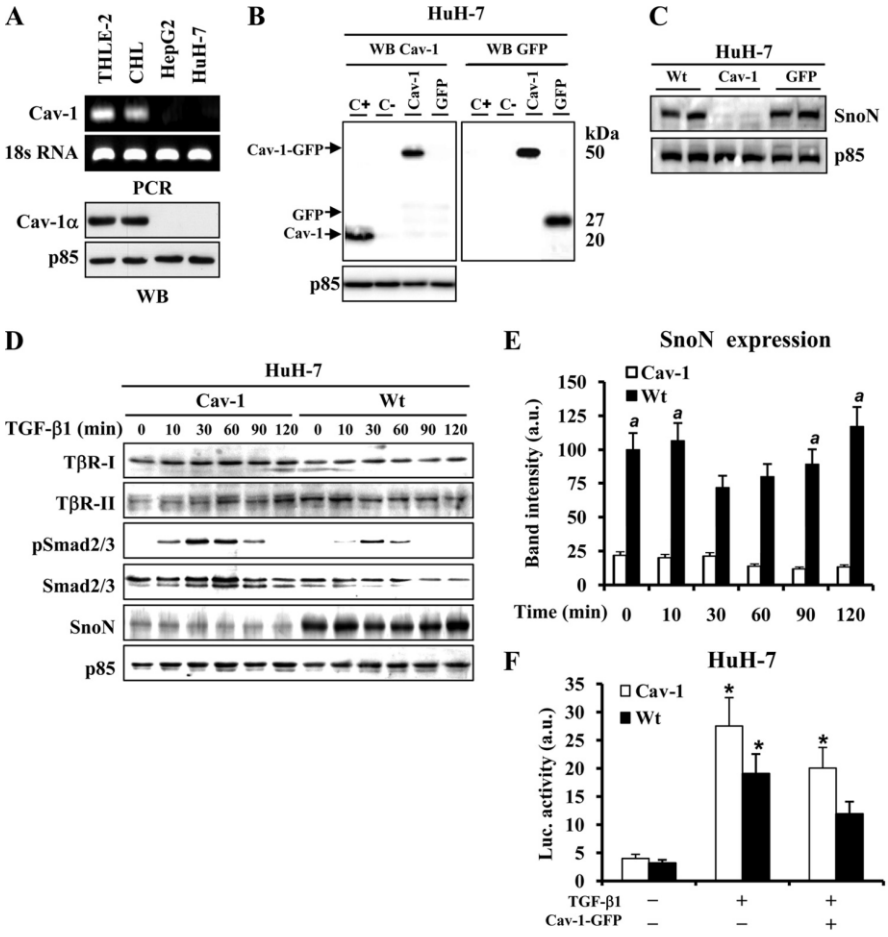

FIGURE 5. **SnoN expression is increased in HCC cells that lack Cav-1.** *A,* mRNA and protein levels of Cav-1 were determined by semiquantitative RT-PCR and Western blot (*WB*) in THLE-2, CHL, HepG2, and HuH-7 cells. *B,* HuH-7 cells were stably transfected with Cav-1-GFP expression vector or GFP control vector. The cells that express Cav-1-GFP or GFP were fluorescence-activated cell sorter-subcloned and selected in the presence of G418. Western blot analysis of the protein, Cav-1-GFP, GFP, or Cav-1, expressed after transfection with the pEGFPN1 vector as a control of the process (*C+*, CHL total extract; *C−*, HuH-7-WT total extract). *C,* SnoN expression in two different clones from HuH-7-WT, HuH-7-Cav-1, and HuH7-GFP cells. *D,* TGF-β-signaling molecules expression analyzed by Western blot in HuH-7-WT and HuH-7-Cav-1 cells after stimulation with TGF-β1 at the indicated times. *E,* densitometric analysis of SnoN protein levels from *D. a.u.,* arbitrary units. *F,* HuH-7-WT and HuH-7-Cav-1 cells were transfected with pEGF-N1 and 3TP-lux vectors as described in the legend from Fig. 4*A*. Results are the means ± S.D. of four independent experiments. *, $p < 0.01$ *versus* the corresponding unstimulated. [a], $p < 0.01$ *versus* the corresponding value at the same condition in HuH-7-Cav-1.

preceding data suggest that SnoN overexpression inhibits TGF-β signaling in the absence of Cav-1. As Fig. 6, *D* and *E*, shows, pretreatment of cells with a SnoN-specific siRNA increased PAI-1 gene expression in NCL Cav-$1^{-/-}$ cells. When the cells were treated with HGF, the expression of PAI-1 induced by TGF-β was partially abolished, and this was also counteracted after treatment of the cells with SnoN-siRNA. To establish a link between SnoN expression and cell proliferation, a cell counting experiment was performed after transfection of the cells with SnoN-siRNA and stimulation with TGF-β1. As Fig. 6*F* shows, TGF-β treatment inhibits cell proliferation by 40 and 20% after 72 h in NCL Cav-$1^{+/+}$ and NCL Cav-$1^{-/-}$ cells, respectively. In the presence of SnoN-siRNA, the inhibition of cell growth promoted by TGF-β1 in NCL Cav-$1^{-/-}$ cells increased up to 70% supporting a role for SnoN in NCL cell proliferation.

DISCUSSION

In this work, we have investigated the contribution of Cav-1 to early TGF-β signaling in regenerating liver after PH, aimed by the observation of an accelerated early commitment to hepatocyte growth in Cav-$1^{-/-}$ mice (16). The role of Cav-1 in the regulation of liver function and regeneration is not clear, and discrepancies exist regarding the requirement of Cav-1 for liver regeneration after PH (15, 16). Our results with hepatoma cell lines show that non-tumor cells and primary cultures of hepatocytes express significant amounts of Cav-1, whereas it was undetectable in the HepG2 and HuH-7 hepatoma cell lines. Besides regeneration and hepatocellular carcinogenesis, recent work proposed a new role for Cav-1 in liver function; in mouse

FIGURE 4. **TGF-β-responsive promoter and PAI-1 expression are impaired in the absence of Cav-1.** *A,* NCL Cav-$1^{+/+}$ and NCL Cav-$1^{-/-}$ cells were transfected with pEGFN1 (encoding wild-type Cav-1-GFP or GFP) and with the 3TP-Lux vectors with FuGENE-6 (Roche Applied Science) for 12 h. After 24 h of transfection, cells were treated with TGF-β1 for 12 h, and the luciferase (*Luc.*) activity was measured by using the luciferase assay system. *Inset,* SnoN expression in NCL cells after transfection with Cav-1-GFP vector. *a.u.*, arbitrary units. *B,* Western blot (*WB*) analysis of the protein, Cav-1-GFP, GFP, or Cav-1, expressed after transfection with the pEGFPN1 vector as a control of the process (*C,* Cav-1; *G,* GFP). *C,* 1 μg of total RNA, extracted with TRIzol reagent (Invitrogen), was reverse-transcribed using SuperScript™ III first-strand synthesis system for RT-PCR. Real time PCR of PAI-1 mRNA was conducted with SYBR Green on a MyiQ real time PCR system, after treatment of the cells with 5 ng/ml TGF-β1 for the indicated times. Results were normalized with the 36B4 expression and were expressed as relative quantity (*RQ*) ($2^{-\Delta\Delta Ct}$). *D,* after the stimulation of the NCL cells with TGF-β1 (5 ng/ml) for 90 min, RNA (2 μg) was used for cDNA synthesis with RT[2] first standard kit (SuperArray Bioscience, Frederick, MD). The mouse TGF-β/BMP signaling pathway PCR array was performed according to the manufacturer's protocol, using the Profiler PCR array system and the SYBR Green/fluorescein qPCR master mix (SuperArray Bioscience) on a MyiQ real time PCR system (Bio-Rad). Gene expression was compared with the web-based software package for the PCR array system; this software automatically performs all $\Delta\Delta Ct$-based fold-change calculations from the specific uploaded raw threshold cycle data. *E,* colorimetric diagram with a selection of the 84 TGF-β signaling related genes analyzed. Genes whose transcription is up/down (*red/green*) 2-fold in gene expression threshold in NCL Cav-$1^{+/+}$ and NCL Cav-$1^{-/-}$ cells are shown. All results presented are the means ± S.D. of four independent experiments. *, $p < 0.01$ *versus* the corresponding unstimulated condition. [a], $p < 0.01$ *versus* the corresponding value at the same condition in NCL Cav-$1^{+/+}$.

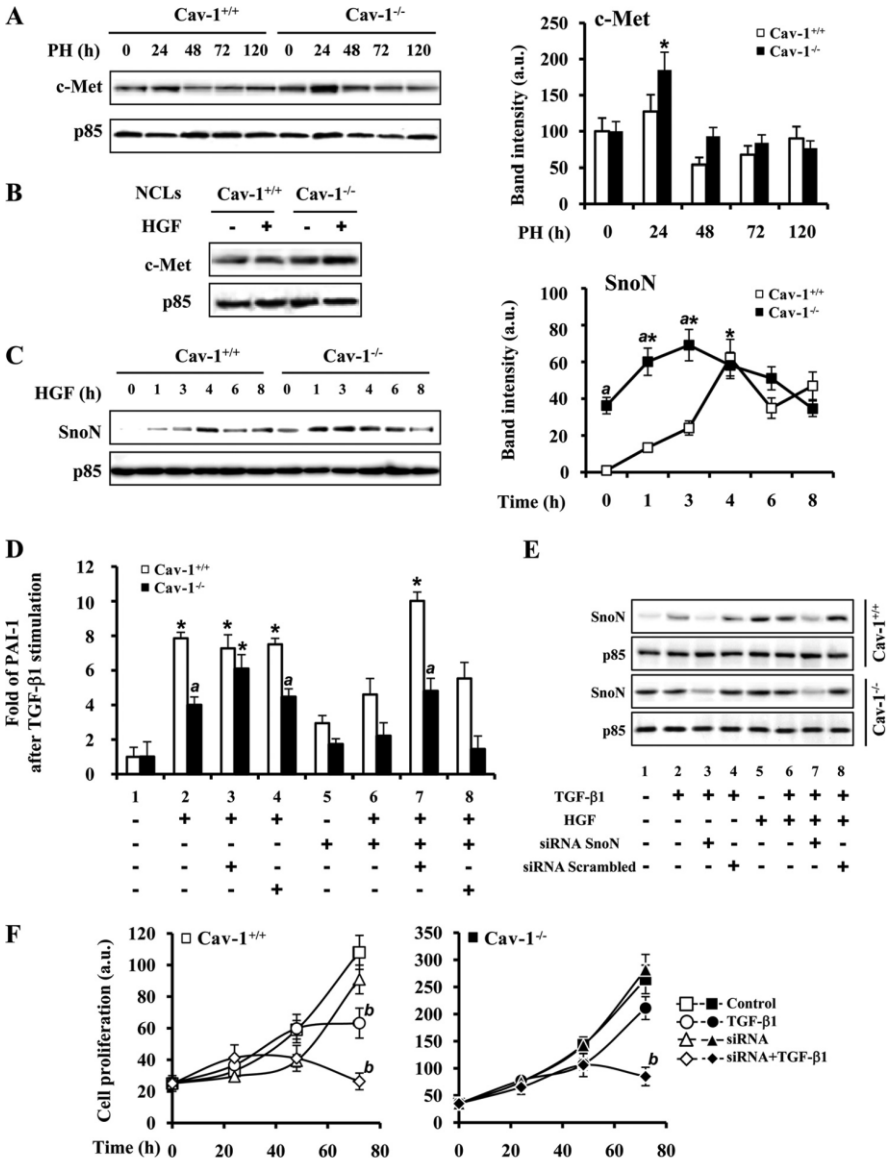

FIGURE 6. **TGF-β and HGF signaling cooperate through SnoN expression to increase the proliferation of Cav-1$^{-/-}$ liver cells after PH.** *A*, representative Western blot and the quantification of c-Met protein levels in total liver extracts from Cav-1$^{+/+}$ and Cav-1$^{-/-}$ mice after PH. *B*, c-Met protein levels in NCL Cav-1$^{+/+}$ and NCL Cav-1$^{-/-}$ cells after treatment with 25 ng/ml HGF for 2 h. *C*, induction of SnoN protein expression by treatment of the NCL cells with HGF for the indicated times. A representative Western blot and a densitometric analysis of the results are shown. *D*, mRNA PAI-1 levels were measured by qPCR after inhibition of SnoN expression with a specific siRNA or treatment with a scrambled control siRNA. NCL Cav-1$^{+/+}$ and NCL Cav-1$^{-/-}$ cells were transfected during 6 h with 20 pmol of SnoN siRNA by using Lipofectamine 2000 (Invitrogen) according to manufacturer's instructions before TGF-β1 (5 ng/ml) and HGF (25 ng/ml) stimulation for 90 min. *E*, after transfection of the cells with siRNA and extraction of the mRNA with TRIzol used in *D*, SnoN protein levels were obtained from organic phase of the TRIzol extraction and analyzed by Western blot. *F*, 48 h after siRNA transfection, 10 × 10^3 cells were seeded in a 24-multiwell plate and treated with TGF-β1 (5 ng/ml). The cells were trypsinized, stained with trypan blue, and counted at the indicated times. Results are the means ± S.D. of four independent experiments. *, $p < 0.01$ *versus* the corresponding value at 0 time (*C*) or the corresponding unstimulated data (*D*). [a], $p < 0.01$ *versus* the corresponding value at the indicated time (*C*) or stimulated data in NCL Cav-1$^{+/+}$ (*D*). [b], $p < 0.01$ *versus* the corresponding untreated data at 72 h (*F*). Blots were normalized with p85 for total extracts. *a.u.*, arbitrary units.

hepatoma cells, Cav-1 expression positively correlated with cell transformation and invasiveness via the activation of the Survivin-mediated pathway (34), and in HepG2 cells Cav-1 negatively regulated the apoptosis induced by tumor necrosis factor-related apoptosis-inducing ligand through the internalization of its receptor DR4, which is localized in caveolae (13).

Although many cytokines and growth factors are involved in the onset of liver regeneration, TGF-β has been proposed as an important regulatory factor controlling cell proliferation and death through the transcriptional regulation of cell cycle inhibitors and activators (17); however, sometimes cells become refractory to TGF-β signaling and can proliferate even in the presence of this cytokine. Several groups and our data show an up-regulation of the TβRs during liver regeneration between 24 and 48 h after PH (18). TβRs localize to caveolae although the functional consequences of their activation differ depending on the receptor and the cell type considered, even suppressing TGF-β-mediated signaling in some cases. For instance, Cav-1 interacts with TβR-I and suppresses TGF-β-mediated phosphorylation of Smad2 and subsequent downstream events in NIH-3T3 and in other fibroblast types (23, 35); however, in human endothelial cells, Cav-1 cooperates with ALK1 as a key mediator of the TGF-β pathway in angiogenesis (25). Our data show no differences in TβR-II expression in Cav-1$^{+/+}$ and Cav-1$^{-/-}$ mice after PH; however, TβR-I levels, although up-regulated after PH, were always reduced in the absence of Cav-1. Moreover, TβR-I and -II do not colocalize in the same membrane fraction in the hepatocytes derived from Cav-1$^{-/-}$ mice. A common model for the TβRs/caveolae interaction proposes that caveolae are involved in receptor degradation, whereas Smad signaling occurs through clathrin-dependent processes (36, 37).

We have used the following three different approaches to analyze the cross-regulation between Cav-1 and the TGF-β signaling pathway: liver regeneration after PH in Cav-1-deficient mice; neonatal hepatocyte cell lines derived from these animals (NCLs); and human hepatoma cell lines lacking Cav-1. In a coherent way, the data support the conclusion that the TGF-β signaling pathway is

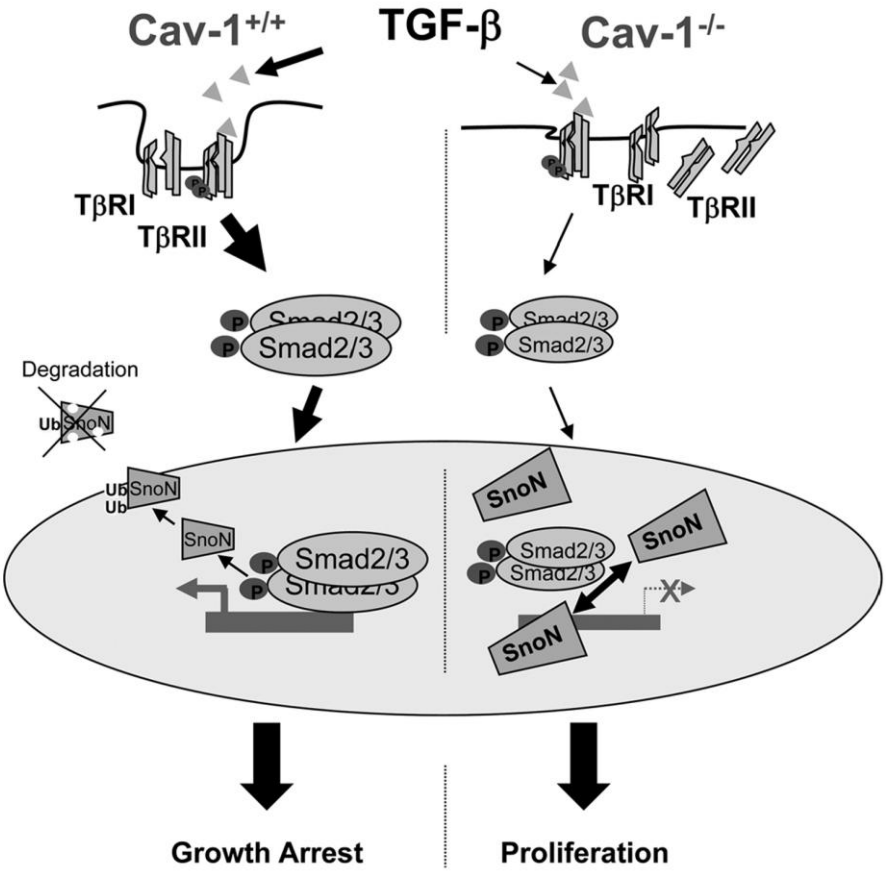

FIGURE 7. **TGF-β signaling in Cav-1-deficient hepatocytes.** In the absence of Cav-1, TβRs delocalize between the membrane and the cytoplasm, leading to a TGF-β-deficient signaling. Lesser activated Smad2/3 translocates to the nucleus, and the higher levels of SnoN impair the transcription of growth-arrest genes and enhance hepatocyte proliferation in the process of liver regeneration. In the presence of Cav-1, TGF-β signaling is sufficient to maintain the balance between cell proliferation and cell growth arrest characteristic of regenerating liver.

impaired in the absence of Cav-1 implicating different levels as follows: (*a*) TβR-I is less abundant in liver from Cav-1$^{-/-}$ mice; (*b*) as expected, both TβR-I and TβR-II do not colocalize in the DRM fraction in the Cav-1$^{-/-}$ NCL; (*c*) total and phosphorylated Smad2/3 proteins are decreased in Cav-1$^{-/-}$ liver, Cav-1$^{-/-}$ NCL, and HuH-7 cells; (*d*) the activity of a Smad2/3-dependent promoter is decreased in Cav-1$^{-/-}$ NCL and in the HuH7 hepatoma cells compared with Cav-1$^{+/+}$ NCL and the HuH7 cells stably transfected with an expression vector for Cav-1; (*e*) the expression of TGF-β target genes, such as PAI-1, is decreased both at the mRNA and protein levels, in the absence of Cav-1; (*f*) good correlation exists between the absence of Cav-1, the decrease in the Smad 2/3 signaling, and the increase of the corepressor SnoN levels in liver from Cav-1$^{-/-}$ mice after PH, in Cav-1$^{-/-}$ NCL cells, and HuH-7 cells. To gain further insight into this differential response of the neonatal cells to TGF-β, we used a specific mouse TGF-β-signaling microarray to compare the expression profile in NCLs cells after TGF-β1 treatment. The down-regulated genes in NCL Cav-1$^{-/-}$ are those implicated in TGF-β signaling or cell cycle.

The induction of TGF-β pathway inhibitors, for example the induction of Smad6 and -7, is one of the mechanisms used by tumor cells to overcome the TGF-β restriction (38). In addition to this, other inhibitors, such as the transcriptional repressors TGIF, Ski, and SnoN, allow cell proliferation by blocking Smad activity (39). Ski and SnoN are members of the Ski proto-oncogene family (40). Elevated levels of Ski or SnoN have been detected in many human tumor cell lines, and SnoN has been proposed as a prognostic marker in breast carcinoma (41). In addition to the up-regulation of Ski or SnoN expression, mislocalization may also contribute to malignant progression. SnoN is localized exclusively in the nucleus in cancer tissues, whereas in normal tissues and nontumorigenic cells, SnoN is predominantly cytoplasmic (42). The mechanism of transformation by Ski and SnoN was not defined until diverse studies converged on the conclusion that Ski/SnoN bind directly to the Smad3/4 complex and negatively regulate TGF-β signaling (39). Longerich *et al.* (43) did not detect mutations or significant pro-tumorigenic expression changes of the *snon* and *ski* genes in human hepatocellular carcinomas; however, it was found that both were induced during liver regeneration/proliferation and recruited activated Smad proteins. It is known that SnoN protein levels were increased in the early stages of liver regeneration, whereas Ski was induced at later time points (22). In the absence of Cav-1 in the three models used, Cav-1$^{-/-}$ mice, NCLs, and the HuH7 cells, SnoN is increased, and surprisingly, when Cav-1 is overexpressed SnoN levels did not change, although the TGF-β-dependent luciferase reporter activity is reduced. It has been reported that overexpression of Cav-1 is sufficient to disrupt Smad3 phosphorylation and translocation to the nucleus and consequently TGF-β signaling (23, 35). In this unphysiological situation, SnoN levels are irrelevant because the pathway is impaired at a very upstream level. In addition to this, the subcellular distribution of SnoN between the nucleus and the cytoplasm might be altered and post-translational modifications of SnoN, yet uncovered, cannot be disregarded upon Cav-1 ectopic expression. Our data show that the absence of Cav-1 is related with an increase in SnoN expression and with cell proliferation both in the *in vivo* model of liver regeneration after PH and in liver cells. According to these data, a schematic representation of TGF-β signaling in Cav-1-deficient hepatocytes is proposed in Fig. 7. In the absence of Cav-1, TβRs, mainly TβRII, delocalize between the membrane and the cytoplasm, leading to a TGF-β-deficient signaling. Lesser acti-

vated Smad2/3 translocates to the nucleus, and the higher levels of SnoN impair the transcription of growth-arrest genes and enhance hepatocyte proliferation in the process of liver regeneration. In the presence of Cav-1, TGF-β signaling is sufficient to maintain the balance between cell proliferation and cell growth arrest characteristic of regenerating liver.

Classic studies in liver regeneration and fibrotic processes have found that HGF specifically counteracts many anti-proliferative and pro-fibrotic actions of TGF-β, suggesting that the balance between HGF and TGF-β might play a pivotal role in the pathogenesis of liver and kidney diseases (17, 44). HGF and TGF-β are induced after PH and tissue injury, suggesting that both are important for the initial wound-healing response and tissue repair. In transient injuries, HGF signaling will predominate resulting in tissue repair and regeneration. In this scenario, TGF-β is important for matrix remodeling, but also for counteracting HGF activity after recovery. In chronic kidney diseases, HGF abolished TGF-β signaling by inducing SnoN in tubular epithelial cells (44). In this regard, the elevated expression of SnoN in the absence of Cav-1 was potentiated by HGF and may be related with the accumulation of c-Met. In summary, in this work we proposed a new cross-talk between TGF-β and HGF signaling and Cav-1 expression during liver regeneration. This cross-talk converges in the Smad transcriptional corepressor, SnoN, which impairs the growth-arrest pathway of TGF-β and thereby might explain why Cav-1$^{-/-}$ mice exhibit an accelerated liver regeneration after PH.

Acknowledgment—We thank Dr. M. A. del Pozo for the vectors encoding WT Cav-1-GFP and GFP.

REFERENCES

1. Yamada, E. (1955) *J. Biophys. Biochem. Cytol.* **1**, 445–458
2. Razani, B., Woodman, S. E., and Lisanti, M. P. (2002) *Pharmacol. Rev.* **54**, 431–467
3. Schnitzer, J. E. (2001) *Adv. Drug Delivery Rev.* **49**, 265–280
4. Fu, Y., Hoang, A., Escher, G., Parton, R. G., Krozowski, Z., and Sviridov, D. (2004) *J. Biol. Chem.* **279**, 14140–14146
5. Okamoto, T., Schlegel, A., Scherer, P. E., and Lisanti, M. P. (1998) *J. Biol. Chem.* **273**, 5419–5422
6. del Pozo, M. A., Balasubramanian, N., Alderson, N. B., Kiosses, W. B., Grande-García, A., Anderson, R. G., and Schwartz, M. A. (2005) *Nat. Cell Biol.* **7**, 901–908
7. Williams, T. M., and Lisanti, M. P. (2005) *Am. J. Physiol. Cell Physiol.* **288**, C494–C506
8. Engelman, J. A., Zhang, X. L., Razani, B., Pestell, R. G., and Lisanti, M. P. (1999) *J. Biol. Chem.* **274**, 32333–32341
9. Galbiati, F., Volonté, D., Liu, J., Capozza, F., Frank, P. G., Zhu, L., Pestell, R. G., and Lisanti, M. P. (2001) *Mol. Biol. Cell* **12**, 2229–2244
10. Calvo, M., Tebar, F., Lopez-Iglesias, C., and Enrich, C. (2001) *Hepatology* **33**, 1259–1269
11. Yokomori, H., Oda, M., Ogi, M., Sakai, K., and Ishii, H. (2002) *Liver* **22**, 150–158
12. Yerian, L. M., Anders, R. A., Tretiakova, M., and Hart, J. (2004) *Am. J. Surg. Pathol.* **28**, 357–364
13. Zhao, X., Liu, Y., Ma, Q., Wang, X., Jin, H., Mehrpour, M., and Chen, Q. (2009) *Biochem. Biophys. Res. Commun.* **378**, 21–26
14. Pol, A., Martin, S., Fernandez, M. A., Ferguson, C., Carozzi, A., Luetterforst, R., Enrich, C., and Parton, R. G. (2004) *Mol. Biol. Cell* **15**, 99–110
15. Fernández, M. A., Albor, C., Ingelmo-Torres, M., Nixon, S. J., Ferguson, C., Kurzchalia, T., Tebar, F., Enrich, C., Parton, R. G., and Pol, A. (2006) *Science* **313**, 1628–1632
16. Mayoral, R., Fernández-Martínez, A., Roy, R., Boscá, L., and Martín-Sanz, P. (2007) *Hepatology* **46**, 813–822
17. Michalopoulos, G. K. (2007) *J. Cell. Physiol.* **213**, 286–300
18. Nishikawa, Y., Wang, M., and Carr, B. I. (1998) *J. Cell. Physiol.* **176**, 612–623
19. Bouzahzah, B., Fu, M., Iavarone, A., Factor, V. M., Thorgeirsson, S. S., and Pestell, R. G. (2000) *Cancer Res.* **60**, 4531–4537
20. Massagué, J., Seoane, J., and Wotton, D. (2005) *Genes Dev.* **19**, 2783–2810
21. Le Scolan, E., Zhu, Q., Wang, L., Bandyopadhyay, A., Javelaud, D., Mauviel, A., Sun, L., and Luo, K. (2008) *Cancer Res.* **68**, 3277–3285
22. Macias-Silva, M., Li, W., Leu, J. I., Crissey, M. A., and Taub, R. (2002) *J. Biol. Chem.* **277**, 28483–28490
23. Razani, B., Zhang, X. L., Bitzer, M., von Gersdorff, G., Böttinger, E. P., and Lisanti, M. P. (2001) *J. Biol. Chem.* **276**, 6727–6738
24. Lee, E. K., Lee, Y. S., Han, I. O., and Park, S. H. (2007) *Biochem. Biophys. Res. Commun.* **359**, 385–390
25. Santibanez, J. F., Blanco, F. J., Garrido-Martin, E. M., Sanz-Rodriguez, F., del Pozo, M. A., and Bernabeu, C. (2008) *Cardiovasc. Res.* **77**, 791–799
26. Chen, Y. G. (2009) *Cell Res.* **19**, 58–70
27. Martín-Sanz, P., Callejas, N. A., Casado, M., Díaz-Guerra, M. J., and Boscá, L. (1998) *Br. J. Pharmacol.* **125**, 1313–1319
28. Valverde, A. M., Burks, D. J., Fabregat, I., Fisher, T. L., Carretero, J., White, M. F., and Benito, M. (2003) *Diabetes* **52**, 2239–2248
29. Wrana, J. L., Attisano, L., Cárcamo, J., Zentella, A., Doody, J., Laiho, M., Wang, X. F., and Massagué, J. (1992) *Cell* **71**, 1003–1014
30. Zhu, Q., Pearson-White, S., and Luo, K. (2005) *Mol. Cell. Biol.* **25**, 10731–10744
31. Cokakli, M., Erdal, E., Nart, D., Yilmaz, F., Sagol, O., Kilic, M., Karademir, S., and Atabey, N. (2009) *BMC Cancer* **9**, 65
32. Tan, R., Zhang, X., Yang, J., Li, Y., and Liu, Y. (2007) *J. Am. Soc. Nephrol.* **18**, 2340–2349
33. Cantiani, L., Manara, M. C., Zucchini, C., De Sanctis, P., Zuntini, M., Valvassori, L., Serra, M., Olivero, M., Di Renzo, M. F., Colombo, M. P., Picci, P., and Scotlandi, K. (2007) *Cancer Res.* **67**, 7675–7685
34. Wang, S., Jia, L., Zhou, H., Wang, X., and Zhang, J. (2008) *IUBMB Life* **60**, 693–699
35. Kim, S., Lee, Y., Seo, J. E., Cho, K. H., and Chung, I. H. (2008) *Cell. Signal.* **20**, 1313–1319
36. Di Guglielmo, G. M., Le Roy, C., Goodfellow, A. F., and Wrana, J. L. (2003) *Nat. Cell Biol.* **5**, 410–421
37. Deheuninck, J., and Luo, K. (2009) *Cell Res.* **19**, 47–57
38. Heldin, C. H., Miyazono, K., and ten Dijke, P. (1997) *Nature* **390**, 465–471
39. Seoane, J. (2006) *Carcinogenesis* **27**, 2148–2156
40. Stavnezer, E., Barkas, A. E., Brennan, L. A., Brodeur, D., and Li, Y. (1986) *J. Virol.* **57**, 1073–1083
41. Zhang, F., Lundin, M., Ristimäki, A., Heikkilä, P., Lundin, J., Isola, J., Joensuu, H., and Laiho, M. (2003) *Cancer Res.* **63**, 5005–5010
42. Krakowski, A. R., Laboureau, J., Mauviel, A., Bissell, M. J., and Luo, K. (2005) *Proc. Natl. Acad. Sci. U.S.A.* **102**, 12437–12442
43. Longerich, T., Breuhahn, K., Odenthal, M., Petmecky, K., and Schirmacher, P. (2004) *Virchows Arch.* **445**, 589–596
44. Liu, Y. (2004) *Am. J. Physiol. Renal Physiol.* **287**, F7–F16

OPEN ACCESS Freely available online

PLOS ONE

Cyclooxygenase-2 Is a Target of MicroRNA-16 in Human Hepatoma Cells

Noelia Agra Andrieu[1], Omar Motiño[1], Rafael Mayoral[1,2], Cristina Llorente Izquierdo[1], Ana Fernández-Alvarez[3], Lisardo Boscá[1,2], Marta Casado[2,3], Paloma Martín-Sanz[1,2]*

1 Instituto de Investigaciones Biomédicas Alberto Sols, (Centro Mixto Consejo Superior de Investigaciones Científicas-Universidad Autónoma de Madrid, CSIC-UAM), Madrid, Spain, **2** Centro de Investigación Biomédica en Red de Enfermedades Hepáticas y Digestivas (CIBERehd), Barcelona, Spain, **3** Instituto de Biomedicina de Valencia del Consejo Superior de Investigaciones Científicas (IBV-CSIC), Valencia, Spain

Abstract

Cyclooxygenase-2 (COX-2) expression has been detected in human hepatoma cell lines and in human hepatocellular carcinoma (HCC); however, the contribution of COX-2 to the development of HCC remains controversial. COX-2 expression is higher in the non-tumoral tissue and inversely correlates with the differentiation grade of the tumor. COX-2 expression depends on the interplay between different cellular pathways involving both transcriptional and post-transcriptional regulation. The aim of this work was to assess whether COX-2 could be regulated by microRNAs in human hepatoma cell lines and in human HCC specimens since these molecules contribute to the regulation of genes implicated in cell growth and differentiation. Our results show that miR-16 silences COX-2 expression in hepatoma cells by two mechanisms: a) by binding directly to the microRNA response element (MRE) in the COX-2 3′-UTR promoting translational suppression of COX-2 mRNA; b) by decreasing the levels of the RNA-binding protein Human Antigen R (HuR). Furthermore, ectopic expression of miR-16 inhibits cell proliferation, promotes cell apoptosis and suppresses the ability of hepatoma cells to develop tumors in nude mice, partially through targeting COX-2. Moreover a reduced miR-16 expression tends to correlate to high levels of COX-2 protein in liver from patients affected by HCC. Our data show an important role for miR-16 as a post-transcriptional regulator of COX-2 in HCC and suggest the potential therapeutic application of miR-16 in those HCC with a high COX-2 expression.

Citation: Agra Andrieu N, Motiño O, Mayoral R, Llorente Izquierdo C, Fernández-Alvarez A, et al. (2012) Cyclooxygenase-2 Is a Target of MicroRNA-16 in Human Hepatoma Cells. PLoS ONE 7(11): e50935. doi:10.1371/journal.pone.0050935

Editor: Rafael Aldabe, Centro de Investigación en Medicina Aplicada (CIMA), Spain

Received June 21, 2012; **Accepted** October 26, 2012; **Published** November 30, 2012

Funding: This work was supported by Ministry of Science and Innovation [SAF2010-16037, SAF2009-12602 and BFU2011-24760] and by Comunidad de Madrid [P2010/BMD-2378]. The funders had no role in study design, data collection and analysis, decision to publish, or preparation of the manuscript.

Competing Interests: The authors have declared that no competing interests exist.

* E-mail: pmartins@iib.uam.es

Introduction

Hepatocellular carcinoma (HCC) is the fifth most common cancer worldwide and has an increasing incidence in western countries [1]. Although the risk factors for HCC are well characterized, the molecular pathogenesis of this tumor type is not well understood [2,3], and thus the identification of new possible targets for the development of non-conventional treatments is urgent and must be improved.

Cyclooxygenase-1 (COX-1) and -2 catalyze the first step in prostanoid biosynthesis. COX-1 is constitutively expressed in many tissues, whereas COX-2 is induced by a variety of stimuli such as growth factors, pro-inflammatory stimuli, hormones and other cellular stresses [4]. Adult hepatocytes fail to induce COX-2 expression regardless of the pro-inflammatory factors used [5,6]. However, our group and others demonstrated that partial hepatectomy (PH) [7,8] induced COX-2 in hepatocytes and contributed to the progression of cell cycle after PH. In addition to liver regeneration after PH or hepatotoxic agents, expression of COX-2 has been detected in animal models of cirrhosis [9], in human hepatoma cell lines [10,11], in human HCC [12] and after HBV and HCV infection [13,14].

COX-2 is widely regarded as a potential pharmacological target for preventing and treating inflammatory and cancer diseases. Therapeutic strategies have focused primarily on selective inhibitors of COX-2 activity; however, considerable less attention has been paid to identifying anticancer agents that suppress the expression of COX-2 [15]. COX-2 overexpression is the result of the activation of many intracellular pathways that regulate COX-2 both at transcriptional and post-transcriptional level. The 5′-UTR of the COX-2 gene contains binding sites for numerous regulatory transcription factors including two NF-κB (nuclear factor κB) motifs, two AP-1 (activator protein 1) sites and two CREs (cAMP-response elements) among others [16]. However, the regulation of the expression of COX-2 is more complex including modifications of genomic DNA and chromatin and at the post-transcriptional level via targeting its 3′-UTR [17]. The 3′-UTR of COX-2 contains multiple copies of AU-rich elements (AREs) and microRNA response element (MRE) motifs which, when bound by specific ARE-binding factors or miRNAs, influence COX-2 stability and translational efficiency [17].

MicroRNAs (miRNAs) are short single-stranded non-coding RNAs that influence post-transcriptional gene regulation by affecting mRNA stability and/or translational repression of their target mRNAs [18]. Alterations of the expression pattern of

miRNAs that regulate genes involved in cellular proliferation, differentiation or apoptosis, have been found in different human tumors including HCC [19,20], suggesting that they may represent a novel class of oncogenes or tumor suppressor genes. Moreover, recent reports of profound phenotypic abnormalities in miRNA-knockout models further demonstrate their crucial roles as regulators of gene expression [21]. Regarding COX-2, Dey's group [22,23] highlighted a miRNA-mediated regulation of COX-2 by mmu-miR-101a and mmu-miR-199a* during embryo implantation and in endometrial cancer cells. Recent works have reported that miR-101 downregulation is involved in COX-2 overexpression in human colon cancer cells (CRC) [24], miRNA-26b regulates the expression of COX-2 in desferrioxamine-treated carcinoma of nasopharyngeal epithelial cells [25] and binding of miR-16 to AREs of TNF-α, IL-6, IL-9 and COX-2 mRNA transcripts could promote their degradation [20,26].

Besides miRNAs, various cytoplasmic proteins have been reported to bind the COX-2 3′UTR [20]. As an example, the RNA-binding protein CUGBP2 interacts directly with specific AREs within the first 60 nucleotides of the COX-2 3′-UTR and that binding stabilizes the COX-2 mRNA yet inhibits its translation [27]; tristetrapolin binds to COX-2 3′UTR and decrease mRNA levels in colon cancer [28], whereas Human Antigen R (HuR) is a translational enhancer of COX-2 in ovarian carcinoma [29] and in colon carcinogenesis [20].

To our knowledge, no data is available concerning the post-transcriptional regulation of COX-2 by miRNAs and RNA-binding proteins in HCC. Our results show that miR-16 silences COX-2 expression in hepatoma cells by two mechanisms: by binding directly to the MRE motif in the COX-2 3′-UTR and by decreasing the levels of HuR. miRNA-16 is able to inhibit cell proliferation, to promote cell apoptosis and to suppress the ability of WRL68 hepatoma cell line to develop tumors in nude mice partially through targeting COX-2 expression. Moreover a reduced miR-16 expression tends to correlate to high levels of COX-2 protein in liver from patients affected by HCC. Our data suggest an important role for miR-16 in HCC and implicate the potential therapeutic application of miR-16 in those HCC with a high COX-2 expression.

Materials and Methods

Chemicals

Antibodies were from Santa Cruz Laboratories (Santa Cruz, CA, USA), Sigma Chemical Co. (St. Louis, MO, USA), Cell Signaling (Boston, MA, USA), Abcam (Cambridge, UK) and Cayman Chemical (Ann Arbor, MI, USA). Prostaglandin E_2 (PGE_2) was from Cayman Chemical. Reagents were from Roche Diagnostics (Mannheim, Germany) or Sigma Chemical Co. Reagents for electrophoresis were obtained from Bio-Rad (Hercules, CA, USA). Tissue culture dishes were from Falcon (Becton Dickinson Labware, Franklin Lakes, NJ, USA). Tissue culture media were from Gibco (Invitrogen™, Grand Island, NY, USA).

Patients

Seven individual tumoral and paired non-tumoral HCC human samples were obtained from de Spanish Tumor Bank Network of the Centro Nacional de Investigaciones Oncológicas (CNIO). Institutional review board approval (N°PI. CEI PI 20_2011) was obtained for these studies from Comité de la Investigación y de Bienestar Animal of CNIO and all participants provided written informed consent. Tissues were evaluated by pathologists by means of hematoxylin/eosin staining. Tissue was snap-frozen in liquid nitrogen and total RNA and protein were isolated as described below.

Cell Culture

The cell lines WRL68, HepG2 and Hep3B were purchased from the American Type Culture Collection, ATCC (Manassas, VA, US). All these cells lines were authenticated by ATCC and were expanded twice, and stored in liquid N_2. Expansions from these clones were used up to 6 months in culture. PLC/PRF/5 [30] was kindly provided by Dr. C Perret (Institut Cochin, CNRS UMR8104, University Paris-Descartes, Paris, France) and HuH-7 [31] by Dr. M. Kern (Department of General Pathology, University Hospital Heidelberg, Heidelberg, Germany). WRL68 was derived from human liver embryo. HepG2, Hep3B and HuH-7 are well differentiated hepatocellular carcinoma cell lines and PLC/PRF/5 is a malignant liver cancer with HBsAg positive cell line. Cells were grown on Falcon tissue culture dishes in EMEM or DMEM supplemented with 10% FBS and antibiotics (50 μg each of penicillin, streptomycin and gentamicin per ml) at 37°C in a humidified air 5% CO_2 atmosphere. Human hepatocytes were from HPCH10 CryostaX™, Single-freeze Cryopreserved Pooled Human Hepatocytes (Xenotech, Lenexa, KA, USA).

RNA Extraction and Quantitative Real-time PCR Analysis

Total RNA from HCC cells or human biopsies was extracted by using TRIzol reagent (Invitrogen, Grand Island, NY, USA). RNA (1 μg) was reverse transcribed using a Transcriptor First Strand cDNA Synthesis Kit following manufacturer's indications (Roche Applied Science). For quantification of mature miRNAs, total RNA was extracted using the miRNeasy Mini Kit (Qiagen, Valencia, CA, USA). RNA (500 ng) was polyadenylated and reverse- transcribed to cDNA using the NCode™ miRNA first-strand cDNA synthesis kit (Invitrogen) in accordance with the manufacturers instructions. The cDNA was used as template for real-time PCR through Taqman probes. Primers for COX-2 (Hs00153133-m1) and 36b4 (Hs99999902-m1) were from Applied Biosystems (Carlsbad, CA, USA). Real-time PCR was performed using a MyiQ detection system (Bio-Rad) and thermocycling parameters were 95°C for 10 min, 50 cycles of 95°C for 15 s followed for 60°C for 1 min and finally 95°C for 1 min. Each sample was run in triplicate and was normalized to 36b4 mRNA. The replicates were then averaged, and fold induction was determined in a ΔΔCt based fold-change calculations.

Levels of miRNAs were quantified using the FastStart Universal SYBR Green Master (Roche) with the universal reverse primer provided in the kit and the following forward primers; hsa-miR-16: 5′- TAGCAGCACGTAAATATTGGCG -3′; hsa-miR-26b: 5′-CGCTTCAAGTAATTCAGGATAGGT -3′; hsa-miR-199a: 5′-CCCAGTGTTCAGACTACCTGTTC -3′; hsa-miR-101: 5′-CCGGTACAGTACTGTGATAACTGAA -3′; hsa-miR-21: 5′-CGGTAGCTTATCAGACTGATGTTGA -3′ and hsa-miR-122: 5′- TGGAGTGTGACAATGGTGTTT -3′. Thermocycling parameters were 95°C for 3 min and 40 cycles of 95°C for 15 s followed by 60°C for 30 sec. The expression of miRNAs was normalized against U6 snRNA levels (U6 primers: forward 5′-CTTCGGCAGCACATATACT -3′; reverse 5′- AAAATATG-GAACGCTTCACG -3′). Melting curve analysis was performed to confirm the specificity of the PCR products.

The miRNAs (miR-16, miR-26b, miR-101, miR-199a, miR-122 and miR-21) were selected by using miRWalk computational analyses, that covers miRNA-targets interactions information produced by 8 established miRNA prediction programs on 3' UTRs of all known genes of Human, Mouse and Rat, i.e., RNA22, miRanda, miRDB, TargetScan, RNAhybrid, PITA,

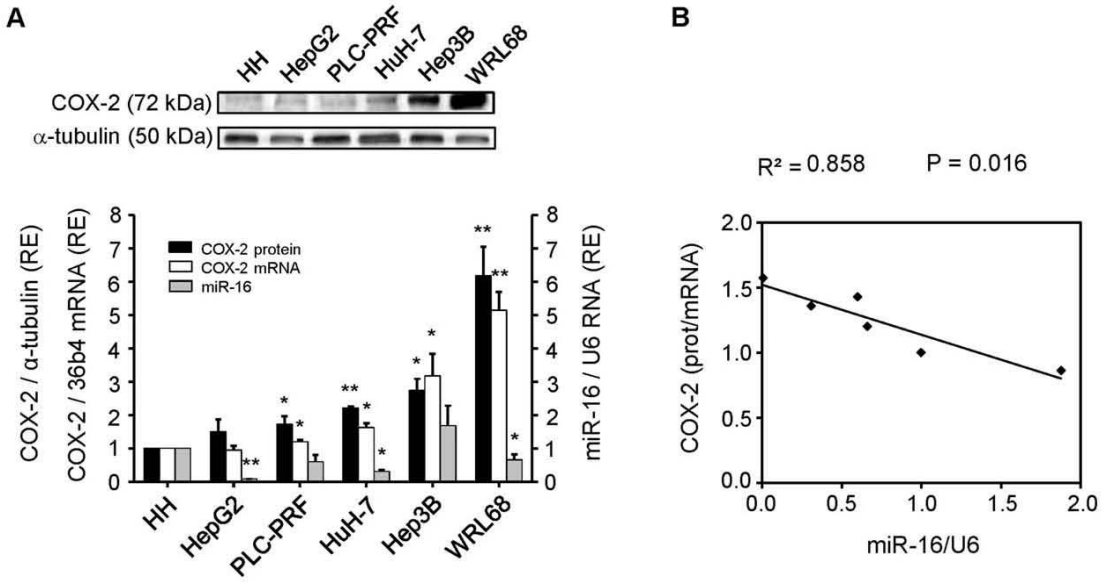

Figure 1. miR-16 and COX-2 correlate inversely in HCC cell lines. Cells were plated in 100-mm dishes and grown to 60–70% confluence in culture medium supplemented with 10% FBS. (**A**) Total cellular extracts were prepared from HCC cells and protein (30–50 µg/lane) was analyzed by Western blot. A representative Western blot showing COX-2 protein. The expression of target protein was normalized to that of α-tubulin. Densitometric analysis of COX-2 expression (black bars) is referring to HH as 1 and expressed as relative expression (RE). Total RNA was prepared from HCC cell lines and COX-2 mRNA was analyzed by real-time PCR. COX-2 mRNA amounts (white bars), normalized to the expression of 36b4 mRNA, and miR-16 expression (grey bars), normalized against U6 RNA levels, were calculated. Values represent fold change relative to human hepatocytes (HH) as 1. Data are reported as means±SD of three independent experiments. $^{**}p<0.01$ and $^{*}p< 0.05$ *vs.* the HH. (**B**) The inverse correlation between COX-2 protein/mRNA ratio and miR-16 expression in HCC cells is graphically depicted. The coefficient of determination (R^2) was calculated.
doi:10.1371/journal.pone.0050935.g001

Table 1. Expression of selected miRNAs is evaluated in HCC cell lines.

Cell Lines			
	miR-16 (R^2 = 0.86)	**miR-26b (R^2 = 0.43)**	**miR-101 (R^2 = 0.71)**
	p = 0.016	*p = 0.297*	*p = 0.018*
HH	1	1	1
HepG2	0.008±0.002	0.023±0.004	0.141±0.003
HuH-7	0.309±0.150	0.114±0.100	0.573±0.250
PLC-PRF	0.601±0.300	0.021.±0.015	0.383±0.800
WRL68	0,661±0.234	0.019±0.009	0.451±0.315
Hep3B	1.578±0.015	0.682±0.261	1.956±0.394
	miR-199a (R^2 = 0.49)	**miR-122 (R^2 = 0.03)**	**miR-21 (R^2 = 0.02)**
	p = 0.226	*p = 0.241*	*p = 0.919*
HH	1	1	1
HepG2	0.583±0.056	0.001±7.65E-05	1.501±0.121
HuH-7	1.084±0.430	0.028±0.005	1.558±0.313
PLC-PRF	0.702±0.359	0.004±1.91E-05	1.130±0.600
WRL68	0.479±0.171	0.001±6.32E-05	0.997±0.006
Hep3B	2.321±0.380	0.012±0.003	1.741±0.154

The miRNAs (miR-16, miR-26b, miR-101, miR-199a, miR-122 and miR-21) were selected by using miRWalk computational analysis as described in Methods. The expression profile was analyzed in HCC cell lines using real-time PCR, normalized against U6 RNA levels and refers to human hepatocytes (HH) as 1. COX-2 protein/mRNA ratio was compared to miRNAs expression in HCC cells and the coefficient of determination (R^2) was calculated.
doi:10.1371/journal.pone.0050935.t001

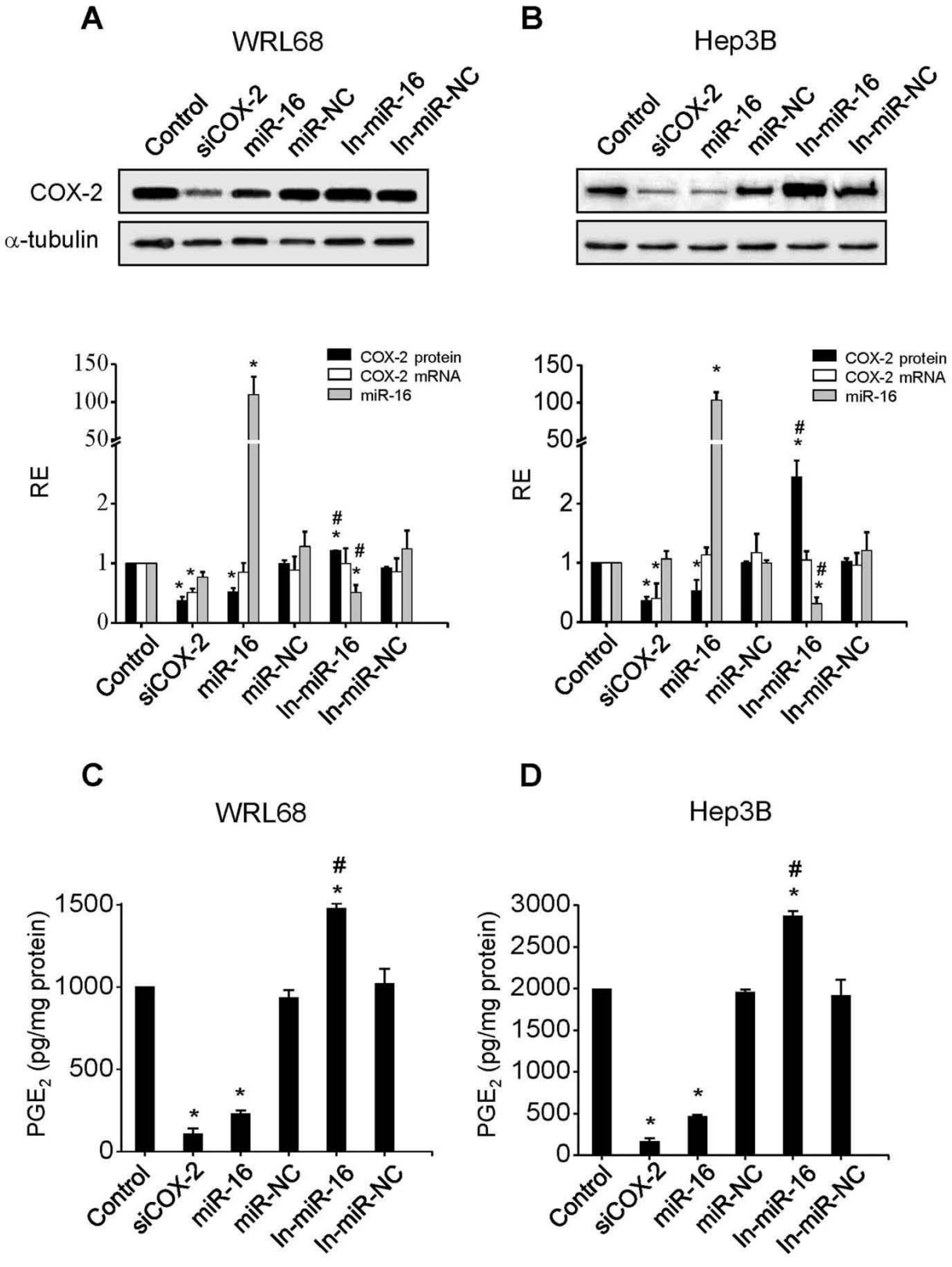
A
WRL68
Control
siCOX-2
miR-16
miR-NC
In-miR-16
In-miR-NC
COX-2
α-tubulin
B
Hep3B
Control
siCOX-2
miR-16
miR-NC
In-miR-16
In-miR-NC
COX-2 protein
COX-2 mRNA
miR-16
RE
150
100
50
2
1
0
C
WRL68
D
Hep3B
PGE2 (pg/mg protein)
1500
1000
500
3000
2500
2000

Figure 2. miR-16 regulates COX-2 expression in HCC cell lines. WRL68 and Hep3B cells were transfected with: 30 nM siRNA anti-COX2 (siCOX-2) or 50 nM of miR-16, miR-16 inhibitor (In-miR-16), miR negative control (miR-NC) or miR negative control inhibitor (In-miR-NC). (**A–B**) COX-2 protein was analyzed by Western blot 48 h after transfection and normalized against α-tubulin protein. COX-2 mRNA and miR-16 expression were analyzed by real-time PCR. COX-2 mRNA and miR-16 expression were normalized against 36b4 mRNA and U6 RNA levels, respectively. Relative expression of each sample refers to control as 1 (cells transfected only with lipofectamine). (**C–D**) PGE_2 concentration was determined by enzyme immunoassay in the supernatant of the cells. Data are reported as means±SD of four independent experiments. *$p< 0.05$ *vs.* the control condition and #$p< 0.05$ *vs.* the miR-16 transfection condition.
doi:10.1371/journal.pone.0050935.g002

PICTAR, and Diana-microT, and comparing the obtained results with data collected from the literature.

Western Blot Analysis

Extracts from cells ($2–3\times10^6$) or from liver tissue were obtained as previously described [32]. For Western blot analysis, whole-cell extracts were boiled for 5 minutes in Laemmli sample buffer, and equal amounts of protein (20–30 μg) were separated by 10–15% SDS-polyacrylamide electrophoresis gel (SDS-PAGE). The relative amounts of each protein were determined with the following polyclonal or monoclonal antibodies: COX-2 (Cayman 160107 and Santa Cruz sc-1747), α-tubulin (Sigma T9026), HuR (Santa Cruz sc-5261), Ago2 (Abcam AB57113) and Caspase-3 (Cell Signaling 9662). After incubation with the corresponding anti-rabbit or anti-mouse horseradish peroxidase conjugated secondary antibody, blots were developed by the ECL protocol (GE Healthcare, Chalfont St Giles, UK). Target protein band densities were normalized with α-tubulin. The blots were revealed, and different exposition times were performed for each blot with a charged coupling device camera in a luminescent image analyzer (Gel-Doc, Bio-Rad) to ensure the linearity of the band intensities. Densitometric analysis was expressed in arbitrary units.

Determination of Metabolites

PGE_2 was determined in culture media by specific immunoassay (Arbor Assays, Ann Arbor, MI, USA). Protein levels were determined with Bradford reagent (Bio-Rad).

Transfection, Constructs and Luciferase Reporter Assay

The miR-16 precursor (PM10339), which was a double-stranded RNA mimicking the endogenous mature miRNA, the miR-16 inhibitor (In-miR-16, AM10339) which was a single stranded nucleic acid designed to specifically bind to and inhibit endogenous microRNA molecule, their negative controls (miR-NC, AM17110; In-miR-NC, AM17010) and anti-COX-2 siRNA (siCOX-2) (positive control, forward 5′- GGGCUGUCC-CUUUACUUCAtt -3′and reverse 5′- UGAAGUAAAGGGA-CAGCCCtt-3′) were purchased from Ambion (Austin, TX, USA). pPyCAGIP-hCOX-2 was prepared as described previously [33]. Briefly, human COX-2 ORF was amplified by PCR from human full-length COX-2 cDNA cloned into pcDNA1/Amp, and then, was subcloned into *Xho*I-*Not*I restriction site of pPyCAGIP vector. WRL68 and Hep3B cells were seeded in a 6-well plate (3×10^5cells/well) at 70% confluence. After 24 h, cells were transfected with 50 nM of miR products or 30 nM siCOX-2 using lipofectamine 2000 (Invitrogen, USA) according to the manufacturers instructions. After 6 h of incubation at 37°C, transfection medium was replaced with 2 ml of complete medium containing 10% FBS. For the analysis of COX-2 mRNA or protein decay, 5 μg/ml actinomycin-D or 10 μg/ml cycloheximide (Sigma, USA) were added after transfection. Cells were lysated after 48 h for Western blot and RT-PCR analyses.

To determine whether COX-2 mRNA was located in processing bodies, p-bodies (PB), as a consequence of translational repression, digitonine permeabilization and cellular fractionation of Hep3B cell lines were performed since PB are enriched in the pellet fraction [34]. Hep3B cell lines were transfected with miR-16 or In-miR16 48 hours prior to harvesting at a final concentration of 50 nM. Cells were harvested by trypsinization, washed with cold phosphate buffered saline (PBS) and resuspended in Buffer C [250 mM sucrose, 10 mM Tris-HCl pH 7.5, 25 mM KCl, 5 mM MgCl2, 2 mM DTT, 30 U/ml RNasin, and 0.1% v/v phosphatase-protease inhibitor cocktail (Sigma) containing 50 mg/ml digitonin (Sigma)]. After incubation on ice for 15 min, samples were centrifuged at 1,000 g for 5 min at 4°C. The supernatant was recentrifuged at 14,000 g at 4°C for 5 min and saved as a soluble fraction. The pellet from 1,000 g centrifugation was washed with Buffer C without digitonin and saved as a cell debris pellet. RNA was isolated from each fraction with Trizol reagent and was used for RT-PCR. 5′-3′ exonucleasa (Xrn1) primers; F:GAGAAGC-GATTATTGGAAGCCA and R:GCACATTAGGCACTCAC-TATGTT were used as PB marker.

Using several programs (RNAhybrid, PITA, and RNA22), miR-16 was predicted to associate with the 3′UTR region of COX-2 to different MRE motifs (Table S1). In the present report, miR-16 target site prediction for COX-2 was performed using RNAhybrid [35] and we found one predicted MRE for miR-16 at positions 1195–1217 taking as position 1 the beginning of the 3′ UTR region. The 3′-UTR sequences of COX-2 were retrieved using Ensembl Data base (available: http://www.ensembl.org). Human miRNA sequences were downloaded from the miRBase website (available: http://www.mirbase.org). A fragment of 3′UTR COX-2 mRNA (region 1195–1217, from NM_000963) which include the MRE binding site for miR-16, and a mutant variant were cloned into pGL3-Promoter vector (pGL3-empty, Promega, USA) downstream firefly luciferase gene (*Sac*I, *Hind*III sites) to obtain the luciferase reporter constructs (pGL3-seed and pGL3-mut, respectively). Sequences cloned: 5′-ctttatctcagtcttgaagccaattcag-taggtgcattggaatcaagcctga-3′ (seed); 5′-ctttatctcagtcttgaataaccttcag-gagggtaattggaatcaagcctga-3′ (mut).

A DNA fragment containing 2.5 kb corresponding to the full length 3′UTR region of the human COX-2 gene was amplified by PCR and cloned into the pGEM-T easy vector (Promega) to construct pGEMCOX-2/3′UTR. The fragment was obtained by XbaI/BamHI digestion and subcloned in the pGL3-Promoter vector (pGL3-empty, Promega) to construct the pGL3-UTR vector. Mutagenesis was performed by means of the QuickChange Site-Directed Mutagenesis Kit (Stratagene, La Jolla, CA. USA) using pGEMCOX-2/3′UTR as a template. All the constructions were confirmed by nucleotide sequencing.

Cells (3×10^4 cells/well) were seeded in 24-wells plate and transfected for 6–12 h with pGL3-empty (750 ng), pGL3-seed (750 ng), pGL3-mut (750 ng), pGL3-UTR (750 ng), pGL3-UTR mut (750 ng), pRL-SV40 vector (50 ng, Promega, USA), miR-16 (50 nM), In-miR-16 (50 nM) or miR-NC (50 nM) or a different combinations of them using lipofectamine 2000 reagent protocol. Cells were harvested 48 h after transfection and cell lysates were used for Dual-Luciferase® Reporter Assay System analysis, according to the manufacturer's instructions (Promega, USA). HuR expression vector, pcDNA3-HuR-GFP, was kindly provided by Dr.M. Gorospe (Laboratory of Molecular Biology and

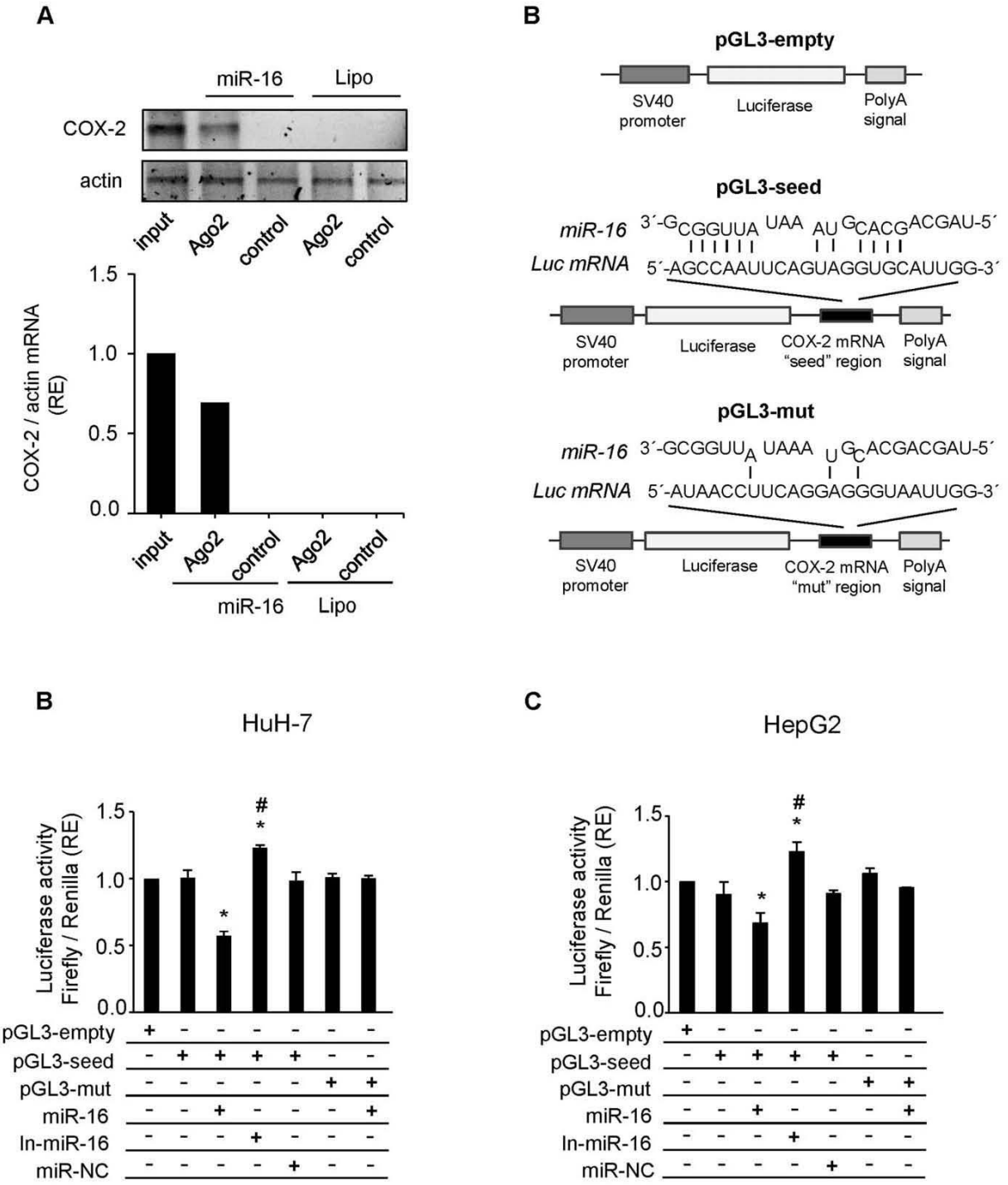

Figure 3. miR-16 binds COX-2 mRNA and inhibits its translation. (**A**) WRL68 cell extracts (500 µg per lane) were immunoprecipitated with Ago-2 or IgG antibodies. Bound RNA was harvested with TRIzol reagent, reverse transcriptased, and PCR amplified with COX-2 primers. PCR products were visualized by electrophoresis in SYBR Safe DNA gel stain agarose gels. The presence of COX-2 mRNA in WRL68 cell transfected with miR-16 or Lipofectamine after Ago2 immunoprecipitation was assessed, and fold differences were plotted. Input, total mRNA in cell extract; and control, bound mRNA after immunoprecipitation with IgG antiboby. (**B**) Scheme of pGL3-empty, pGL3-seed and pGL3-mut reporter vectors. In pGL3-seed, the putative binding site of miR-16 on COX-2 mRNA 3′-UTR region (as detected by RNAhybrid software) was introduced downstream luciferase gene. In pGL3-mut this region was mutated in order to avoid the binding between miR-16 and Luc mRNA. (**C–D**) A luciferase assay was carried out on HuH-7 and HepG2 cell lines using pGL3-seed and pGL3-mut reporter vectors. Firefly luciferase activity was evaluated 48 h after co-transfection with pGL3-

empty/seed/mut (750 ng), miR-16 (50 nM), In-miR-16 (50 nM) and miR-NC (50 nM) as indicated. Data were normalized against renilla luciferase activity (all samples were co-transfected with 50 ng pRL vector and refer to the positive control, pGL3 empty vector). Data are reported as means±SD of three independent experiments. *$p < 0.05$ *vs.* the pGL3-empty condition and # $p < 0.05$ *vs.* the miR-16 transfection condition.
doi:10.1371/journal.pone.0050935.g003

Immunology, NIA-IRP, NIH, Baltimore, USA). When transfection was performed with pcDNA3-HuR-GFP (4 μg) and pPyCAGIP-hCOX-2 or control vector (4 μg) cells were seeded in 6-wells plate.

Immunoprecipitation and PCR Analysis

The binding of miR-16 to COX-2 mRNA, HuR to COX-2 mRNA and the binding of HuR to miR-16 were analyzed by immunoprecipitation and PCR analysis. The immunoprecipitation was carried out in the lysis buffer (10 mM Tris/HCl, pH 8, 150 mM NaCl, 1% NP40, 0.1% azide, and protease inhibitor cocktail). Total crude extracts (500 μg) from WRL68 and Hep3B cells were immunoprecipitated with 10 μg Ago2, HuR, or IgG antibody and mixed 2 hours at 4°C. An equal volume of protein A/G sepharose was added per immunoprecipitation and mixed overnight at 4°C. The protein/G sepharose was pelleted at 1500 rpm for 2 minutes at 4°C. For the elution of bound RNA, beads were resuspended in the lysis buffer described above, supplemented with 10 μg tRNA from *Escherichia coli* and 80 μg of proteinase K. The mixture was incubated at 50°C for 45 minutes. The RNA was purified using TRIzol reagent (Invitrogen, Carlsbad, CA), reverse transcriptased and PCR amplified with COX-2, miR-16, U6 or actin primers. The PCR reaction was performed at 95°C for 5 min, followed by 30 cycles of 95°C for 30 s, 52°C for 30 s, and 72°C for 1 min, with the following primers; hCOX-2 forward 5′- ATCTACCCTCCTCAAGTCCC-3′and reverse 5′- TACCAGAAGGGCAGGATACAG-3′, actin forward 5′- GCTCACGGAGGCACCCCTGAA -3′and reverse 5′- CTGATAGGACATTGTTAGCAT -3′, miR-16 forward 5′- TAGCAGCACGTAAATATTGGCG -3′and the universal reverse primer provided in the NCode™ miRNA first-strand cDNA synthesis kit (Invitrogen), U6 snRNA forward 5′-CTTCGGCAGCACATATACT -3′and reverse 5′- AAAATATGGAACGCTTCACG -3′. PCR products were visualized by electrophoresis in SYBR Safe DNA gel stain (Invitrogen) agarose gels.

Analysis of Cell Proliferation

Cell proliferation was determined by the MTT (3-[(4, 5-dimethylthiazol-2-yl)-2, 5′diphenyltetrazolium bromide]) assay (Sigma). Cells (8×10^3) were seeded on 96-well plates in DMEM supplemented with 10% FBS. After transfection with different conditions, cells were treated with 20 μl of MTT solution (2 mg/ml) for 4 h at 37°C. The medium was removed and DMSO was added to dissolve the blue formazan residue. The optical density was measured at 570 nm.

Evaluation of Apoptosis

Apoptosis was detected by flow cytometry using Annexin V-FITC Apoptosis Detection Kit (BD Pharmingen, San Diego, CA, USA). Briefly, cells were collected and washed in cold PBS. After centrifugation at 4°C for 5 min at 1000 rpm, cells were double stained with Annexin V-FITC and PI for 15 min at room temperature in the dark. Early apoptosis is defined by Annexin V^+/PI^- staining and late apoptosis is defined by Annexin-V^+/PI^+ staining as determined in a Cytomics FC500.

Analysis of Tumorigenicity in Nude Mice

Female athymic *nu/nu* mice (6 weeks old) were obtained from Charles River Laboratories (Wilmington, MA). All the experiments were performed in accordance with the animal care guidelines of the European Union (2010/63/EU), and approved by the Bioethical Committee from Consejo Superior de Investigaciones Científicas (reference project SAF2010/16037). The animals were kept under pathogen-free conditions and were given an autoclaved standard diet and water *ad libitum* and treated according to the Institutional Care Instructions (Bioethical Commission from Consejo Superior de Investigaciones Científicas, CSIC, Spain). WRL68 cells were transfected *in vitro* with 50 nM miR-NC or miR-16 and pPyCAGIP-hCOX-2 ORF (hCOX-2 expression vector lacking COX-2 3′ UTR) by using lipofectamine 2000. At 24 h after transfection, 5×10^6 viable cells suspended in PBS were injected subcutaneously into both flanks of the *nu/nu* mice (5 mice per group). Tumor growth was measured every 2 or 3 days. At 21 days after injection, mice were killed and tumors were weighed after necropsy. Tumor volume (V) was monitored by measuring the length (L) and width (W) with calipers and calculated with the formula $(L\times W^2)\times0.5$.

Data Analysis

Data are expressed as mean ± S.D. (n ranged from three to five independent experiments). Statistical significance was estimated with the Student's two-tailed *t* test for unpaired observations, Spearman r test for nonparametric correlations and the Mann-Whitney U test was used for ordinal variables using the statistical software GraphPad Prism 5. A p value < 0.05 was considered significant.

Results

miR-16 and COX-2 Correlate Inversely in Hepatoma Cell Lines

To examine whether COX-2 expression is under the control of miRNAs, we determined the expression pattern of COX-2 and selected miRNAs in four hepatoma (HCC) cell lines (HepG2, PLC/PRF/5, HuH-7, Hep3B) and in a cell line derived from human liver embryo (WRL68), using human hepatocytes (HH) as control (Fig. 1A). We found that each cell line expresses different levels of COX-2 protein and mRNA. WRL68 exhibited the highest COX-2 mRNA levels whereas HepG2 and PLC/PRF/5, two differentiated liver carcinomas, showed low levels of COX-2 mRNA and protein (Fig. 1A). The expression profile of six miRNAs (miR-16, miR-26b, miR-101, miR-199a, miR-122 and miR-21) was analyzed in HCC cell lines (Table 1). In almost all HCC lines analyzed, miR-16 expression was lower than in control hepatocytes (HH), whereas COX-2 protein levels were higher (Fig. 1A). We decided to compare the COX-2 protein/mRNA ratio (as an index of translational inhibition) of the cell lines with the selected miRNAs levels. Among the six miRNAs analyzed, the expression of miR-16 showed the highest inverse correlation with the COX-2 protein/mRNA ratio ($R^2 = 0.858$, $p = 0.016$) (Fig. 1B), suggesting that miR-16 is involved in COX-2 regulation in hepatoma cell lines.

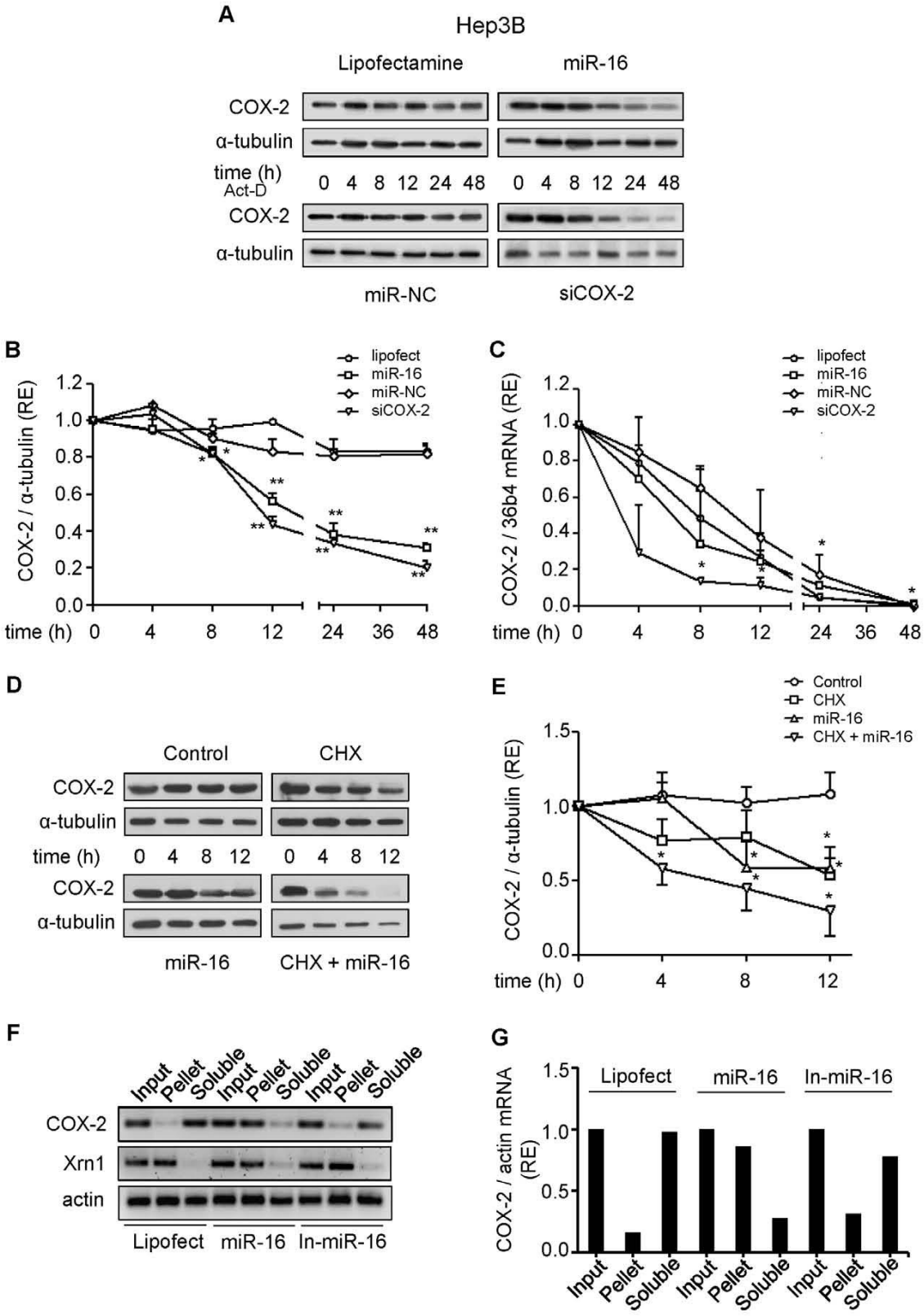
A
Hep3B
Lipofectamine
miR-16
COX-2
α-tubulin
time (h)
Act-D
0 4 8 12 24 48 0 4 8 12 24 48
COX-2
α-tubulin
miR-NC
siCOX-2
B
lipofect
miR-16
miR-NC
siCOX-2
COX-2 / α-tubulin (RE)
time (h) 0 4 8 12 24 36 48
C
lipofect
miR-16
miR-NC
siCOX-2
COX-2 / 36b4 mRNA (RE)
time (h) 0 4 8 12 24 36 48
D
Control
CHX
COX-2
α-tubulin
time (h) 0 4 8 12 0 4 8 12
COX-2
α-tubulin
miR-16
CHX + miR-16
E
Control
CHX
miR-16
CHX + miR-16
COX-2 / α-tubulin (RE)
time (h) 0 4 8 12
F
Input Pellet Soluble Input Pellet Soluble Input Pellet Soluble
COX-2
Xrn1
actin
Lipofect
miR-16
In-miR-16
G
Lipofect
miR-16
In-miR-16
COX-2 / actin mRNA (RE)
Input Pellet Soluble Input Pellet Soluble Input Pellet Soluble

Figure 4. Effect of miR-16 on COX-2 mRNA and protein stability. Hep3B cells were transfected with 50 nM miR-16 or miR-NC, or 30 nM siCOX-2. 5 μg/ml actinomycin-D (Act D) or 10 μg/ml cycloheximide (CHX) were added after transfection. (**A–B**) COX-2 protein was analyzed by Western blot at different time after actinomycin-D treatment. Corresponding densitometry analysis is shown and the relative expression of each sample is related to sample at 0 h as 1. (**C**) mRNA COX-2 levels were analyzed by real time PCR. COX-2 mRNA amounts were calculated as relative expression and normalized to the expression of 36b4 mRNA. Values represent fold change relative to sample at 0 h. (**D–E**) COX-2 protein levels were analyzed by Western blot in the presence or absence of cycloheximide. Corresponding densitometric analysis is shown and the relative expression of each sample is related to the value at 0 h as 1. **F)** Hep3B cells were transfected with 50 nM miR-16, miR-16 inhibitor (In-miR-16) or lipofectamine and permeabilized with digitonine to obtain soluble and pellet fractions enriched in PB as described in Methods. RNA was isolated from each fraction with Trizol reagent, reverse transcriptased, and PCR amplified with COX-2, Xrn1 and actin primers. Input, RNA extracted from cells prior to fractionation. PCR products were visualized by electrophoresis in SYBR Safe DNA gel stain agarose gels. **G)** The presence of COX-2 mRNA in soluble and PB fractions was assessed and fold differences were plotted. Data are reported as means±SD of three independent experiments. **$p<0.01$ and *$p<0.05$ vs. the value of sample at 0 h.
doi:10.1371/journal.pone.0050935.g004

miR-16 Regulates COX-2 Expression in HCC Cell Lines

Major approaches to validate miRNA targets use *in vitro* gain-of-function and loss-of-function analyses. We overexpressed miR-16 in HCC cell lines and examined whether it decreases endogenous COX-2 levels. The effect of miR-16 transfection on COX-2 protein expression was evaluated in WRL68 and Hep3B cells and it was compared to one positive control, cells transfected with siCOX-2, and with two different negative controls, cells treated only with lipofectamine and cells transfected with miR-NC. As a further control, the effect of both miR-16 and miR-NC inhibitors were analyzed. WRL68 and Hep3B cells were chosen since they express higher levels of COX-2 protein. miR-16 caused a decrease in COX-2 protein levels within 48 h of transfection in both cell lines (Fig. 2A–B). Moreover, the transfection of In-miR-16 induced an increase of COX-2 protein mainly in Hep3B cells. COX-2 mRNA levels were also evaluated and no significant changes was observed following the different treatments with the exception of siCOX-2 transfection (Fig. 2A–B). These results provide further evidence that COX-2 mRNA is post-transcriptionally controlled by miR-16. Released PGE_2 levels are in good agreement with COX-2 protein changes (Fig. 2C–D).

miR-16 Binds COX-2 mRNA and Inhibits its Translation

To establish whether the effect of miR-16 on COX-2 expression was mediated through a direct miRNA:mRNA interaction, we performed a RNA immunoprecipitation (RNA-IP) assay in WRL68 cells transfected with miR-16. Immunoprecipitation of total lysates was carried out with an antibody against Argonaute 2 (Ago2), a major component of the microRNA associated to multiprotein RNA-induced-silencing complex (RISC) [36]. As shown in Fig. 3A, COX-2 mRNA was present in the Argo2 immunoprecitation samples where miR-16 was expressed whereas capture of the negative control actin mRNA was unchanged. Using several programs (RNAhybrid, PITA, and RNA22), miR-16 was predicted to associate with the 3′UTR region of COX-2 to different MRE motifs (Table S1) and we found one predicted MRE for miR-16 at positions 1195–1217 taking as position 1 the beginning of the 3′ UTR region. To ensure that miR-16 can bind to this predicted region and cause translational repression, we performed a luciferase reporter gene assay in HuH-7 and HepG2 cells with low levels of miR-16. We cloned the 3′UTR region of COX-2 containing the miR-16 putative binding site (seed region) and a mutant variant downstream the Luc gene in pGL3-vector (pGL3-seed and pGL3-mut, respectively) (Fig. 3B). The luciferase activity significantly decreased after cotransfection with both pGL3-seed and miR-16, when compared to positive control (cells transfected only with pGL3-seed). The transfection of In-miR-16 increased the luciferase activity while the transfection of miR-NC had no effects. Moreover, we did not observe variations of the luciferase activity in cells cotransfected with pGL3-mut and miR-16, in comparison to cells transfected only with pGL3-mut (Fig. 3C–D). The results suggest that miR-16 could specifically bind to the 3′UTR region of COX-2 and represses COX-2 translation reinforcing the hypothesis that COX-2 mRNA is a direct target for miR-16. The effect was similar using 3′ UTR full length region of COX-2 (Figure S1).

To further support the hypothesis that miR-16 is involved in the down-regulation of COX-2 translation, we tested the expression of COX-2 in Hep3B cells after transfection with siCOX-2 or miR-16, in the presence of the transcription inhibitor actinomycin-D. We found a decrease of COX-2 protein in both cases (Fig. 4A–B). However, siCOX-2 induced a rapid decay of COX-2 mRNA ($t_{1/2}$ = 3 h) while the transfection of miR-16 did not show significant mRNA decay when compared to negative controls (cells treated only with lipofectamine and cells transfected with miR-NC; $t_{1/2}$ = 7 to 9 h) (Fig. 4C). We performed a similar experiment in the presence of the protein synthesis inhibitor, cycloheximide (CHX) and the results obtained reveal that both miR-16 and CHX induced a rapid decay of COX-2 protein with a synergistic effect (Fig. 4D–E). Furthermore, when Hep3B cells were treated with digitonin and fractionated after transfection with miR-16 in order to localize COX-2 mRNA in soluble or P-bodies (PB) fractions [34], the amount of COX-2 mRNA present in PB was more than 90%, suggesting inhibition of translation. Instead, in Hep3B cells transfected with lipofectamine, COX-2 mRNA is present in the soluble fraction, where polysomes are located. A similar distribution of COX-2 mRNA was observed upon transfection of Hep3B cells with In-miR-16 (Fig. 4F–G). The results demonstrate that miR-16 interacts with COX-2 mRNA and promotes COX-2 protein decrease mostly through a translational repression mechanism.

HuR Antagonizes miR-16 Activity in Regulating COX-2 Expression in Hepatoma Cell Lines

It is well known that HuR and other RNA-binding proteins bind to and regulate COX-2 expression and determine the fate of COX-2 translation [37,38]. However, a recent work [39] has demonstrated that miR-16 inversely correlates with HuR protein levels in human breast carcinoma. RNA immunoprecipitation (RNA-IP) was performed to determine whether HuR would associate with COX-2 and whether there is a direct interaction between HuR and miR-16 in WRL68 cell line. As shown in Fig. 5A, COX-2 mRNA was present in the HuR immunoprecipitates, whereas capture of the negative control actin mRNA was unchanged. Moreover, when RNA-IP was performed, miR-16 was also present in the HuR immunoprecipitates (Fig. 5B). To study the relationship between miR-16 and HuR in HCC cell lines, we determined whether HuR levels were altered by miR-16 transfection. As shown in Fig. 5C–D, overexpression of miR-16 in WRL68 and Hep3B cell lines led to a substantial decrease in HuR

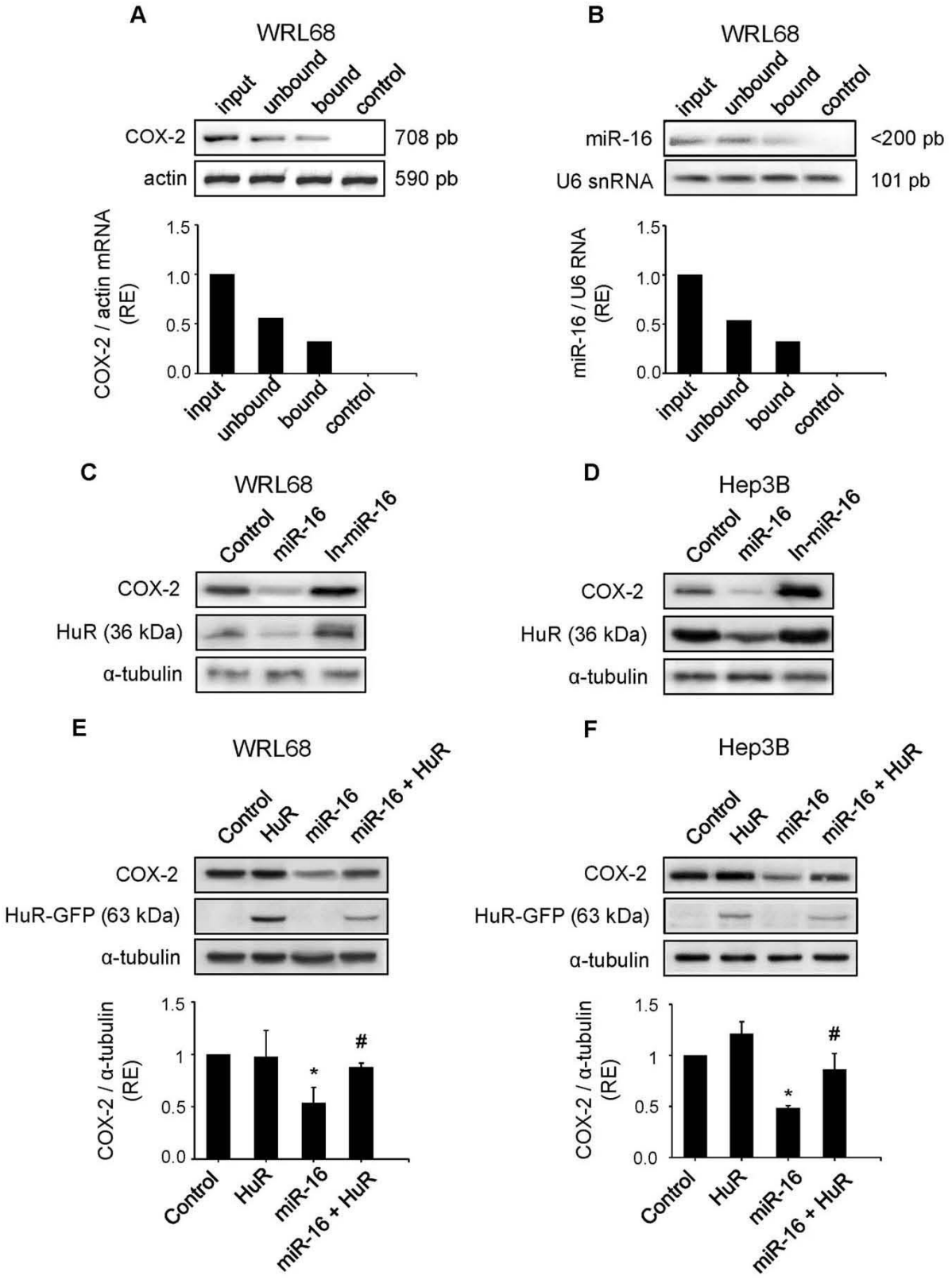
A
WRL68
input
unbound
bound
control
COX-2
708 pb
actin
590 pb
COX-2 / actin mRNA (RE)
1.5
1.0
0.5
0.0
input
unbound
bound
control
B
WRL68
input
unbound
bound
control
miR-16
<200 pb
U6 snRNA
101 pb
miR-16 / U6 RNA (RE)
1.5
1.0
0.5
0.0
input
unbound
bound
control
C
WRL68
Control
miR-16
In-miR-16
COX-2
HuR (36 kDa)
α-tubulin
D
Hep3B
Control
miR-16
In-miR-16
COX-2
HuR (36 kDa)
α-tubulin
E
WRL68
Control
HuR
miR-16
miR-16 + HuR
COX-2
HuR-GFP (63 kDa)
α-tubulin
COX-2 / α-tubulin (RE)
1.5
1
0.5
0.0
*
#
Control
HuR
miR-16
miR-16 + HuR
F
Hep3B
Control
HuR
miR-16
miR-16 + HuR
COX-2
HuR-GFP (63 kDa)
α-tubulin
COX-2 / α-tubulin (RE)
1.5
1
0.5
0.0
*
#
Control
HuR
miR-16
miR-16 + HuR

Figure 5. HuR antagonizes the downregulation of COX-2 expression caused by miR-16 in hepatoma cell lines. WRL68 cell extracts (500 µg per lane) were immunoprecipitated with HuR or IgG antibodies. Bound RNA was harvested with TRIzol reagent, reverse transcriptased, and PCR amplified with COX-2 (**A**) or miR-16 primers (**B**). PCR products were visualized by electrophoresis in SYBR Safe DNA gel stain agarose gels. The abundance of the transcripts present in WRL68 cells after HuR immunoprecipitation was assessed, and fold differences were plotted. Input, total mRNA in cell extract; unbound, unbound mRNA after immunoprecipitation with HuR antibody; bound, bound mRNA after immunoprecipitation with HuR antibody; and control, bound mRNA after immunoprecipitation with IgG antiboby. (**C–D**) WRL68 and Hep3B cell lines were transfected with miR-16 or In-miR-16 (50 nM). COX-2 and HuR protein levels were analyzed by Western Blot. (**E–F**) WRL68 and Hep3B cell lines were cotransfected with miR-16 (50 nM) and pcDNA3-HuR-GFP expression vector (4 µg). COX-2 and HuR protein levels were analyzed by Western Blot. Data are reported as means±SD of three independent experiments. *$p< 0.05$ *vs.* the control condition and #$p< 0.05$ *vs.* the miR-16 transfection condition.
doi:10.1371/journal.pone.0050935.g005

protein levels. To determine whether miR-16-mediated COX-2 protein loss was due in part to a decrease in HuR expression, Hep3B and WRL68 cell lines were cotransfected with miR-16 and HuR expression vectors. As shown in Fig. 5E–F, miR-16 inhibited the COX-2 and HuR protein levels in both cellular types; however, in the presence of HuR, the ability of miR-16 to downregulate COX-2 protein levels was partially abolished.

miR-16 Down Regulation of COX-2 Sensitizes HCC Cells to Apoptosis

To further establish a functional relationship between miR-16 and COX-2, we tested whether COX-2 expression was required to miR-16-dependent induction of apoptosis. Overexpression of miR-16 promoted apoptosis in Hep3B hepatoma cells. However, the effect of miR-16 on apoptosis was partially attenuated by treatment of cells with PGE_2 (Fig. 6A). Western blot analysis of active caspase-3 showed an increase in the pro-apoptotic protein by the effect of miR-16 and this effect was also reverted in the presence of PGE_2 (Fig. 6B). These results suggest that miR-16 may exert its pro-apoptotic function partially through decreasing COX-2 expression.

mir-16 Suppresses the Growth of Hepatoma Cells in vitro and *in vivo*

We sought to determine whether miR-16 affects the growth of hepatoma cell lines assessed by the MTT reduction assay. As indicate in Fig. 7A, the growth of Hep3B cells transfected with miR-16 was significantly decreased relative to control cells. Transfection of the cells with miR-16 decreased cell growth up to 40%, being restored to 70% in the presence of PGE_2. To further analyze the effect of miR-16 on hepatoma cell growth *in vivo*, the WRL68 cells were transiently transfected with miR-16, miR-NC or miR-16 together with a human COX-2 expression vector that lacks the 3′ UTR and, therefore, it cannot be regulated by miR-16. Then the transfected cells were subcutaneously injected into athymic *nu/nu* mice. The mice were followed by the observation of xenograft growth for 3 weeks. We found that miR-16 led to a significant reduction in the volume and weight of the tumor comparing with the mice injected with miR-NC. COX-2-dependent production of PGE_2 increased the volume and the weight of tumors comparing with miR-16 (Fig. 7B–C). The expression of intratumoral miR-16, measured by real-time PCR, increased in tumors injected with cells transfected with miR-16 compared with miR-NC without being modified by COX-2 overexpression (Fig. 7D). Moreover, human COX-2 expression was detected in the tumors 21 days after the injection (Fig. 7E). These results agree with the *in vitro* data (Fig. 7A) and suggest that miR-16 inhibits the proliferation of hepatoma cells, among other mechanisms, through downregulation of COX-2.

Inverse Correlation between miR-16 and COX-2 Expression is Observed in HCC Human Biopsies

Since miR-16 regulates COX-2 expression by binding to the MRE in the 3′-UTR COX-2 and by inhibition of HuR in HCC cell lines, we evaluated the relationship between miR-16, HuR and COX-2 mRNA/protein expression in individual tumoral (T) and paired non-tumoral (NT) HCC human samples. COX-2 mRNA and protein were higher in NT tissue compared to T counterparts, like HuR protein and mRNA (Figure S2A-C) whereas miR-16 levels in HCC tissues tended to be higher in T than in NT tissue (Figure S2D) and inversely correlated with COX-2 protein levels (Figure S2E).

Discussion

In this study we have analyzed whether COX-2 could be regulated by miRNAs or RNA-binding proteins in human hepatoma cell lines and human HCC specimens and whether COX-2 levels in human HCC correlate with an altered expression of these miRNAs. Our results show that miR-16 directly silences COX-2 expression in hepatoma cells and indirectly through the downregulation of HuR. Moreover, a reduced miR-16 expression correlates with high levels of COX-2 in liver from HCC patients. From a functional point of view, COX-2 down-regulation by miR-16 increased apoptosis and decreased cell proliferation in human hepatoma cell lines.

Several lines of evidence suggest that COX-2 signaling is implicated in hepatocarcinogenesis and that COX-2 inhibitors prevent HCC cell growth *in vitro* and in animal models [40]. Increased COX-2 expression has been found in human HCC; however, although COX-2 expression is elevated in the early stages of HCC, many questions remain unsolved regarding the sufficiency of COX-2 to induce/contribute to tumorigenesis. The mechanisms regulating the expression of COX-2 at specific stages of HCC development remain unknown. Moreover, recent data and our present results indicate that COX-2 mRNA levels are significantly higher in the adjacent liver than in the HCC and lower in HCC than in nonalcoholic steatohepatitis [12]. Our previous work demonstrated that COX-2 expression is not sufficient to enhance malignant transformation induced by dyethylnitrosamine in a model of transgenic mice expressing COX-2 in hepatocytes [33]. These results suggest that COX-2 could be related to the inflammatory response occurring in the early phases of chronic liver disease and eventually contribute to the induction of hepatocarcinogenesis.

Several reports describe COX-2 overexpression as a critical step contributing to various facets of colon cancer and growing evidence indicates that this overexpression is facilitated through loss of ARE-mediated mRNA decay [41]. In CRC cells, a variant of COX-2 mRNA lacking the distal region of the 3′UTR was stabilized upon cell growth to confluence [28]. These findings suggest that COX-2 mRNA can escape rapid decay through the use of alternative polyadenylation sites, resulting in deletion of potential 3′UTR regulatory elements. This phenomenon appears

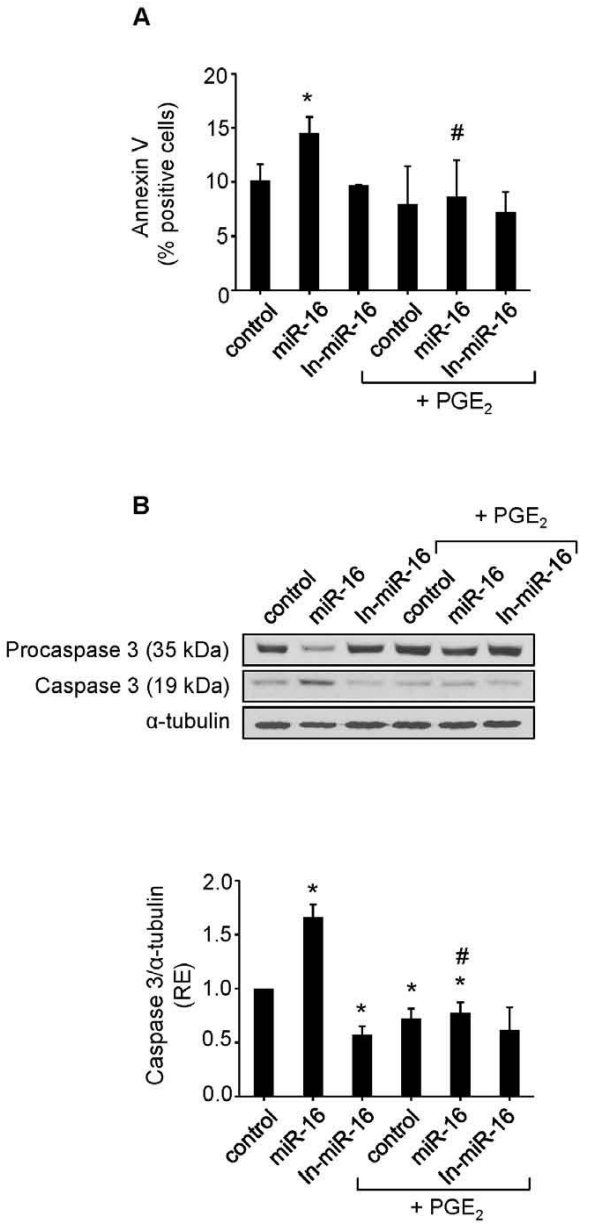

Figure 6. Downregulation of COX-2 by miR-16 increases apoptosis in HCC cells. Hep3B cells were transfected with 50 nM miR-16 or In-miR-16 in the presence or absence of 5 μM PGE_2 (**A**) Apoptosis was measured with Annexin V-FITC Apoptosis Detection Kit (**B**) Western blot analysis of caspase-3. Results are the means ± SD of three different experiments. *$p< 0.05$ *vs.* the corresponding control cells $^{\#}$ $p< 0.05$ *vs.* miR-16 condition.
doi:10.1371/journal.pone.0050935.g006

to be common in colon cancer cells [42]. Moreover, it has been described a common polymorphism in the 3′UTR of COX-2 and this variant is associated with lung cancer risk [43]. Nevertheless, no data are available concerning the loss of ARE-mediated post-transcriptional regulation of COX-2 or even polymorphisms in the ARE elements in HCC.

There are several miRNAs abundantly expressed in adult liver tissue [44,45] and the liver displays a differential miRNA expression profile in HCC. Microarray analysis showed altered expression of some miRNAs in hepatomas such as let-7a, miR-21, miR-23, miR-130, whereas the hepato-specific miR-122a and others were found downregulated in 70% of HCCs and in HCC-derived cell lines [20,46,47], as reported in our data (Table 1). Murakami et al. [48] showed a correlation between miR-222, miR-106a, miR-92, miR-17-5p, miR-20 and miR-18 and the degree of differentiation suggesting an involvement of specific miRNAs in the progression of the disease. However, the molecular mechanisms underlying transcriptional regulation of miRNA genes in the liver remain poorly established and different transcription factors, such as hepatocyte nuclear factor 1α, c-myc, STAT-3 and NF-κB have been implicated [25,49]. Understanding the contribution of desregulated miRNAs to HCC requires the identification of gene targets and in this sense, cyclin G1 and the PTEN tumor suppressor gene have been found to be regulated by miR-122a and miR-21, respectively [50,51].

The 3′-UTR of COX-2 is complex and contains multiple copies of AREs and MREs which, when bound to specific ARE-binding factors or miRNAs, influence COX-2 stability and translational efficiency [17]. Work investigating the role of COX-2 during embryo implantation identified the miRNAs, miR-101a and miR-199a as regulators of COX-2 [22,23]. miR-101a also controls mammary gland development by regulating COX-2 expression [52]. In the context of colon cancer cell lines and colon tumors, miR-101 inhibited COX-2 translation [24]. Young et al. [36] demonstrated that miR-16 binds the COX-2 3′UTR and inhibits COX-2 expression by promoting mRNA decay in colon cancer. However, the functional consequences of miR-16 associated with HCC progression have not been established. The present results demonstrate that miR-16 regulates COX-2 expression in HCC cells by binding directly to the MRE response element in the COX-2 3′UTR and this binding inhibits mainly COX-2 translation without affecting significantly mRNA decay. It has been described by Huang et al. that miR-16 decreased the association of its target mRNA with polysomes in 293T and HeLa cells by mediating the association of mRNA with processing bodies (P-bodies), since localization of mRNAs to these structures is a consequence of translational repression [34]. A similar assay has been used previously to support the PB-to-cytosol relocalization of mRNAs relieved from miRNA repression by treatment with antisense oligonucleotides [53]. Our results clearly show that COX-2 mRNA was located in P-bodies (>90%) after transfection with miR-16, inhibiting its translation.

Next, we investigated the effect of COX-2-mediated inhibition by miR-16 in hepatocarcinogenesis. Our data show that the ectopic expression of miR-16 repressed cell proliferation of hepatoma cells *in vitro* and tumor growth *in vivo*, and these effects were partially reverted by treatment with PGE_2. Furthermore, COX-2 inhibition mediated by miR-16 promoted apoptosis in HCC cells by increasing apoptotic proteins such as caspase-3.

Various cytoplasmic proteins have been observed to bind to the COX-2 ARE. To date, 16 different RNA-binding proteins bind the COX-2 3′UTR promoting mRNA decay, mRNA stabilization or translational silencing [41]. The HuR protein is a ubiquitously expressed member of the ELAV (Embryonic-Lethal Abnormal Vision in Drosophila) family of RNA-binding proteins. HuR contains three RNA recognition motifs with a high affinity and specificity for AREs and its overexpression stabilizes transcripts and promotes their translation [54]. HuR is localized predominantly in the nucleus and the ability of HuR to promote mRNA stabilization requires its translocation to the cytoplasm.

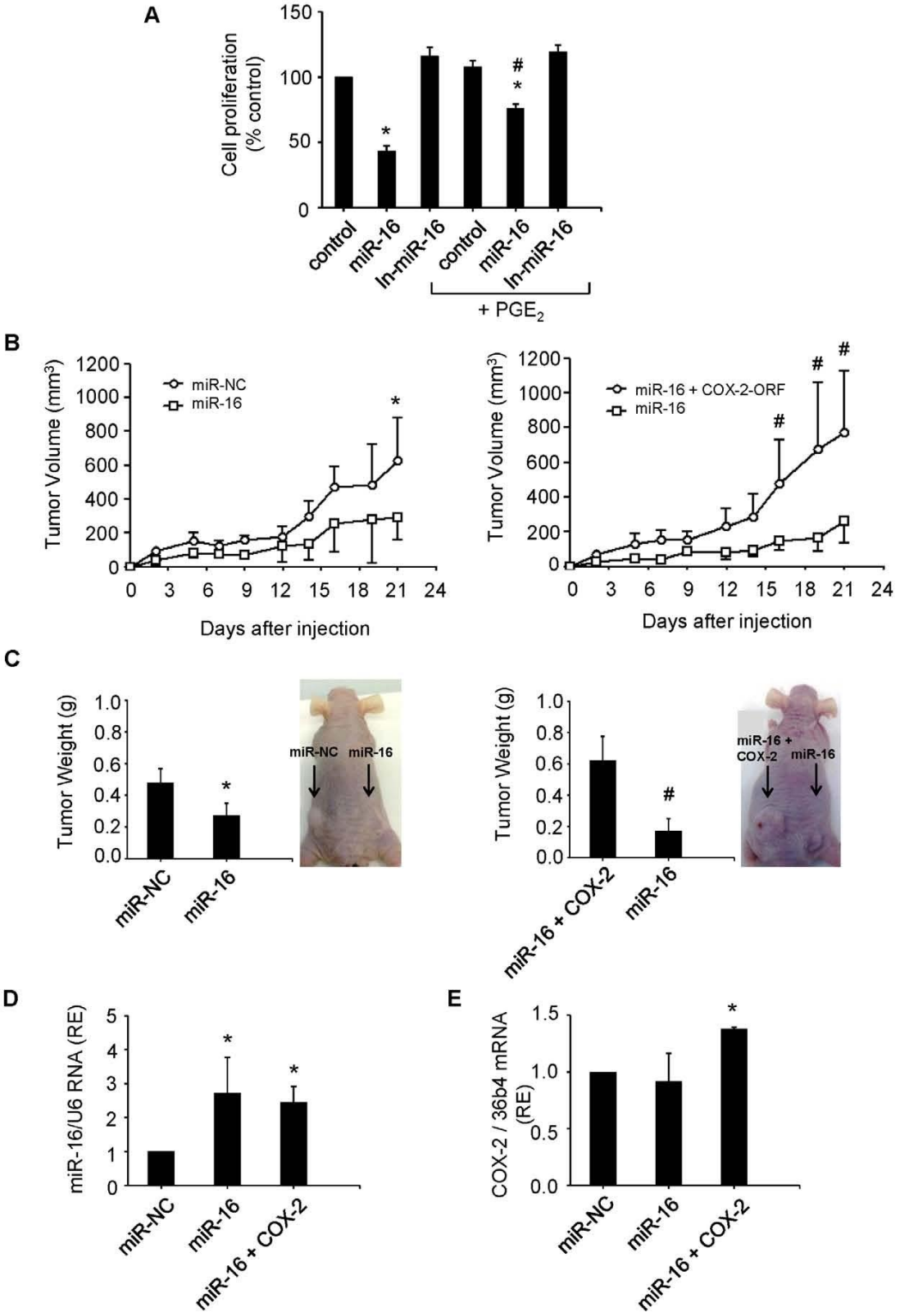
A
Cell proliferation (% control)
150
100
50
0
control
miR-16
ln-miR-16
control
miR-16
ln-miR-16
+ PGE2
B
Tumor Volume (mm3)
miR-NC
miR-16
Days after injection
miR-16 + COX-2-ORF
miR-16
Days after injection
C
Tumor Weight (g)
miR-NC
miR-16
miR-NC
miR-16
Tumor Weight (g)
miR-16 + COX-2
miR-16
miR-16 + COX-2
miR-16
D
miR-16/U6 RNA (RE)
miR-NC
miR-16
miR-16 + COX-2
E
COX-2 / 36b4 mRNA (RE)
miR-NC
miR-16
miR-16 + COX-2

Figure 7. miR-16 suppresses growth of hepatoma cells in vitro and tumorigenicity *in vivo*. (**A**) Hep3B cells were transfected with 50 nM miR-16 or In-miR-16. The effect on cell proliferation was determined by MTT assay at 48 h after transfection. *$p< 0.05$ *vs.* the control and # $p< 0.05$ *vs.* the miR-16 transfection condition. (**B**) Tumor growth curves measured after subcutaneous injection of WRL68 cells transiently transfected with miR-16, miR-NC or miR-16 with a hCOX-2 expression vector lacking 3′ UTR (miR-16+COX-2). Tumor volume (V) was monitored by measuring the length (L) and width (W) with calipers and calculated with the formula ($L \times W^2$)×0.5. Tumor growth was measured every 2–3 days. *$p< 0.05$ *vs.* the miR-NC and # $p<0.05$ *vs.* miR-16 (**C**) Tumor weight and a representative picture of the tumors. At 21 days after injection, mice were killed and tumors were weighed after necropsy. *$p< 0.05$ *vs.* the miR-NC or # *vs.* the miR-16+ COX-2 condition. (**D–E**) miR-16 and human COX-2 expression in tumors using real-time PCR normalized against U6 RNA levels and refers to miR-NC as 1 or 36b4 mRNA, respectively. *$p< 0.05$ *vs.* the miR-NC Data are reported as means±SD of three independent experiments or five animals per condition.
doi:10.1371/journal.pone.0050935.g007

Different cellular signals known to activate MAPK pathways, the PI-3 kinase pathway and the Wnt signaling pathway have been shown to trigger cytoplasmic HuR localization [55]. HuR has been identified as a trans-acting factor that promotes COX-expression and it is known that cytoplasmic HuR expression correlates with poor clinical outcome and with COX-2 expression in ovarian carcinoma [29], human keratinocytes after UVB irradiation [56] and in colon carcinogenesis [37,57]. It is known that HuR is overexpressed in CRC cells and tumors, where elevated HuR levels can impede ARE-mediated decay [37]. However, the expression of HuR in HCC is not reported. HuR binds to COX-2 and increases/maintains COX-2 expression in HCC cells. Moreover, miR-16 is also present in the HuR immunoprecipitated and the analysis of miR-16 predicted target genes determined by using the algorithms miRWalk showed that among miR-16 target genes one is HuR. miR-16 interacts with HuR mRNA in the 3′UTR and represses HuR translation in human breast cancer cells [39]. Indeed, Dixon et al. [37] reported a direct interaction between HuR and miR-16 promoting the downregulation of miR-16 and targeting COX-2 in colon cancer cells. Our data are in agreement with the proposed interaction between miR-16 and HuR mRNA in HCC cells and suggest two different mechanisms for miR-16 to inhibit COX-2: by binding directly to the MRE response element in the COX-2 3′-UTR and by decreasing the levels of HuR through a direct interaction. Our results show HuR expression, protein and mRNA, in both NT and T tissue from HCC biopsies, paralleling COX-2 expression. Moreover a reduced miR-16 expression tends to correlate to high levels of COX-2 protein in liver from patients affected by HCC. Therefore, the reduced expression of miR-16 in those HCC with a high COX-2 expression may contribute to the promotion of cell proliferation and the inhibition of apoptosis and consequently facilitate the development of these types of tumors. Our data suggest an important role for miR-16 in HCC and implicate the potential therapeutic application of miR-16 in those HCC with a high COX-2 expression.

Supporting Information

Figure S1 miR-16 downregulates COX-2 by binding its 3′UTR. A luciferase assay was carried out on HuH-7 cell line using pGL3-UTR reporter vectors. Firefly luciferase activity was evaluated 48 h after co-transfection with pGL3-empty, pGL3-UTR or pGL3-UTR mut (750 ng) and miR-16 (50 mM). Data were normalized against renilla luciferase activity (all samples were co-transfected with 50 ng pRL vector and refer to the positive control, pGL3 empty vector). Data are reported as means ± SD of three independent experiments. *$p<0.05$ vs. the pGL3-UTR condition and #$p<0.05$ vs. the miR-16 transfection condition.
(TIFF)

Figure S2 COX-2 correlates inversely with miR-16 and directly with HuR in HCC human biopsies. (**A**) COX-2 and HuR protein expression were analyzed in both tumor (T) and their paired non tumor (NT) tissues by Western Blot in a total of 7 pairs of matched tissue specimens. Corresponding densitometry analysis is shown and the relative expression of each sample is refer to that in one non tumor tissue sample NT. (**B–D**) The expression of COX-2 mRNA, HuR mRNA and miR-16 were analyzed using real-time PCR in NT and T tissue. *$p< 0.05$ *vs.* NT samples (**E**) COX-2 protein levels were compared to miR-16 expression in T samples. Data were normalized against α-tubulin and U6 RNA levels, respectively.
(TIFF)

Table S1 Several binding sites for miR-16 wihtin COX-2 3′UTR, predicted by diferent algorithms. Using several programs (RHAhybrid, RNA22, PITA, targeScan, microRNA.org), miR-16 was predicted to associate with the 3′UTR region of COX-2 to different MRE motifs. The number of binding sites, the positions and the folding energy are indicated for each program. The 3′UTR sequence of human COX-2 was retrieved using Ensembl Data base, and miR-16 sequence for Homo Sapiens was downloaded from mirBase website.
(DOC)

Author Contributions

Conceived and designed the experiments: NAA PMS. Performed the experiments: NAA OM CLI AFA. Analyzed the data: NAA RM LB MC PMS. Contributed reagents/materials/analysis tools: NAA RM LB MC PMS. Wrote the paper: NAA LB MC PMS.

References

1. Llovet JM, Bruix J (2008) Molecular targeted therapies in hepatocellular carcinoma. Hepatology 48: 1312 1327.
2. Hoshida Y, Nijman SM, Kobayashi M, Chan JA, Brunet JP, et al. (2009) Integrative transcriptome analysis reveals common molecular subclasses of human hepatocellular carcinoma. Cancer Res 69: 7385 7392.
3. Lee JS, Chu IS, Mikaelyan A, Calvisi DF, Heo J, et al. (2004) Application of comparative functional genomics to identify best-fit mouse models to study human cancer. Nat Genet 36: 1306 1311.
4. Simmons DL, Botting RM, Hla T (2004) Cyclooxygenase isozymes: the biology of prostaglandin synthesis and inhibition. Pharmacol Rev 56: 387 437.
5. Ledwith BJ, Pauley CJ, Wagner LK, Rokos CL, Alberts DW, et al. (1997) Induction of cyclooxygenase-2 expression by peroxisome proliferators and non-tetradecanoylphorbol 12,13-myristate-type tumor promoters in immortalized mouse liver cells. J Biol Chem 272: 3707 3714.
6. Martin-Sanz P, Callejas NA, Casado M, Diaz-Guerra MJ, Bosca L (1998) Expression of cyclooxygenase-2 in foetal rat hepatocytes stimulated with lipopolysaccharide and pro-inflammatory cytokines. Br J Pharmacol 125: 1313 1319.
7. Casado M, Callejas NA, Rodrigo J, Zhao X, Dey SK, et al. (2001) Contribution of cyclooxygenase 2 to liver regeneration after partial hepatectomy. FASEB J 15: 2016 2018.
8. Rudnick DA, Perlmutter DH, Muglia LJ (2001) Prostaglandins are required for CREB activation and cellular proliferation during liver regeneration. Proc Natl Acad Sci U S A 98: 8885 8890.
9. Yamamoto H, Kondo M, Nakamori S, Nagano H, Wakasa K, et al. (2003) JTE-522, a cyclooxygenase-2 inhibitor, is an effective chemopreventive agent against rat experimental liver fibrosis1. Gastroenterology 125: 556 571.

10. Kern MA, Haugg AM, Koch AF, Schilling T, Breuhahn K, et al. (2006) Cyclooxygenase-2 inhibition induces apoptosis signaling via death receptors and mitochondria in hepatocellular carcinoma. Cancer Res 66: 7059 7066.
11. Mayoral R, Fernandez-Martinez A, Bosca L, Martin-Sanz P (2005) Prostaglandin E2 promotes migration and adhesion in hepatocellular carcinoma cells. Carcinogenesis 26: 753 761.
12. Cusimano A, Fodera D, Lampiasi N, Azzolina A, Notarbartolo M, et al. (2009) Prostaglandin E2 receptors and COX enzymes in human hepatocellular carcinoma: role in the regulation of cell growth. Ann N Y Acad Sci 1155: 300 308.
13. Cheng AS, Yu J, Lai PB, Chan HL, Sung JJ (2008) COX-2 mediates hepatitis B virus X protein abrogation of p53-induced apoptosis. Biochem Biophys Res Commun 374: 175 180.
14. Nunez O, Fernandez-Martinez A, Majano PL, Apolinario A, Gomez-Gonzalo M, et al. (2004) Increased intrahepatic cyclooxygenase 2, matrix metalloproteinase 2, and matrix metalloproteinase 9 expression is associated with progressive liver disease in chronic hepatitis C virus infection: role of viral core and NS5A proteins. Gut 53: 1665 1672.
15. Cha YI, DuBois RN (2007) NSAIDs and cancer prevention: targets downstream of COX-2. Annu Rev Med 58: 239 252.
16. Kang YJ, Mbonye UR, DeLong CJ, Wada M, Smith WL (2007) Regulation of intracellular cyclooxygenase levels by gene transcription and protein degradation. Prog Lipid Res 46: 108 125.
17. Harper KA, Tyson-Capper AJ (2008) Complexity of COX-2 gene regulation. Biochem Soc Trans 36: 543 545.
18. Nicoloso MS, Spizzo R, Shimizu M, Rossi S, Calin GA (2009) MicroRNAs the micro steering wheel of tumour metastases. Nat Rev Cancer 9: 293 302.
19. Garzon R, Marcucci G, Croce CM (2010) Targeting microRNAs in cancer: rationale, strategies and challenges. Nat Rev Drug Discov 9: 775 789.
20. Ji J, Shi J, Budhu A, Yu Z, Forgues M, et al. (2009) MicroRNA expression, survival, and response to interferon in liver cancer. N Engl J Med 361: 1437 1447.
21. Zhao Y, Ransom JF, Li A, Vedantham V, von Drehle M, et al. (2007) Dysregulation of cardiogenesis, cardiac conduction, and cell cycle in mice lacking miRNA-1 2. Cell 129: 303 317.
22. Chakrabarty A, Tranguch S, Daikoku T, Jensen K, Furneaux H, et al. (2007) MicroRNA regulation of cyclooxygenase-2 during embryo implantation. Proc Natl Acad Sci U S A 104: 15144 15149.
23. Daikoku T, Hirota Y, Tranguch S, Joshi AR, DeMayo FJ, et al. (2008) Conditional loss of uterine Pten unfailingly and rapidly induces endometrial cancer in mice. Cancer Res 68: 5619 5627.
24. Strillacci A, Griffoni C, Sansone P, Paterini P, Piazzi G, et al. (2009) MiR-101 downregulation is involved in cyclooxygenase-2 overexpression in human colon cancer cells. Exp Cell Res 315: 1439 1447.
25. Aguda BD, Kim Y, Piper-Hunter MG, Friedman A, Marsh CB (2008) MicroRNA regulation of a cancer network: consequences of the feedback loops involving miR-17 92, E2F, and Myc. Proc Natl Acad Sci U S A 105: 19678 19683.
26. Jing Q, Huang S, Guth S, Zarubin T, Motoyama A, et al. (2005) Involvement of microRNA in AU-rich element-mediated mRNA instability. Cell 120: 623 634.
27. Mukhopadhyay D, Houchen CW, Kennedy S, Dieckgraefe BK, Anant S (2003) Coupled mRNA stabilization and translational silencing of cyclooxygenase-2 by a novel RNA binding protein, CUGBP2. Mol Cell 11: 113 126.
28. Sawaoka H, Dixon DA, Oates JA, Boutaud O (2003) Tristetraprolin binds to the 3'-untranslated region of cyclooxygenase-2 mRNA. A polyadenylation variant in a cancer cell line lacks the binding site. J Biol Chem 278: 13928 13935.
29. Erkinheimo TL, Lassus H, Sivula A, Sengupta S, Furneaux H, et al. (2003) Cytoplasmic HuR expression correlates with poor outcome and with cyclooxygenase 2 expression in serous ovarian carcinoma. Cancer Res 63: 7591 7594.
30. de La Coste A, Romagnolo B, Billuart P, Renard CA, Buendia MA, et al. (1998) Somatic mutations of the beta-catenin gene are frequent in mouse and human hepatocellular carcinomas. Proceedings of the National Academy of Sciences of the United States of America 95: 8847 8851.
31. Kern MA, Schubert D, Sahi D, Schoneweiss MM, Moll I, et al. (2002) Proapoptotic and antiproliferative potential of selective cyclooxygenase-2 inhibitors in human liver tumor cells. Hepatology 36: 885 894.
32. Casado M, Molla B, Roy R, Fernandez-Martinez A, Cucarella C, et al. (2007) Protection against Fas-induced liver apoptosis in transgenic mice expressing cyclooxygenase 2 in hepatocytes. Hepatology 45: 631 638.
33. Llorente Izquierdo C, Mayoral R, Flores JM, Garcia-Palencia P, Cucarella C, et al. (2011) Transgenic mice expressing cyclooxygenase-2 in hepatocytes reveal a minor contribution of this enzyme to chemical hepatocarcinogenesis. Am J Pathol 178: 1361 1373.
34. Huang J, Liang Z, Yang B, Tian H, Ma J, et al. (2007) Derepression of microRNA-mediated protein translation inhibition by apolipoprotein B mRNA-editing enzyme catalytic polypeptide-like 3G (APOBEC3G) and its family members. J Biol Chem 282: 33632 33640.
35. Rehmsmeier M, Steffen P, Hochsmann M, Giegerich R (2004) Fast and effective prediction of microRNA/target duplexes. RNA 10: 1507 1517.
36. Young LE, Moore AE, Sokol L, Meisner-Kober N, Dixon DA (2012) The mRNA stability factor HuR inhibits microRNA-16 targeting of COX-2. Mol Cancer Res 10: 167 180.
37. Dixon DA, Tolley ND, King PH, Nabors LB, McIntyre TM, et al. (2001) Altered expression of the mRNA stability factor HuR promotes cyclooxygenase-2 expression in colon cancer cells. J Clin Invest 108: 1657 1665.
38. Sureban SM, Murmu N, Rodriguez P, May R, Maheshwari R, et al. (2007) Functional antagonism between RNA binding proteins HuR and CUGBP2 determines the fate of COX-2 mRNA translation. Gastroenterology 132: 1055 1065.
39. Xu F, Zhang X, Lei Y, Liu X, Liu Z, et al. (2010) Loss of repression of HuR translation by miR-16 may be responsible for the elevation of HuR in human breast carcinoma. J Cell Biochem 111: 727 734.
40. Kern MA, Schoneweiss MM, Sahi D, Bahlo M, Haugg AM, et al. (2004) Cyclooxygenase-2 inhibitors suppress the growth of human hepatocellular carcinoma implants in nude mice. Carcinogenesis 25: 1193 1199.
41. Young LE, Dixon DA (2010) Posttranscriptional Regulation of Cyclooxygenase 2 Expression in Colorectal Cancer. Curr Colorectal Cancer Rep 6: 60 67.
42. Mayr C, Bartel DP (2009) Widespread shortening of 3'UTRs by alternative cleavage and polyadenylation activates oncogenes in cancer cells. Cell 138: 673 684.
43. Hu Z, Miao X, Ma H, Wang X, Tan W, et al. (2005) A common polymorphism in the 3'UTR of cyclooxygenase 2/prostaglandin synthase 2 gene and risk of lung cancer in a Chinese population. Lung Cancer 48: 11 17.
44. Chen XM (2009) MicroRNA signatures in liver diseases. World J Gastroenterol 15: 1665 1672.
45. Viswanathan SR, Powers JT, Einhorn W, Hoshida Y, Ng TL, et al. (2009) Lin28 promotes transformation and is associated with advanced human malignancies. Nat Genet 41: 843 848.
46. Kutay H, Bai S, Datta J, Motiwala T, Pogribny I, et al. (2006) Downregulation of miR-122 in the rodent and human hepatocellular carcinomas. J Cell Biochem 99: 671 678.
47. Xu C, Liu S, Fu H, Li S, Tie Y, et al. (2010) MicroRNA-193b regulates proliferation, migration and invasion in human hepatocellular carcinoma cells. Eur J Cancer 46: 2828 2836.
48. Murakami Y, Yasuda T, Saigo K, Urashima T, Toyoda H, et al. (2006) Comprehensive analysis of microRNA expression patterns in hepatocellular carcinoma and non-tumorous tissues. Oncogene 25: 2537 2545.
49. Chen XM, Splinter PL, O'Hara SP, LaRusso NF (2007) A cellular micro-RNA, let-7i, regulates Toll-like receptor 4 expression and contributes to cholangiocyte immune responses against Cryptosporidium parvum infection. J Biol Chem 282: 28929 28938.
50. Gramantieri L, Ferracin M, Fornari F, Veronese A, Sabbioni S, et al. (2007) Cyclin G1 is a target of miR-122a, a microRNA frequently down-regulated in human hepatocellular carcinoma. Cancer Res 67: 6092 6099.
51. Meng F, Henson R, Wehbe-Janek H, Ghoshal K, Jacob ST, et al. (2007) MicroRNA-21 regulates expression of the PTEN tumor suppressor gene in human hepatocellular cancer. Gastroenterology 133: 647 658.
52. Tanaka T, Haneda S, Imakawa K, Sakai S, Nagaoka K (2009) A microRNA, miR-101a, controls mammary gland development by regulating cyclooxygenase-2 expression. Differentiation 77: 181 187.
53. Bhattacharyya SN, Habermacher R, Martine U, Closs EI, Filipowicz W (2006) Relief of microRNA-mediated translational repression in human cells subjected to stress. Cell 125: 1111 1124.
54. Brennan CM, Steitz JA (2001) HuR and mRNA stability. Cell Mol Life Sci 58: 266 277.
55. Yang X, Wang W, Fan J, Lal A, Yang D, et al. (2004) Prostaglandin A2-mediated stabilization of p21 mRNA through an ERK-dependent pathway requiring the RNA-binding protein HuR. J Biol Chem 279: 49298 49306.
56. Zhang J, Bowden GT (2008) UVB irradiation regulates Cox-2 mRNA stability through AMPK and HuR in human keratinocytes. Mol Carcinog 47: 974 983.
57. Young LE, Sanduja S, Bemis-Standoli K, Pena EA, Price RL, et al. (2009) The mRNA binding proteins HuR and tristetraprolin regulate cyclooxygenase 2 expression during colon carcinogenesis. Gastroenterology 136: 1669 1679.

Supplementary Table S1: Several binding sites for miR-16 wihtin COX-2 3´UTR, predicted by diferent algorithms. Using several programs (RHAhybrid, RNA22, PITA, targeScan, microRNA.org), miR-16 was predicted to associate with the 3´UTR region of COX-2 to different MRE motifs. The number of binding sites, the positions and the folding energy are indicated for each program. The 3´UTR sequence of human COX-2 was retrieved using Ensembl Data base, and miR-16 sequence for Homo Sapiens was downloaded from mirBase website.

Software	Sites	Position	Folding energy (Kcal/mol)
RNAhybrid	1	1195-1214	-22.5
RNA22	1	169-190	-25.9
PITA	5	179	-11,86
		182	-14.2
		185	-12.9
		702	-9.5
		1238	-15.64
targetScan	0		
microRNA.org	0		

Supplementary Fig.S1- miR-16 downregulates COX-2 by binding its 3´UTR. A luciferase assay was carried out on HuH-7 cell line using pGL3-UTR reporter vectors. Firefly luciferase activity was evaluated 48 h after co-transfection with pGL3-empty, pGL3-UTR or pGL3-UTR mut (750 ng) and miR-16 (50 mM). Data were normalized against renilla luciferase activity (all samples were co-transfected with 50 ng pRL vector and refer to the positive control, pGL3 empty vector). Data are reported as means ± SD of three independent experiments. *p<0.05 vs. the pGL3-UTR condition and #p<0.05 vs. the miR-16 transfection condition.

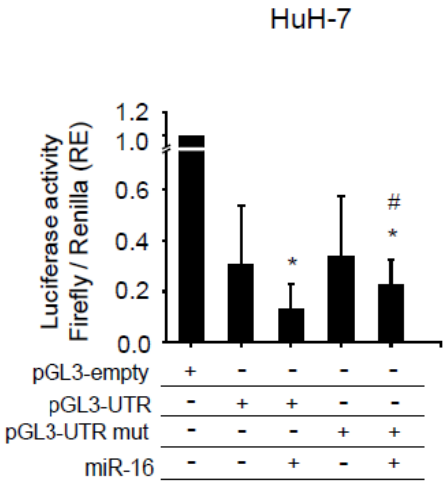

Supplementary Fig.S2- ***COX-2 correlates inversely with miR-16 and directly with HuR in HCC human biopsies.*** **(A)** COX-2 and HuR protein expression were analyzed in both tumor (T) and their paired non tumor (NT) tissues by Western Blot in a total of 7 pairs of matched tissue specimens. Corresponding densitometry analysis is shown and the relative expression of each sample is refer to that in one non tumor tissue sample NT. **(B-D)** The expression of COX-2 mRNA, HuR mRNA and miR-16 were analyzed using real-time PCR in NT and T tissue. *$p< 0.05$ *vs*. NT samples **(E)** COX-2 protein levels were compared to miR-16 expression in T samples. Data were normalized against α-tubulin and U6 RNA levels, respectively.